# Mobility Solutions for 5G New Radio over Low-Earth Orbit Satellite Networks

Martinez, Enric Juan

*DOI (link to publication from Publisher):*
10.54337/aau504484796

*Publication date:*
2022

*Document Version*
Publisher's PDF, also known as Version of record

# MOBILITY SOLUTIONS FOR 5G NEW RADIO OVER LOW-EARTH ORBIT SATELLITE NETWORKS

**BY**
**ENRIC JUAN MARTÍNEZ**

DISSERTATION SUBMITTED 2022

AALBORG UNIVERSITY
DENMARK

# Mobility Solutions for 5G New Radio over Low-Earth Orbit Satellite Networks

Ph.D. Dissertation

Enric Juan Martínez

Aalborg University
Department of Electronic Systems
Fredrik Bajers Vej 7
DK - 9220 Aalborg

Dissertation submitted: September 2022

PhD supervisor: Prof. Preben Mogensen
Aalborg University

Assistant PhD supervisors: Dr. Mads Lauridsen
Nokia

Dr. Jeroen Wigard
Nokia

PhD committee: Associate Professor Beatriz Soret (chairman)
Aalborg University, Denmark

Professor Michele Zorzi
Università degli Studi di Padova, Spain

Master Researcher Helka-Liina Määttänen
Ericsson Research Finland, Finland

PhD Series: Technical Faculty of IT and Design, Aalborg University

Department: Department of Electronic Systems

ISSN (online): 2446-1628
ISBN (online): 978-87-7573-834-2

Published by:
Aalborg University Press
Kroghstræde 3
DK – 9220 Aalborg Ø
Phone: +45 99407140
aauf@forlag.aau.dk
forlag.aau.dk



Printed in Denmark by Stibo Complete, 2022

# Curriculum Vitae

Enric Juan Martínez

Enric Juan received the B. Sc. and M. Sc. in telecommunications engineering from Universitat Politécnica de Catalunya, Spain, in 2015 and 2018, respectively. He is pursuing a Ph.D. degree in wireless communications at Aalborg University, Denmark, in collaboration with Nokia, Aalborg, Denmark. His research interests include radio propagation, low-Earth orbit satellite communications, and radio mobility management algorithms for non-terrestrial networks.

# Abstract

Low-Earth orbit (LEO) satellite constellations emerge as a cost-effective technology to provide ubiquitous and seamless broadband access. Very large constellation projects are planned by private companies such as SpaceX (Starlink), OneWeb, and Amazon (Project Kuiper); thousands of LEO satellites have been already deployed and many more will be launched over the next decade. Motivated by these *new space* ventures and the growing demand for broadband-based applications, the 3rd generation partnership project (3GPP) is working on the development of non-terrestrial networks (NTNs), which aims to efficiently ensure fifth generation (5G) service availability everywhere, at any time. To that end, the specification of NTN seeks to provide 5G New Radio (NR) access over LEO satellite systems, among other systems.

As compared with geosynchronous equatorial orbit (GEO) satellites, LEO satellites present reduced path loss, shorter propagation delay and less expensive launch and manufacturing costs. However, these advantages come at the cost of highly mobile systems and challenging radio propagation conditions; LEO satellites revolve at approximately 7.8 km/s relative to the Earth at altitudes between 500 km and 1500 km. These particular aspects compromise the 5G protocols in areas such as the radio mobility management algorithms, which are fundamental to ensure seamless service as user equipments (UEs) handover across cells. Unlike terrestrial networks (TNs) where radio access network (RAN) nodes are fixed, LEO satellite networks are characterized by a high frequency of mobility events that is primarily caused by the satellite movement. Aiming to support the development of 5G NR over Earth-moving cells (EMC)-based LEO satellite networks, this thesis investigates enhancements for the connected-mode mobility procedure known as handover (HO). These moving satellite systems introduce important mobility challenges, however, they follow deterministic trajectories. Thus, this thesis works on the hypothesis that the 5G NR HO procedures can be modified to exploit the known trajectories of LEO satellites, enhancing the UE mobility performance. The PhD project answers research questions such as: Which are the main mobility challenges to enable 5G NR over LEO satellite networks? Can measurement-based 5G NR HO procedures ensure service con-

tinuity? Can the predictable satellite movement be exploited to improve the UE mobility performance? Can the fact that there are fully correlated radio propagation conditions among adjacent intra-satellite cells be exploited?

Firstly, the large-scale radio propagation parameters of LEO-to-Ground links are studied focusing on time-correlated aspects. We develop a geometrical radio propagation model driven by the lack of models suitable for mobility investigations that realistically capture the varying radio propagation conditions. The proposed model is validated against ray-tracing simulations in rural and urban scenarios. Secondly, the UE mobility performance of the conventional break-before-make UE-assisted network-controlled 5G NR HO and the 5G NR conditional HO (CHO) - both based on NR measurement events and designed for TNs -, are analyzed to identify the limitations of measurement-based HO procedures in 5G LEO satellite networks. The assessment is based on extensive system-level simulations, which results show that the conventional HO cannot ensure service continuity due to a late HO decision that leads to a large number of radio link failures (RLFs). On the other hand, the CHO procedure eliminates the RLFs but increases more than 60 % the signalling overhead and the measurement reporting. To reduce the impact of the observed limitations and enhance UE mobility performance, we propose, simulate, and analyze two novel HO procedures that exploit the known satellite movement. The first contributed solution is a location-based HO procedure, which is assisted with the distance between UE location and the cells centre location. System-level simulation results demonstrate that this procedure can eliminate RLFs and unnecessary HO (UHO) events, while maximizes the time-of-stay (ToS) in a cell. With similar UE mobility performance, we also propose a fully network-controlled HO solution for intra-satellite mobility that uses antenna gain predictions of the satellite beams to bypass cell radio measurements and avoid the non-negligible UE measurement error. This solution is built on the assumption that large-scale radio propagation conditions are fully-correlated between adjacent intra-satellite cells.

This thesis explores novel HO solutions to improve the UE mobility performance in 5G LEO satellite networks with EMC. The PhD studies demonstrate that measurement-based 5G NR HO procedures, which present a sub-optimal mobility performance, can be enhanced by using UE location and satellite location information apart from cell radio measurements. Even though system-level simulation results indicate that the use of the satellite trajectory is beneficial to enhance mobility performance, there are remaining issues to be addressed in the research field of radio mobility algorithms. While we focus on intra-satellite mobility and Earth-moving cells, the suitability of the proposed HO solutions for inter-satellite mobility and Earth-fixed cells is yet to be investigated.

# Resumé

Konstellationer bestående af satellitter i lav jordhøjde (LEO) er en priseffektiv teknologi til at levere allestedsnærværende og problemfri adgang til bredbånd. Firmaer som SpaceX (Starlink), OneWeb og Amazon (Project Kuiper) planlægger projekter med meget store konstellationer, tusindvis af LEO satellitter er allerede i drift, og mange flere vil blive opsendt det kommende årti. Motiveret af disse new space satsninger og den voksende efterspørgsel efter bredbåndsbaserede applikationer arbejder 3rd generation partnership project (3GPP) på udviklingen af non-terrestrial networks (NTNs), som sigter efter effektivt at sikre femte generations (5G) services tilgængelighed alle steder og til enhver tid. Derfor søger standardiseringen af NTN at levere 5G New Radio (NR) adgang via LEO satellitsystemer blandt flere andre systemer.

Sammenlignet med geostationære (GEO) satellitter resulterer LEO satellitter i lavere radioudbredelsestab, kortere udbredelsesforsinkelse og billigere opsendelse samt konstruktion. Disse fordele kommer dog med en pris i form af et meget mobilt system og udfordrende radioudbredelse; LEO satellitter roterer om jorden med omkring 7.8 km/s relativt til jorden i højder imellem 500 km og 1500 km. Disse aspekter kompromitterer 5G protokollerne indenfor felter som algoritmer til håndtering af radiomobilitet, hvilke er fundamentale for at sikre servicekontinuitet når slutbrugernes telefoner (UEs) laver overdragelse fra en celle til en anden. I modsætning til netværk på jorden (TN) hvor radio access network (RAN) noderne er fikserede er LEO satellitnetværk karakteriserede af meget ofte fremkommende mobilitetshændelser der primært skyldes satellittens bevægelse. Med målet om at understøtte udviklingen af 5G NR LEO netværk med celler som bevæger sig på jordoverfladen (EMC) undersøger denne afhandling forbedringer for mobilitetsprocedurer (HO) for forbundne (Connected mode) enheder. De bevægelige satellitsystemer resulterer i store udfordringer for mobilitetsprocedurerne, men systemerne bevæger sig i deterministiske baner. Derfor arbejder denne afhandling ud fra hypotesen om at 5G NR HO procedurerne kan ændres til at udnytte LEO satellitternes kendte baner og dermed forbedre niveauet for UE mobilitet. PhD projektet besvarer forskningsspørgsmål som inkluderer: hvad er hovedudfordringerne for at sikre mobilitet i 5G NR LEO satellit-

netværk? Kan målebaserede 5G NR HO procedurer sikre servicekontinuitet? Kan satellitternes forudsigelse bevægelser udnyttes til at forbedre niveauet for UE mobilitet? Kan det faktum at radioudbredelsen fra nærliggende celler på samme satellit er fuldt korreleret udnyttes?

Først undersøges parametre for storskala radioudbredelse for LEO-til-jord forbindelser med fokus på korrelation i tid. Vi udvikler en geometrisk radioudbredelsesmodel på grund af manglen af modeller, som kan anvendes til undersøgelser af mobilitet og samtidig redegøre for varierende radioudbredelsesforhold på realistisk vis. Modellen, som foreslås, er valideret med ray-tracing simuleringer i landlige og bymæssige miljøer. Derefter undersøges ydeevnen for UE mobilitet for den konventionelle break-before-make UE-assisterede og netværks-kontrollede 5G NR HO procedure og 5G NR conditional HO (CHO) proceduren – begge er baseret på NR målebegivenheder og designet for TN. De analyseres endvidere for at identificere begrænsninger for målebaserede HO procedurer i 5G LEO satellitnetværk. Undersøgelserne er baseret på omfattende simuleringer på systemniveau og resultaterne viser at den konventionelle HO procedure ikke kan sikre servicekontinuitet fordi beslutningen om HO foretages sent og dermed leder til et højt antal af radiolinkfejl (RLF). På den anden side kan CHO proceduren eliminere RLF, men samtidig forøges signaleringsoverhead og målerapporter med mere end 60 %. For at mindske påvirkningen af de identificerede begrænsninger og forbedre ydeevnen af UE mobilitet foreslår, simulerer og analyserer vi to nye HO procedurer som udnytter satellitternes kendte bevægelser. Den første løsning er en HO procedure, som er baseret på positioner og mere specifikt assisteres af distancen imellem en UE's position og positionen for cellernes centre. Simuleringer på systemniveau viser at denne procedure kan eliminere RLF og unødvendige HO begivenheder og samtidig maksimere tiden en UE er i en celle (ToS). Vi foreslår også en fuldt netværks-kontrolleret HO løsning for intra-satellitet mobilitet som opnår tilsvarende mobilitetsydeevne ved at forudsige antenneforstærkningen for satellittens stråler og dermed omgår radiocellemålinger og den ikke ubetydelige målefejl i en UE. Denne løsning er baseret på antagelsen om at storskala radioudbredelse er fuldt korreleret for nærliggende radioceller på samme satellit.

Denne afhandling udforsker nye HO løsninger for at forbedre UE mobilitetsydeevne i 5G LEO satellitnetværk med EMC. PhD studiet demonstrerer at målebaserede 5G NR HO procedurer, som resulterer i suboptimal mobilitetsydeevne, kan forbedres ved at bruge positionerne for UE og satellitten udover radiocellemålinger. Selvom resultaterne baseret på simuleringer på systemniveau indikerer at brugen af viden om satellitternes baner er fordelagtig for at forbedre mobilitetsydeevnen, er der tilbageværende forskningsproblemer indenfor algoritmer til radiomobilitet. Vi har fokuseret på intra-satellit mobilitet og EMC, men det er endnu ikke undersøgt om de foreslåede HO løsninger kan anvendes i celler som er fikseret på jorden (EFC) og

inter-satellit mobilitet.

# Contents

# Glossary

**2G** second generation

**3GPP** 3rd generation partnership project

**5G** fifth generation

**6G** sixth generation

**AG** antenna gain

**AGHO** antenna gain based HO

**BHO** baseline HO

**CDF** cumulative distribution function

**CHO** conditional HO

**CI** confidence interval

**CL** coupling loss

**CN** core network

**DL** downlink

**DL SIR** downlink signal-to-interference ratio

**DL SINR** downlink signal-to-interference-plus-noise ratio

**DPM** dominant path model

**EFC** Earth-fixed cells

**EMC** Earth-moving cells

**FR** frequency reuse

**FR1** frequency reuse 1

**GEO** geosynchronous equatorial orbit

**GNSS** global navigation satellite system

**HAPS** high altitude platform systems

**HO** handover

**HOF** HO failure

**HOM** HO margin

**HST** high-speed train

**ISD** inter-site distance

**ITU** international telecommunications union

**ITU-R** ITU radio communication sector

**KPI** key performance indicator

**LCHO** location-based CHO

**LEO** low-Earth orbit

**LHT** location-based HO triggering

**LOS** line-of-sight

**LTE** Long-Term Evolution

**ME** measurement error

**MEO** medium-Earth orbit

**MHT** measurement-based HO triggering

**MR** measurement report

**NLOS** non line-of-sight

**NR** New Radio

**NTN** non-terrestrial network

**NW** network

**PDCCH** physical downlink control channel

**PP** ping-pong

**PRB** physical resource block

**QoS** quality of service

**RA** random access

**RACH** random access channel

**RAN** radio access network

**RAT** radio access technology

**RF** radio frequency

**RLF** radio link failure

**RMSE** root mean square error

**RRC** radio resource control

**RSRP** reference signal received power

**RSRQ** reference signal received quality

**SINR** signal-to-interference-plus-noise ratio

**TN** terrestrial network

**ToO** time-of-stay-in-outage

**ToS** time-of-stay

**TSG** technical specification group

**TTT** time-to-trigger

**UE** user equipment

**UHO** unnecessary HO

**UL** uplink

**UMa** urban macro

**WCN** Wireless Communication Networks

# Thesis Details

| | |
|---|---|
| **Thesis Title:** | Mobility Solutions for 5G New Radio over Low-Earth Orbit Satellite Networks |
| **PhD Student:** | Enric Juan Martínez |
| **Supervisors:** | Prof. Preben Mogensen, Aalborg University<br>Dr. Mads Lauridsen, Nokia, Aalborg<br>Dr. Jeroen Wigard, Nokia, Aalborg |

This PhD thesis is the result of three years of research at the Wireless Communication Networks (WCN) section (Department of Electronic Systems, Aalborg University, Denmark) in collaboration with Nokia (Aalborg). The work was carried out in parallel with mandatory courses required to obtain the PhD degree. The papers supporting the work presented in the thesis were published in peer-reviewed IEEE journals and conferences.

The main body of the thesis consists of the following papers:

Paper A: Enric Juan, Mads Lauridsen, Jeroen Wigard, and Preben Mogensen, "A Time-correlated Channel State Model for 5G New Radio Mobility Studies in LEO Satellite Networks", *IEEE 93rd Vehicular Technology Conference (VTC2021-Spring)*, April 2021, pp. 1–5.

Paper B: Enric Juan, Ignacio Rodriguez, Mads Lauridsen, Jeroen Wigard, and Preben Mogensen, "Time-correlated Geometrical Radio Propagation Model for LEO-to-Ground Satellite Systems", *IEEE 94th Vehicular Technology Conference (VTC2021-Fall)*, September 2021, pp. 1–5.

Paper C: Enric Juan, Mads Lauridsen, Jeroen Wigard and Preben Mogensen, "5G New Radio Mobility Performance in LEO-based Non-Terrestrial Networks", *IEEE Globecom Workshops (GC Wkshps)*, December 2020, pp. 1-6.

Paper D: Enric Juan, Mads Lauridsen, Jeroen Wigard, and Preben Mogensen, "Performance Evaluation of the 5G NR Conditional Han-

dover in LEO-based Non-Terrestrial Networks", *IEEE 23rd Wireless Communications and Networking Conference (WCNC)*, April 2022, pp. 2488–2493.

Paper E: Enric Juan, Mads Lauridsen, Jeroen Wigard, and Preben Mogensen, "Location-Based Handover Triggering for Low-Earth Orbit Satellite Networks", *IEEE 95th Vehicular Technology Conference (VTC2022-Spring)*, June 2022, pp. 1-6.

Paper F: Enric Juan, Mads Lauridsen, Jeroen Wigard, and Preben Mogensen, "Handover Solutions for 5G New Radio over Low-Earth Orbit Satellite Networks", *IEEE Access*, 2022.

This thesis has been submitted for assessment in partial fulfilment of the PhD Degree. The PhD thesis is composed by the submitted and published papers, which are listed above. Parts of the papers are used directly or indirectly in this thesis. As part of the thesis assessment, co-author statements are available to the assessment committee and at the Faculty.

# Acknowledgements

This thesis is an attempt to capture the work conducted throughout the PhD journey. These more than three years represent professional and emotional growth, that would not be possible without the support of many people.

First, I would like to thank my supervisors for their constant support and advice during these years. I thank Mads Lauridsen for thoroughly reviewing all my work (even when he had no time for it) and teaching me what high-quality research means. I thank Jeroen Wigard for always being available to help and for trusting me. Last but not least, I thank to Preben Mogensen for his *punching* questions and for reminding me constantly to take ownership over my work. I thank the three of them for *shaping* me into a better professional.

I would also like to thank all my colleagues at Aalborg University and Nokia for the always-good technical discussions and making the office a very friendly and social place to work. Thanks for so many good mental breaks while having coffee, cake, and breakfast. I would like to give a special mention to István Z. Kovács, Jens Steiner, Mads Brix and Dorthe Sparre for always efficiently address all my questions.

On the personal side, I am grateful to many people that contributed on their own way to make the process easier. Dani, for the climbing afternoons, the half-marathons and the great talks (specially the ones about politics). Roberto and Majken, for being such attentive listeners and advisors. Pilar, for her endless energy and support, especially in times of a pandemic. Francesco and David, for hosting so many nights that helped to disconnect the mind. Filipa and Joao, for that proximity that made me feel a bit less far from home. Elisa, for the refreshing walks and the ice-cream. Manel, Ruben and Toni, for always caring about me from the far distance. I cannot forget Silvia, for teaching me how to properly listen, talk and treat myself.

There is a special place in this acknowledgements to David, for always being by my side, caring, listening, understanding, supporting, and advising since the very beginning. You are family.

If there is a person to blame for this achievement that one is Melisa. Thank you for showing me the value of day-dreaming and what really matters in

life. Thank you for being always a friend, an adventure mate, a partner in crime since that very first day of university. For all those great memories and the ones are about to come. You are my past, my present and my future.

Last, I would like to thank my parents for giving me far beyond everything they could. For every inch of your effort to make possible that I had a better future. For teaching me your values of integrity, unconditional love and caring. You are also part of this. *Por último, me gustaría dar las gracias a mis padres por darme absolutamente todo lo que pudieron y más. Por los incontables esfuerzos que hicieron posible que tuviera un futuro mejor. Por enseñarme vuestros valores de integridad, esfuerzo y amor. Vosotros también sois parte de esto.*

Enric Juan Martínez
Aalborg University, August, 2022

# Part I

# Introduction

# Introduction

Wireless communications have become essential in our personal and professional lives with a major role in the global economy and in the society development [1]. Despite wireless technologies were designed for human-centric communication, e.g. voice and data services, the rapid advance of technology has motivated the need to support new applications and use cases. The definition of the fifth generation (5G) standard has become fundamental to introduce novel technologies that are able to support these new services.

The 5G technology aims to serve emerging use cases grouped in three categories: i) enhanced mobile broadband (eMMB), ii) ultra-reliable low-latency communications (URLLC), and iii) massive machine type communications (mMTC). The first case refers to all human-centric communications, which focuses on providing high-data rates and seamless user experience. The second covers those services requiring high reliability, low latency and high availability. Finally, the last one refers to services with a large number of low-power devices which usually transmit small amounts of latency-tolerant data.

Among other requirements, 5G systems are expected to support ubiquitous and seamless connectivity [2]. However, the current roll-out of cellular networks, including 5G and older generations, fall short to provide adequate global broadband connectivity, especially in remote and underserved areas [3]. Even in the most developed countries, the cellular infrastructure may lack the expected reliability and availability, also being vulnerable to natural disasters. Despite there has been an increase in recent years, currently less than 64 % of the world's population uses the Internet [4]. This means that an estimate of 3 billion people remain unconnected and with an increased risk of digital exclusion. The main reason for this, is the absence of available infrastructure in those areas where deploying a cellular network is not cost-effective. The 5G development process had less focus on providing coverage to rural and remote areas compared to increasing capacity in densely populated areas where revenue generation is higher [5].

Satellites, traditionally used for application such as television broadcasting, navigation and remote sensing, emerge as a technology enabler able to

provide ubiquitous broadband service across the world [2]. Their inherent nature, not being constrained to a geographical location, makes them the ideal cost-effective solution to complement terrestrial network (TN). Low-Earth orbit (LEO) satellite constellations have received the most attention from academia and industry. As compared with geosynchronous equatorial orbit (GEO) satellites, satellite systems in LEO orbits - from 500 km to 1500 km -, improves the radio link budget, cuts down the propagation delay and reduces manufacturing and launching costs [6].

The private space sector, led by SpaceX, Amazon and OneWeb, is already deploying hundreds and thousands of LEO satellites as part of its ambitious plans to deliver broadband from space [7]. SpaceX, as the frontrunner of the race, has already launched more than 2300 satellites of its Starlink constellation. Furthermore, the company envisions to scale the constellation up to approximately 30 000 systems in orbit. OneWeb project consists of an initial constellation composed by 716 satellites, followed by a final network with 6372 satellites. Amazon Kuiper system will bring the constellation up to 3236 satellites. According to [7], the three constellations could offer a total capacity of around tens of Tbps. That means they will not compete against TNs that achieve thousands of Tbps [8], but instead complement them in underserved areas where it is not cost-effective or feasible to deploy the network infrastructure.

Apart from proprietary solutions to deliver global broadband access, the 3rd generation partnership project (3GPP) standardization activities are also working to include the satellite technology as part of the 5G standard. The 3GPP is a consortium of standard organizations and market players which together have invested their resources in developing the different cellular telecommunications technologies. The partnership provides system description and specifications for each cellular technology and their multiple use cases. After the definition of the 5G standard there has been increasing interest and participation from academia, satellite industry and telecommunications companies convinced of the potential of an integrated satellite and terrestrial network infrastructure.

# 1 Satellite Systems in 5G

## 1.1 The Role of Satellites in Mobile Networks in the Past

Satellite and cellular networks have been developed separately from each other, using independent protocol architectures which made difficult the integration of both worlds. Satellite technology was developed decades earlier than cellular networks. The first communication satellite systems were deployed more than fifty years ago at geosynchronous orbits [9]. This is

because satellites appeared to remain stationary in their orbit and ground stations could point constantly to the same location. The large path loss of GEO-to-Ground links and the high cost to launch and operate those systems indicated that non-geostationary orbits, thirty to forty times closer to ground, could present advantages. However, operating satellites at lower altitudes also involved a constellation of satellites to provide global coverage. The concept of private companies that could deploy satellite services at non-geostationary orbits did not emerge until the demand for cellular services really began to dominate. At the beginning of the 1990s, cell phone services were minimal and centered only in big urban areas. The following years, the roll-out was fast and determined, and base stations started to provide reliable and robust service. When pioneering systems such as Iridium and Globalstar started to offer communication services using non-geostationary satellites, the market of subscribers was nonexistent since terrestrial deployments were cheaper and offered better service [6]. Despite these projects rapidly filed bankruptcy due to lack of economic viability caused by a small market and the high costs of these LEO satellites, they gained the attention of the research community.

There have been attempts to integrate satellite communications in previous mobile network generations but those consisted in proprietary tailored solutions, where the satellites were primarily deployed for backhaul purposes as a costly non-flexible transport network [10].

## 1.2 3GPP Non-Terrestrial Networks

The growing market pull, coming from the demand for broadband access and the advances in satellite technology, reducing launching and manufacturing costs, seem to indicate the time to develop a fully-fledged architecture integrating cellular and satellite technologies. To that end, the 3GPP standardization efforts target the development of non-terrestrial network (NTN) systems as a cost-effective solution to provide 5G New Radio (NR) access across areas where the TN infrastructure is not available. The roll-out of NTN systems aims not only to serve isolated and remote areas, but to deliver service continuity for moving platforms such as aircraft and ships. It is also expected to be used as a responsive solution for areas affected by natural disasters, e.g. earthquakes and flooding.

The benefits of satellites in 5G were studied by the 3GPP in Release 15, leading to concrete requirements to support satellite access in [11]. Later on, the 3GPP addressed a study item to support 5G NR over NTN [12]. The objective was to study channel models, define deployment scenarios and identify potential impacted areas of the standard. In the fall of 2018, the technical report [13] followed with solutions for the identified key impact on the radio access network (RAN) protocols. After the study items in Release 16,

the 3GPP included in Release 17 the satellite technology for the first time as part of the 5G NR standard with the work item [14]. This work item defined the required changes to enable basic operations of NR over NTN. Furthermore, the Release 17 specification will also support satellite-based access for internet-of-things use cases. At the time of writing, 3GPP is finalizing Release 17 and working on enhancements to support 5G NR over NTN in the context of Release 18. The work item [15] targets new deployments in frequency bands above 10 GHz, enhanced coverage for handset terminals and mobility solutions for TN-NTN and NTN-NTN scenarios.

According to [12], an NTN refers to a network operating through satellite systems and/or high altitude platform systems (HAPS) where these systems act as RAN nodes. HAPS are *airborne* platforms that stay quasi-static in the sky and they are typically placed at altitudes around 20 km. On the other hand, *spaceborne* platforms are categorized below depending on orbit altitude and beam footprint size (see Fig. I.1):

- **GEO satellites** orbit around Earth at 35 786 km altitude and the orbital period is equal to the Earth rotation period, which makes them quasi-static to an observer on the ground. It is the satellite system with the largest beam footprint size, i.e. from 200 to 3500 km.
- **Medium-Earth orbit (MEO) satellites** feature circular orbits at an altitude varying from 7000 to 25 000 km with beam footprint sizes from 50 to 1000 km.
- **LEO satellites** revolves around the Earth at an altitude between 600 km and 1200 km with footprint sizes from 100 to 1000 km.

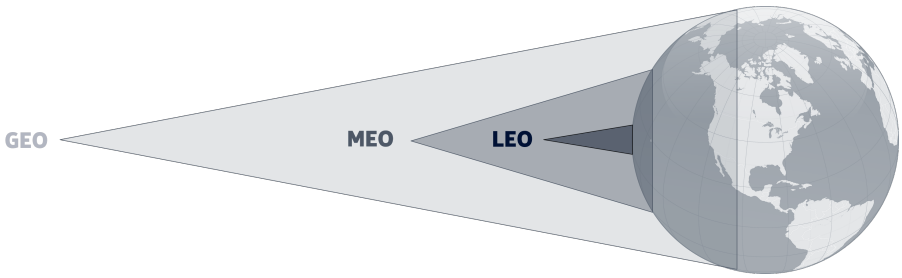


**Fig. I.1:** General comparison of GEO, MEO and LEO orbits satellite systems.

The typical scenario of an NTN consists of a NTN platform that provides NR access to user equipments (UEs) through the service link, where multiple satellite beams enable multiple NR cells. Fig. I.2 contains the main elements envisioned by the 3GPP. As described in [13], the 3GPP considers two payload implementations for NTN systems: *transparent* and *regenerative*.

The former, also known as bent-pipe, considers the NTN platform acting as a relay node between the UE and the network (NW) on the ground. The latter entails a payload with full, or partial, gNB capabilities able to work as a moving base station. The connection between the NTN system and the 5G core network (CN) goes through the feeder link enabled by one or several NTN gateways.

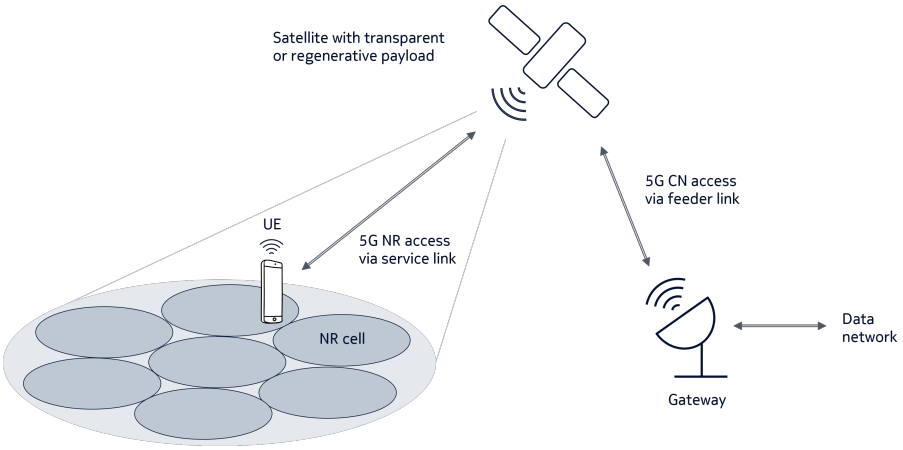


**Fig. I.2:** Overview of a typical NTN scenario.

Among the deployment scenarios discussed in 3GPP, the Earth-fixed cells (EFC) and the Earth-moving cells (EMC) implementations are included in Release 17. Satellites using EFC continuously adjust the satellite beam pointing direction to fix the cell to a specific point on Earth for a period of time, while EMC-based systems entail a fixed satellite beam pointing direction, i.e. nadir, and thus the beam footprint, i.e. NR cell, is moving on Earth.

## 1.3 From GEO to LEO Satellites

Each satellite category has its own characteristics that may impact the 5G standard differently. The work done by 3GPP is focusing on GEO and LEO systems, the last one being the most attention-grabbing. Table I.1 captures some of the main differences between GEO and LEO satellite systems and it also includes a typical rural macro deployment to provide a baseline reference. LEO systems present several advantages but also pose disadvantages as compared with GEO satellites. GEO satellites can provide backhauling and broadband access to users over wide areas such as entire countries or continents due to its altitude, i.e. 35 786 km. However, the high altitude of these orbits implies long signal propagation delay, i.e. one-way delay of 270 ms, and significantly increases the launching costs as compared with lower or-

bits. The long communication distances not only impact the latency but also the path loss, which results in a challenging link budget. LEO satellites partially solve the distance issue since these systems orbit at lower altitude, i.e. 600–1200 km. Even though LEO satellites reduce the link distance, these can be up to 3131 km [13]. Furthermore, lower orbit altitudes come at the expense of highly mobile satellites and smaller coverage. Unlike GEO deployments that precise three satellites to provide global coverage, in LEO it is required a large number of satellites, which are distributed in a mesh known as *constellation*. One of the key aspects of LEO satellites is their high-speed mobility. These systems revolve faster than the rotational speed of the Earth; a LEO satellite can circle the Earth in around 90 min moving at a speed of approximately 7.5 km/s, i.e. 27 000 km/h. The fast movement of LEO platforms involve large Doppler frequency shifts, i.e. 24–21 ppm [13], which will impact the signals synchronization.

| **Network specific** | **GEO satellite** | **LEO satellite** | **Rural deployment** |
|---|---|---|---|
| Altitude RAN node | 35 786 km | 600–1200 km | 10–35 m |
| RAN node speed (relative to Earth) | 0 km/s | 7.5–7.1 km/s | 0 km/s |
| Max beam footprint size | 3500 km | 1000 km | 10 km |
| Max propagation delay (10° elevation angle) | 270.73 ms | 12.89–20.89 ms | 0.03 ms |
| RAN lifetime | 15 years | 5 to 10 years | 5 to 10 years |
| Visibility time window (10° elevation angle) | ∞ | 7–12 min | ∞ |

**Table I.1:** Comparison of the key characteristics of GEO and LEO satellite systems for non-terrestrial networks [13] and a terrestrial rural macro deployment [16].

# 2 Radio Mobility in 5G LEO Satellite Networks

The use of LEO satellites allows shorter propagation delay, higher data-rates and reduced deployment and manufacturing costs as compared with GEO systems. Therefore, LEO systems are considered a cost-effective solution to complement TN and extend the 5G availability.

The 5G specifications were defined to efficiently work considering radio links where the RAN nodes were fixed in terrestrial environments (e.g. rural,

urban or dense urban). These static RAN nodes typically provide NR access from some tens of meters above the ground with communication distances shorter than a few kilometers. For LEO satellite-based access, the physics of the scenario, i.e. RAN node mobility and TX-RX distance, vastly increases requiring changes in the 5G standard (see Table I.1). One of the most impacted areas is the radio mobility management, which procedures aim to ensure adequate service while users change serving cells. In particular, this thesis focuses on the handover (HO) procedure that is the procedure in charge to ensure service continuity in connected-mode.

## 2.1 Mobility Challenges

This section aims to explain the key aspects that should be considered to investigate mobility in 5G LEO satellite networks. The Fig. I.3 supports the following explanation summarizing the main mobility challenges.

A. **High-speed satellite movement and altitude.** If in a TN the mobility events are triggered by UE mobility, in LEO satellite networks the satellite movement - approximately 28 000 km/h - is expected to cause, and increase, the triggering of mobility events. This means that even when users are stationary, the satellite movement will trigger additional mobility events as well as high Doppler frequency shifts that can compromise the mobility performance. Another aspect to consider is the communication distance. LEO satellites aim to provide NR access from hundreds or thousands of kilometers; 1932 km for a satellite at an altitude of 600 km and 10° elevation angle. However, 5G specifications support a maximum distance of 100 km, while the maximum distance in a typical rural deployment is 10 km. The satellites movement and the magnitude of the communication distances introduce important challenges in terms of radio propagation conditions and propagation delay, which will be commented further down.

B. **Varying radio channel.** In LEO-to-Ground links, the satellite movement introduces changes in the radio propagation conditions in terms of path loss, shadowing and visibility conditions, i.e. line-of-sight (LOS)/non line-of-sight (NLOS). Even stationary users in rural low-scattered areas may experience varying signal attenuation because distances and LOS conditions change as satellites move.

C. **Low reference signal received power (RSRP) variation.** In TN there is a clear difference between the RSRP at cell centre and at cell edge. Typically, in a rural deployment with high probability of LOS, the path loss may differ more than 40 dB depending on the position in the cell. This effect is not as pronounced in LEO satellite networks. For a satellite altitude of

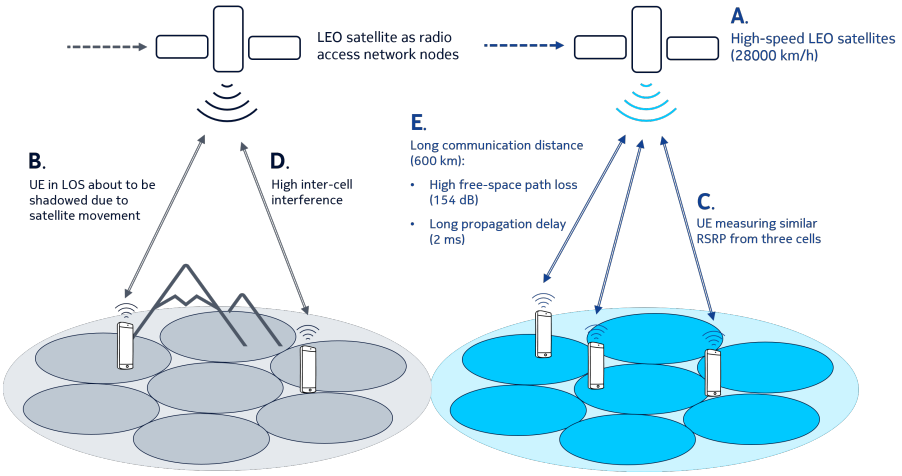


**Fig. I.3:** Mobility challenges caused by LEO satellites providing 5G NR access to UEs on the ground.

600 km, a cell size of 50 km and a carrier frequency of 2 GHz (S-band), the free-space path loss ranges from 154.03 dB at cell centre to 154.04 dB at cell edge. Distance between UE location and satellite location is usually orders of magnitude longer than the cell size, which leads to very little variation of the path loss within a cell. Thus, the RSRP variations are dominated by the satellite beam antenna pattern.

D. **High inter-cells interference.** Similar as cell sites in TN, satellite coverage will be dimensioned via multiple satellite spot beams. This translates into a single transmission/reception point radiating multiple NR cells that might generate high inter-cells interference to users on the ground. This limitation may deteriorate the service radio link quality especially in a deployment with frequency reuse 1 (FR1) scheme.

E. **Long propagation delay.** Even though LEO satellites reduce drastically the latency issue as compared with GEO systems, satellite systems feature much larger delays than TNs; the maximum one-way propagation delay supported in 5G NR is 1 ms, whereas LEO systems might require up to 20.89 ms (see Table I.1). Long propagation delays may result in outdated measurements. Furthermore, the propagation delay changes as the satellite move, which introduces new requirements for procedures relying on time synchronization.

## 2.2 Why 5G NR HO Procedures Could Require Enhancements

This PhD started as 3GPP was working on the study items [12] and [13] for Release 15 and 16. Both technical reports acknowledged that the fast pace of LEO satellites creates problems for paging and handovers and, therefore, potential adaptations should be studied. Despite procedures in inactive and idle-mode also presented interesting fields to explore, we considered the HO procedure as the most attractive area of research.

The HO procedure is fundamental to avoid service interruptions and data loss. In essence, it is responsible for ensuring service continuity. Furthermore, if the HO is not executed quickly enough, the UE may not use target cell resources efficiently. The NR HO procedures were not designed to address aspects such as fast satellite movement, large and varying propagation delays and small RSRP variation in regions of cell overlap. Thus, Release 16 NR HO procedures require analysis with two principal purposes: i) assess the impact of these aspects in the mobility performance and ii) define new HO schemes to improve the mobility performance and ensure service continuity and satisfactory user experience.

Similarly as in TN, there are different types of HO depending on the context where the procedure is triggered. In NTN, the HO types will differ depending on the network architecture and configuration but in general they can be categorized among the classes included in Fig. I.4. Further details are given below:

- **Intra-satellite HO** is defined as the mobility event that occurs when a UE connects to a neighbouring cell enabled by a satellite beam that belongs to the same satellite. In LEO satellite networks, this scenario is characterized by a high HO rate due to satellite mobility, especially if the satellite enables a large number of cells with relatively small size, e.g. 25-100 km. As a reference, for a EMC-based satellite, altitude of 600 km and 50 km cell size, the minimum HO rate is approximately 0.2 HO/UE/s.

- **Inter-satellite HO** refers to a handover where serving cell and target cell belong to different satellites. For a regenerative satellite with the full gNB on board, it requires inter-gNB mobility.

- **Inter-radio access technology (RAT) HO** occurs between satellites belonging to different RAT networks (i.e. NTN-NTN), or between non-terrestrial and terrestrial access networks (i.e. TN-NTN and NTN-TN).

We consider the intra-satellite HO scenario as the most challenging and interesting area to address. Satellite movement triggers a high intra-satellite HO rate. High inter-cell interference might cause a fast degradation of the serving cell radio link quality. Low RSRP variation can further increase the

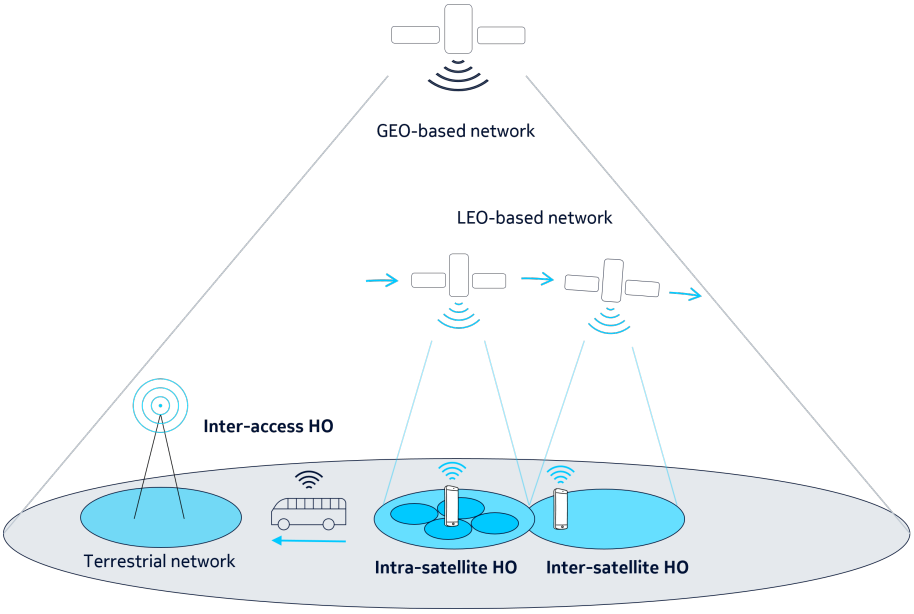


**Fig. I.4:** Overview of the intra-satellite HO, inter-satellite HO and inter-access HO scenarios.

number of undesired HO events because the NR HO procedures are triggered by NR measurements events that only consider cell radio measurements. Aiming for seamless and continuous service, research on the topic is required as these challenging conditions might lead the NR HO procedures to malfunction in 5G LEO satellite networks.

## 2.3 State-of-the-art HO Solutions for LEO Satellite Networks

Several research works have addressed HO solutions for LEO satellite networks. Early examples of these works are [17] and [18], which were motivated by the appearance of Iridium and Globalstar constellations. Several investigations followed the rise and fall of these projects designed to support second generation (2G) mobile services with a data rate up to 14.4 kbps [19]. These works were mainly focused on ensuring communication resources, considering a simple quality of service (QoS) criteria, and tailored to the specifics of each constellation.

The last decade has seen a wind of change in the space market with the decrease of the manufacturing and launching costs. Furthermore, the emergence of the 5G technology has opened a wide variety of use cases. The involvement of academia and industry pushing towards the same direction has led to a large body of literature on the topic. Y. Wu *et al.* presented in [20] an inter-satellite HO approach that was based on the *potential game*

theory; in the network system there are many devices competing for satellites resources and spectrum. The goal was to minimize the HO rate as well as reducing the HO time and maintaining a balanced traffic load in the constellation. In [21], Y. Li *et al.* proposed a multi-layer network which consisted in GEO and LEO satellites, HAPS and terrestrial relay nodes. The goal was to reduce the call dropping as well as to increase the throughput. The results showed an enhanced performance which reduced the HO latency and signalling costs compared with traditional HO methods. Due to the complexity of satellite constellations, the use of reinforcement learning is becoming popular to optimize network-specific key performance indicators (KPIs). To minimize the satellite HO rate, S. He *et al.* proposed a new algorithm in [22] that satisfies the limited channel budgets of each satellite. The relationship between user and satellite service availability is formulated as an optimization problem that is transformed into a multi-agent reinforcement learning optimization framework. The simulation evaluation results shows that the proposed HO solution reduces the average number of HOs and it improves the channel utilization of the system. Another example is the one presented by Y. Cao *et al.* in [23] to address the frequent HO problem. They proposed a reinforcement learning scheme where UEs make autonomous decisions to improve throughput while avoid frequent HOs.

The reviewed works mostly address HO solutions to improve the performance in terms of HO rate and traffic load. In many cases, the proposed solutions do not account for 5G, or any cellular, technology. Thus, to the best of our knowledge, none of the above-mentioned addresses HO procedures to support the development of 5G NR over LEO satellite networks. Furthermore, in the available literature there exists a lack of proposals supported by system-level simulations compliant with 3GPP specifications for NTN.

## 2.4 LEO Satellites Follow Predictable Trajectories

We have discussed the important challenges that LEO satellites entail and how these challenges introduce new requirements to the NR HO procedures that require investigation. The 3GPP is working to address these issues and the technical reports [12] and [13] captured a promising way forward.

The 3GPP suggested in [12] that UEs could benefit from geo-location information. The UE could report its own location to the NW - e.g. included in the measurement report (MR) - or the NW broadcasts the satellite *ephemeris*[1]. Despite the challenging nature of LEO satellites, it is possible to know current and future satellite locations because these systems follow deterministic orbits that are predictable. On the other hand, it is feasible that UEs are

[1]Table or data file giving the calculated positions of a celestial object at regular intervals throughout a period.

aware of their locations since most 3GPP-compliant handhelds, e.g. smartphones, have global navigation satellite system (GNSS) receivers and NTN targets primarily outdoor users.

Using UE location and satellite location, the cells coverage and its velocity can be estimated. One possibility is that new HO triggering events based on location and/or time information are used. Additional triggers can be determined based on the distance between the UE and the cells centre, the elevation angles of serving and target cells or the remaining serving cell radio coverage time. Furthermore, these triggers could be evaluated independently or jointly with measurement-based HO triggers (i.e. NR measurement events). In essence, the known satellite trajectory and the UE location should be exploited to determine the most appropriate target cell to handover to and, ultimately, enhance the UE mobility performance.

# 3 Objectives of the Thesis

The goal of this thesis is to tailor HO solutions that overcome the challenges of 5G LEO satellite networks and ensure a service continuity similar to the equivalent terrestrial deployments. The study focuses on LEO satellites with on-board gNB capabilities and EMC. The current 5G NR HO procedures, which are based on cell radio measurements, might lead to a sub-optimal mobility performance. To that purpose, this investigation considers the predictable movement of LEO satellites as a key element to design HO enhancements. The aim is to propose, simulate and evaluate HO solutions that are able to improve the mobility performance as compared with Release 16 5G NR HO procedures. The mobility performance targets are to maximize the downlink signal-to-interference-plus-noise ratio (DL SINR), prevent radio link failures (RLFs) and avoid unnecessary HO (UHO) events.

These objectives were used to establish the following hypothesis (H) and research questions (Q), which have been addressed during the PhD study:

H1 The continuous movement of LEO satellites causes varying radio propagation conditions for LEO-to-Ground links. Static users in rural environments could experience a fast degradation of the service radio link quality due to shadowing of surrounding elements, e.g. buildings and mountains.

Q1 For a given satellite elevation angle, what is the LOS probability for static users in rural and urban environments? What is the probability to transition from/to LOS/NLOS? What is the variability of the shadow fading?

H2 LEO satellites move at 28 000 km/h relative to the Earth. The fast movement of these satellite systems, acting as moving base stations from a

high altitude, may challenge the UE mobility performance. Constraints such as long propagation delays and varying radio propagation conditions can lead to a malfunctioning of the measurement-based NR HO procedures.

Q2 What is the RSRP variability experienced by UEs at cell centre and at cell edge? How the inter-cell interference from intra-satellite cells can impact the radio signal quality and the overall mobility performance? What is the optimal HO rate? What kind of enhancements can be done to improve the conventional HO procedure performance?

H3 Due to the characteristics of LEO satellite networks, location-based HO triggering criteria may improve the UE mobility performance of HO procedures purely based on cell radio measurements.

Q3 Can satellite *ephemeris* and UE location be used in the HO triggering criteria to initiate the HO at cell edge and towards the optimal target cell? Can location-based HO solutions maximize DL SINR, optimize the HO rate while reducing RLFs and UHO events?

H4 Intra-satellite mobility is characterized by fully-correlated radio propagation conditions - i.e. path loss, shadow fading and LOS - because cells are radiated from the same satellite. In such predictable scenario, a UE could handover across cells without requiring cell radio measurements.

Q4 Can the fact that there is a fully-correlated shadow fading be exploited? Can intra-satellite HO be triggered without using cell radio measurements bypassing the non-negligible UE measurement error?

# 4 Research Methodology

A classical research approach is adopted to accomplish the objectives stated above. The working methodology can be summarized as follows:

1. **Identification of the problem**. First, the 5G NR over LEO satellites use cases are analyzed to understand the requirements in terms of radio mobility, communication latency and radio propagation characteristics. Second, the available literature is examined to identify the limitations of the 5G NR specifications and to explore the state-of-the-art HO solutions over cellular networks and over satellite systems.

2. **Formulation of hypothesis and research questions**. Once the problems and limitations are identified, the respective hypothesis is formulated. Research questions are formulated to have a clearly-defined research problem and know exactly how to contribute to resolve the problem.

3. **Solutions development**. After defining hypothesis and research questions, feasible and applicable solutions are discussed and proposed to validate the hypothesis and find answers for the research questions. As part of this step, it is important to carry out preliminary and simple analysis to determine the expected outcomes.

4. **Determination of the KPIs**. To evaluate the proposed solutions, several KPIs are determined. These include widely accepted mobility performance metrics and new ones designed to understand the benefits and limitations of the proposals.

5. **Evaluation of the proposed solutions**. The proposed solutions are evaluated by means of system-level Monte Carlo simulations [24]. The proposals are implemented in the Nokia proprietary system-level simulator. This tool offers a high-level of realistic analysis, which would be very difficult to achieve through theoretical approaches. The simulator is built over mathematical models to reproduce the stochastic and complex behaviour of wireless communication networks and accounts for the main elements impacting the mobility performance, e.g. 5G radio resource management techniques, 3GPP-compliant channel propagation models, UE radio frequency (RF) receiver chain, etc. A sufficient number of samples is collected during the Monte Carlo simulations to obtain statistically reliable results. This implies multiple realizations of the same simulated scenario where each realization varies the pseudo-random seed to randomize, for instance, the UE location and the impact of different sources of error. Once the multiple simulations are completed, the results are combined together to provide an estimate.

6. **Performance analysis**. The simulation results are compared against the formulated hypothesis and preliminary analysis. Typically, the analysis of the performance based on the KPIs help to identify further requirements of the scenario as well as limitations of the proposed solutions not previously considered. This phase involves repeatedly redefinitions and fine-tuning of the proposed solutions.

7. **Dissemination of the main findings**. The validated solutions and the respective performance are presented in form of six scientific publications to the research community. The acquired knowledge is also disseminate in project-related meetings at Wireless Communication Networks (WCN) section and Nokia. The performance results has impacted Nokia contributions to 3GPP for NTN. Parts of the novel work are disclosed via patent applications.

# 5 Contributions

The main contributions of the PhD study are summarized as follows:

C1: **Development of a time-correlated radio propagation model of LEO-to-Ground links for mobility investigations.**

This thesis proposes a two-stage framework to model the large-scale radio propagation parameters of LEO-to-Ground links. The model realistically captures the time variations of the radio propagation conditions caused by the movement of LEO satellites. In a first stage, a Markov-based approach defines the channel states, i.e. LOS and NLOS, and its transitions as a function of the elevation angle for the rise and fall of the LEO satellite with respect to a stationary UE on the ground. Path loss and shadow fading are then estimated based on geometrical parameters that define the environment surrounding the UE. The model is built on the basis of classical well-known channel models and validated against ray-tracing simulations in rural and urban scenarios.

C2: **Identification of the key challenges to ensure service continuity in 5G LEO satellite networks.**

This thesis provides a comprehensive study of the key aspects limiting the UE mobility performance when using 5G NR HO procedures in 5G LEO satellite networks. Characteristics of the scenario such as high-speed satellite movement, inter-cell interference, low RSRP variability and UE measurement error are the main factors impacting the mobility performance. The analysis also underlines that the upper bound performance of LEO satellites deploying EMC feature an inherent high HO rate and a low serving cell radio link quality.

C3: **Mobility performance evaluation through system-level simulations of the 5G NR HO procedures in 5G LEO satellite networks.**

The thesis analyzes the 5G NR mobility performance in a EMC-based LEO satellite network of two NR HO procedures available in Release 16 specifications: the conventional HO procedure and the conditional HO (CHO) procedure. The conventional break-before-make UE-assisted NW-controlled HO, also referred in this thesis as baseline HO (BHO), and the CHO are assessed using different HO configurations to identify the best achievable performance and understand the limitations of using HO procedures based on cell radio measurements.

C4: **Proposal of a HO solution that combines cell radio measurements and cell distance measurements to reduce undesired signalling and measurement reporting.**

This thesis proposes a HO procedure that exploits the location information of UEs and the satellite beams radio coverage. This solution modifies the NR measurement events by introducing an offset that changes its value depending on the distance between the UE and the cells centre on the ground. System-level simulation results are provided to show the UE mobility performance. The procedure has been contributed as a potential solution in 3GPP.

C5: **Proposal of a HO solution that delivers enhanced UE mobility performance without using cell radio measurements.**

This thesis proposes a fully NW-controlled HO procedure designed for intra-satellite mobility. It exploits the assumption of fully-correlated path loss and shadow fading among adjacent cells belonging to the same satellite. Based on that hypothesis and using satellite beam antenna gain predictions, the UE is able to handover across cells without using cell radio measurements and bypassing the inherent non-negligible UE measurement error.

C6: **Sensitivity Analysis of error sources that can potentially impact the UE mobility performance.**

This thesis presents a sensitivity analysis to assess the impact of several sources of error on the HO solutions proposed in contributions C4 and C5. 3GPP does not cover errors on the satellite side that can impact the HO performance. Thus, the study covers as source of error the radiated antenna gain, the precision of the satellite beam antenna to steer its beams towards a given location on the ground and the accuracy of the UE to determine its location.

The thesis is composed of a collection of papers. The main findings and contributions are included in the following publications:

Paper A: Enric Juan, Mads Lauridsen, Jeroen Wigard, and Preben Mogensen, "A Time-correlated Channel State Model for 5G New Radio Mobility Studies in LEO Satellite Networks", *IEEE 93rd Vehicular Technology Conference (VTC2021-Spring)*, April 2021, pp. 1–5.

Paper B: Enric Juan, Ignacio Rodriguez, Mads Lauridsen, Jeroen Wigard, and Preben Mogensen, "Time-correlated Geometrical Radio Propagation Model for LEO-to-Ground Satellite Systems", *IEEE 94th Vehicular Technology Conference (VTC2021-Fall)*, September 2021, pp. 1–5.

Paper C: Enric Juan, Mads Lauridsen, Jeroen Wigard and Preben Mogensen, "5G New Radio Mobility Performance in LEO-based

Non-Terrestrial Networks", *IEEE Globecom Workshops (GC Wkshps)*, December 2020, pp. 1-6.

Paper D: Enric Juan, Mads Lauridsen, Jeroen Wigard, and Preben Mogensen, "Performance Evaluation of the 5G NR Conditional Handover in LEO-based Non-Terrestrial Networks", *IEEE 23rd Wireless Communications and Networking Conference (WCNC)*, April 2022, pp. 2488–2493.

Paper E: Enric Juan, Mads Lauridsen, Jeroen Wigard, and Preben Mogensen, "Location-Based Handover Triggering for Low-Earth Orbit Satellite Networks", *IEEE 95th Vehicular Technology Conference (VTC2022-Spring)*, June 2022, pp. 1-6.

Paper F: Enric Juan, Mads Lauridsen, Jeroen Wigard, and Preben Mogensen, "Handover Solutions for 5G Low-Earth Orbit Satellite Networks", *IEEE Access*, 2022.

Paper A-F represent the core publications of this thesis. Furthermore, three patent applications have been filed:

Patent Application 1: "UE-specific autonomous hysteresis adjustment for NTN". Target: 3GPP Release 18.

Patent Application 2: "New measurement triggers for networks with moving network nodes". Target: 3GPP Release 17. First contributed to 3GPP in [25].

Patent Application 3: "Antenna gain-based HO procedure for NTN". Target: 3GPP Release 17. First contributed to 3GPP in [26].

A large part of this PhD study was dedicated to system-level simulator development. Different simulation tools were used depending on the nature of the problem but the main body of simulation results were obtained with a Nokia proprietary system-level simulation tool. The objected-oriented C++ based simulator offers a realistic analysis of the mobility procedures because it models the NR physical (PHY) and medium-access control (MAC) layers according to 3GPP specifications. The simulator has been calibrated against system-level simulations from several 3GPP members and it is being used in 3GPP standardization and scientific publications, e.g. [27] and [28]. Part VI provides further details of the system-level simulation methodology. As a result of the time invested in understanding the key functionalities of the tool, developing, debugging, testing and documenting new implementations, the main contributions to the system-level tool are summarized as follows:

SLS1: **Extension to operate with NTN systems.** At the starting point of this PhD the system-level simulator was designed to support terrestrial deployments without even considering the curvature of the Earth. A new whole functional framework is implemented to enable NTN systems with on-board gNB capabilities revolving around the Earth. Long propagation delays, movement of the gNBs and adjustable pointing of the cell antennas were included to accommodate the NTN scenario characteristics. In addition, new UE mobility models were developed for users on a spherical scenario.

SLS2: **NTN channel model.** Built on the previous point, a specific channel model for NTN reported by the 3GPP is implemented in the simulator. The model, which is calibrated against measurements reported by other 3GPP members, supports satellite operations in outdoor conditions including atmospheric, scintillation and cloud attenuation. Several user environments are included and it models large-scale radio propagation parameters as well as fast fading. This model was used to contribute to Paper C. Part VI describes the calibration process and offers a comparison against results from other 3GPP members.

SLS3: **Two-stages framework to model LEO-to-Ground links.** As an alternative to the 3GPP channel model (used for Paper C), the model reported in Papers A-B is implemented in the system-level simulator for mobility studies. The model, that supports the radio propagation changes caused by the satellites movement, is implemented following a two-stages approach. First, a LOS model defines the LOS/NLOS states as a function of the satellite elevation angle for specific satellite-user pairs. Second, path loss and correlated shadow fading are added accordingly. The model is used for Papers D-F. Part VI contains calibration results (as compared with the 3GPP model) and testing results obtained with the simulator in terms of LOS probability for rural and urban environments.

SLS4: **Modelling of the CHO procedure.** For the studies conducted in Papers D, E and F, the CHO procedure is modelled modifying the existing implementation of the conventional HO.

SLS5: **Development of NTN-specific metrics.** To support the studies, new metrics were enabled to correctly evaluate the UE mobility performance. Among others, the metrics covered: undesired HO events, distance at HO completion time between user position and serving cell ground centre, distinction between intra-satellite mobility events and inter-satellite mobility events as well as numerous logs for debugging and testing purposes.

SLS6: **HO procedure based on location criteria.** HO solutions proposed in Papers E and F exploit the satellite movement by using UE location and satellite-specific information. The HO implementation is modified to consider and monitor UE location, satellite location and cells centre location. For Paper E, the UE implementation includes a functionality to periodically acquire its own location and measure the distance changes with regard to cells centre. The HO triggering conditions are modified to combine cell radio and cell distance measurements under three configuration schemes.

SLS7: **Intra-satellite fully NW-controlled HO procedure.** For Paper F, a new HO framework is implemented to predict the satellite beam antenna gains from serving cell and target cells. The implementation considers the periodic signalling of the UE location to the NW and the HO decision based on these predictions that consider the known satellite trajectory. Furthermore, the HO decision algorithm implementation aims to avoid UHO events.

SLS8: **Additional sources of error.** For Paper F, several error sources were added to the simulator to conduct a sensitivity study and validate the performance of the proposed HO algorithms. The radiation of the satellite beam antenna, the UE location and the satellite beam antenna pointing were modified to introduce normally distributed errors.

Finally, during this thesis there were work activities not directly reflected in the aforementioned contributions. The following article has been accepted for publication as part of a collaborative work not related to the thesis topic:

Collaboration A: Alejandro Perez-Conesa, Wahyudin P. Syam, David Scott, Ignacio Rodriguez, Melisa Maria Lopez Lechuga, Enric Juan Martinez and Rigas T. Ioannidis, "Low RF-based Navigation for Emergencies in Difficult Environments", The Institute of Navigation (ION) GNSS+ 2022.

An overview of all the produced contributions during this thesis categorized per research topics and thesis parts is shown in Fig. I.5.

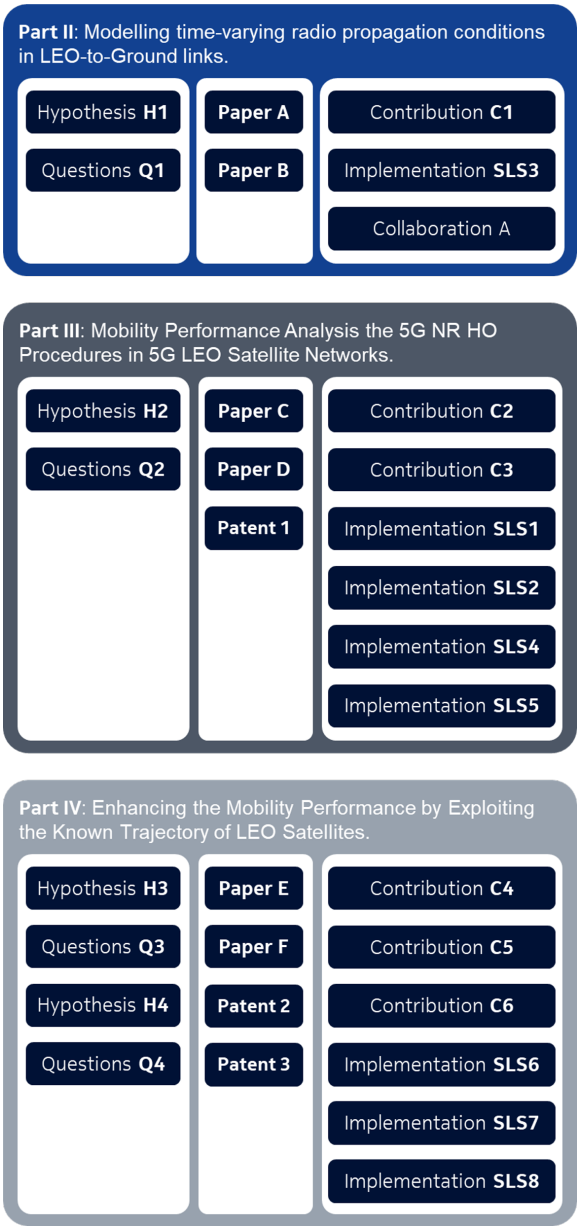


**Fig. I.5:** Overview of the contributions generated during this thesis.

# 6 Thesis Outline

The thesis is written as a collection of papers and it is structured in six parts. The current part presents an introduction of the thesis topic and the conducted work. The main contributions are included in Part II, III, and IV. Papers A and B are given in Part II, while Papers C and D and Paper E and F are included in Part III and Part IV, respectively. Each of these parts contain a summary of the problem addressed, the main findings and the papers supporting them. Conclusions are given in Part V, while Part VI includes an appendix about the system-level simulation methodology.

- **Part I: Introduction**. This part introduces the PhD topic, the motivation behind the research and summarizes the main contributions.
- **Part II: Modelling time-varying radio propagation conditions in LEO-to-Ground links**. This part covers a channel model designed to capture the time variations of the signal introduced by the movement of the satellite.
- **Part III: Mobility Performance Analysis the 5G NR HO Procedures in 5G LEO Satellite Networks**. This part includes the mobility performance analysis of the 5G NR HO procedures. System-level simulations of UEs in a rural scenario are given.
- **Part IV: Enhancing the Mobility Performance by Exploiting the Known Trajectory of LEO Satellites**. This part focuses on novel HO solutions that exploit the deterministic movement of the satellites to enhance the mobility performance. The evaluation is supported by system-level simulations in rural and urban environments.
- **Part V: Conclusions**. The conclusions of the studies during the PhD are presented in this part. It summarizes the main findings and discusses the recommendations that could be addressed as future work.
- **Part VI: Appendix**. This part presents several analysis to evaluate the statistical confidence of the system-level simulation results. Furthermore, it offers a description of some of the assumptions taken in this thesis and the calibration process for the NTN channel model and the model in Part II. Some of the calibration and testing results obtained through the simulator development are also included.

# References


[1] R. Katz and F. Callorda, "The economic contribution of broadband, digitization and ICT regulation," *International Telecommunication Union*, 2018. [Online]. Available: https://www.itu.int/en/ITU-D/Regulatory-Market/Documents/FINAL_1d_18-00513_Broadband-and-Digital-Transformation-E.pdf

[2] K. Liolis, A. Geurtz, R. Sperber, D. Schulz, S. Watts, G. Poziopoulou, B. Evans, N. Wang, O. Vidal, B. Tiomela Jou *et al.*, "Use cases and scenarios of 5G integrated satellite-terrestrial networks for enhanced mobile broadband: The SaT5G approach," *International Journal of Satellite Communications and Networking*, 2019.

[3] E. Yaacoub and M.-S. Alouini, "A Key 6G Challenge and Opportunity -— Connecting the Base of the Pyramid: A Survey on Rural Connectivity," *Proceedings of the IEEE*, 2020.

[4] ITU, "2021 Measuring digital development: Facts and figures," ITU Publications, 2021. [Online]. Available: https://www.itu.int/en/ITU-D/Statistics/Pages/facts/default.aspx

[5] E. Oughton and W. Lehr, "Next-G Wireless: Learning from 5G Techno-Economics to Inform Next Generation Wireless Technologies," *Available at SSRN 3898099*, 2021.

[6] J. N. Pelton and S. Madry, *Handbook of Small Satellites: Technology, Design, Manufacture, Applications, Economics and Regulation*. Springer, 2020.

[7] N. Pachler, I. del Portillo, E. F. Crawley, and B. G. Cameron, "An Updated Comparison of Four Low Earth Orbit Satellite Constellation Systems to Provide Global Broadband," in *2021 IEEE International Conference on Communications Workshops (ICC Workshops)*, 2021, pp. 1–7.

[8] "Cisco visual networking index: Forecast and trends, 2017–2022 white paper," Cisco, VNI, Cisco Systems San Jose, CA, Tech. Rep., 2019. [Online]. Available: https://twiki.cern.ch/twiki/pub/HEPIX/TechwatchNetwork/HtwNetworkDocuments/white-paper-c11-741490.pdf

[9] J. M. Steele, W. Markowitz, and C. Lidback, "Telstar Time Synchronization," *IEEE Transactions on Instrumentation and Measurement*, no. 4, pp. 164–170, 1964.

[10] E. Feltrin and E. Weller, "New Frontiers for the Mobile Satellite Interactive Services," in *IEEE Advanced Satellite Multimedia Systems Conference*, 2010.

[11] "Study on Scenarios and Requirements for Next Generation Access Technologies (Release 15)," 3GPP, TR 38.913 V15.0.0, 2018. [Online]. Available: https://www.3gpp.org/ftp/Specs/archive/38_series/38.913/

[12] "Study on New Radio (NR) to support Non-Terrestrial Networks (Release 15)," 3GPP, TR 38.811 V15.2.0, 2019. [Online]. Available: https://www.3gpp.org/ftp/Specs/archive/38_series/38.811/

[13] "Solutions for NR to support Non-Terrestrial Networks (NTN) (Release 16)," 3GPP, TR 38.821 V1.0.0, 2019. [Online]. Available: https://www.3gpp.org/ftp/Specs/archive/38_series/38.821/

[14] "Solutions for NR to support Non-Terrestrial Networks (NTN) (Release 17)," 3GPP, RP-202908, TSG RAN Meeting 90-e, 2020. [Online]. Available: https://www.3gpp.org/ftp/tsg_ran/TSG_RAN/TSGR_90e/Docs

[15] "NR Non-Terrestrial Networks (NTN) enhancements (Release 18)," 3GPP, RP-213690, TSG RAN Meeting 94-e, 2021. [Online]. Available: https://www.3gpp.org/ftp/tsg_ran/TSG_RAN/TSGR_94e/Docs

[16] "Study on channel model for frequencies from 0.5 to 100 GHz (Release 17)," 3GPP, TR 38.901 V17.0.0, 2022. [Online]. Available: https://www.3gpp.org/ftp/Specs/archive/38_series/38.901/

[17] E. Del Re, R. Fantacci, and G. Giambene, "Efficient Dynamic Channel Allocation Techniques with Handover Queuing for Mobile Satellite Networks," *IEEE Journal on Selected Areas in Communications*, 1995.

[18] G. Maral, J. Restrepo, E. del Re, R. Fantacci, and G. Giambene, "Performance Analysis for a Guaranteed Handover Service in an LEO Constellation with a Satellite-Fixed Cell System," *IEEE Transactions on Vehicular Technology*, vol. 47, no. 4, pp. 1200–1214, 1998.

[19] X. Lin, S. Cioni, G. Charbit, N. Chuberre, S. Hellsten, and J.-F. Boutillon, "On the Path to 6G: Embracing the Next Wave of Low Earth Orbit Satellite Access," *IEEE Communications Magazine*, vol. 59, no. 12, pp. 36–42, 2021.

[20] Y. Wu, G. Hu, F. Jin, and J. Zu, "A Satellite Handover Strategy based on the Potential Game in LEO Satellite Networks," *IEEE Access*, vol. 7, pp. 133 641–133 652, 2019.

[21] Y. Li, W. Zhou, and S. Zhou, "Forecast based Handover in an Extensible Multi-Layer LEO Mobile Satellite System," *IEEE Access*, vol. 8, pp. 42 768–42 783, 2020.

[22] S. He, T. Wang, and S. Wang, "Load-aware satellite handover strategy based on multi-agent reinforcement learning," in *GLOBECOM 2020-2020 IEEE Global Communications Conference*. IEEE, 2020, pp. 1–6.

[23] Y. Cao, S.-Y. Lien, and Y.-C. Liang, "Deep Reinforcement Learning for Multi-User Access Control in Non-Terrestrial Networks," *IEEE Transactions on Communications*, vol. 69, no. 3, pp. 1605–1619, 2020.

[24] R. Coates, G. Janacek, and K. Lever, "Monte Carlo Simulation and Random Number Generation," *IEEE Journal on Selected Areas in Communications*, vol. 6, no. 1, pp. 58–66, 1988.

[25] Nokia, Nokia Shanghai Bell, "On connected mode mobility for NTN," 3GPP, R2-2103335, TSG RAN WG2 Meeting #113bis-e, 2021. [Online]. Available: https://www.3gpp.org/ftp/tsg_ran/WG2_RL2/TSGR2_113bis-e/Docs

[26] ——, "Resolving open NTN issues for IDLE mode," 3GPP, R2-2205528, 3GPP TSG-RAN WG2 Meeting #118-e, 2022.

[27] "E-UTRA Mobility Enhancements in Heterogeneous Networks (Release 11)," 3GPP, TR 36.839 V0.7.1, 2012. [Online]. Available: https://www.3gpp.org/ftp/Specs/archive/36_series/36.839/

[28] G. Pocovi, K. I. Pedersen, and P. Mogensen, "Joint Link Adaptation and Scheduling for 5G Ultra-Reliable Low-Latency Communications," *IEEE Access*, vol. 6, pp. 28 912–28 922, 2018.

# Part II

# Modelling Time-Varying Radio Propagation Conditions in LEO-to-Ground Links

# Modelling Time-Varying Radio Propagation Conditions in LEO-to-Ground Links

System-level simulations are fundamental to evaluate, understand, and develop the performance of cellular technologies [1]. To that purpose, modelling the time-varying propagation conditions of radio links is a first mandatory step to realistically evaluate the UE mobility performance. This part of thesis focuses on the development of a new radio propagation model for LEO-to-Ground links, that accounts for radio propagation changes caused by the movement of LEO satellites.

## 1 Motivation

As implementation tests in the real world are expensive and laborious, simulations are crucial to design, test, and optimize procedures for the development of cellular standards. These are especially important to gain insights on the mutual information among all involved elements in the simulated scenario. The simulation process is conducted at two levels: the physical layer (link-level) and the network (system) level. Link-level are used to analyze the link performance of, for example, multiple-input multiple-output systems [2] or channel encoding and decoding [3]. On the other hand, scheduling algorithms [4], interference coordination [5] or mobility management [6] are investigated by means of system-level simulations. Among other areas, the 3GPP has adopted this work methodology for analyzing the mobility performance [7].

In terrestrial deployments, the UE mobility causes RSRP fluctuations because radio conditions between TX and RX change, e.g. path loss increase

due to distance increase, obstacles shadowing the UE or destructive interference of multipath components. These RSRP variations, caused by large-scale and small-scale fading, impacts the UE mobility performance. Thus, a first step towards solid solutions for cellular technologies is a good understanding and modelling of the radio propagation conditions. The 3GPP channel models are one of the most widely employed models because are applicable to a broad variety of scenarios and frequencies. In [8], the 3GPP published the findings on 5G channel modelling and provides channel parameters such as path loss models, path delays and LOS probabilities.

In LEO satellite networks, the UE RSRP variation is also due to satellite movement. Even for stationary UEs, LEO satellites cause changes in the UE's radio propagation conditions. The magnitude of these changes are determined by the UE environment and the satellite trajectory (i.e. orbit). These assumptions lead to the following formulation:

(**H1**) The continuous movement of LEO satellites causes varying radio propagation conditions for LEO-to-Ground links. Static users in rural environments could experience a fast degradation of the service radio link quality due to shadowing of surrounding elements, e.g. buildings and mountains.

Fig. II.1 illustrates how the LOS conditions of a static UE changes according to the satellite movement. At $t = T$, i.e. high satellite elevation angle, the UE experiences LOS conditions. As the satellite moves to lower elevation angles, at $t = T + \Delta_t$ the UE's signal path becomes blocked (i.e. NLOS) due to surrounding clutter. e.g. household. The signal shadowing decreases the UE RSRP, which deteriorates the serving cell radio link quality. Once the serving cell radio link becomes sufficiently weak, the UE needs to handover towards a new cell to maintain the data session active. It is therefore particularly important for mobility studies that radio propagation models consider *when* LOS conditions can change and *how* the UE RSRP varies accordingly.

The topic of modelling radio propagation conditions for LEO-to-Ground links is not new. Some of the most important research works have been available in the literature since the 1980s. A statistical model for mobile satellite-to-Ground channels was first introduced by C. Loo in [9]. The model assumed that the amplitude of the signal in LOS under foliage attenuation follows a log-normal distribution while the multipath component has a Rayleigh distribution. In [10], the authors proposed the Corazza model, which combines Rice and log-normal statistics to model LOS and shadowing states. Ever since, many research works have proposed the use of Markov chains based on different states, to capture the changes in the radio propagation conditions in different environments. The basic idea is that every state of the Markov

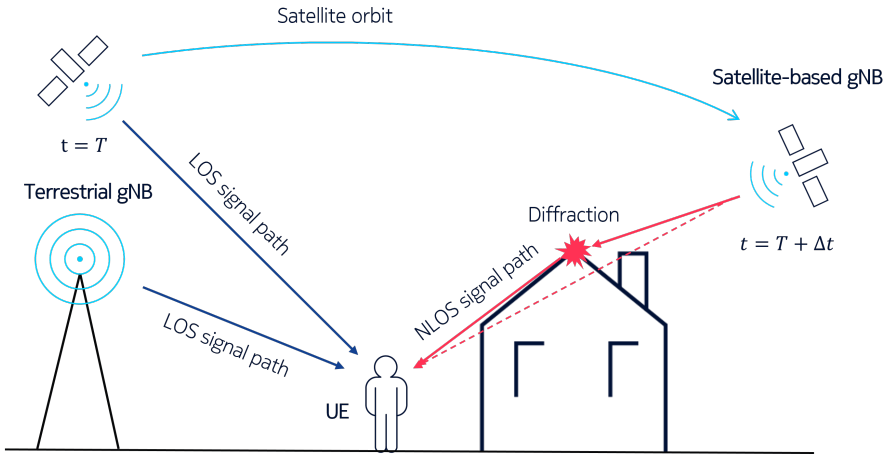


**Fig. II.1:** LEO-to-Ground links: UE's radio propagation conditions change due to the movement of LEO satellites.

chain models a visibility condition to which the signal is subjected; the user moves from one state to the next one based on a set of transition probabilities. E. Lutz *et al.* presented in [11] a two-state Markov model distinguishing between intervals with LOS conditions, i.e. *good* channel state, and time intervals in shadowed conditions, i.e. *bad* channel state. The model assumed that the user remains in a state for a certain time before re-evaluating and deciding to transit towards the other state or stay in the same state. In [12], F. Fontán *et al.* proposed a three-state Markov model to produce time-series that describe the slow and fast fluctuations of the RSRP. The three states account for LOS conditions, moderate shadowing and deep shadowing conditions. The parameters of the model were extracted from measurement campaigns with planes, helicopters and geostationary satellites in different environments and elevation angles. Other works have also proposed four-state, five-state and multi-state Markov approaches as captured in [13]. Recent works such as [14] and [15], presented propagation models to characterize the Satellite-to-Ground path loss and its corresponding LOS probability. The latter model was tuned based on signal measurements from GNSS receivers, while the former propagation model used ray-tracing simulations in dense urban and suburban scenarios.

Some of the most relevant studies on the topic of Satellite-to-Ground links are driven by the international telecommunications union (ITU) and the 3GPP. Based on some of the aforementioned works, the ITU reported in the Recommendation P.681 [16] a two-state Markov model to produce time-series of channel states, i.e. *good* and *bad* states, where the duration of each state follows a log-normal distribution and the RSRP follows a Loo distribution.

The 3GPP reported in the technical report [17] a channel model for NTN, which targets GEO, MEO, LEO systems and HAPS for users in rural, urban and dense urban environments. However, the mobility of NTN systems is not addressed since the model can only be used for drop-based simulations (i.e. simulations that only consider a single time sample where the NTN system is at a given elevation angle). The LOS probability is characterized as a function of the satellite elevation angle and the UE environment. After determining the LOS/NLOS state, path loss, shadow fading, and fast fading are applied accordingly.

To the best of our knowledge, none of the previous works are valid for system-level mobility studies in 5G LEO satellite networks because these works do not consider the time correlations of LEO-to-Ground links. Most of the models allow to determine the radio propagation conditions only at a given particular satellite elevation angle, without considering previous and coming radio conditions caused by the satellite movement. As an example of this, the 3GPP model for NTN is not valid because the radio propagation parameters must be re-evaluated at each elevation angle experienced by satellite and UE during the simulation. This methodology results in frequent and inconsistent changes of the LOS/NLOS conditions and, therefore, the RSRP levels.

The following aims to describe the time correlations in a LEO-to-Ground link as well as to motivate why these should be considered in a propagation model for mobility studies. Fig. II.2 shows a time-trace of the clutter loss as function of the experienced satellite elevation angle of a UE. The trace, which is obtained by means of ray-tracing simulations, is characterized by the following:

i) At 50° elevation angle, the visibility conditions change from NLOS to LOS. Once the UE is in LOS, it is likely that stays in LOS as the satellite moves to higher elevation angles.

ii) The clutter loss starts decreasing prior to 50° elevation angle. For elevation angles lower than 50°, clutter loss and shadow fading vary according to a NLOS-to-LOS transition ahead in time.

Based on the above observations, path loss, shadow fading, and LOS conditions should change considering past and future radio propagation events. Thus, a model should capture these time-correlations to realistically predict the RSRP changes.

This part of the thesis explores the design of a radio propagation model that captures the time-correlated changes of the radio conditions caused by the satellite movement. The main goal was to understand the dynamics of radio channels in LEO-to-Ground links and develop a model valid for researching radio mobility aspects in rural and urban scenarios. First, the

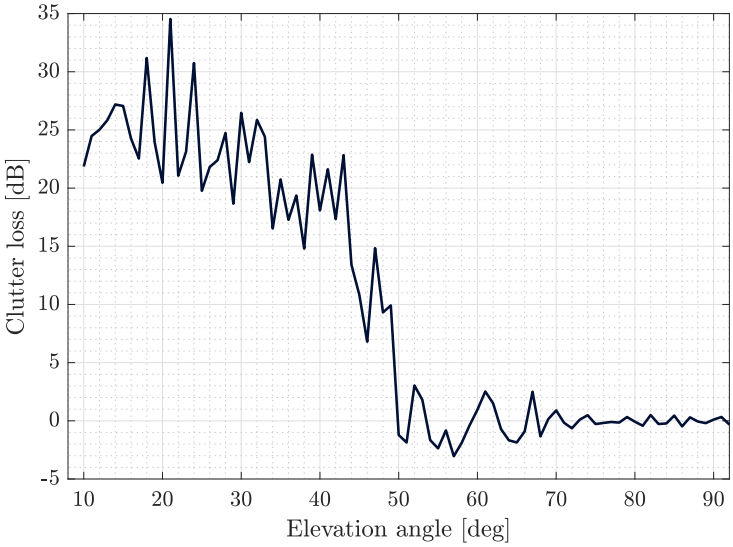


**Fig. II.2:** Simulated clutter loss trace as a function of satellite elevation angle.

model was implemented in MATLAB, parameterized and calibrated using data from ray-tracing simulations. Then, the designed model was implemented in the system-level simulator that was used in later studies of the PhD thesis.

# 2 Objectives

To validate the formulated hypothesis H1, the end goal is to design a radio propagation model suitable for mobility investigations that realistically captures the time-correlated variations of path loss, shadow fading and LOS conditions. Furthermore, the model should be implemented and validated in the system-level simulator to be used in later PhD studies. To that purpose, the following tasks are required:

A. Design a statistical Markov-based LOS model that captures the time-correlated channel state changes caused by the movement of LEO satellites. The model should be built on the ITU basis and valid for stationary UEs in rural and urban environments.

B. Conduct ray-tracing simulations of LEO satellites flying over stationary UEs in rural and urban environments to collect data of the channel states and the RSRP. The simulator provides UE's visibility conditions and UE RSRP based on the radio waves path and the geometry of the scenario.

C. Use the LOS traces from ray-tracing simulations to fit the LOS model and evaluate whether the model is able to produce realistic results.

D. Use the RSRP traces from ray-tracing simulations to study the clutter loss and shadow fading variations focusing on the transitions from NLOS to LOS, and viceversa.

# 3 Included Articles

The work related to this part is collected in the following papers:

**Paper A. A Time-correlated Channel State Model for 5G New Radio Mobility Studies in LEO Satellite Networks**

This paper addresses the issue of modelling channel states for LEO-to-Ground links. The article proposes a new model based on a two-state Markov chain where the states corresponds to LOS and NLOS states. The stochastic process models over time whether a LEO-to-Ground link maintains its current channel state or transitions from one state to the other. The state transitions depend on probability distributions that change as a function of the satellite elevation angle and UE environment. Ray-tracing simulations are conducted to collect time-traces of the channel states of LEO satellites flying over static UEs in suburban and dense urban scenarios. The traces are used to calculate the transition probabilities of the Markov chain. The model includes the transition probabilities from NLOS to LOS and from LOS to NLOS, which emulates the rise and fall of a LEO satellite that ranges from 10° to 170° elevation angle. The performance of the model is evaluated by analysing the LOS probabilities as a function of the satellite elevation angle and the distribution of time periods in LOS. The LOS/NLOS time-sequences generated using the proposed model are compared against the traces from the ray-tracing simulations and the traces obtained using the 3GPP model for NTN deployments.

**Paper B. Time-correlated Geometrical Radio Propagation Model for LEO-to-Ground Satellite Systems**

This paper completes the modelling started in Paper A. The goal of this paper is to define a radio propagation model that can be used for system-level mobility studies in LEO satellite networks. To that end, this work proposes a radio propagation model that realistically predicts the time-variations of the path loss and the shadow fading. The UE RSRP varies as a function of the given *switching angles*, i.e. the elevation angles where the LOS/NLOS transitions occur, which are obtained using the Markov chain proposed in

Paper A. The model is built on the basis of the knife-edge diffraction model and the Ikegami and Walfisch models, designed for terrestrial deployments. Furthermore, the radio propagation losses are calculated considering a set of geometric parameters that define the surrounding environment of the UE. The small-scale fading is out of the scope of this work because it is assumed that fast fading variations of the signal are filter out by the UE. Ray-tracing simulations are conducted for UEs in a suburban scenario. The simulated time-traces of the RSRP are analyzed, focusing on the variations of the clutter loss for those UEs in NLOS conditions. The ray-tracing simulations are also used to validate the signal traces generated with the proposed model, which accuracy is quantified in terms of root mean square error.

# 4 Main Findings

**First stage: predicting LOS and NLOS visibility conditions**

The two-state Markov-based model reported in Paper A accomplishes to predict realistically channel state traces for UEs in suburban and dense urban scenarios. The validation of the model conducted in the paper shows that the traces generated by the model are able to mimic the signal behaviour observed in the ray-tracing simulations. Therefore, the model captures the time-correlations among channel states of the LEO-to-Ground links when LEO satellites trace a full pass from 10° to 170° elevation angle. The low-complexity and effectiveness of the model allows to use it as a convenient extension of the snapshot-based simulation-oriented 3GPP channel model for NTN.

The LOS probabilities are modelled as a function of the satellite elevation angle and fitted with ray-tracing simulations. To validate the model, we calculate the LOS probabilities from LOS traces generated with the model. These probabilities show mismatches as compared with the probabilities reported by the 3GPP for NTN in [17]. These differences are more evident for the dense urban case where the LOS probabilities at low elevation angles are 20-30 % below the values found in the 3GPP model. This is likely due to the following aspects. First, the LOS probabilities from the 3GPP model are based on ray-tracing simulations with HAPS at fixed heights. Second, these ray-tracing simulations were conducted with a 15 m spatial resolution for the suburban case while the dense urban case considered a resolution of 20 m. The combination of these two aspects resulted in a limited elevation angle diversity and, therefore, sample size. To overcome this limitation, the ray-tracing simulations conducted for this work used a spatial resolution of 2 m and considered a LEO satellite at 600 km tracing a full pass, i.e. from 10° to 170°, sampled every 1° elevation angle.

**Second stage: predicting time-correlated path loss and shadow fading**

The work done as part of Paper B proposed a radio propagation model based on geometric parameters that is able to realistically predict path loss and shadow fading according to the satellite elevation angle, the channel state and the distance to the *switching angles*, i.e. elevation angles where visibility conditions change.

The prediction of the clutter loss is composed by two elements: i) a variable rooftop-to-street diffraction-based contribution and ii) a constant reflection-based contribution. This modelling criteria is chosen after analyzing the ray-tracing simulation data. For UEs that transition from NLOS to LOS, the following was observed: for low elevation angles, the clutter loss remains constant, i.e. 15-18 dB. However, as satellite elevation angle increases, the clutter loss decreases steadily from 15-20 ° prior to the *switching angle*. The clutter loss reaches 0 dB when the satellite reaches the *switching angle*. This effect is physically consistent considering that the reflected ray is dominant for low elevation angles and the rooftop-to-street diffraction increases its relevance as the satellite rises moving to LOS, where the UE is no longer obstructed. The clutter loss traces generated by the proposed model show close conformity with traces from ray-tracing simulations. The traces with *switching angles* ranging from 20° to 80° present a root mean square error from 0.9 to 1.5 dB, when the model and the ray-tracing simulations are compared.

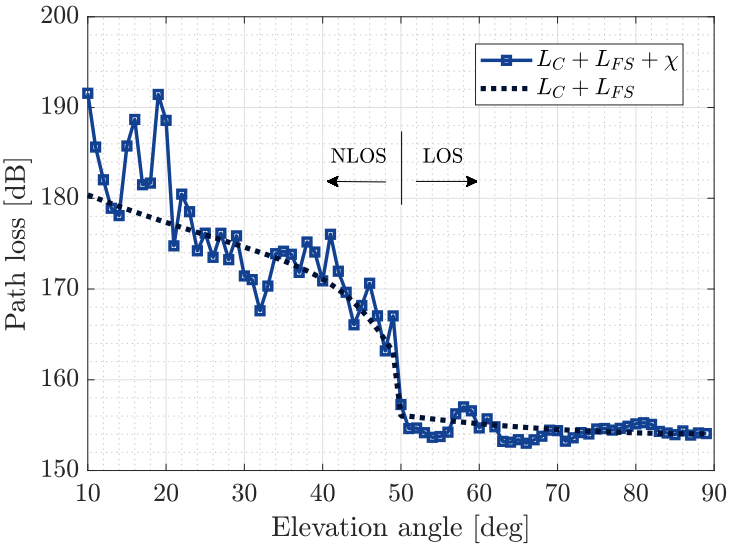


**Fig. II.3:** Overall path loss trace including free-space path loss ($L_{FS}$), clutter loss ($L_C$) and shadow fading ($\chi$) for a user transitioning from non line-of-sight to line-of-sight at 50° satellite elevation angle. (Source: Paper B, [18, Fig. 5])

The combined work in Papers A and B present a two-stages propagation model that predicts realistically the path loss, the shadow fading and the LOS conditions of LEO-to-Ground links. Fig. II.3 shows a path loss trace generated by the complete model. First, the model in Paper A defines the channel states and the *switching angles* (i.e. 50°). Second, the mean path loss is calculated split in: i) free-space path loss ($L_{FS}$) and ii) clutter loss ($L_C$), when applicable. Finally, correlated shadow fading ($\chi$) is computed and applied accordingly.

The result of this part of the thesis is a radio propagation model that can be conveniently used for system-level simulation studies targeting mobility aspects in 5G LEO satellite networks.

# References


[1] J. C. Ikuno, M. Wrulich, and M. Rupp, "System Level Simulation of LTE Networks," in *2010 IEEE 71st Vehicular Technology Conference*. IEEE, 2010, pp. 1–5.

[2] H. Yang, "A Road to Future Broadband Wireless Access: MIMO-OFDM-based Air Interface," *IEEE communications Magazine*, vol. 43, no. 1, pp. 53–60, 2005.

[3] J. C. Ikuno, M. Wrulich, and M. Rupp, "Performance and modeling of LTE H-ARQ," in *Proc. International ITG Workshop on Smart Antennas (WSA 2009), Berlin, Germany*, 2009.

[4] G. Pocovi, K. I. Pedersen, and P. Mogensen, "Joint Link Adaptation and Scheduling for 5G Ultra-Reliable Low-Latency Communications," *Ieee Access*, vol. 6, pp. 28 912–28 922, 2018.

[5] B. Soret, H. Wang, K. I. Pedersen, and C. Rosa, "Multicell Cooperation for LTE-Advanced Heterogeneous Network Scenarios," *IEEE Wireless Communications*, vol. 20, no. 1, pp. 27–34, 2013.

[6] K. I. Pedersen, P. H. Michaelsen, C. Rosa, and S. Barbera, "Mobility Enhancements for LTE-Advanced Multilayer Networks with Inter-Site Carrier Aggregation," *IEEE Communications Magazine*, vol. 51, no. 5, pp. 64–71, 2013.

[7] "E-UTRA Mobility Enhancements in Heterogeneous Networks (Release 11)," 3GPP, TR 36.839 V0.7.1, 2012. [Online]. Available: https://www.3gpp.org/ftp/Specs/archive/36_series/36.839/

[8] "Study on channel model for frequencies from 0.5 to 100 GHz (Release 17)," 3GPP, TR 38.901 V17.0.0, 2022. [Online]. Available: https://www.3gpp.org/ftp/Specs/archive/38_series/38.901/

[9] C. Loo, "A Statistical Model for a Land Mobile Satellite Link," *IEEE transactions on vehicular technology*, vol. 34, no. 3, pp. 122–127, 1985.

[10] G. E. Corazza and F. Vatalaro, "A Statistical Model for Land Mobile Satellite Channels and Its Application to Nongeostationary Orbit Systems," *IEEE Transactions on vehicular technology*, vol. 43, no. 3, pp. 738–742, 1994.

[11] E. Lutz, D. Cygan, M. Dippold, F. Dolainsky, and W. Papke, "The Land Mobile Satellite Communication Channel-Recording, Statistics, and Channel Model," *IEEE transactions on vehicular technology*, vol. 40, no. 2, pp. 375–386, 1991.

[12] F. P. Fontan, M. Vázquez-Castro, C. E. Cabado, J. P. Garcia, and E. Kubista, "Statistical Modeling of the LMS Channel," *IEEE Transactions on vehicular technology*, vol. 50, no. 6, pp. 1549–1567, 2001.

[13] M. Tropea and F. De Rango, "A Comprehensive Review of Channel Modeling for Land Mobile Satellite Communications," *Electronics*, vol. 11, no. 5, p. 820, 2022.

[14] F. Hsieh and M. Rybakowski, "Propagation Model for High Altitude Platform Systems Based on Ray Tracing Simulation," in *2019 13th European Conference on Antennas and Propagation (EuCAP)*. IEEE, 2019, pp. 1–5.

[15] A. Al-Hourani and I. Guvenc, "On Modeling Satellite-to-Ground Path-Loss in Urban Environments," *IEEE Communications Letters*, vol. 25, no. 3, pp. 696–700, 2020.

[16] "Propagation data required for the design systems in the land mobile-satellite service," ITU, Rec. ITU-R P.681-11, 2019. [Online]. Available: https://www.itu.int/rec/R-REC-P.681/en

[17] "Study on New Radio (NR) to support Non-Terrestrial Networks (Release 15)," 3GPP, TR 38.811 V15.2.0, 2019. [Online]. Available: https://www.3gpp.org/ftp/Specs/archive/38_series/38.811/

[18] E. Juan, I. Rodriguez, M. Lauridsen, J. Wigard, and P. Mogensen, "Time-correlated Geometrical Radio Propagation Model for LEO-to-Ground Satellite Systems," in *2021 IEEE 94th Vehicular Technology Conference (VTC2021-Fall)*, 2021, pp. 1–5.

# Paper A

## A Time-correlated Channel State Model for 5G New Radio Mobility Studies in LEO Satellite Networks

Enric Juan, Mads Lauridsen, Jeroen Wigard, Preben Mogensen

The paper has been published in the
*IEEE 94th Vehicular Technology Conference (VTC2021-Spring), 2021.*

*The layout has been revised.*

# Abstract

*Low Earth orbit (LEO) satellite networks will play a major role in future broadband communications. To study LEO satellite mobility performance, and guarantee reliable service, accurate channel characterization is necessary. Current models, such as the ones reported by 3GPP and ITU, define channel parameters as a function of elevation angle, frequency and deployment scenario. However, key parameters including the line-of-sight (LOS) probability and the shadow fading do not describe any time component or correlation and, therefore, the movement of the satellite is not captured. This fact might result in unrealistic changes of the LOS/NLOS states hampering the radio mobility studies for 5G-based LEO satellite networks. In this paper, we present a Markov-based channel state model that takes into consideration the time correlations of the LOS variations along the satellite's orbit. The proposed model is based on ray-tracing measurements of suburban and dense urban scenarios and it can accurately reflect the behaviour of the channel state variations of those scenarios, essentially leading to a realistic number of state changes per satellite pass.*


# 1 Introduction

LEO satellite networks are called upon to play an essential role in the development of cellular networks by supporting 5G NR communications [1] and paving the way towards the 6th generation [2]. Current networks lack adequate global coverage and responsiveness to natural disasters. To address these issues, the potential of constellations of satellites in LEO orbits to provide seamless and ubiquitous connectivity has been acknowledged [3]. Proprietary projects such as SpaceX's Starlink, Amazon's Kuiper and OneWeb are state-of-the-art examples of a new space market determined to bring internet to the most distant corners of the Earth. On the other hand, 3GPP standardization activities for Rel-17 are focusing on the development of 5G NR based NTNs [4]. This concept envisions a fully fledged architecture where terrestrial cellular networks are complemented by HAPS and satellites to bring broadband services in unserved or disaster-affected areas.

The use of LEO orbits, i.e. at altitudes of 600 km to 1200 km, implies satellite systems with small ground coverage, which move rapidly (7.5 km/s) with respect to the Earth's surface. Such high mobility poses new and major challenges to the conventional radio mobility mechanisms [5]. In order to address these challenges, a solid understanding of the radio channel propagation is required.

Therefore, the characterization of the propagation channel will be key for the study, design and planning of broadband satellite networks. In terrestrial networks, as users move in a certain area, shadowing and multipath conditions might change abruptly causing large-scale variations in the received

signal. Channel modelling is used to generate time-series of the slow and fast variations of the signal. In a LEO-based network not only users' mobility might cause large-scale fading. Movement of LEO systems will also introduce signal disturbances in the propagation channel between the satellite and the users on the ground, in terms of LOS/NLOS state changes. Thus, it is paramount to realistically model such changes caused by the mobility of satellites and users.

Different approaches for state modelling are available in the literature. As stated by authors in [6], land mobile-satellite channel models produce time series of channel states using Markov concepts. Changes in the propagation states were described by a first-order Markov chain in [7], discriminating between *good* (i.e., LOS/light shadowing) and *bad* (i.e., NLOS/heavy shadowing) states. Further on, research in [8] proposed a third state by splitting the NLOS state into *shadowed* and *blocked* to improve the accuracy of the prediction. However, first-order Markov models may result in unrealistic durations of the states as exposed by [9]. Following a similar approach as in [9], the ITU in its Recommendation P.681 [10] adopted a semi-Markov two-state model where the duration of each state follows a log-normal distribution.

The majority of models available in the aforementioned literature were mostly designed for geostationary satellites and they consider only mobility on the user's end. Even when other satellite systems were addressed, the research focused on models where the mobility of the LEO satellite was neglected as in the study item reported by 3GPP in [1]. In the latter, the model developed for NTNs was conceived for drop-based simulations, i.e. considering a single time sample where the satellite is at a given angle and, therefore, does not describe how long a user might be in LOS state along a satellite pass.

Current state-of-the-art models do not allow to characterize LEO satellite propagation channels since they do not describe any time or spatial correlation component across channel states. In this paper, we introduce an enhanced LOS model for LEO satellites, which is built on ITU and 3GPP bases and it is able to comprise time correlation components to capture realistically the motion of the LEO systems. This model is based on a 2-state Markov chain where the transition matrix is composed by probabilities calculated from ray-tracing simulations for suburban and dense urban scenarios.

The remainder of the paper is structured as follows: Section 2 summarizes the channel models from ITU and 3GPP. A theoretical description of the model proposed in this work is introduced in Section 3, while in Section 4 we describe the methodology used to perform the ray-tracing simulation campaign. Finally, Section 5 discusses the impact of the model and future work and conclusions are drawn in Section 6 and 7, respectively.

# 2 ITU-R Recommendation and 3GPP channel model for NTN

In the field of radio engineering, recommendations from the ITU are defined by the ITU radio communication sector (ITU-R) and work as an international standard. Most recent works and measurements on satellite channel models are covered by the ITU-R in the recommendation P.681-11 [10]. There, the ITU-R comprises a statistical model to design systems for land mobile-satellite services in mixed propagation conditions. This model describes the long-term variations of the received RF signal by decomposing the channel states into *good* and *bad* states. A two-state semi-Markov chain describes these states where the duration of each of them follows a log-normal distribution. Furthermore, the fading within each state is modeled by a set of Loo laws. Even though the model is able to generate realistic time series of the channel, the Markov chain is only used to simulate the time-variations introduced by the mobility of the user, while considering a static satellite at a given elevation angle.

Aside from ITU recommendations, 3GPP initiated a new channel model for NTNs reported in the study item [4]. This work started with Rel-15 and it targets satellite and HAPS operations for several environments. The objective was to support two frequency bands in particular (i.e., S and Ka bands) and to accommodate UE mobility speed up to 1000 km/h. This model intends to be valid for all non-terrestrial platforms but only drop-based simulations were considered. The model defines the LOS probability as a function of elevation angle and deployment scenario. Once the LOS/NLOS state is determined, large and small-scale parameters are selected accordingly. This means that the model only allows to analyze the channel characteristics at a particular satellite's location without establishing any time correlation between the current position and the next one. In other words, if we use the 3GPP model to study the radio mobility performance, we will have to reevaluate the channel parameters for each elevation angle. This fact results in frequent, and unrealistic, changes of the channel state and, therefore, might lead to inconsistent results (see Section 5).

# 3 Channel state model for mobile LEO satellite systems

As mentioned in Section 1, land mobile-satellite channels have been typically modeled by Markov processes. However, these processes were designed to capture only the channel state variations introduced by the mobility of the receiver on the ground. In this Section, we present a Markov-based channel

state model intended for mobility investigations which considers those variations stemmed from the motion of the LEO satellites. Hence, the channel changes will not only depend on the elevation angle but also in the previous state and the rising or setting trajectory of the satellite. We focus on extending the 3GPP model since our intention is to enable radio mobility studies compliant with the 3GPP specifications for NTNs.

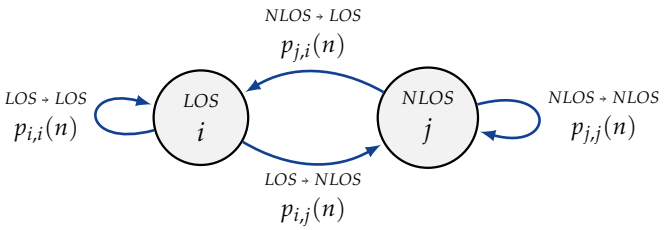


**Fig. II.1:** The state model is based on a Markov chain that assumes two states. This model takes into consideration the state transitions as a function of time sample $n$.

## 3.1 Generalization of the model

By definition, a Markov model is a random process used to generate discrete sample sequences corresponding to a set of $M$ discrete categories, also named states, of a predefined sample length. A Markov chain of finite order $m = 1$, i.e., a first order Markov process, allows the signal to be in one of $M$ states with a probability depending only on the previous state.

To realize time-correlated channel state sequences, we consider a 2-state Markov chain, where the states correspond to LOS and NLOS. Hence, the stochastic process models over time if the channel maintains its current state or transitions from one state to the other. These state transitions depend on a certain probability distribution which changes as a function of the elevation angle. Fig. II.1 illustrates the Markov process considered for this work.

As mentioned earlier, the Markov chain describes the state transitions with a certain likelihood that changes over time. The collection of these probabilities constitutes a matrix known as transition matrix. Thus, we define the transition probability matrix, $P(n)$, as the matrix of probabilities showing the likelihood of staying unchanged or moving to another state at time sample $n$ and where each element of the matrix, $p_{i,j}(n)$, corresponds to a transition probability. Eq. A.1 defines the one-step transition probability as the probability of changing from state $i$ to state $j$ at time sample $n$.

$$p_{i,j}(n) = Pr\{X_n = j \mid X_{n-1} = i\} \tag{A.1}$$

### 3.2 Estimation of the state transition matrix

The modelling of the state transitions is a challenge difficult to address since it highly depends on the vicinity and the mobility of the receiver. For instance, a more cluttered environment might lead to shorter time periods in LOS where the LOS/NLOS transitions will occur at elevation angles near 90°. On the other hand, in a rural or suburban area with low-rise buildings it is expected that the receiver will experience most of its time in LOS. However, it is possible to estimate the transition matrix when individual transitions are known from experimental measurements. This process is conducted by observing the sequence of states for each individual unit of observation. To generalize this definition, we denote $s_{i,j}(n)$ as the number of individuals moving from state $i$ at instant $n-1$ to state $j$ at instant $n$. Thereby, the probability $p_{i,j}(n)$ is equal to the fraction of individuals that started in state $i$ and transitioned to state $j$ as a proportion of all individuals that started in state $i$ at time sample $n-1$:

$$p_{i,j}(n) = \frac{s_{i,j}(n)}{s_{i,i}(n) + s_{i,j}(n)} \tag{A.2}$$

Thus, it is possible to estimate a three-dimensional transition matrix by using experimental data, where the probabilities of LOS/NLOS change are captured as a function of time. However, carrying out a measurement campaign may be cumbersome due to the proprietary nature of most of the LEO systems and the lack of publicly available data. To this end, ray-tracing tools offer a good compromise for channel modelling [11]. The following Section summarizes the methodology that the authors of this work used to obtain channel state time-traces based on ray-tracing measurements. Furthermore, we include the transition probabilities estimated from the simulated observations used to complete our model.

## 4 Modelling with Ray-Tracing measurements

### 4.1 Ray-Tracing simulations

Ray-tracing simulations are conducted to study LEO satellite signal propagation in two different environments. The first one is a street canyon based dense urban scenario with high-rise buildings. The cluttered environment poses challenging conditions for LOS signal propagation. Figure II.2 shows the map of Chicago downtown used to model this scenario. This map has an area of 1070 m × 1070 m, an average building height of 150 m and a maximum building height of 526 m. For the second scenario, we used a map of Arlington Heights village to simulate a suburban environment with scattered

low residential houses. It is situated in the west suburb of Chicago with an area of 840 m $\times$ 780 m and a maximum building height of 10 m.

We perform ray-tracing simulations for both scenarios using WinProp simulator [12]. In these simulations, we compute time traces of the geometric LOS/NLOS states between pixels on ground and satellites covering different orbits. For the purpose of this work, we choose the dominant path model (DPM) as the propagation model, which consists on the determination of the dominant signal reaching the receiver [13]. Each available outdoor pixel, with a spatial resolution of 2 m, corresponds to an UE at 1.5 m height. 12 LEO satellites are simulated orbiting at 600 km altitude. Each of them covers an orbit from 10° to 170° elevation angle, rising from azimuth angles ranging from 0° (north) to 165° (counterclockwise). Furthermore, the simulations are conducted with a discrete spatial resolution of 1° along the orbit, i.e., 161 time samples.

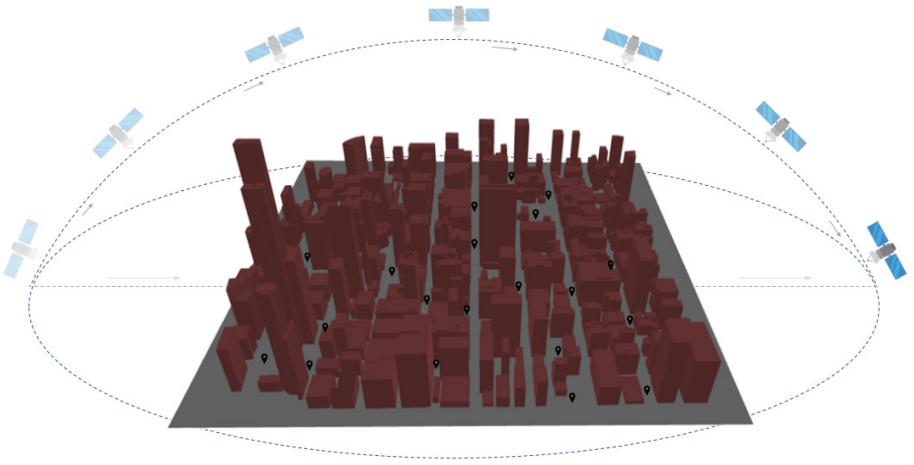

**Fig. II.2:** View of Chicago downtown (dense urban environment) together with a satellite flying over from West to East. Note the orbit and positions of the satellites are not to scale, but merely to exemplify the simulation assumptions.

## 4.2 Approximation of the state transition statistics

Table II.1 depicts the transition probabilities calculated after processing the ray-tracing measurements for suburban and dense-urban scenarios. It includes the likelihood of changing from NLOS to LOS and from LOS to NLOS. As one can observe, the probability of going from NLOS to LOS covers only the range from 10° to 90° where the likelihood of switching to LOS reaches a 100 % when the satellite moves to nadir, i.e., 90° elevation angle. This is due to the fact that the event of transitioning from NLOS to LOS hardly oc-

curs when the satellite is in upward trajectory. The probability of moving from LOS to NLOS comprises the range from 90° to 170° since it captures the downward movement of the satellites. This case draws a distinction between suburban and dense urban scenarios since a more cluttered environment leads to a higher probability of changing from LOS to NLOS, especially for lower elevation angles.

| $P_{NLOS \to LOS}$ | | | $P_{LOS \to NLOS}$ | | |
|---|---|---|---|---|---|
| Elevation | Suburban | Dense urban | Elevation | Suburban | Dense urban |
| 15° | 6.5 | 0.3 | 15°-85° | 0.0 | 0.0 |
| 25° | 4.2 | 0.5 | 90° | 0.0 | 0.0 |
| 35° | 3.5 | 0.9 | 95° | 0.1 | 3.0 |
| 45° | 3.3 | 1.2 | 105° | 0.1 | 3.2 |
| 55° | 3.5 | 1.7 | 115° | 0.1 | 3.4 |
| 65° | 4.3 | 2.5 | 125° | 0.1 | 4.1 |
| 75° | 6.6 | 4.9 | 135° | 0.2 | 5.4 |
| 85° | 21.1 | 19.4 | 145° | 0.3 | 7.8 |
| 90° | 100 | 100 | 155° | 0.5 | 12.1 |
| 95°-165° | 0 | 0 | 165° | 1.6 | 24.7 |

**Table II.1:** Transition probabilities (in %) estimated from ray-tracing simulations

# 5 Evaluation of the channel state model

In this Section, we evaluate the performance of the channel state model proposed in this work by comparing the behaviour of our model against the 3GPP model. As elaborated in Section 2, the channel model defined by the 3GPP was not designed to support satellite's mobility, leading to inconsistent transitions. However, it is included in this evaluation to prove the statement of lack of mobility support and to demonstrate the validity of our model as an applicable extension to the 3GPP model.

Fig. II.3 shows the stationary LOS probability as a function of the satellite elevation angle from the ray-tracing samples, the Markov model and the 3GPP model. We provide the statistics for suburban and dense urban scenarios. For the case of our model, $10^6$ realizations were randomly generated to estimate the probabilities. Regarding the 3GPP case, the LOS probabilities are publicly available in [4]. In general, the LOS probability increases with increasing satellite elevation, however, there are two further aspects to analyze in this figure. On the one hand, we can observe that the Markov-based

model presents a precise match with the probabilities calculated from the ray-tracing measurements. This matter might be noticed for both environments and validates the correct implementation of our model. On the other hand, there exists a gap between the 3GPP probabilities and our model, which it is notable for the dense urban case. These differences are caused by the larger and highly randomized dataset produced by our ray-tracing simulations. It is worth mentioning that the LOS probabilities from the 3GPP model are based on the work reported in [14], where authors focused their research in HAPS platforms.

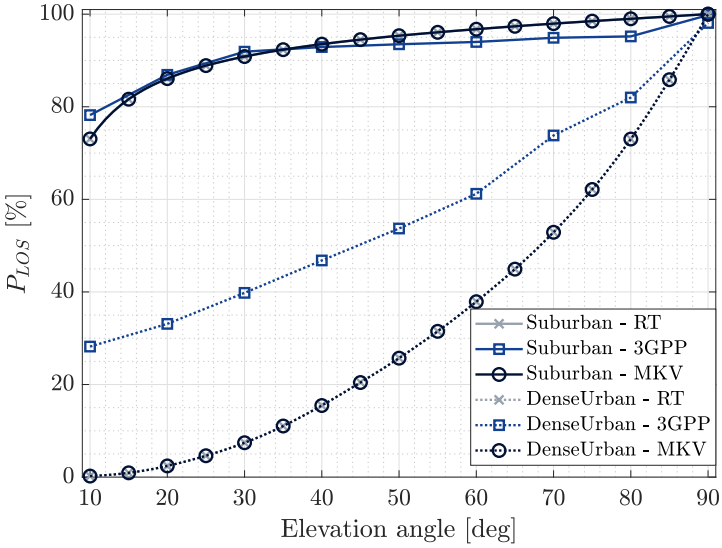


**Fig. II.3:** Line-of-sight probabilities as a function of satellite elevation angle from ray-tracing simulations (RT), the 3GPP model and the Markov model (MKV) for suburban and dense urban environments.

The cumulative distribution function (CDF) of the time in LOS that a receiver experiences is depicted in Fig. II.4. This key performance indicator allows us to quantify the degree of reality that each model achieves according to the scenario. As shown in Fig. II.3, we compare the results against the 3GPP model and the ray-tracing measurements. The goal of this figure is twofold: (i) to illustrate the distribution of time periods in LOS and (ii) analyze the number of transitions, i.e., LOS/NLOS state changes. One can observe that there exists a significant difference between the behaviour of the 3GPP model and the rest. The explanation is that an unrealistic number of transitions occurs due to the inability of the 3GPP model to support satellite movement. More precisely, an average of 21.75 and 65.7 state changes takes place for suburban and dense urban scenarios by using the 3GPP model. As

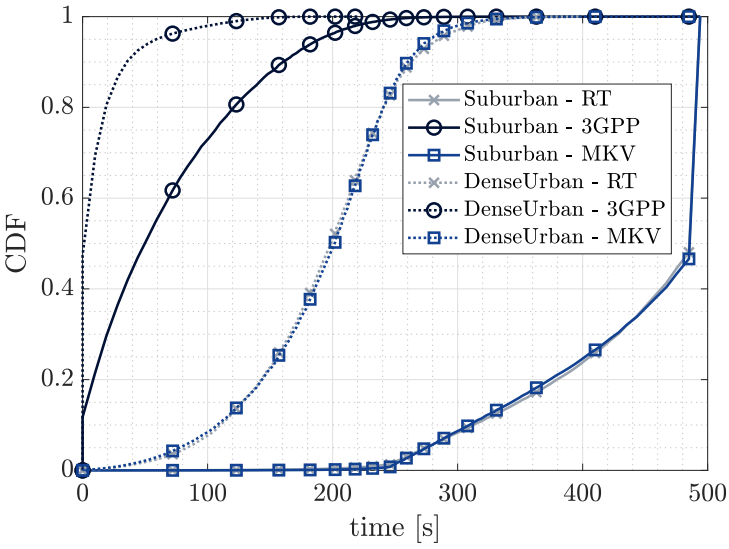


**Fig. II.4:** Distribution of the time periods in line-of-sight from ray-tracing simulations (RT), the 3GPP model and the Markov model (MKV) for suburban and dense urban environments.

a consequence, the receiver is not able to remain in the same state for a long period of time. A good example of this can be seen in the 3GPP curve when suburban environment is analyzed. There, the majority of realizations are only able to remain in LOS for time periods below 200 s, when the maximum achievable is approximately 500 s. On the contrary, it might be seen how the ray-tracing and the Markov curves provide longer periods in LOS. This fact underlines the importance of the model that we report here. This means that our model is not only able to reproduce realistic time windows in LOS but also to mimic a reasonable number of transitions. Indeed, a further analysis exposed that the Markov model was able to emulate an average of 0.57 and 2 state transitions for the suburban and dense urban scenarios, respectively.

Finally, we present in Fig. II.5 random realizations of the Markov and 3GPP models. Both outcomes are shown for suburban and dense urban scenarios. This figure reinforces the discussion above showing the appropriateness of the Markov model for mobility studies. It is observed that our model is able to achieve a high degree of reality by emulating a single LOS state with a length consistent with the scenario. As seen in the ray-tracing simulations, the Markov model reproduces longer periods in LOS with transitions at low elevations for the suburban case, while it generates short LOS time windows at high elevation angles for dense urban environments. Furthermore, it exemplifies the aforementioned inapplicability of the 3GPP model.

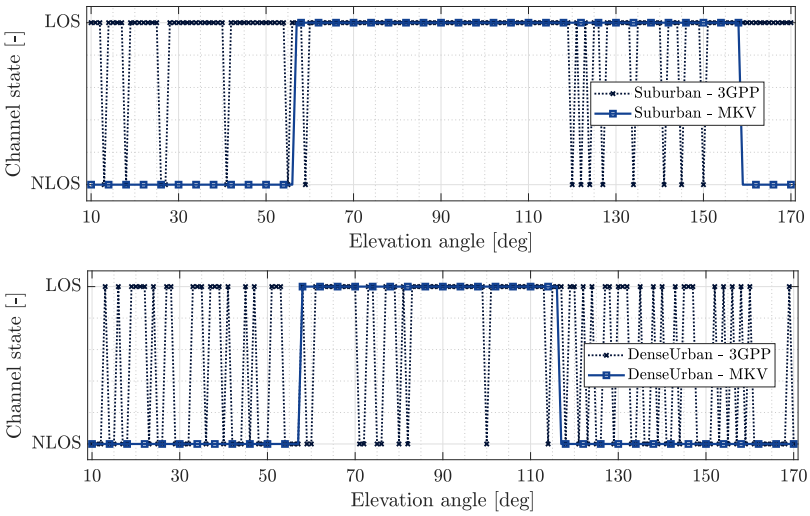


**Fig. II.5:** Example of the channel states for a satellite pass as a function of elevation angle. Comparison between the outcomes of the 3GPP and the Markov (MKV) models for suburban and dense urban scenarios.

# 6 Future Work

The modelling of the channel state variations is a necessary step in the channel characterization process. Nevertheless, once the channel states are generated, in a second phase the large-scale fluctuations of the received signal must be addressed. Typically, Markov processes might describe the transitions across channel states while statistical models define the signal variations within each state. The statistical modelling of channel propagation time series aims to capture the slow fading components of the channel due to shadowing conditions and blockages between the satellite and the receiver. Such signal fluctuations will depend on parameters such as the channel state, the near environment of the receiver, the radio-link distance and the frequency of the signal. Therefore, the authors of this work target as future steps to propose a complete channel propagation model for satellite mobility studies. This complete model shall not only model the state changes but also the slow signal variations experienced by a receiver for a moving LEO satellite scenario.

# 7 Conclusions

In this paper, a time-correlated Markov-based channel state model has been presented for radio mobility investigations in low Earth orbit satellite net-

works. Such satellite systems are a key component to achieve seamless and global 5G New Radio connectivity and, therefore, a realistic channel characterization is essential. This work acknowledged the gaps in the literature by proposing a state model able to capture the time correlations of the channel variations when highly mobile low Earth orbit satellites serve users on ground. Our model is based on a Markov process, extending the current snap-shot simulation-oriented 3GPP model, which does not facilitate simulations of moving satellites. The Markov model is based on ray-tracing simulations of suburban and dense urban 3GPP-compliant scenarios. Furthermore, we evaluate and validate the model by comparing its behaviour against the channel model reported by the 3GPP for non-terrestrial networks. Such analysis underlines that the Markov-based model is able to mimic the realistic behaviour observed in the ray-tracing simulations and, therefore, its applicability for studies where satellite mobility is included.

# References

[1] 3GPP, "Solutions for NR to support Non-Terrestrial Networks (NTN) (Release 16)," TR 38.821 V1.0.0, Dec. 2019.

[2] M. Giordani and M. Zorzi, "Non-Terrestrial Communication in the 6G Era: Challenges and Opportunities," *arXiv preprint arXiv:1912.10226*, 2019.

[3] G. Denis, D. Alary, X. Pasco, N. Pisot, D. Texier, and S. Toulza, "From New Space to Big Space: How Commercial Space Dream is Becoming a Reality," *Acta Astronautica*, 2020.

[4] 3GPP, "Study on New Radio (NR) to support non-terrestrial networks (Release 15)," TR 38.811 V15.2.0, Sept. 2019.

[5] E. Juan, M. Lauridsen, J. Wigard, and P. Mogensen, "5G New Radio Mobility Performance in LEO-based Non-Terrestrial Networks," in *2020 Global Communications Conference (GLOBECOM)*. IEEE.

[6] D. Arndt, A. Ihlow, T. Heyn, A. Heuberger, R. Prieto-Cerdeira, and E. Eberlein, "State Modelling of the Land Mobile Propagation Channel for Dual-Satellite Systems," *EURASIP Journal on Wireless Communications and Networking*, vol. 2012, no. 1, p. 228, 2012.

[7] E. Lutz, D. Cygan, M. Dippold, F. Dolainsky, and W. Papke, "The Land Mobile Satellite Communication Channel-Recording, Statistics, and Channel Model," *IEEE transactions on vehicular technology*, vol. 40, no. 2, pp. 375–386, 1991.

[8] L. E. Braten and T. Tjelta, "Semi-Markov Multistate Modeling of the Land Mobile Propagation Channel for Geostationary Satellites," *IEEE Transactions on Antennas and Propagation*, vol. 50, no. 12, pp. 1795–1802, 2002.

[9] M. Milojevic, M. Haardt, E. Eberlein, and A. Heuberger, "Channel Modeling for Multiple Satellite Broadcasting Systems," *IEEE Transactions on Broadcasting*, vol. 55, no. 4, pp. 705–718, 2009.

[10] ITU-R, "Propagation data required for the design systems in the land mobile-satellite service," Recommendation ITU-R P.681-11, Aug. 2019.

[11] J. Wu and P. Fan, "A Survey on High Mobility Wireless Communications: Challenges, Opportunities and Solutions," *IEEE Access*, 2016.

[12] Altair HyperWorks. WinProp proagation modeling. [Online]. Available: https://altairhyperworks.com/product/FEKO/WinProp-Propagation-Modeling

[13] R. Wahl, G. Wölfle, P. Wertz, P. Wildbolz, and F. Landstorfer, "Dominant Path Prediction Model for Urban Scenarios," *14th IST Mobile and Wireless Communications Summit, Dresden (Germany)*, 2005.

[14] F. Hsieh and M. Rybakowski, "Propagation Model for High Altitude Platform Systems Based on Ray Tracing Simulation," in *2019 13th European Conference on Antennas and Propagation (EuCAP)*. IEEE.

# Paper B

## Time-correlated Geometrical Radio Propagation Model for LEO-to-Ground Satellite Systems

Enric Juan, Ignacio Rodriguez, Mads Lauridsen, Jeroen Wigard, Preben Mogensen

The paper has been published in the
*IEEE 95th Vehicular Technology Conference (VTC2021-Fall), 2021.*

*The layout has been revised.*

# Abstract

*Low-Earth orbit (LEO)-based satellite communication systems are envisioned to be a next-generation key asset for telecom industry due to their potential to deliver global and seamless mobile broadband services. The high-speed mobility relative to Earth, that characterizes LEO orbits, will pose time-varying propagation conditions impacting the system performance in terms of mobility, availability and user throughput. Therefore, in LEO satellite systems, it is fundamental to understand accurately the signal variations between mobile satellites and users on the ground. This paper presents a radio propagation model able to describe realistically the time variations of the LEO-to-Ground path loss, including the line-of-sight changes and the impact of the surrounding built-up structures. We propose a low-complexity geometrical approach based on intelligent ray-tracing that considers the general dependencies on the elevation angle. The resulting model has been validated for a suburban scenario, exhibiting an overall root mean square error of 1.1 dB. Furthermore, the time-correlated geometry-based model is suitable for system-level radio mobility simulations with LEO-to-Ground satellite systems.*


# 1 Introduction

LEO satellite networks have become a reality with the initial deployments of constellations by SpaceX and OneWeb. Driven by the development of new low-cost space technologies and the reduction of launching costs, space is a rising market with many new players convinced of its potential [1]. Organizations and companies in the 3GPP continue working towards the integration of satellites into 5G networks, which aim at meeting the high-demand for internet services by providing global and seamless broadband access. Proof of this is the completion of two study items [2] [3] for Rel-15 and Rel-16 and the ongoing work item [4] for Rel-17.

The deployment of satellite constellations at relatively low altitude, between 600 km and 1200 km, has unique capabilities such as a reduced latency and a more favourable link budget compared to higher orbits like the geostationary orbit (i.e. 35.786 km height). A key challenge for LEO-based systems is the rapid movement of the satellites with respect to the Earth's surface, i.e. approximately 7.5 km/s. Even for ground stationary UEs, this translates into fast and continuous changes of the propagation conditions which have a clear impact on the system performance.

To enable LEO-based 5G access, it is paramount to understand and address the time-varying dynamics of the radio propagation links between LEO systems and the UEs on the ground. Many research efforts have acknowledged the importance of the channel modelling, however, satellite-to-ground channels, considering time-varying satellite mobility, have not received as

much attention as in terrestrial deployments. The most relevant and up-to-date studies are the works done by the ITU and the 3GPP. In the report P.681 [5], the ITU defines its recommendations to predict the propagation impairments in the land mobile-satellite links. Even though the model includes some considerations regarding LEO satellites, only UE mobility is considered. On the other hand, 3GPP addressed the channel modelling for NTN in [2]. Despite the technical report considers model parameters for LEO satellites such as the probability of LOS, clutter loss and shadow fading, movement of the satellites is not supported. Hence, the model does not define the correlations over time of the channel parameters.

Modelling the time correlations is fundamental to facilitate the design, development and planning of LEO-based NTN, as the mobility performance of the system needs to be carefully evaluated to ensure satisfactory end user experience. In [6] we conducted system-level simulations to evaluate the 5G New Radio mobility performance in LEO-based NTN, where we had to assume a constant LOS for the satellite-to-UE links due to the lack of a suitable channel model in terms of mobility. Later on, initial steps were done towards a model able to capture the time correlations in [7], where we proposed a Markov-based model to realistically determine the LOS state transitions. In this paper, we complete our previous work by proposing a model that predicts the signal strength variations caused by effect of LOS obstructions considering stationary users on the ground and mobile satellites. The model describes the path loss and the shadow fading as a function of a given channel state transition point. The model is built on the basis of models for terrestrial radio deployments to define how the diffraction and reflection physical phenomena changes over elevation angle. Furthermore, the developed large-scale propagation model is able to achieve a compromise between accuracy and simplicity resulting in a useful extension to the channel model for NTN reported by the 3GPP.

The remainder of the paper is structured as follows: Section 2 introduces the terrestrial models used as a baseline for our model. Section 3 describes our proposed geometrical model and illustrates its dynamics. The ray-tracing simulations used for validation of the model are presented in Section 4, while in Section 5 we discuss the overall accuracy of the model. Section 6 elaborates on the extraction of applicable shadow fading parameters and, finally, 7 concludes the paper.

## 2 Baseline Radio Propagation Models

Several terrestrial radio propagation models have described radio link situations in built-up areas that are close to the one experienced in the LEO-to-Ground scenario. Hereafter, we provide a brief description of the models

used as baseline for developing our model.

### 2.1 Knife-edge diffraction model

The ITU collected in its recommendation P.526 [8] several models to study the effect of diffraction on the received field strength, including the widely used model known as knife-edge diffraction. This model ignores the roughness of the material by considering an ideal and infinite edge and adjusts the loss based on the dimensionless parameter $v$ (see [8, Eq. (26-29)]). Further details of this parameter are discussed in Section 3.

### 2.2 Ikegami and Walfisch models

Ikegami *et al.* published in [9] a model based on geometrical optics assuming a simple two-ray approach; a direct rooftop-to-street diffracted ray and a ray reflected by a building across the street. Later on, Walfisch and Bertoni proposed in [10] a model addressing the impact of buildings in the propagation between base stations and UEs. Both models were later combined in [11] to address the limitations of each individual model. Nonetheless, the accuracy of the resulting model is limited to an environment where the range of parameters such as the slant range and the transmitter antenna height are up to 5 km and 50 m, respectively.

## 3 Proposed Geometrical Model

### 3.1 Geometry description

Radio signals from LEO satellites can be attenuated by buildings located near the UE. These signals propagate blockage-free over long distances and interact with the built-up area prior to reaching the UE. We denote the free-space segment as the path that the radio signal covers under free-space conditions, while we refer to the clutter segment as the portion of the path where the signal propagates in built-up areas. This scenario is depicted in Fig. II.1, where the LEO satellite is at an altitude of $h_{sat}$, at a distance $d_{sat}$ and with an elevation angle of $\alpha_{sat}$ with regards to the UE, located at a height of $h_{UE}$ surrounded by buildings. The LOS path is obstructed by *Building 1* with a height of $h_B$. The signal reaches the rooftop of *Building 1* with angle $\alpha_1$, measured from the satellite-UE plane, and grazes towards the UE with angle $\alpha_{sp}$. We term $\alpha_{sp}$ as the *switching point* because the angle denotes the line between NLOS and LOS conditions.

The model assumes a geometrical approach based on two-rays: a ray diffracted at the rooftop of *Building 1* and a ray reflected by *Building 2* after

grazing over *Building 1*. For further clarification, both rays are illustrated in Fig. II.1. We assume *Diffraction 1* varies depending on angles $\alpha_1$, $\alpha_{sat}$ and $\alpha_{sp}$, while *Diffraction 2* remains constant with the edge of *Building 1* just in line between the satellite and the reflection spot on *Building 2*.

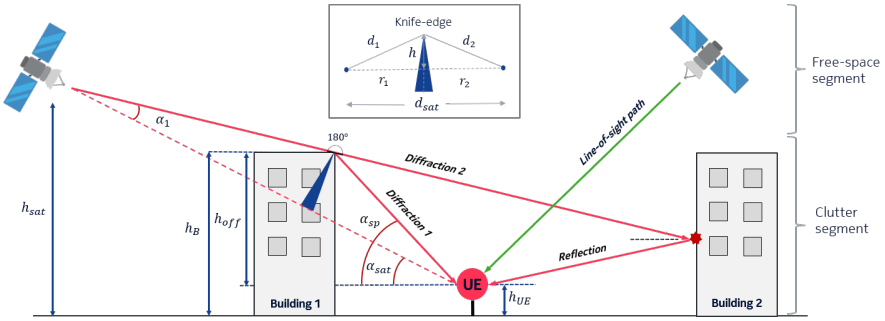


**Fig. II.1:** Geometric concept to illustrate the radio wave interactions of LEO-to-ground links.

## 3.2 Formulation

Following the scenario just described, the overall path loss ($PL$) is estimated in Eq. B.1 according to the channel conditions. We use the model in [7] to generate time-correlated LOS and NLOS states as a function of $\alpha_{sat}$ and define the values of $\alpha_{sp}$. Once the LOS/NLOS states are computed, the geometrical-based radio propagation loss is calculated for the different states by splitting $PL$ in three components: free-space $L_{FS}$, clutter $L_C$ and shadow fading $\chi$, where $L_C$ is negligible when the UE is in LOS conditions.

$$PL = \begin{cases} L_{FS} + \chi, & \text{if LOS} \\ L_{FS} + L_C + \chi, & \text{if NLOS} \end{cases} \quad \text{[dB]} \quad \text{(B.1)}$$

Signal attenuation under free-space conditions is calculated in Eq. B.2 according to the carrier frequency $f_c$ (GHz) and the distance $d_{sat}$ (m), where $R_E$ denotes Earth radius. The term $d_{sat}$, shown in Eq. B.3, is computed as the 3GPP reports in [2].

$$L_{FS} = 20\ \log_{10}\left(d_{sat}\right) + 20\ \log_{10}\left(f_c\right) + 32.45 \quad \text{[dB]} \quad \text{(B.2)}$$

$$d_{sat} = \sqrt{R_E^2\ \sin\left(\alpha_{sat}\right)^2 + h_{sat}^2 + 2h_{sat}R_E} - R_E\ \sin\left(\alpha_{sat}\right) \quad \text{[m]} \quad \text{(B.3)}$$

The clutter loss $L_C$ addresses the shadowing loss caused by surrounding buildings and objects. As shown in Eq. B.4, the term is computed by the root mean square and comprises two components: a variable contribution

accounting for the rooftop-to-street diffraction $L_D$ and a constant attenuation derived from the reflection on the building on the opposite side of the street $L_R$. Both components are estimated independently and described below.

$$L_C = -10 \log_{10} \left( 10^{-\frac{L_D}{10}} + 10^{-\frac{L_R}{10}} \right) \quad \text{[dB]} \quad \text{(B.4)}$$

The component loss $L_R$ is calculated in Eq. B.5 and accounts for the reflection loss in *Building 2* and the grazing diffraction in *Building 1*. The first part is computed based on a given reflection coefficient ($\Gamma_R$) and assuming the parity of the angles of incidence and reflection on *Building 2*. The diffraction-based loss ($L_{D,180^\circ}$), with the obstruction just in line, is half of the value in free-space conditions, i.e. a loss of 6 dB.

$$L_R = -20 \log_{10} (\Gamma_R) + L_{D,180^\circ} \quad \text{[dB]} \quad \text{(B.5)}$$

The diffraction-based contribution $L_D$ is computed as a knife-edge diffraction loss by approximating *Building 1* as an ideal absorbing edge. For that purpose, we use the expression in Eq. B.6 which accounts for an approximation of the Fresnel-Kirchoff loss $J(v)$ reported in [8, Eq. (30)].

$$L_D = 6.9 + 20 \log_{10} \left( \sqrt{(v - 0.1)^2 + 1} + v - 0.1 \right) \quad \text{[dB]} \quad \text{(B.6)}$$

The value of $L_D$, in Eq. B.6, is considered valid for values of $v$ greater than zero. The term $v$, defined in Eq. B.7, is key to capture the dynamics of the model by adjusting the diffraction loss with regards to the position of the satellite, the knife-edge and the UE. Moreover, note that we tune $v$ to depend on the wavelength $\lambda$, the slant range $d_{sat}$ and the angular difference $\Delta_{sp}$, which is defined as the absolute difference between the angles $\alpha_{sp}$ and $\alpha_{sat}$ in radians.

$$v = \sqrt{\frac{2}{\lambda} d_{sat} \, \alpha_1 \, |\alpha_{sp} - \alpha_{sat}|} = \sqrt{\frac{2}{\lambda} d_{sat} \, \alpha_1 \, \Delta_{sp}} \quad [-] \quad \text{(B.7)}$$

For the estimation of the angle $\alpha_1$, in Eq. B.8, we use the approximation $r_1 \approx d_{sat}$, which is valid for values of $r_1 \gg r_2$.

$$\alpha_1 = \arctan (h / d_{sat}) \quad \text{[rad]} \quad \text{(B.8)}$$

We compute the height of the knife-edge ($h$) as follows:

$$h = h_{off} \sin (\Delta_{sp}) \sqrt{1 + \cot^2 (\alpha_{sp})} \quad \text{[m]} \quad \text{(B.9)}$$

$$h_{off} = h_B - h_{UE} \quad \text{[m]} \quad \text{(B.10)}$$

Further, the model considers log-normal shadow fading ($\chi$) with zero mean and variance $\sigma_\chi^2$, i.e. $\chi \sim N(0, \sigma_\chi^2)$, and as a function of the angular term $\Delta_{sp}$. Further details are discussed in Section 6.

### 3.3 Model Discussion

In this section we have defined a model for the estimation of the large-scale aspects of the propagation. The small-scale fading caused by interference of multipath is out of the scope of this work and it is covered by 3GPP in [2].

Together with the work in [7], we address the novelty of modelling the time correlations of LEO-to-Ground satellite systems. The modelling is done as a function of the elevation angle instead of time to facilitate the calculations - we propose a geometrical model - and is based on the fact that time and space are intrinsically related.

The model automatically adjusts the propagation conditions and path loss according to values of $\alpha_{sat}$ and $\alpha_{sp}$. The dynamics of the model have been checked to model elevation angles from 10° to 170°, as defined by the 3GPP in [2]. The angle $\alpha_{sp}$ may take any value in the application range of $\alpha_{sat}$. We neglect the estimation of the horizontal distance from *Building 1* to the UE since it is self-contained in $\alpha_{sp}$.

## 4 Ray-Tracing Simulations

Ray-tracing simulations are conducted to validate the theoretical model as well as to study LEO-to-Ground signal propagation. Similarly as in [7], we simulate a suburban environment since we consider suburban and rural key scenarios for NTNs. For that purpose, we use a map of Arlington Heights village (western Chicago) with scattered low residential houses, an area of 840 m × 780 m and a maximum building height of 10 m. Despite ray-tracing is a valid tool for validation, real measurements can be useful to refine the model and enable further scenarios. Therefore, further study is encouraged to gain more insight on the topic.

The simulations are done in WinProp [12] using 3D intelligent ray-tracing, considering a limit of 2 diffractions and 1 reflection per ray with a spatial pixel resolution of 1 m. We use a limitation of 10 rays per pixel and set a carrier frequency of 2 GHz. We compute time traces of the received power at outdoor pixels at 1.5 m height. A LEO satellite flies over the area at an altitude of 600 km and at elevation angles ranging from 10° to 170°.

We simulate the received power ($P_{RX}$) over roughly 456 000 pixels, where the contribution of each ray is coherently superposed. The path loss at the $i^{th}$ pixel is calculated by considering isotropic transmitter power $P_{TX} = 10$ W. Fig. II.2 shows the path loss heat-map of one of the simulations considering a

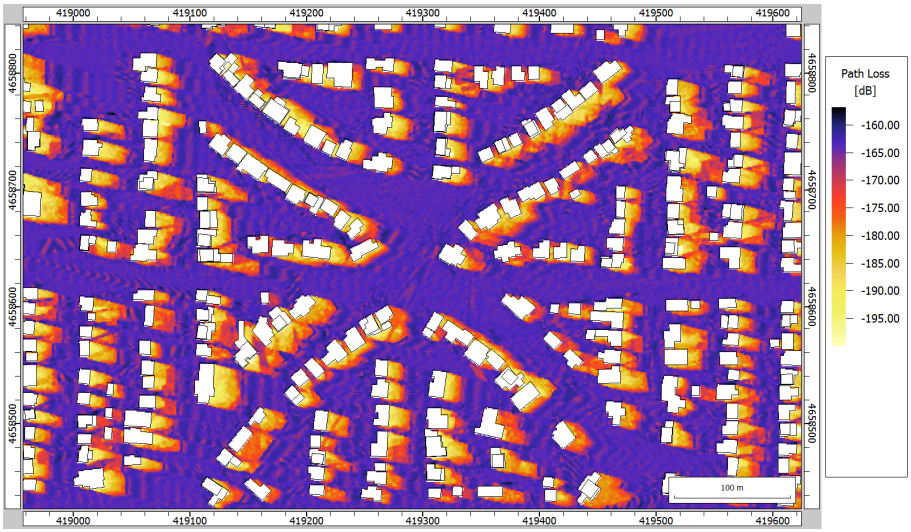


**Fig. II.2:** Path loss map of Arlington Heights for a LEO satellite rising from North-West at 10° elevation angle and at 600 km height.

transmitting LEO satellite at an altitude of 600 km with coordinates 44° N and 109° W, which corresponds to an elevation angle of 10°. From the resulting path loss, the clutter loss at the $i^{th}$ pixel location can be estimated as detailed below.

$$CL_i = P_{TX,i} - P_{RX,i} - L_{FS,i} \qquad \text{[dB]} \quad \text{(B.11)}$$

Fig. II.3 shows the angular clutter loss variations at a given location as the LEO satellite flies over the scenario varying its $\alpha_{sat}$. The traces, obtained from the ray-tracing data, correspond to locations with different NLOS/LOS angular transition characteristics, i.e. switching points $\alpha_{sp}$ at 30°, 50° and 70°.

# 5 Validation of the Model

This section presents the validation of the time-correlated geometrical model against ray-tracing simulations for a carrier frequency of 2 GHz. To that end, we tune the model by considering a building height of $h_B = 6$ m and a UE placed at $h_{UE} = 1.5$ m. To choose the building height value we consider two-storey houses with an average floor height of 3 m, which is well in line with the average building profiles in suburban areas. The satellite is at an altitude of 600 km with $\alpha_{sat}$ ranging from 10° to 90°. We account a constant value of 16.45 dB for $L_R$ (Eq. B.5) by considering a reflection coefficient of $|\Gamma_R| = 0.3$ and $L_{D,180^\circ} = 6$ dB.

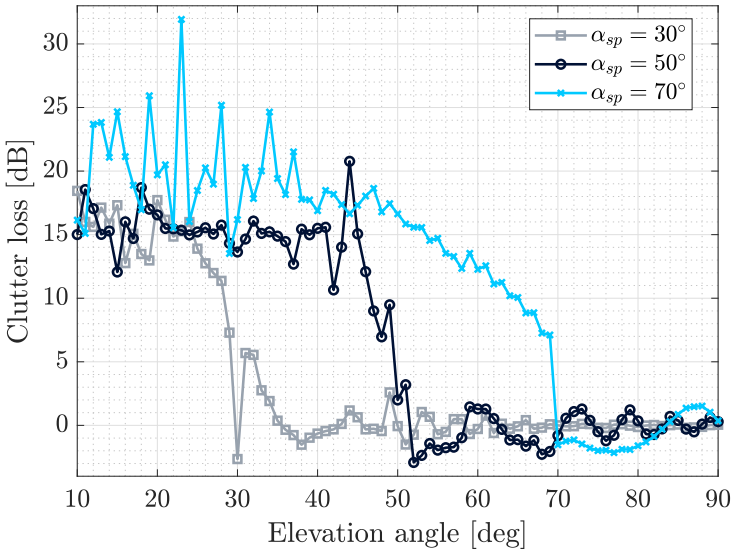


**Fig. II.3:** Ray-tracing simulated clutter loss traces as a function of the elevation angle, at three different locations with non line-of-sight to line-of-sight transitions at 30°, 50° and 70° elevation angle.

The model is compared against the ray-tracing simulations described in Section 4 in terms of mean clutter loss. For illustrative purposes, we compute the clutter loss $L_C$ using Eq. B.4 for three switching points; $\alpha_{sp} = 30°, 50°, 70°$. Regarding the ray-tracing, we average the clutter loss values from all locations in the scenario that have the same switching angle. Fig. II.4 shows the predicted and the simulated mean clutter loss as a function of $\alpha_{sat}$. As one can observe, the model predicts the same trend observed in the ray-tracing. The traces follow a similar pattern which can be split in two stages. A first part where the clutter loss at low elevation angles remains constant or falls gently, showing a loss response around 15–18 dB. The second part begins approximately 20° before the NLOS-LOS transition where the loss value decreases steadily until the switching point, i.e. $\alpha_{sat} = \alpha_{sp}$. For values of $\alpha_{sat} \geq \alpha_{sp}$, the model predicts exactly 0 dB, while the ray-tracing traces show values near 0 dB. By analysing the propagation of the rays in the simulations, we observe that these effects are physically consistent if we consider that the reflected ray is the dominant for low elevation angles. Then, as long as the satellite rises, the rooftop-to-street diffraction gains relevance until the switching point, where the UE is no longer obstructed.

Even though the 3GPP model do not support satellite's mobility, another aspect to underline is the close conformity between the clutter loss obtained with our model and the clutter loss for suburban and rural scenarios, in the range of 16–19 dB, reported in [2, Table 6.6.2-3].

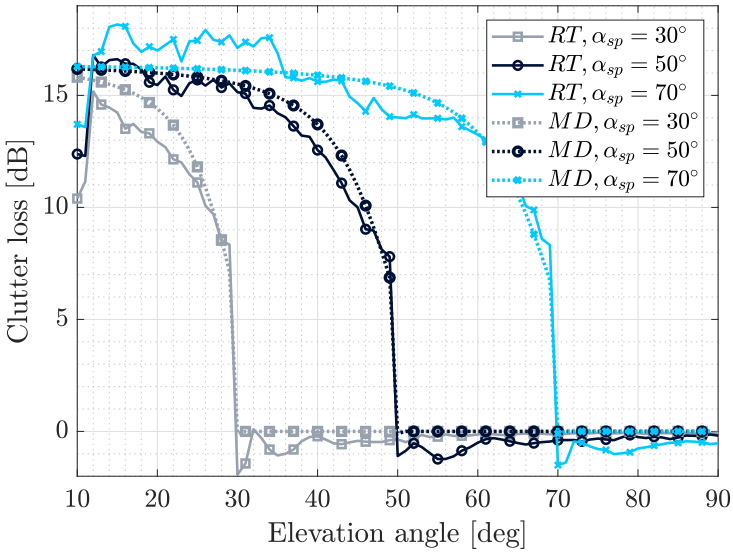


**Fig. II.4:** Average clutter loss traces from ray-tracing (RT) and model (MD) for non line-of-sight to line-of-sight transitions at 30°, 50° and 70° elevation angle.

To quantify the accuracy of the model we calculate the root mean square error (RMSE). Regarding traces where $\alpha_{sp}$ ranges from 20° to 80°, the RMSE is in the range of 0.9–1.5 dB with a mean of 1.1 dB. The maximum RMSE is observed at $\alpha_{sp} = 80°$ and is due to the low number of NLOS to LOS transitions at high elevation angles.

# 6 Modelling of the Shadow Fading

This section analyses and models the shadow fading $\chi$ as a function of $\Delta_{sp} = |\alpha_{sp} - \alpha_{sat}|$ and is based on the ray-tracing simulations. We compute the shadow fading samples with the procedure detailed as follows. We first create a grid $SF$ composed by the path loss values from each pixel location. $SF$ is generated per elevation angle and the samples are labeled with regards to the LOS conditions. Discerning between NLOS and LOS pixels, we subtract the mean path loss to the individual samples of $SF$. As a result, we obtain distributions per elevation angle and LOS conditions. Such approach assumes that all pixels at a given elevation angle are at the same distance $d_{sat}$ from the satellite, which dominates over any ground distance.

The analysis of the processed data shows that $\sigma_{\chi,nlos}$ decreases as $\Delta_{sp}$ decreases. Table II.1 reflects the standard deviation of the shadow fading ($\sigma_\chi$) as a function of $\Delta_{sp}$ with a 10° step, where $\sigma_\chi$ is taken from the nearest reference value of $\Delta_{sp}$. It is worth noting that values of $\sigma_\chi$ for LOS conditions

| **Angular distance** $\Delta_{sp}$ (°) | **std deviation** $\sigma_\chi$ (dB) | | **Decorrelation distance** $\alpha_{corr}$ (°) | |
|---|---|---|---|---|
| | LOS | NLOS | LOS | NLOS |
| **10** | 2.3 | 4.2 | 2.6 | 2.5 |
| **20** | 1.4 | 5.1 | 2.8 | 3.1 |
| **30** | 1.1 | 5.6 | 2.9 | 4.5 |
| **40** | 0.9 | 6.1 | 2.9 | 6.4 |
| **50** | 0.6 | 6.2 | 3.0 | 8.7 |
| **60** | 0.4 | 6.5 | 3.1 | 10.5 |
| **70** | 0.3 | 7.1 | 3.1 | 11.9 |
| **80** | 0.3 | 7.4 | 3.2 | 12.6 |

**Table II.1:** Shadow fading parameters for non line-of-sight conditions modeled from the ray-tracing simulations.

are in the range of 0.3–2.3 dB. Compared with NLOS conditions, this results in a lower impact when modelling as a function of $\Delta_{sp}$.

Table II.1 also provides the decorrelation distance ($\alpha_{corr}$). Typically in system-level simulations, shadow fading is computed independently in time. However, the shadow fading effect of the same radio link is usually highly correlated. In a similar fashion, we model this parameter as a function of $\Delta_{sp}$. For that purpose, we compute the autocorrelation function of the shadow fading ($R(\Delta_{sp}, \Delta_{sp} - \tau)$) and estimate $\alpha_{corr}$ for those values of $\alpha_{sat}$ that meets the condition $R = 1/e$ based on [13].

Fig. II.5 depicts a time-correlated trace generated by the complete channel model. Firstly, the LOS model in [7] defines the channel states of a LEO-to-Ground link with a NLOS-LOS transition at 50°. Secondly, the model computes the mean path loss split in two parts: the free-space and the clutter components, as described in Section 3. Finally, the correlated shadow fading is generated and applied accordingly.

# 7 Conclusions

In this paper we have presented a model which captures the time-varying radio propagation conditions for low-Earth orbit satellite-to-ground links. We have analysed the large-scale changes of the received signal's power caused by obstructions appearing in the line-of-sight path due to the movement of the satellite. We have proposed a model that predicts the overall path loss

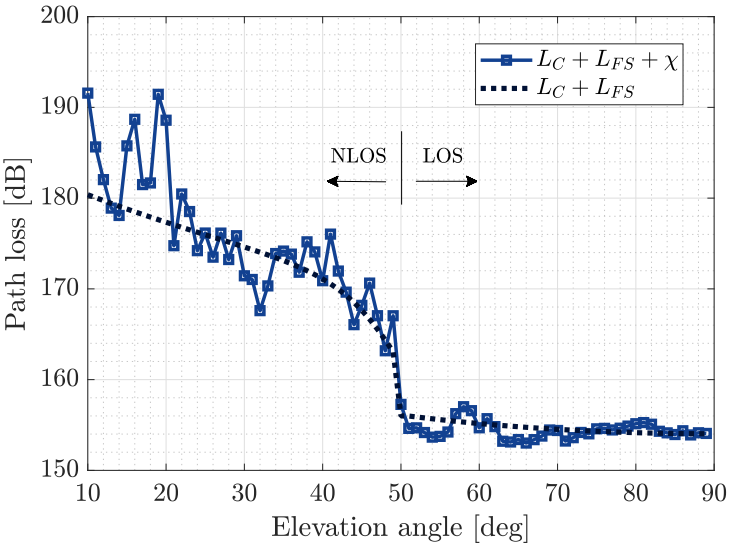


**Fig. II.5:** Time-correlated overall path loss trace including free-space path loss, clutter loss and shadow fading for a user transitioning from non line-of-sight to line-of-sight at 50° elevation angle.

discerning between free-space path loss, clutter loss and shadow fading. For the modelling of the clutter loss we have extended a combination of existing models for terrestrial deployments by including the full range of motion of a satellite in terms of elevation angle dependency. Furthermore, the model is geometry-based and it can be tuned accordingly. The results show a close agreement between the mean clutter loss from the designed model and the ray-tracing with an average root mean square error of 1.1 dB, regardless at what elevation angle the channel state transition occurs. The model can be conveniently used for system-level simulations targeting LEO satellite-to-Ground mobility aspects.

# References

[1] G. Denis, D. Alary, X. Pasco, N. Pisot, D. Texier, and S. Toulza, "From New Space to Big Space: How Commercial Space Dream is Becoming a Reality," *Acta Astronautica*, 2020.

[2] 3GPP, "Study on New Radio (NR) to support Non-Terrestrial Networks (Release 15)," TR 38.811 V15.2.0, Sept. 2019.

[3] ——, "Solutions for NR to support Non-Terrestrial Networks (NTN) (Release 16)," TR 38.821 V1.0.0, Dec. 2019.

[4] ——, "Solutions for NR to support Non-Terrestrial Networks (NTN) (Release 17)," RP-202908, 3GPP TSG RAN Meeting 90-e, Dec. 2020.

[5] ITU, "Propagation data required for the design systems in the land mobile-satellite service," Rec. ITU-R P.681-11, 2019.

[6] E. Juan, M. Lauridsen, J. Wigard, and P. Mogensen, "5G New Radio Mobility Performance in LEO-based Non-Terrestrial Networks," *IEEE GLOBECOM*, 2020.

[7] ——, "A Time-correlated Channel State Model for 5G New Radio Mobility Studies in LEO Satellite Networks," *IEEE VTC-Spring*, 2021.

[8] ITU, "Propagation by diffraction," Rec. ITU-R P.526-15, 2019.

[9] F. Ikegami, S. Yoshida, T. Takeuchi, and M. Umehira, "Propagation Factors Controlling Mean Field Strength on Urban Streets," *IEEE Transactions on Antennas and Propagation*, 1984.

[10] J. Walfisch and H. Bertoni, "A Theoretical Model of UHF Propagation in Urban Environments," *IEEE Transactions on Antennas and Propagation*, 1988.

[11] E. Damosso and L. Correia, "Digital mobile radio towards future generation systems communications. cost 231 final report," *CEC*, 1999.

[12] Altair HyperWorks. WinProp propagation modelling. [Online]. Available: https://altairhyperworks.com/product/FEKO/WinProp-Propagation-Modeling

[13] M. Gudmundson, "Correlation model for shadow fading in mobile radio systems," *Electronics letters*, vol. 27, no. 23, pp. 2145–2146, 1991.

# Part III

# Mobility Performance Analysis of the 5G NR HO Procedures in 5G LEO Satellite Networks

# Mobility Performance Analysis of the 5G NR HO Procedures in 5G LEO Satellite Networks

Before starting to design, simulate and analyze new HO solutions, it is important to understand the achievable performance of the state-of-the-art HO solutions. This part focuses on analyzing the mobility performance of the conventional *make-before-break* UE-assisted NW-controlled 5G NR HO procedure (referred as BHO) and the 5G NR CHO procedure, both available in Release 16 specifications.

## 1 Motivation

In cellular communications, a HO is the mobility procedure that allows to transfer an ongoing user data session from the current cell, i.e. *serving cell*, to a new cell, i.e. *target cell*, without noticeable interruption for the UE. This process is usually triggered when the UE moves away from the serving cell radio coverage and enters in the target cell radio coverage.

In TNs, factors such as UE speed, cells working at different frequencies and large number of UEs present challenging and interesting scenarios for the mobility management. Extensive studies in the literature have been conducted to improve the terrestrial HO performance and to address issues such as long HO interruption time that impact the user experience [1], frequent UHO and ping-pong (PP) events that use unnecessary resources [2], and RLF/HO failure (HOF) caused by poor radio conditions [3]. As a result, the 3GPP has standardized the *break-before-make* UE-assisted NW-controlled HO procedure as well as several mobility enhancements such as the dual active protocol stack (DAPS) based HO procedure and the CHO procedure.

As discussed in Part I, the NR HO procedures were created considering certain deployment characteristics: base stations that are fixed, air-interface propagation delays almost negligible and a clear difference in RSRP between cell edge and cell centre. In LEO satellite networks, the scenario is completely different and so do the challenges. Unlike in TNs where the HO procedure is mainly triggered by the UE mobility, in LEO satellite networks the mobility events are triggered by the movement of these satellite systems. The characteristics of this new scenario led to the formulation of the following hypothesis:

(**H2**) LEO satellites move at 28 000 km/h relative to the Earth. The fast movement of these satellite systems, acting as moving base stations from a high altitude, may challenge the UE mobility performance. Constraints such as long propagation delays and varying radio propagation conditions can lead to a malfunctioning of the measurement-based NR HO procedures.

The NR HO procedures include three important functions: the HO measurements, the HO triggering and the HO decision. The HO measurements function monitors the cells radio link strength or quality (i.e. RSRP, reference signal received quality (RSRQ) or DL SINR) to detect when a neighbouring cell becomes suitable for handover. The HO triggering is based on conditions known as NR measurement events. The UE is configured with these measurement-specific conditions to decide when the MR must be reported to the NW, i.e. HO initiation. Finally, the HO decision is made by the NW based on the reported HO measurements. The mobility studies of this thesis have been conducted using the NR A3 measurement event which is based on two HO control parameters: the HO margin (HOM), or hysteresis, and the time-to-trigger (TTT). When a neighbour cell is HOM dB stronger than the serving cell for a certain TTT, the UE initiates the HO process. Fig. III.1 illustrates how the NR A3 event is triggered depending on the HOM and TTT. The UE mobility performance depends on these parameters that are configured by the NW; a sub-optimal configuration might increase the number of UHOs and RLFs. For instance, a sufficiently low TTT can be configured to address long propagation delays and fast radio link quality decay (caused by satellite movement, high-gain satellite beams and high inter-cell interference). On the other hand, the HOM is used to avoid UHOs but due to the low RSRP variability needs to be carefully selected.

As stated in H2, the characteristics of LEO satellite networks can limit the UE mobility performance when using the measurement-based NR HO procedures. This part of the thesis focuses on studying the performance of the measurement-based BHO and CHO procedures. The motivation behind

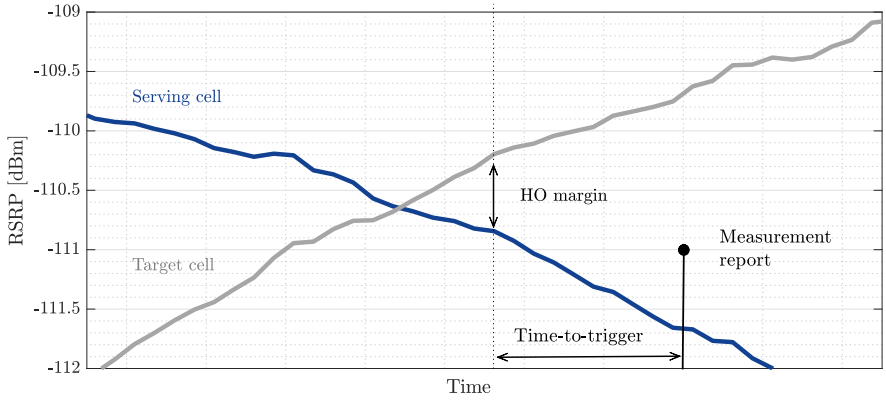


**Fig. III.1:** Triggering of the MR based on HOM and TTT control parameters.

is built on the following:

i) it is required greater understanding of the achievable performance of these procedures,

ii) the analysis allows to establish a baseline for later performance studies and,

iii) the analysis allows to identify and analyze further limitations of these HO procedures, which is important for the proposal of enhancements.

Furthermore, even though the 3GPP has acknowledged the CHO as a potential mobility enhancement for NTN, no simulation results have been reported to support such agreement.

The analysis are conducted using system-level simulations in a multi-user, multi-cell 5G LEO satellite network, where: i) satellites operate with EMC and gNB on-board capabilities and ii) UEs are in a rural environment. For this purpose, the system-level simulation assumptions proposed by the 3GPP in [4] are used. Both 5G NR HO procedures, i.e. BHO and CHO, are studied using several HO configurations to find the best achievable mobility performance.

# 2 Objectives

This part of the thesis pursues to test hypothesis H2 by simulating and analyzing the UE mobility performance of the BHO procedure and the CHO procedure. To that purpose, the following objectives are defined:

A. By means of system-level simulations, find the best achievable performance of the BHO and the CHO in EMC-based 5G LEO satellite networks.

B. Based on the best achievable performance of the BHO procedure, establish a mobility performance baseline for future mobility studies.

C. Based on the best achievable performance of the BHO procedure, compare the performance against typical terrestrial deployments.

D. Based on system-level simulation results, analyze the mobility performance of the BHO and CHO focusing on identifying critical limitations.

# 3 Included Articles

The articles that form the main body of this part are:

**Paper C. 5G New Radio Mobility Performance in LEO-based Non-Terrestrial Networks**

This paper studies the mobility performance when using the conventional *break-before-make* UE-assisted NW-controlled 5G NR HO procedure, i.e. BHO, in a LEO satellite network. Highly scattered users are covered by a network of LEO satellites that provides NR access. The LEO satellites have gNB capabilities and satellite beams implement the EMC scheme. The study is conducted by means of system-level simulations that follow a Monte Carlo approach. The simulation methodology is based on simulation assumptions specified by the 3GPP. The observed KPIs are the HOF rate, the RLF rate, the PP rate, the time-of-stay-in-outage (ToO), and the geometric DL SINR. The UEs are configured with the NR A3 measurement event. The mobility performance of the BHO procedure is analyzed configuring the NR A3 event with different values of the HOM and the TTT. The observed results are compared against two 3GPP-specific terrestrial scenarios commonly used in mobility studies: 21-cells urban macro and 500 km/h high-speed train.

**Paper D. Performance Evaluation of the 5G NR Conditional Handover in LEO-based Non-Terrestrial Networks**

This paper extends the study started in Paper C. In this paper, the study evaluates the mobility performance of the Release 16 CHO procedure to enhance the mobility robustness in LEO satellite networks. The main goal is to leverage the earlier HO initiation that characterizes the CHO to improve the baseline performance set by the BHO. The performance evaluation is again

conducted by means of system-level simulations and by configuring UEs with the NR A3 measurement event and different values of HOM and TTT. As in Paper C, the study follows simulation assumptions defined by the 3GPP. The 3GPP channel model defined for NTN is replaced by the time-correlated channel model reported in Papers A-B in order to realistically characterize the changes of LOS conditions.

# 4 Main Findings

**The BHO procedure leads to a sub-optimal mobility performance**

The mobility performance analysis in Paper C shows that the BHO cannot ensure service continuity and, therefore, satisfactory user experience. Even with a very low density of users (i.e. 0.005 users/km$^2$) under favourable LOS conditions, the system-level simulation results indicate that the best achievable performance cannot provide service continuity due to a large number of service failures (i.e. RLFs and HOFs) and PPs. When the best configuration is compared with terrestrial deployments, the BHO performs 10 times worse in LEO satellite networks than in TNs.

The analysis of several NR A3 measurement event configurations showed a trade-off between service failures and PPs: small HOMs (i.e. 0-1 dB) and short TTTs (i.e. 0-100 ms) decrease the RLFs/HOFs rates but also increase the number of PPs. Low HOM and TTT allow the UEs to react quicker to the fast serving cell radio link quality decay but it results in more HOs towards the wrong target cells. The latter is caused by the low RSRP difference at cell edge between serving cell and neighbouring cells which makes the UE difficult to distinguish the appropriate target cell.

Further analysis of the simulation results revealed that a majority of HOF were due to radio link problems in uplink (UL) and downlink (DL) transmissions. In UL, serving cells could not receive the MRs, whereas in the DL, UEs could not receive the corresponding HO commands. It was observed for these two cases, that very poor radio conditions were caused by UEs already out of the serving cell radio coverage. This highlights two important findings: i) the fast movement of the cells causes UEs to rapidly fall out of the serving cell radio coverage and ii) the BHO procedure does not react sufficiently fast to access on time the appropriate target cell. Even when the UE initiates the HO access sufficiently early, there is a high PP penalty.

Fig. III.2 is provided to support the mentioned findings. The figure shows the DL SINR as a function of time for a randomly selected UE, which is configured with three different HO configurations. Furthermore, the figure also includes the *optimal HO* as an upper bound performance. This upper bound reference is obtained with the aim of optimizing the DL SINR (further

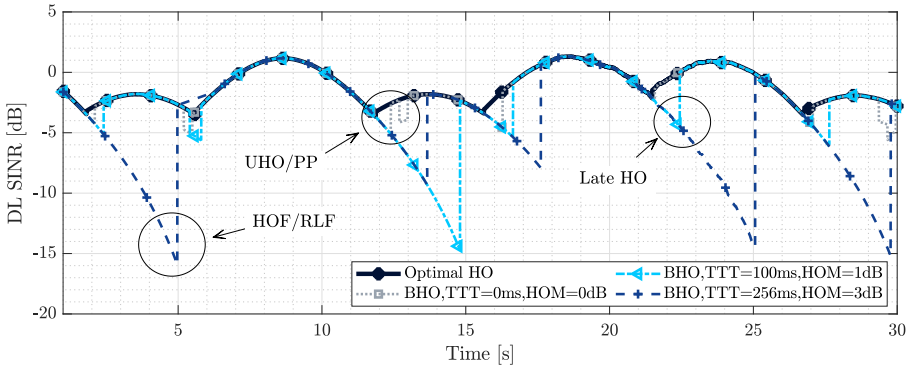


**Fig. III.2:** Mobility performance of the BHO procedure: time-trace of the DL SINR experienced by a UE (Source: Paper F).

details can be found in Papers D-F). The *optimal HO* presents a DL SINR that ranges from $-4$ to 1 dB, which highlights the challenging radio link budget. Examples of HOF/RLF, UHO/PP and late HO are given at $t = 5$ s, $t = 12$ s and $t = 22.5$ s.

### Impact of an earlier HO initiation

Paper D showed the benefits of using the CHO as compared with the BHO. In the CHO procedure, the UE receives a HO command containing an execution condition to handover to a candidate target cell. The UE keeps the connection with the serving cell until the execution condition is met based on cell radio measurements performed by the UE. This allows: i) to initiate the HO process earlier and ii) to access the target cell when the target cell radio link is reliable enough, without need for further communication with the serving cell.

As shown in Fig. III.3, the CHO achieves the goal of eliminating RLFs, which reduces service interruptions and data loss. As a result, the UE experiences better DL SINR (depicted in Fig. III.3 as the $5^{th}$ percentile DL SINR). This is important because directly impacts on the user experience since higher DL SINR enables higher modulation coding schemes and higher data rates. The improvement in terms of RLFs and DL SINR comes with an UHO penalty. With the aim of optimizing the DL SINR, the CHO configuration with highest DL SINR (i.e. HOM $= 0$ dB and TTT $= 0$ ms) shows a 75 % increase of UHOs. The CHO set with HOM $= 3$ dB and TTT $= 256$ ms reaches the optimal HO rate but it presents the worst $5^{th}$ percentile DL SINR performance, i.e. $-7$ dB. The best compromise is shown by the CHO set with HOM $= 1$ dB and TTT $= 100$ ms. The CHO procedure avoids RLFs by initiating earlier the HO process to the target cell. However, in many cases the early HO initiation leads to a sub-optimal choice of candidate cells. This

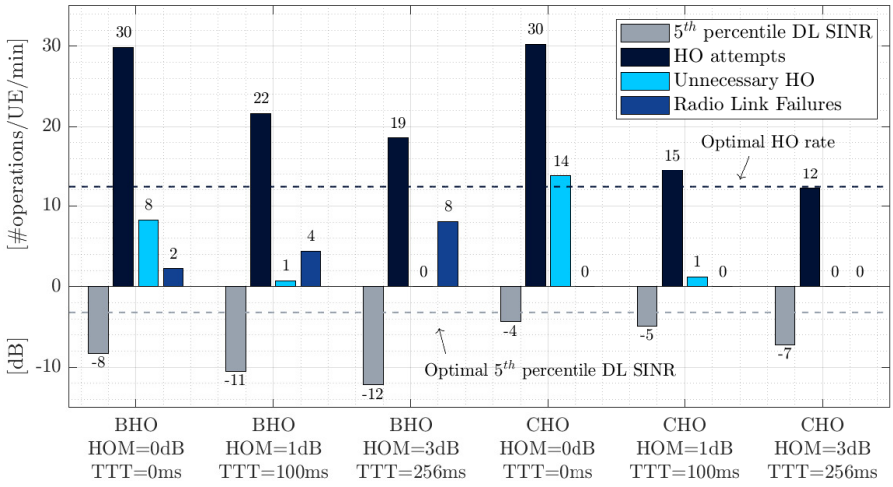


**Fig. III.3:** Mobility performance of the BHO and CHO procedures in terms of DL SINR, HO attempts, UHO events and RLFs.

is partly explained by the fact that the CHO in the system-level simulator is used blindly by the NW, i.e. there is no smartness at NW side that filters out undesired target cells.

### Impact of NR measurement events purely based on cell radio measurements

The system-level simulation results in Paper D showed that the CHO procedure addresses the high number of service failures that results by using the BHO. Short HOM and TTT leads to better DL SINR, but increases UHOs/PPs. The increase of these KPIs translates into an increase of the HO control signalling, measurement reporting and, ultimately, an undesired use of the available resources that can impact the user experience.

The end goal of a HO procedure is to avoid RLFs/HOFs and UHO/PP events, while maximizing the DL SINR. The BHO and the CHO lead to sub-optimal mobility performance because these HO procedures cannot jointly optimize the DL SINR and the HO rate. These procedures limit the HO triggering to measurement-specific conditions, i.e. NR measurements events. This means that: i) UEs only consider cell radio measurement quantities to initiate the HO process and ii) serving cells only consider cell radio measurements to decide the appropriate target cell.

The system-level simulation results in Papers C and D indicate that the characteristics of LEO satellite networks can lead to a sub-optimal mobility performance when using NR measurement events purely based on cell radio

measurements. Fig. III.4 support this statement with a RSRP trace from the system-level simulation results. The key aspects to highlight from this figure are:

i) There is a 1-3 dB RSRP variability between cell centre and cell edge.

ii) UEs feature a certain measurement error that can be as high as the RSRP variation (the 3GPP specifies in [5] a relative RSRP accuracy requirement of $\pm 2$ dB).

The combination of these two aspects challenges the HO triggering and the HO decision because the UE cannot correctly monitor the RSRP variations and, therefore, distinguish the appropriate target cell to handover to.

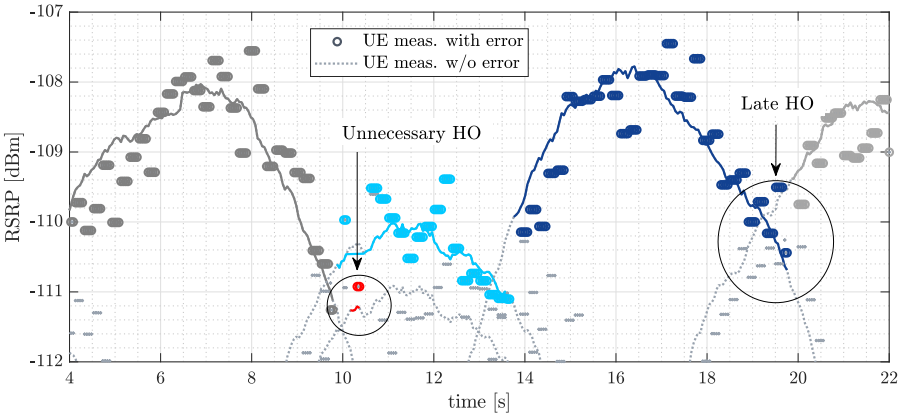


**Fig. III.4:** Time-trace of the RSRP measured by a UE showing the impact of the low RSRP variability and the UE measurement error (Source: Paper F).

# References

[1] L. C. Gimenez, P. H. Michaelsen, K. I. Pedersen, T. E. Kolding, and H. C. Nguyen, "Towards Zero Data Interruption Time with Enhanced Synchronous Handover," in *2017 IEEE 85th VTC Spring*, 2017.

[2] A. Alhammadi, M. Roslee, M. Y. Alias, I. Shayea, S. Alraih, and K. S. Mohamed, "Auto Tuning Self-Optimization Algorithm for Mobility Management in LTE-A and 5G HetNets," *IEEE Access*, vol. 8, pp. 294–304, 2019.

[3] H. Martikainen, I. Viering, A. Lobinger, and T. Jokela, "On the Basics of Conditional Handover for 5G Mobility," in *2018 IEEE 29th PIMRC*.

[4] "Solutions for NR to support Non-Terrestrial Networks (NTN) (Release 16)," 3GPP, TR 38.821 V1.0.0, 2019. [Online]. Available: https://www.3gpp.org/ftp/Specs/archive/38_series/38.821/

[5] “NR; Requirements for support of radio resource management (Release 16),” 3GPP, TS 38.133 V16.5.0, 2020. [Online]. Available: https://www.3gpp.org/ftp/Specs/archive/38_series/38.133/

# Paper C

## 5G New Radio Mobility Performance in LEO-based Non-Terrestrial Networks

Enric Juan, Mads Lauridsen, Jeroen Wigard, Preben Mogensen

The paper has been published in the
*IEEE Global Communications Conference (IEEE GLOBECOM), 2020.*

*The layout has been revised.*

# Abstract

*As part of 3GPP standardization work for Release 17, non-terrestrial networks (NTNs) aim to bring 5G New Radio (NR) communications to unserved and isolated areas. Constellations of low Earth orbit (LEO) satellites have emerged as a promising asset for NTNs and a key enabler technology to provide truly seamless and ubiquitous connectivity through 5G. Varying and longer propagation delays compared to terrestrial networks, limited radio link budget and the inherent high-speed movement of LEO satellites introduce new challenges in the mobility management procedures. To guarantee robust service continuity and satisfactory user experience, the handover (HO) procedure in LEO satellite systems is critical. Motivated by this fact, this paper presents a first performance analysis of the conventional 5G NR HO algorithm in a LEO-based NTN deployment. We provide system-level simulations obtained for different values of HO margin and time-to-trigger. Furthermore, we compare the HO performance in NTN with two 3GPP terrestrial scenarios - urban macro and high-speed train. The simulation results show HO failures and radio link failures are a factor 10 higher for the NTN scenario, while the corresponding time in outage is 5 times longer. Finally, we analyze the key issues and suggest potential mobility enhancements.*


# 1 Introduction

The massive growth and demand for wireless technologies led towards the definition of a new standard known as 5G New Radio (NR). Future services such as the Internet of Things, e-Health and Industry 4.0 will play a fundamental role in the global society and economy [1]. The 5G technology sets a milestone for a technological revolution that aims to meet challenging requirements such as ultra-high reliability and global and seamless connectivity [2]. Nonetheless, according to [3], still an estimated 53 % of the world's population remains unconnected to the internet. To this end, the integration of satellite and terrestrial networks is crucial for the realization of a global and heterogeneous 5G network.

In previous mobile network generations, the integration of satellite communications was based on proprietary tailored solutions. Even when integrated solutions were addressed, the satellite network was mainly used to provide backhaul as a non-flexible and expensive transport network [4].

The definition of the 5G standard in Rel-15 and the emergence of a new space market [5] increased the interest and participation in 3GPP activities from the satellite communications industry. As a result, current 3GPP standardization efforts focus on the development of NTNs, where companies and organizations are convinced of the market potential. Proof of this is the completion of two study items [6] [7] as part of 3GPP Rel-16 and the work item [8]

recently approved for Rel-17.

LEO satellites might become a key component for the realization of a communication network providing worldwide coverage and ubiquity. Unlike geostationary orbits, the use of lower orbits - from 600 km to 1200 km - allows to cut down the propagation delay, improve the radio link budget and reduce the deployment and manufacturing costs. However, LEO satellites have smaller coverage footprints and move at a very high speed relative to Earth, e.g. 7.5 km/s for an altitude of 600 km. Thus, LEO systems require dense satellite constellations to guarantee continuous coverage. Commercial missions such as SpaceX's Starlink, OneWeb and Telesat were the first movers in a space market aiming to establish global networks through constellations [5].

To enable 5G through LEO satellite networks, mobility mechanisms play a key role in ensuring service continuity and a satisfactory user performance. Communication distances up to 10 times longer than in terrestrial networks, imply longer propagation delays and higher path loss. These factors, together with the satellite movement and a high downlink interference from adjacent satellite beams, might lead to a possible malfunctioning of the HO procedure, requiring enhancements.

Despite the technical report [7] discussed mobility challenges, no simulation results were provided to support the discussion. In this paper, we present, to the best of our knowledge, the first publicly available system-level simulations of the conventional 5G NR HO algorithm performance in a LEO-based NTN scenario. In a first phase, the conventional 5G NR HO is assessed under different design settings - HOM and TTT - to identify the configuration achieving the best performance. In a second phase, the obtained mobility KPIs are compared against two 3GPP-compliant terrestrial environments - urban macro (UMa) and high-speed train (HST).

The remainder of the paper is structured as follows: Section 2 introduces the NTN concept within the 3GPP context and Section 3 describes the mobility issues in LEO-based NTN. Methodology and simulation results are found in Section 4 and 5, respectively. Section 6 discusses the results, while Section 7 presents potential mobility enhancements. Final conclusions are drawn in Section 8.

## 2 Non-Terrestrial Networks in 3GPP

NTNs refer to networks operating through air/spaceborne vehicles aiming to provide 5G service in unserved remote areas where the terrestrial service is not available or it is too costly to build the infrastructure. Apart from providing global service availability, it will reinforce service reliability by providing service continuity for moving platforms such as aircraft and ships as well

as enabling 5G network scalability by providing multicast and broadcast resources. Initial steps were taken by 3GPP in Rel-15, where the use of satellite systems to provide global coverage was introduced. As part of Rel-16, the study items reported in [6] and [7], provided a description of the envisioned concept defining the deployment scenarios, the key potential impacts in NR as well as the challenges to tackle. Based on the outcomes of the mentioned study items, Rel-17 work item [8] aims to continue addressing new solutions and specify the enhancements identified to support NTNs for NR.

3GPP addresses not only LEO and geostationary satellites but also high altitude platforms covering altitudes from 8 km to 35 786 km. Two payload implementations are conceptualized for these platforms: transparent and regenerative [6]. In the transparent architecture, satellites work as a relay node between the UE and the gNB on the ground, whereas regenerative satellites embark a payload with gNB capabilities. Fig. III.1 depicts the main differences between these two architectures.

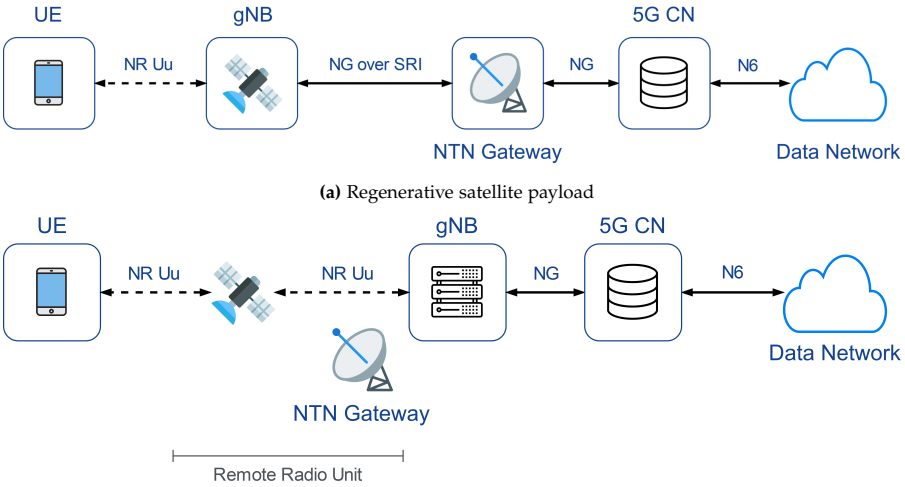


**(a)** Regenerative satellite payload

**(b)** Transparent satellite payload

**Fig. III.1:** NTN architectures in 3GPP.

# 3 NR mobility in LEO-based NTN

In terrestrial networks, mobility management focuses on ensuring the service continuity for users moving in deployments with fixed cells. LEO-based NTN overturns the mobility paradigm. LEO satellites will operate as high-speed moving cells providing 5G connectivity to UEs on the ground. The satellite movement together with the long communication distances will not

only trigger additional mobility events, it will challenge the UE's mobility performance.

One of the challenges of LEO-based NTN is to handle frequent HOs without resulting in an increased number of RLFs, HOFs and PPs [9]. Nonetheless, frequent mobility events are not the only driving factor. 5G NR was designed for terrestrial communications with relatively short cell-to-UE distances (i.e., a maximum distance of 300 km). In LEO-based NTN, communication distances can reach up to 3131 km involving a round trip delay of 20.89 ms for a satellite at 1200 km altitude and 10° elevation angle. This fact has a direct impact on the link budget and the HO latency. Furthermore, the HO latency varies depending on the implemented architecture and whether HO is executed among cells of the same satellite or they belong to different satellites. Longer propagation delays can lead to outdated UE measurements, late HO decisions and, ultimately, a failure in the HO procedure. Therefore, propagation delays, fast cell mobility and a constrained link budget must be considered in the design of an optimal HO mechanism.

## 3.1 Conventional Handover mechanism

The HO mechanism is designed to enable users to move from one cell to another while guaranteeing the service connectivity without noticeable service interruption. In NR, as Fig. III.2 introduces, the conventional HO algorithm implements a UE-assisted, network controlled break-before-make scheme. Such scheme means that the UE experiences a certain interruption time after disconnecting from the serving cell and until the new connection with the target cell is established. The procedure uses specific downlink channel measurements performed by the UE. If certain conditions configured by the network are fulfilled, the UE sends a MR to the serving cell. With this information, the serving cell decides if the UE needs to be handed over to a new cell and starts the HO preparation phase. During this phase, the serving cell requests the target cell to prepare the resources to allocate the UE. Once the target cell acknowledges the UE to be handed over, the HO execution starts and the UE releases its connection with the serving cell. Then, the UE proceeds to access the target cell via the random access channel (RACH). Upon successful synchronization with the new cell, the HO is completed with a confirmation notification from the UE to the network.

The HO algorithm has been thoroughly designed to provide the best performance in terrestrial scenarios. Besides, it can be tuned according to the requirements of the network. Factors such as UE speed, radio network deployment, propagation conditions and system load are considered during the configuration of the HO. To this end, the network signals the UE with a set of HO parameters - among them there are the HOM and the TTT [10]. Furthermore, different events define the criteria for MR triggering [10]. A commonly

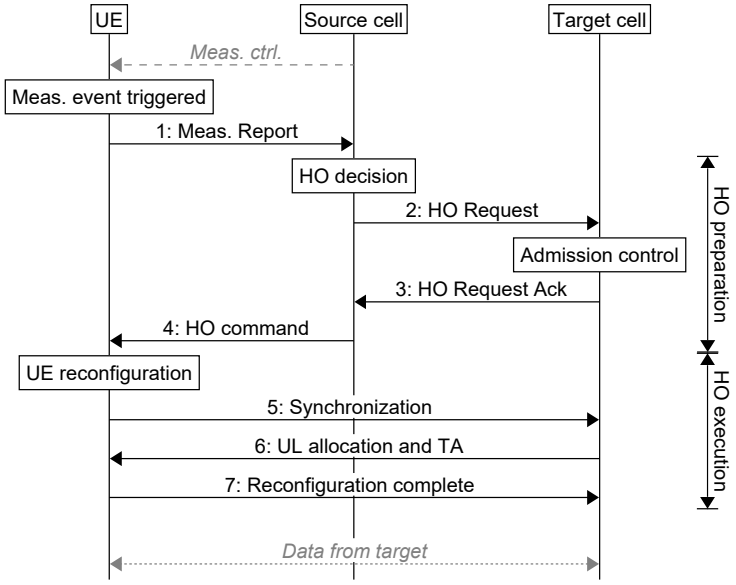


**Fig. III.2:** Conventional UE-assisted network-controlled HO procedure.

used trigger is the NR event A3. Based upon RSRP measurements, the event A3 is triggered when the RSRP of a neighbouring cell becomes HOM dB better than the RSRP of the serving cell for a period of TTT ms.

The HO configuration needs the suitable adjustments of its control parameters to achieve optimal performance. Several mobility related KPIs are defined by 3GPP to evaluate the mobility performance [9]. The following section presents the KPIs used in this paper to conduct the HO study.

## 3.2 Mobility Key Performance Indicators

The following statistics have been collected in the course of our simulations:

- Geometric DL SINR as a function of time [dB].
- Number of RLF events per UE over time [RLF/UE/s]. A RLF event is declared after N310 consecutive out-of-sync indications (e.g., SINR below -8dB) and expiration of timer T310 [10].
- HOF rate defined as the total number of HO failures relative to the total number of HO attempts. A HOF is counted if a RLF occurs after event A3 entering condition is satisfied but before the UE receives the HO command or a downlink control channel failure is detected after event A3 entering condition but before HO completion.

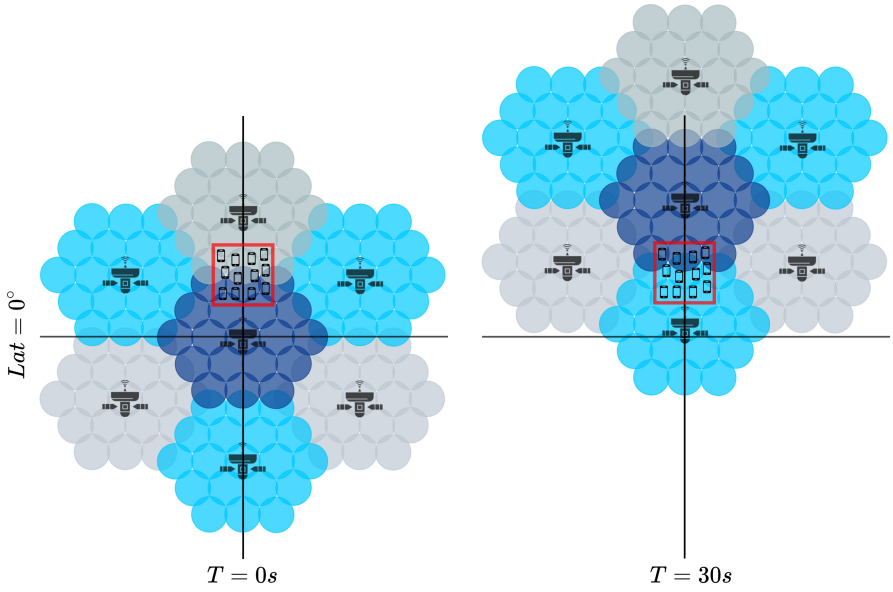


**Fig. III.3:** Simulation scenario: stationary UEs being served by a constellation of 7 satellites operating with Earth-moving cells and a regenerative payload. Beams with the same colour belong to single satellite. Note the area and size of the UEs is not to scale, but merely included to indicate approximate location and satellite movement.

- PP rate [%]. A PP event is declared when a UE experiences a HO from cell A to B and handovers back to cell A within ping-pong-time (1 sec). The PP rate is defined as the number of PP relative to the total number of successful HO.
- Average time in outage [%] defined as the ratio between the total time in outage (i.e., interruption time during HO, HOF and radio link problems) and the total service time.

A wrong choice of HO settings can lead to unnecessary HO (i.e., PP effect), HOFs and RLFs. On the one hand, a growth in number of PPs comes with a signalling overhead including a load on the RACH of the target cell. On the other hand, RLFs and HOFs involve a long time in outage and it might cause a call drop if re-establishment fails.

# 4 Methodology

## 4.1 Simulation assumptions

In this study, we evaluate a constellation of 7 LEO satellites implementing a regenerative payload. The satellite network is organized in 3 polar orbital planes with an inclination of 90° and a longitude offset of the ascending node of 1.36°. An NR cell corresponds to a satellite beam in our study. Each LEO satellite operates 19 satellite beams with a footprint diameter on the ground of 50 km and an inter-cell distance of 43.3 km. As reported in [7], a 50 % beam overlapping is used for outer beams neighbouring an adjacent satellite coverage. As it can be observed from our scenario depicted in Fig. III.3, satellite beams are continuously moving on Earth. In other words, the satellite is generating beams which footprint is sweeping on the ground. Moreover, ideal Doppler compensation is assumed at satellite payload side.

From the UE's standpoint, a rural environment is used considering continuous LOS between satellite and terminal. 20 stationary UEs are uniformly distributed within an area of 55 km $\times$ 55 km close to the equator. UEs establish the connection to the optimal cell based on the strongest RSRP criteria. Besides, a Gaussian error process is introduced in the UE's measurement model. Such measurements are filtered by the UE at layer 1 and layer 3 where the latter is using a single tap IIR filter [10]. We employ a simplified random access (RA) scheme, which models the RA message propagation delays but not potential RA message failures. The satellite payload characteristics and the channel propagation model are defined according to 3GPP technical report [6] and [7], respectively. An aspect to underline is the elevation angle dependency of this model. This means that both shadow fading and fast fading parameters are recalculated depending upon satellite and UE positions. Regarding the traffic network load, 30 % of the Resource Blocks available in a cell are loaded, generating uniform downlink interference conditions. The MR is triggered using the NR event A3 explained in Section 3. The main simulation parameters are included in Table III.1.

Furthermore, we conduct system-level simulations of two terrestrial environments; UMa and HST. Although there are differences between terrestrial and non-terrestrial deployments, specially the channel conditions, we provide the terrestrial simulation results to facilitate a comparison of the NTN mobility performance with two well-known scenarios, where user mobility experience is satisfactory. To obtain the results, we use the same system-level simulator and the optimal HO configuration for each case (see Table III.2). The UMa scenario consists in a network composed by 21 wrapped around cells (7 sites) with 200 m ISD. UEs are uniformly distributed with random initial positions and moving at 3 km/h and 30 km/h speeds. In the HST case, UEs on board of a train at 500 km/h are simulated. The network is built upon 5 sites, with 2 cell per site and 1000 m ISD, and 2 wrap-around areas from both ends. The distance between cells and railroad track is 100 m. Both

scenarios are 3GPP compliant and further details of the simulation assumptions can be found in [9] and [11].

**Table III.1:** System-level simulation assumptions

| **Parameter** | **Values** |
|---|---|
| Satellite altitude | 600 km |
| Satellite antenna pattern | Section 6.4.1 in [6] |
| Satellite equivalent isotropic radiated power density | 34 dBW/MHz |
| 3 dB beamwidth | 4.4127° |
| Satellite Tx max Gain | 30 dBi |
| Satellite beam diameter | 50 km |
| UE Tx power | 23 dBm |
| Deployment scenario [6] | NTN Rural |
| Shadow Fading ($\sigma$) [6] | 1.79 to 0.72 dB |
| Fast Fading, K-factor ($\mu, \sigma$) [6] | 24.72 to 3.59 dB,<br>5.07 to 1.77 dB |
| Carrier frequency | 2 GHz (S-Band) |
| System Bandwidth | 10 MHz |
| Sub-carrier spacing | 15 kHz |
| Traffic model | Full Buffer |
| Traffic load | 30 % |
| Radio Link Failure [10] | Qin/Qout threshold: $-6$ dB/$-8$ dB<br>T310 timer: 1000 ms<br>N310/N311: 1 |
| UE's measurement error ($\sigma$) | 1.72 dB |
| L3 filter coefficient K | 4 |
| Time-to-trigger | 0 ms, 100 ms and 256 ms |
| HO margin | 0 dB, 1 dB, 2 dB and 3 dB |
| Simulation time | 30 s |

## 4.2 Simulation tool

Performance results in this study were generated by using a fully dynamic system-level simulation tool modelling NR PHY and MAC layers with a high level of detail following 3GPP specifications. The simulator offers a realistic

analysis of mobility and handovers while operating on an OFDM symbol-subcarrier resolution. It has been widely used in 3GPP standardization as well as in scientific publications [9] [12]. To obtain reliable results it includes a validated stochastic NTN channel model; implemented according to the specifications in [6] and calibrated against similar models used in 3GPP as stated in [7]. To achieve statistically stable results, 50 simulations are realized and combined for each pair of HOM and TTT values in Table III.1.

# 5 Performance Results

## 5.1 Handover performance in LEO-based NTN

Fig. III.4 shows the system-level simulated DL SINR experienced by a UE as a function of time. Two HO configurations have been included; 0 dB and 3 dB HOM and 0 ms and 256 ms TTT. Furthermore, the theoretical optimal DL SINR is included to provide a view on the upper bound. This metric is calculated by comparing the UE's best RSRP measurement per simulation step with the RSRP of all other cells. It is interesting to point the gap between the optimal and the simulated DL SINR reflecting the impact of the HO latency in the metric performance. The UE is establishing the connection to the serving cells at a late stage, i.e. when the beam signal starts to fade. Moreover, the majority of HOs occur when the DL SINR levels are very low. This might be explained by a re-establishment occurring after potential HOF or RLF.

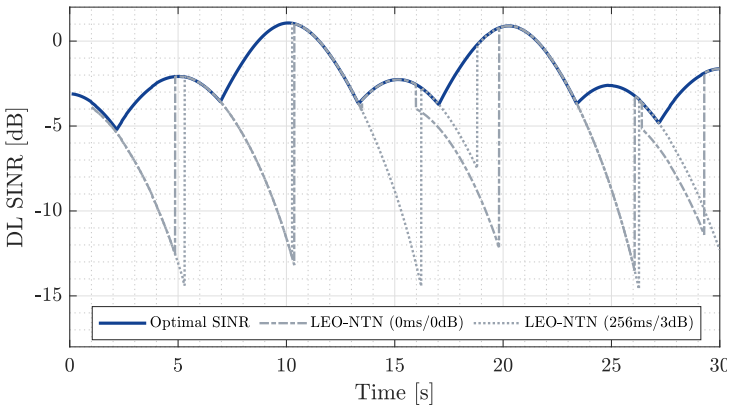


**Fig. III.4:** Optimal and simulated DL SINR as a function of time for a UE configured with 0 dB and 3 dB HO margin and 0 ms and 256 ms time-to-trigger.

Fig. III.5 depicts the ratio of HOFs as a function of HOM and TTT. As expected, HOFs increase with HOM and TTT. Interestingly, HOM has a higher

influence on the HOF metric than TTT. This fact can be observed when HOM increases from 0 dB to 1 dB, irrespectively of the TTT. The lowest HOF rates - about 20 to 40 % - are achieved when HOM is 0 dB with a global minimum of 20 % when TTT is 0 ms. Therefore, the best achievable performance is reached when HOM and TTT are both set to 0.

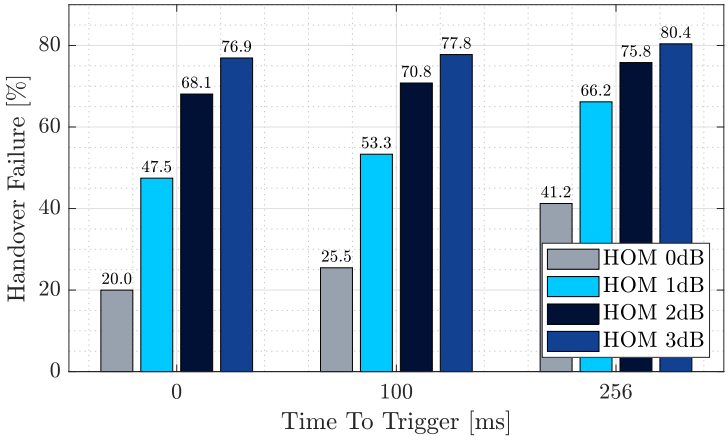


**Fig. III.5:** HOF rate dependency on HO margin and time-to-trigger for LEO-based NTN.

The RLF and PP rates are shown in Fig. III.6. One can observe that both RLFs and PPs are heavily impacted by increasing the HOM and the TTT. Confirming the performance observed in Fig. III.5, RLFs significantly grow with HOM. In fact, the RLF rate rises by a factor of 2 when no TTT is used and HOM transitions from 0 dB to 3 dB. In contrast, the PP metric is affected by aggressive HO configurations (i.e., low HOM and low TTT) due to the effect of fading variations and the measurement model. A PP rate of 30 % can be seen when 0 dB HOM and 0 ms TTT are used and it drops to 10 % when TTT is extended. The rate is significantly reduced as soon as the HOM is non-zero with a marginal impact when HOM is set above 1 dB. Thus, a similar trade-off as in terrestrial networks can be seen when comparing RLFs and PPs. In the case under study, the best compromise is achieved when HOM is 0 dB and TTT is 256 ms. Nonetheless, this HO configuration involves more than 40 % of HOFs (see Fig. III.5). In general, a certain level of PPs are acceptable if RLFs are mitigated but in NTN deployments, to cope with long delays and challenging link budgets, unnecessary HOs (PPs) should be reduced.

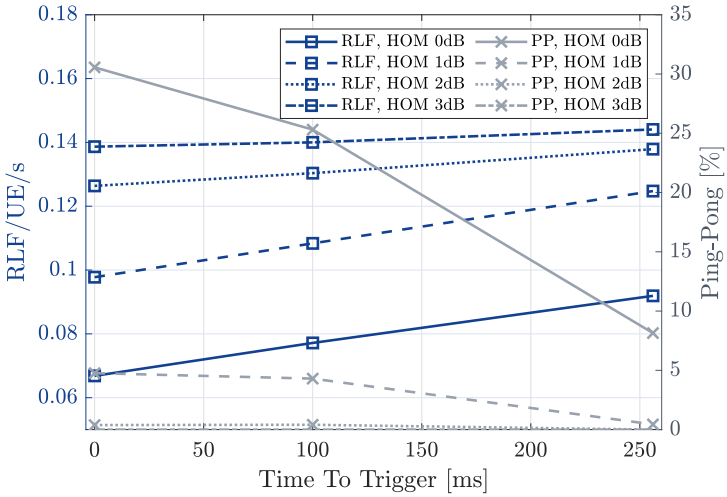


**Fig. III.6:** RLF and PP rates dependency on HO margin and time-to-trigger for LEO-based NTN.

## 5.2 Comparison with terrestrial cases

In this section, we compare the LEO-based NTN performance with UMa and HST scenarios using the HO parameters indicated in Table III.2. Fig. III.7 reflects the HOF rate for the aforementioned deployments. Mobility optimization processes usually aim to target the HOF rate below 2 %. This fact can be noted since UMa deployment establishes an upper bound for the terrestrial scenarios of 2 % of failures. In contrast, the most optimal HO configuration in LEO-NTN presents a performance loss by a factor 10 relative to the UMa case.

**Table III.2:** HO parameters used to compare LEO-based NTN, UMa and HST scenarios

| **Deployment scenario** | HO margin | Time-to-trigger |
|---|---|---|
| LEO-based NTN | 0 dB | 0 ms |
| UMa | 2 dB | 160 ms |
| HST | 1 dB | 0 ms |

The results in Fig. III.8 depict mobility performance in terms of RLFs and PPs. Regarding the RLFs, all the terrestrial scenarios manage to maintain a marginal number of RLFs compared to LEO-NTN where the proportion of RLFs is roughly one order of magnitude higher. Nonetheless, UMa deployment, when UEs move at 3 km/h, show the largest PP proportion of the terrestrial scenarios and is similar to LEO-NTN performance. This can be jus-

tified by the fact that these UEs, with low mobility, will stay longer periods in cell edge conditions increasing the probability of PP. Eventually, it has to be noted that terrestrial performance present a clear trade-off between RLFs and PPs whereas LEO-NTN is not able to reach similar low RLF rate when allowing high number of PPs.

The final result in Fig. III.9 demonstrates the time in outage, which is the KPI that directly impacts the user experience. The distribution reflects that in LEO-NTN 60 % of the UEs experience an outage time larger than 5 %, relative to the call time. In our simulations the call time corresponds to the simulation time. In addition, 5 % of those UEs can experience outages for longer periods than 15 % of the call. Compared to terrestrial networks that show an average time in outage below 2.5 % of the call, UEs connected to a LEO-NTN deployment experiences an average time in outage from 8 % to 18 % depending upon the configuration.

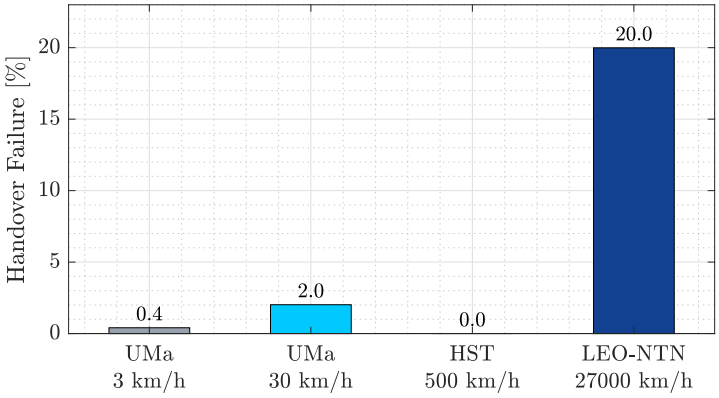


**Fig. III.7:** HOF rate comparison for UMa, HST and LEO-NTN scenarios.

# 6 Discussion

Our simulations indicate the conventional 5G NR HO algorithm fails to provide seamless connectivity in LEO-based NTN. Even in a favourable scenario without LOS blockages, the conventional 5G NR HO cannot guarantee an acceptable user experience. The major challenge for mobility management is to address HO lateness and unnecessary HOs. Analysis of the HOF and RLF indicate a majority of failures occur during UE reception of the HO command from the serving cell. Typically in terrestrial networks, more aggressive HO configurations are used to handle HO lateness and improve the HO reliability. However, this strategy proved not sufficient in LEO-NTN.

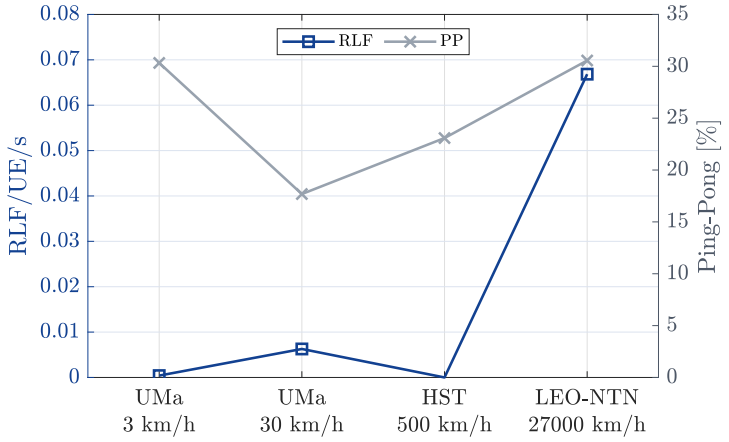


**Fig. III.8:** RLF and PP rate comparison for UMa, HST and LEO-NTN scenarios.

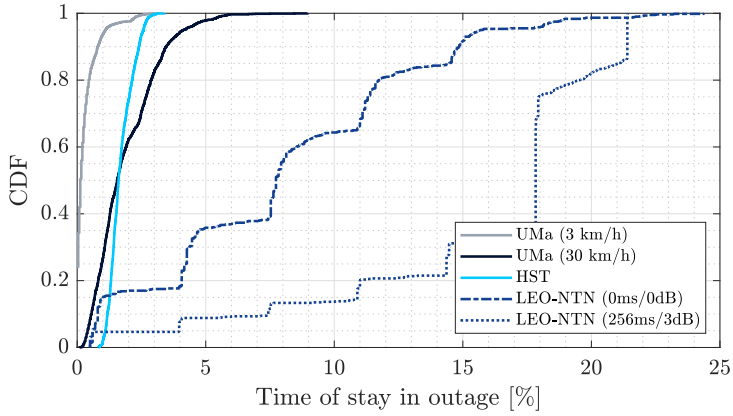


**Fig. III.9:** Distribution of the time of stay in outage for UMa, HST and LEO-NTN scenarios.

We observed that the high number of failures and PPs is due to a combination of factors but intrinsic to LEO satellites. Firstly, there is a low signal variation between the cell centre and cell edge conditions. The propagation distance is orders of magnitude longer than the cell size hindering the UE measurements. Secondly, there exists a high downlink interference from adjacent satellite beams. This fact results in a lower average DL SINR of $-2$ dB for LEO-NTN compared to 2–3 dB and 9 dB for UMa and HST, respectively. Thirdly, there is fast signal fading as a consequence of the high-speed cell mobility and the narrow antenna pattern. Finally, propagation delays, owing to long communication distances, delays all control messages and, hence, the HO latency.

# 7 Future work

Based on the results in Section 5, we conclude that LEO-based NTNs demand new mobility solutions to ensure service continuity. A promising enhancement is related to the knowledge of satellite movement. LEO constellations imply several challenges but the orbits are deterministic and, therefore, the network may predict which beam covers best a given UE, the duration that the UE will remain covered and the best next beam candidate to handover to. Such approach may optimize the triggering of the HO events and, in case of failure, improve the connection reestablishment process. The approach may be supported by the use of conditional HO (C-HO). Simulation results indicate the HO preparation phase is the most vulnerable since the HO process starts when the serving cell radio link is too weak (see Fig. III.4). The C-HO enables the preparation phase to occur early, when the serving cell link is still reliable. Thus, the network may prevent HOFs due to late HOs using the C-HO and, together with the knowledge of satellites movement, foresee the most appropriate target cell.

# 8 Conclusions

This work has analysed the handover performance in a low Earth orbit based non-terrestrial network scenario. System-level simulations indicate that mobility based on a conventional 5G NR break-before-make, UE-assisted, network-controlled handover algorithm cannot guarantee robust service continuity, even under favourable propagation channel conditions. The best achievable performance is obtained by the most aggressive configuration, i.e. 0 ms time-to-trigger and no handover margin. The results obtained for this configuration showed a handover failure ratio of 20 % together with a ping-pong rate equal to 30 %. Further analysis exposed that mobility performance is dominated by handovers happening too late. This is caused by cells moving at a relative speed of 7.5 km/s, long communication distances and high downlink interference. Additionally, the handover performance is compared with two 3GPP terrestrial scenarios - urban macro and high-speed train - showing that non-terrestrial networks perform 10 times worse in terms of handover failures and radio link failures. Therefore, based on the simulations, it is concluded that new mobility solutions are necessary to address the challenges introduced by these satellite systems. These challenges underline the lack of scalability and robustness of the conventional terrestrial handover mechanism, which was not designed to meet non-terrestrial network requirements. Finally, some potential new directions were discussed and include a fully network-controlled handover exploiting the knowledge of satellites' movement and the use of the conditional handover.

# References

[1] A. Guidotti, A. Vanelli-Coralli, M. Conti, S. Andrenacci, S. Chatzinotas, N. Maturo, B. Evans, A. Awoseyila, A. Ugolini, T. Foggi *et al.*, "Architectures and Key Technical Challenges for 5G Systems Incorporating Satellites," *IEEE Transactions on Vehicular Technology*, 2019.

[2] 3GPP, "Study on Scenarios and Requirements for Next Generation Access Technologies (Release 15)," TR 38.913 V15.0.0, Jun. 2018.

[3] I. Philbeck, "Connecting the Unconnected: Working Together to Achieve Connect 2020 Agenda Targets," in *Broadband Commission and the World Economic Forum at Davos Annual Meeting*, 2017.

[4] E. Feltrin and E. Weller, "New frontiers for the mobile satellite interactive services," in *IEEE Advanced Satellite Multimedia Systems Conference*, 2010.

[5] G. Denis, D. Alary, X. Pasco, N. Pisot, D. Texier, and S. Toulza, "From New Space to Big Space: How Commercial Space Dream is Becoming a Reality," *Acta Astronautica*, 2020.

[6] 3GPP, "Study on New Radio (NR) to support Non-Terrestrial Networks (Release 15)," TR 38.811 V15.2.0, Sept. 2019.

[7] ——, "Solutions for NR to support Non-Terrestrial Networks (NTN) (Release 16)," TR 38.821 V1.0.0, Dec. 2019.

[8] ——, "Solutions for NR to support Non-Terrestrial Networks (NTN) (Release 17)," RP-193234, 3GPP TSG RAN Meeting 86, Dec. 2019.

[9] ——, "E-UTRA Mobility Enhancements in Heterogeneous Networks (Release 11)," TR 36.839 V0.7.1, Aug. 2012.

[10] ——, "Radio Resource Control (RRC) protocol specification (Release 15)," TS 38.331 V15.8.0, Dec. 2019.

[11] ——, "System simulation results and RRM Requirements NR HST," R4-1914538, 3GPP TSG RAN WG4 Meeting 93, Nov. 2019.

[12] S. Barbera, L. C. Gimenez, L. L. Sánchez, K. I. Pedersen, and P. H. Michaelsen, "Mobility Sensitivity Analysis for LTE-Advanced HetNet Deployments with Dual Connectivity," in *IEEE 81st Vehicular Technology Conference (VTC Spring)*, 2015.

# Paper D

## Performance Evaluation of the 5G NR Conditional Handover in LEO-based Non-Terrestrial Networks

Enric Juan, Mads Lauridsen, Jeroen Wigard, Preben Mogensen

The paper has been published in the
*IEEE Wireless Communications and Networking Conference (IEEE WCNC), 2022.*

*The layout has been revised.*

# Abstract

*The development of non-terrestrial networks (NTN) aims to satisfy the requirements of ubiquitous and seamless coverage for fifth-generation (5G) services. Low Earth orbit (LEO) satellites introduce challenging mobility requirements to the 5G New Radio (NR) radio resource management procedures. Current research shows that the baseline 5G NR UE-assisted network-controlled handover (HO) procedure, meant for terrestrial scenarios, fails to ensure continuous and satisfactory service in LEO-based NTN. The conditional handover (CHO), specified by 3GPP in Rel-16, was designed for terrestrial networks to enhance mobility robustness by making HO decisions earlier. In this work, we conduct system-level simulations to evaluate the 5G NR mobility performance of the CHO in a LEO-based NTN with Earth-moving cells scenario. The simulation results show that the CHO procedure reduces the radio link failures and handover failures to 0 but increases the unnecessary HO rate by more than 60% in comparison with the baseline HO, which leads to an increase of the signalling and measurement reporting. Finally, future research directions are identified to address the increase of the signalling overhead by exploiting the predictability of the satellite's movement.*


# 1 Introduction

While the 5G of mobile communications continues its roll-out, the idea of providing Internet from space through constellations of LEO satellites strengthens. Private mega-projects such as SpaceX's Starlink and Amazon's Kuiper continue to make progress on the road towards non-terrestrial data services. These massive constellations aim to cover Earth's areas that lack adequate connectivity with at least 4425 and 3236 satellites, respectively [1]. This new space race fuels the development of NTN in 3GPP [2]. After the study item in NR Rel-16, 3GPP decided to start a work item on NTN for NR Rel-17 [3]. This release, due out in early 2022, will be the first to address the satellite technology as part of the 5G NR ecosystem.

LEO-based NTN are characterized by highly mobile satellites able to provide global broadband access on Earth. Compared with TNs, the radio access nodes are constantly in motion. This inherent nature causes frequent HOs, which leads to an increase of the signalling overhead and potential service outages [4]. Unless HO mechanism is carefully designed, the required QoS cannot be guaranteed.

The HO over LEO satellite networks has been addressed in the literature since the 1990s with the emergence of projects like Iridium and Globalstar. The studies reported in [5] and [6] proposed HO schemes to guarantee resources to maintain the user's communication but they only considered specific constellations and simple QoS criteria. In recent years, the new broad-

band LEO constellations demanded more stringent QoS requirements. In [7], the authors proposed a Reinforcement Learning scheme to optimize the UEs decisions and avoid frequent HOs among non-terrestrial base stations. Li *et al.* proposed in [8] a user-centric HO which exploits satellite's storage capability to address the frequent HO problem. Nonetheless, to the best of our knowledge, none of the works in past literature considered HO solutions supported by 3GPP-compliant 5G-based NTN systems.

Our work in [4] highlighted that 3GPP NR LEO-based NTNs require new mobility solutions for EMC since the baseline break-before-make UE-assisted network-controlled HO cannot provide a robust and reliable service. The key issue is that UEs experience frequent outages due to late HO decisions where the serving cell signal quality is too low to complete the HO signalling.

3GPP specified in Rel-16 the CHO as a mobility enhancement to reduce the number of outages and improve the service robustness. The CHO performs an early HO preparation when serving cell radio conditions are still good and allows the UE to access the target cell late when target cell link is reliable.

Despite the CHO has been proposed as a potential procedure to improve the HO robustness in NTN [9], no simulation results have been provided to prove it. To address an optimal design of the mobility management algorithms, simulation results are necessary to determine the advantages and also to pinpoint the associated costs. In this paper, we contribute with a 5G NR mobility performance study of the use of the CHO in LEO-based NTNs. System-level simulation results are presented where the CHO performance is compared against the BHO in a 3GPP-compliant scenario.

The rest of the paper is organized as follows. Section 2 describes the limitations of the conventional BHO procedure in NTN. Section 3 introduces the CHO procedure and its advantages. The KPIs collected during our simulations are detailed in Section 5, while in Section 4 the system-level simulation methodology is explained. Section 6 presents the performance results, discussion and future work are elaborated in Section 7 and, finally, Section 8 concludes the paper.

## 2 5G NR Baseline Handover and its limitations in Earth Moving Cells scenarios

5G NR baseline HO procedure is defined in [10] and [11]. The HO mechanism is a key procedure that ensures UEs can move from one cell to another without noticeable service interruption. Based on DL channel measurements, the UE initiates a HO from its serving cell to a target cell when a signal strength condition is fulfilled for a certain time called TTT. A common condition is

the NR event A3, which is based on RSRP and is triggered when target cell's RSRP becomes HOM dB better than the serving cell's RSRP.

Once the event condition is met, the UE sends a MR to the serving cell. The HO preparation starts with the serving cell deciding whether the UE shall be handed over to the target cell. After the target cell preparation, the serving cell sends a HO command to the UE with instructions to establish a new connection towards the target cell. Nonetheless, the break-before-make HO procedure can fail due to several factors such as an abrupt degradation of the serving cell radio link. In that case, the MR transmission could never reach the network or, even if it does, the UE may never receive the HO command. This results in a failure that brings the UE into connection re-establishment, which translates into a service interruption and a higher UE's energy consumption.

HO failures are usually triggered by channel impairments, a sub-optimal configuration of the HO parameters, UE's mobility and target cell interference. These failures can be defined as wrong decisions categorized as: i) too early HO, ii) too late HO and iii) HO to a wrong cell. The first case results in a successful connection but the UE handovers back to the previous serving cell due to cell edge conditions and inaccuracies in the UE's measurements. This effect is defined as PP. The second case occurs when the serving cell channel quality drops too low before HO completion and the UE goes into cell re-establishment. The third case refers to a UE which connects to a new cell for a very short time before the UE initiates the HO procedure again.

In LEO-based NTN, the mobility of the satellites characterizes a highly dynamic environment which motivates the need for new HO solutions. The work in [4] evaluated the BHO performance in LEO-based NTN implementing EMC which refers to cells that sweep the ground and move with the speed of the satellite, i.e. 7.5 km/s, while the satellite points always towards nadir. The study showed that the BHO presents a best achievable HOF ratio of 20 %, which is not compatible with a sufficient service robustness. The combination of the fast moving cells, the high DL interference and the limiting link budget causes that the serving signal quality is too low at the time of the HO decision and, hence, the UE goes into cell re-establishment. Even when the HO is successfully completed, the connection towards the target cells is established late and at that time the new serving signal quality is already decreasing. Fig. III.1 illustrates how the signal quality, expressed in terms of DL SINR, rapidly drops below $-6$ dB, which is a lower bound for physical downlink control channel (PDCCH) decoding. The figure includes the upper bound that the system can achieve plus the BHO performance using two configurations, i.e. one set with 0 ms TTT and 0 dB HOM and another one with 256 ms TTT and 3 dB HOM.

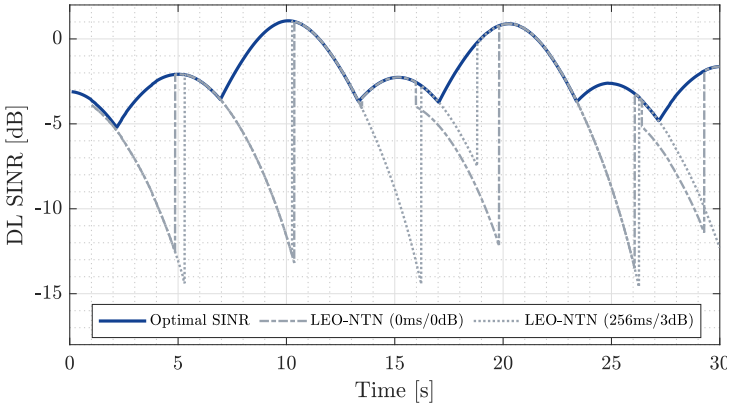


**Fig. III.1:** Downlink SINR as a function of time experienced by a UE served by a LEO-based NTN [4, Fig. 3].

# 3 Conditional Handover

Most of the HO solutions studied for TN, such as the make-before-break HO and the random access channel-less HO [12], were mainly focused on reducing the HO interruption time. The CHO procedure, which conducts an early HO preparation when the serving cell link is still reliable, is the only enhancement proposed for HOF mitigation in environments where the UE experiences rapid received signal attenuation. The CHO allows to initiate the HO earlier but also to delay the access attempt to the target cell until the target cell radio link is strong enough. This reduces the risk of failure since ensures that the transmission of the MR and the reception of the HO command occur in good radio conditions. The authors in [13] showed that even the simplest CHO implementation improved the UE's mobility performance in TNs by reducing the HOF and, hence, the time in outage. The CHO procedure, defined in [10] and [11], was standardized for 5G NR Rel-16 and it has been identified as a potential solution for NTN [2].

Fig. III.2 shows the operational flow of the CHO mechanism. It is characterized by two event conditions denoted as the preparation event ($C_{prep}$) and the execution event ($C_{exec}$). Both events can be configured differently, which allows a HO triggering based on different measurement quantities like RSRP and RSRQ. The $C_{prep}$ condition functions as the BHO triggering condition and, when is fulfilled, the UE sends a MR to the serving cell (see Steps 1–2 in Fig. III.2). This event is configured with values close to zero, even negative ones, to prompt an early HO preparation. The process continues with the serving cell requesting the target cell for preparation and, if the target cell accepts, the serving cell forwards the HO command to the UE (Steps 3–7).

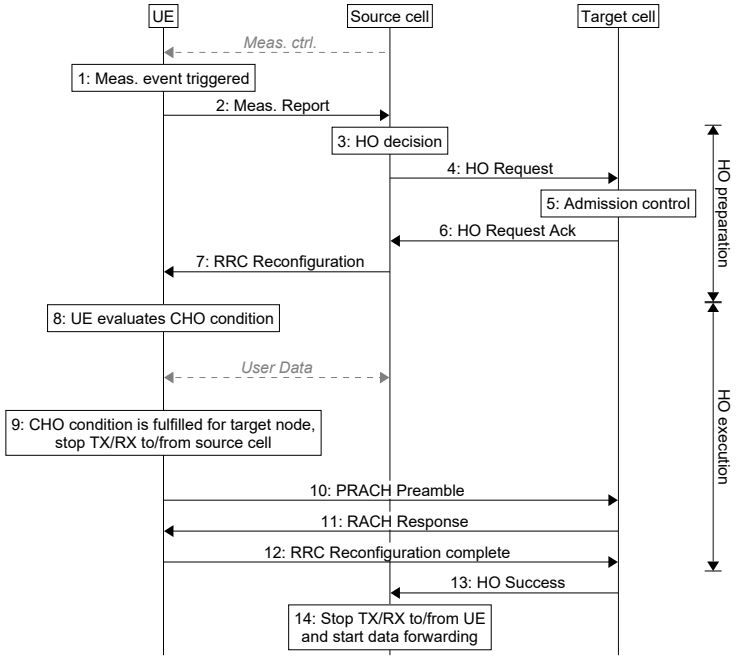


**Fig. III.2:** Basic operational steps of the Conditional Handover.

At this step, the UE stores the HO command instead of initiate the access to the target cell. As part of the HO command, the UE receives the $C_{exec}$ to be monitored and a list of prepared target cells. Now the UE is measuring and evaluating the list of prepared cells against $C_{exec}$ condition (Step 8). When $C_{exec}$ is fulfilled, the UE autonomously starts the HO execution (Steps 9–12).

# 4 System Simulation Methodology

## 4.1 Scenario Overview

Fig. III.3 depicts the simulated scenario with a constellation of 7 LEO satellites mounting a regenerative payload, i.e. a payload with gNB capabilities. The constellation is constituted by 3 polar orbits with an inclination of 90° and a longitude offset of the ascending node of 1.36°. The satellites operate with EMC where a satellite beam corresponds to an NR cell. A satellite implements 19 satellite beams/NR cells with a footprint diameter on the ground of 50 km and an inter-cell distance of 43.3 km. For each satellite, the NR cells on the ground are distributed in 3 tiers, i.e. one central cell circled by two outer rings. There is a 50 % cell overlap for those cells neighbouring an adjacent satellite coverage as indicated in [2].

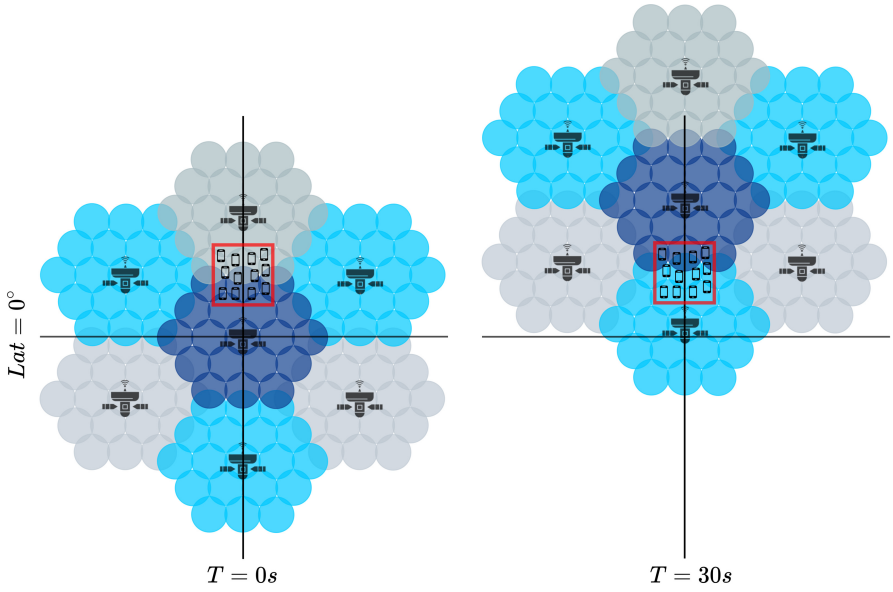


**Fig. III.3:** Simulation scenario: stationary UEs being served by a constellation of 7 satellites operating with Earth-moving cells. Beams with the same colour belong to a single satellite. Size of UEs, satellites and coverage area are not to scale [4, Fig. 3].

## 4.2 UE and Network parameters

A rural environment is simulated with 20 stationary UEs uniformly distributed within an area of 55 km × 55 km close to the equator. The UEs connects to the best cell based on the strongest RSRP. The UE has one omnidirectional antenna for reception. The UE's measurement model considers a Gaussian error process. UE measurements are filtered at layer 1 and layer 3 where the latter uses a single tap IIR filter [11]. A simplified random access (RA) scheme, which models the RA message propagation delays but not potential RA message failures, is used. The satellite payload characteristics are set following the 3GPP technical report [2]. 25 % of the physical resource blocks (PRBs) available in each cell are loaded in order to generate uniform DL interference conditions. We assume ideal Doppler compensation. Table III.1 contains the main simulation parameters.

## 4.3 Radio Propagation Model

We use the radio channel model reported in [15]. This large-scale propagation model describes realistically the time variations of the LEO-to-Ground path loss, including the LOS changes and the impact of the surrounding buildings

**Table III.1:** System-level simulation assumptions.

| **Parameter** | **Values** |
|---|---|
| Satellite altitude | 600 km |
| Satellite antenna pattern | Section 6.4.1 in [14] |
| Satellite equivalent isotropic radiated power density | 34 dBW/MHz |
| 3 dB beamwidth | 4.4127° |
| Satellite Tx max Gain | 30 dBi |
| Satellite beam diameter | 50 km |
| UE Tx power | 23 dBm |
| Deployment scenario | Rural [15] |
| Shadow Fading ($\sigma$) | 0.3 to 7.4 dB [15] |
| Carrier frequency | 2 GHz (S-Band) |
| Frequency reuse | FR1 |
| System Bandwidth | 10 MHz |
| Sub-carrier spacing | 15 kHz |
| Traffic model | Full Buffer |
| Traffic load | 25 % PRBs |
| Radio Link Failure [11] | Qin/Qout threshold: $-6$ dB/$-8$ dB<br>T310 timer: 1000 ms<br>N310/N311: 1 |
| UE's measurement error ($\sigma$) | 1.72 dB |
| L3 filter coefficient K | 4 |
| Receiver type | LMMSE-IRC [2] |
| Time-to-trigger | 0 ms, 100 ms and 256 ms |
| HO margin | 0 dB, 1 dB and 3 dB |
| Simulation time | 30 s |

and objects near the UE. The time-correlated model considers the general dependencies as a function of the elevation angle and the angular distance to the LOS state transition angle. It is assumed that the fast fading is averaged out by the UE's recursive measurements.

### 4.4 System-level Simulation Tool

Performance results are obtained using a fully dynamic system-level simulation tool which models NR PHY and MAC layers according to 3GPP specifications. It provides a realistic evaluation of the mobility procedures while operating at an OFDM symbol-subcarrier resolution. The proprietary tool has been broadly used in 3GPP standardization [16] and scientific publications [4]. 50 simulations are conducted and combined to achieve statistically stable results.

### 4.5 Modelling of the Conditional Handover

To model the CHO, we introduce a set of modifications to the existing HO implementation. The steps in Fig. III.2 are used to support the description. Steps 2–7 are set as zero-time and error-free. By doing this, Step 1 acts as Step 8 and, then, the BHO triggering condition becomes CHO condition $C_{exec}$. It is assumed that condition $C_{prep}$ and the following CHO preparation phase (Steps 1–7) are free of errors since it always occurs when the serving cell link is reliable and, therefore, no radio link failures are expected.

## 5 Key Performance Indicators

The following statistics have been collected to evaluate the 5G NR mobility performance:

### 5.1 Signal-to-interference-plus-noise Ratio

The DL SINR is defined as the ratio of the received signal power relative to the sum of interference power from neighbouring cells and noise. It indicates the quality of the radio channel and has a direct impact on the UE's throughput.

### 5.2 Radio Link Failure and Handover Failure

A relevant metric to assess the mobility robustness is the number of radio link failures. The timer *T310* is started when UE's SINR falls below the threshold $Q_{out}$, typically $-8$ dB. After *T310* expiration, a RLF is declared. This timer is stopped if the signal-to-interference-plus-noise ratio (SINR) exceeds the threshold $Q_{in}$, typically $-6$ dB. Further details about the complete procedure are found in [11].

As a subset of the RLF, the HOF is defined for RLFs declared during the HO procedure in two cases: i) if a RLF is declared after an event entering condition is satisfied but before the UE receives the HO command or ii) if

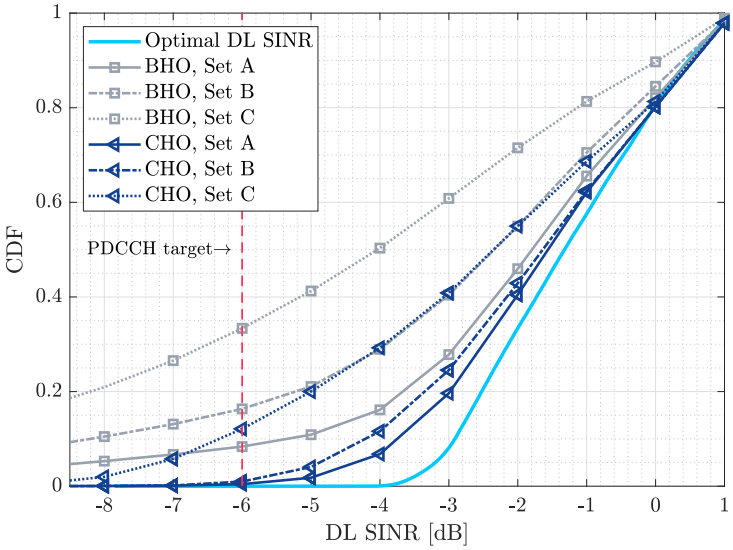


**Fig. III.4:** Distribution of the DL SINR for BHO and CHO procedures.

a DL control channel failure is detected after event entering condition but before HO completion.

### 5.3 Time of Stay and Time in Outage

The time that a UE stays in a cell, also called time-of-stay (ToS), is used to evaluate the HO frequency and the PP behaviour. We define the ToS in *cell A* as the duration from when the UE sends a *HO complete* message to *cell A* to when the UE sends a *HO complete* message to *cell B*.

The ToO is defined as the time that a UE spends in HO interruption time, HOF and in radio link problem conditions.

### 5.4 Unnecessary Handover and Ping-pong

We consider an UHO when a UE handovers from *cell A* to *cell B*, stays in *cell B* less than 1 s, and immediately handovers again to *cell C*.

A PP event is declared when a UE handovers from *cell A* to *cell B* and handovers back to *cell A* within a certain ToS (typically 1 s).

## 6 Performance Results

This section presents the mobility performance of the CHO procedure compared against the BHO procedure. Both procedures are configured with the

NR A3 triggering event and set according to the parameters in Table III.2. Regarding the CHO, these HO parameters are applied to the execution event condition $C_{exec}$.

**Table III.2:** Simulated HO configuration sets.

| **HO parameter** | **Set A** | **Set B** | **Set C** |
|---|---|---|---|
| HO margin (dB) | 0 | 1 | 3 |
| Time-to-trigger (ms) | 0 | 100 | 256 |

Fig. III.4 illustrates the CDF of the system-level DL SINR. Apart from the six cases compared - three HO configurations per each HO mechanism - the figure includes the optimal DL SINR to provide the upper bound limit of the performance. This bound is obtained considering that the UEs always select the best cell based on the simulated UE's RSRP measurements. The figure shows that the CHO procedure improves the BHO performance, regardless the HO configuration. The CHO configured with *Set A* presents the closest performance to the optimal DL SINR. The CHO presents approximately a 2 % and 12 % of users below the PDCCH target, i.e. $-6$ dB, where the latter corresponds to *Set C* and the former to *Set A* and *Set B*. For the BHO cases this percentage grows until 9 %, 17 % and 35 % for *Set A*, *Set B* and *Set C*, respectively.

Fig. III.5 depicts the $5^{\text{th}}$ percentile DL SINR against the successful HO rate. It also includes the optimal value of each metric. Such references are estimated by considering an ideal HO procedure where UEs always select the most suitable target cell at the right time. The figure presents the cost of improving the DL SINR at the expense of a higher HO rate. The three configurations sets of the BHO show DL SINR values 5–9 dB below the optimal, while regarding the CHO these values drop to 1–4 dB. In terms of the successful HO rate, the CHO procedure when is configured with *Set B* and *Set C* performs closest to the optimal with an increase of 11 % and a decrease of 5 %, respectively. Regarding configuration *Set A*, the CHO presents an increase of the successful HO rate of 106 %. A successful HO rate above the optimal value suggests that there is an increase in the number of RLFs and HOFs, while a rate above the optimal indicates an increase in the UHO rate.

The RLF and HOF, the UHO and the PP rates are depicted in Fig. III.6. While the BHO results in a high RLF and HOF rate - 2.2, 4.4 and 8.1 operations/UE/min. - the CHO procedure reduces this metric to zero, no matter the configuration set. This is consistent with the numbers seen in Fig. III.4, since the declaration of RLF/HOF is directly related to the levels of DL SINR. The price for improving the robustness of the radio link is an increase of the HO rate. BHO and CHO procedures exhibit a larger amount of UHOs and PPs, especially when configured with *Set A*. For the latter set, the use of the

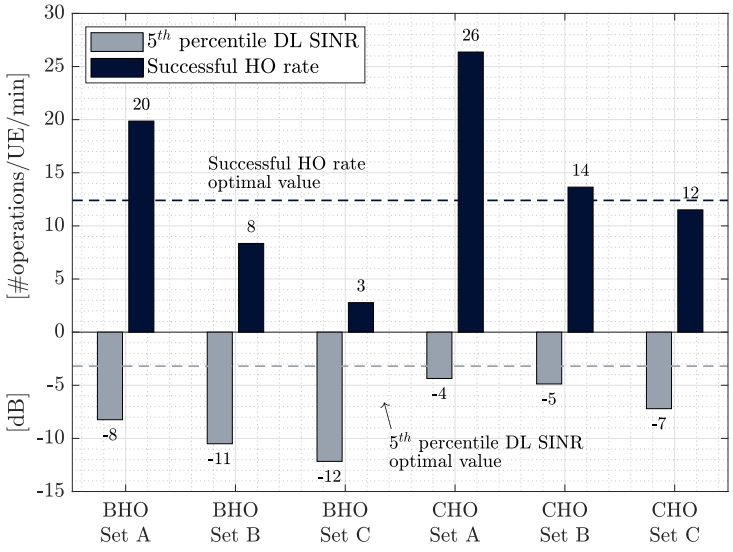


**Fig. III.5:** 5th percentile DL SINR and successful HO rate for BHO and CHO procedures.

CHO represents an increase of the UHO and the PP rates of 66 % and 64 %, respectively and compared against the BHO. Similarly, the CHO configured with *Set B* involves an increase of the UHO and the PP rates of 71 % and 67 %.

Finally, the CDF of the ToS is depicted in Fig. III.7. As seen in Fig. III.5, a consequence of improving the DL SINR is the increase of the signalling overhead. This fact has a direct impact on the time that a UE spends in the serving cell. It is worth mentioning that the optimal mean ToS is 4.9 s. This provides an idea of the scale of the frequent HOs problem; even with an optimal HO procedure, the network has to manage a HO every a few seconds per UE. The configuration *Set A*, which shows the best DL SINR performance and the highest signalling overhead, presents a mean ToS of 1.8 s and 0.6 s for the BHO and the CHO, respectively. This fact entails a gap above 4 s with respect to the optimal mean value. In referring to *Set B*, it presents a mean ToS of approximately 4.7 s for both HO procedures. *Set C* exhibits a similar mean ToS of 4.9 s. Even though *Set B* and *Set C* present similar mean ToS values, which nearly attain the optimal, relevant differences are seen at the ends of the CDFs. When *Set B* is used, 20 % of users present a ToS below 2.5 s and 3.2 s for the BHO and the CHO procedures, respectively. This value rises up to 4.2 s when the *Set C* is employed and regardless of the HO procedure. On the upper end of the distributions, the BHO procedure shows longer ToS values as compared with the CHO procedure. This is probably due the late HO effect of the BHO procedure, which ultimately leads to higher a RLF/HOF rates.

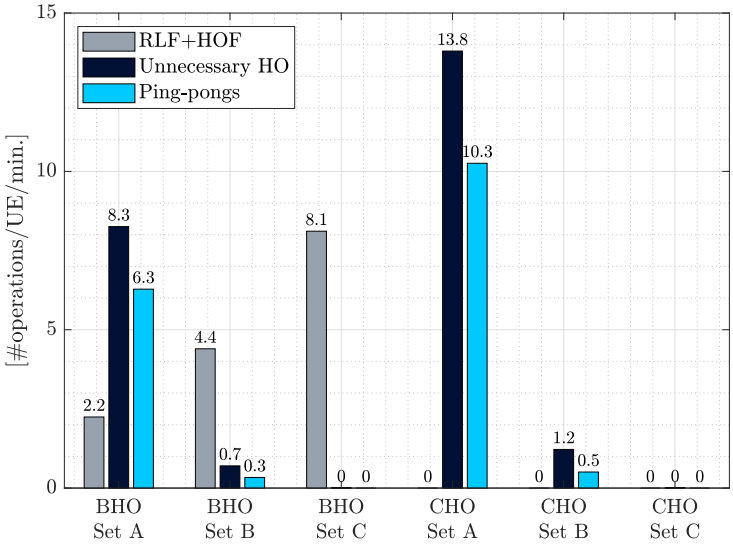


**Fig. III.6:** Radio link failure plus HO failure, ping-pong and unnecessary HO rates for BHO and CHO procedures.

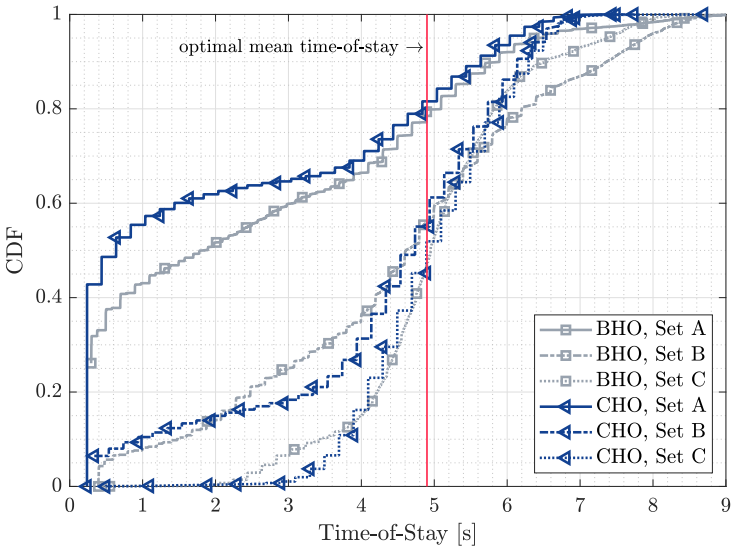


**Fig. III.7:** Distribution of the time-of-stay in the serving cell for BHO and CHO procedures.

# 7 Discussion and Future work

We have presented the first study that evaluates the CHO performance in LEO-based NTN by means of system-level simulations. The simulation re-

sults show that the 5G NR CHO procedure enhances the mobility performance as compared with the baseline 5G NR HO. As remarked in [4], the major challenge was to address the HO lateness and the high HOF rate. The performance results in Section 6 indicate that the CHO procedure leads to a higher DL SINR and reduces the number of RLF and HOF to zero by triggering the HO earlier. This fact lowers the mean time in outage (i.e. HO interruption time, RLF/HOF and radio link problems) in relation with the total service time from 4.5–18 % to 0.7–1.2 % as compared with the BHO. Nonetheless, the CHO procedure results in an increase of the UHO and PP rates above 60 %, which must be addressed. Further optimization of the mobility management implies reducing the HOF rate without increasing the signalling overhead. An increase of the signalling overhead has a direct impact on UE's throughput since it spends less time transferring user's data. This is due to longer periods of control signalling between the UE and the network. Furthermore, each time that a UE initiates a HO, it comes associated with an interruption time and a higher outage probability.

Recent discussions in 3GPP remark the suitability of the CHO in NTN [9]. Although we certainly observe benefits by using the CHO, the results shown in this paper suggest that the CHO performance can be improved. We have shown that EMC imply a high HO frequency, even in an optimal scenario. This, added to the fact that the CHO presents an excess of signalling in a rural environment with a low density of users, the 5G NR mobility performance can be compromised. The mobility of LEO satellites introduces stringent radio conditions and major challenges to the radio resource management. Nonetheless, satellites move following orbits that are deterministic, which means that the trajectories can be predicted and the knowledge of satellites' future positions can be exploited. New conditions to trigger mobility events based on UE's and satellite's location can be used to enhance the existing measurement-based triggering conditions. If the network can estimate how cells on the ground will move, it can prevent the UEs to access certain cells. This is suggested as future work to reduce the number of UHO and PP.

# 8 Conclusions

In this article, we have studied the mobility performance of the 5G NR conditional handover algorithm in low Earth orbit based non-terrestrial networks with Earth-moving cells. We have presented system-level simulations comparing the mobility performance of the 5G NR conditional handover against the baseline 5G NR UE-assisted network-controlled handover. The conditional handover enhances the mobility performance due to an early handover preparation phase. In contrast with the baseline handover, the conditional handover shows an increase of 4–6 dB of the $5^{\text{th}}$ percentile DL SINR. The

boost of the DL SINR improves the UE's outage behaviour and completely removes the number of radio link failures and handover failures. Nonetheless, the conditional handover increases the proportion of unnecessary handovers and ping-pongs more than 60 %, which translates into additional signalling and UE measurement reporting. Overall, and based on the simulation results, the conditional handover enhances the mobility robustness and stands as a potential mobility solution for non-terrestrial networks, however, the problem of the excessive signalling overhead must be addressed in the future. Finally, we discuss a potential way forward that leverages the cell coverage location to avoid the increase of signalling overhead.

# References

[1] O. B. Ogutu and E. J. Oughton, "A Techno-Economic Cost Framework for Satellite Networks Applied to Low Earth Orbit Constellations: Assessing Starlink, OneWeb and Kuiper," *arXiv preprint arXiv:2108.10834*, 2021.

[2] 3GPP, "Solutions for NR to support Non-Terrestrial Networks (NTN) (Release 16)," TR 38.821 V1.0.0, Dec. 2019.

[3] 3GPP, "Solutions for NR to support Non-Terrestrial Networks (NTN) (Release 17)," RP-202908, 3GPP TSG RAN Meeting 90-e, Dec. 2020.

[4] E. Juan, M. Lauridsen, J. Wigard, and P. E. Mogensen, "5G New Radio Mobility Performance in LEO-based Non-Terrestrial Networks," *IEEE GLOBECOM*, 2020.

[5] E. Del Re, R. Fantacci, and G. Giambene, "Efficient Dynamic Channel Allocation Techniques with Handover Queuing for Mobile Satellite Networks," *IEEE Journal on Selected Areas in Communications*, 1995.

[6] G. Maral *et al.*, "Performance Analysis for a Guaranteed Handover Service in an LEO Constellation with a Satellite-Fixed Cell System," *IEEE Transactions on Vehicular Technology*, 1998.

[7] Y. Cao, S.-Y. Lien, and Y.-C. Liang, "Deep Reinforcement Learning for Multi-User Access Control in Non-Terrestrial Networks," *IEEE Transactions on Communications*, vol. 69, no. 3, pp. 1605–1619, 2020.

[8] J. Li, K. Xue, J. Liu, and Y. Zhang, "A User-Centric Handover Scheme for Ultra-Dense LEO Satellite Networks," *IEEE Wireless Communications Letters*, vol. 9, pp. 1904–1908, 2020.

[9] Ericsson, "Connected mode aspects for NTN," R2-2009821, 3GPP TSG-RAN WG2 Meeting #112-e, Nov. 2020.

[10] 3GPP, "TSG RAN, NR, NR and NG-RAN Overall Description (Release 16)," TS 38.300 V16.6.0, Jun. 2021.

[11] 3GPP, "TSG RAN, NR, RRC protocol specification (Release 16)," TS 38.331 V16.5.0, Jun. 2021.

[12] L. C. Gimenez, P. H. Michaelsen, K. I. Pedersen, T. E. Kolding, and H. C. Nguyen, "Towards Zero Data Interruption Time with Enhanced Synchronous Handover," in *2017 IEEE 85th VTC Spring*, 2017.

[13] H. Martikainen, I. Viering, A. Lobinger, and T. Jokela, "On the Basics of Conditional Handover for 5G Mobility," in *2018 IEEE 29th PIMRC*.

[14] 3GPP, "Study on New Radio (NR) to support Non-Terrestrial Networks (Release 15)," TR 38.811 V15.2.0, Sept. 2019.

[15] E. Juan, M. Lauridsen, J. Wigard, and P. E. Mogensen, "Time-correlated Geometrical Radio Propagation Model for LEO-to-Ground Satellite Systems," *IEEE VTC-Fall*, 2021.

[16] 3GPP, "E-UTRA Mobility Enhancements in Heterogeneous Networks (Release 11)," TR 36.839 V0.7.1, Aug. 2012.

# Part IV

# Enhancing the Mobility Performance by Exploiting the Known Trajectory of LEO Satellites

# Enhancing the Mobility Performance by Exploiting the Known Trajectory of LEO Satellites

This part of the thesis aims to improve the mobility performance by addressing a critical limitation: the HO triggering and the HO decision are purely based on cell radio measurements. Therefore, HO enhancements, based on the deterministic movement of LEO satellites, are proposed. These enhancements use as starting point Release 17 discussions about mobility for NR over NTN.

## 1 Motivation

The work in this thesis has closely followed the 3GPP standardization work in the 3GPP technical specification group (TSG) RAN2, which at the time of writing is focusing on NTN mobility enhancements for Release 17. In addition, this thesis has also reviewed the state-of-the-art HO solutions available in the literature.

Many solutions have been proposed in the literature to support mobility in cellular networks. The ultimate goal of these procedures is to ensure no data loss and seamless connection as UEs handover across cells. Typically, the HO procedure mainly uses cell radio measurements to perform the HO decision. However, some research works tried to exploit additional information. The work in [1] aimed to improve the HO performance proposing a HO algorithm based on the RSRP measured by the UE and the distance from the UE to the neighbouring base station. Later on, the works [2] and [3] investigated adaptive HO algorithms to dynamically adjust the HOM considering the distance UE-to-serving base station, the UE location and the UE velocity.

In [4], the authors proposed an algorithm to improve the HO decision in HST scenarios exploiting the train speed and the UE location.

Many studies have addressed methods to optimize the HO control parameters, i.e. HOM and TTT, especially in scenarios where each cell might have different loads and radio conditions. The UE initiates the HO process based on the HO control parameters, hence, the HO performance can be optimized by suitably adjusting these parameters. [5] and [6] proposed techniques to automatically self-optimize HO parameters. The former adjusts the HOM based on the change in HOF events, whereas the latter proposes a fuzzy logic controller to adjust HOM and TTT based on the call dropping rate and the HO rate. As stated in [7], the optimization is centralized based on the performance of the network and all the UEs utilize the same parameters regardless of their individual radio conditions, movement in the cell, direction or mobility speed. This might lead to an increase of the HO issues for some UEs. Finally, in the past years, methods to predict UE mobility such as Markov models, neural networks and Bayesian networks have attracted increasing attention as captured in [8].

Despite the large body of methods in the literature, no technique can entirely tackle all mobility scenarios. The above-mentioned works aim to enhance mobility performance but none of the proposed solutions are suitable for NTN scenarios because these solutions are tailored for TNs, which mostly focus on UE mobility and the optimization of measurement-specific parameters. In Part I, a literature review of HO solutions for LEO satellite networks was provided with similar conclusion: none of the reviewed research works address solutions considering the 3GPP specifications for NR over NTN and, therefore, specific solutions supported by system-level simulation results are required.

As explained in Part III, measurement-based HO procedures lead to suboptimal mobility performance. Therefore, the characteristics of the NTN scenario require to change how typically the HO procedure operates. To that purpose, the 3GPP has been working on connected-mode mobility enhancements in the context of Release 17. After the acknowledgement in [9] that mobility procedures should be improved considering the satellite movement aspect, additional HO triggering conditions based on either time or distance have been proposed. As follows, some of the agreements taken as part of Release 17 work in the TSG RAN2 are listed:

i) Only UEs with GNSS capabilities are supported [10].

ii) The satellite *ephemeris* should be provided to UE, at least for satellite *ephemeris* based cell selection and re-selection [10].

iii) Location-based and time/timer-based CHO triggering event, in combination with the existing Release 16 CHO measurement based event,

should be introduced [11].

The 3GPP has taken initial steps towards new NR HO procedures for NTN that could benefit from additional information such as time or location. Based on the findings in Part III and the directions taken by 3GPP for NTN, the following hypothesis is formulated:

(**H3**) Due to the characteristics of LEO satellite networks, location-based HO triggering criteria may improve the UE mobility performance of HO procedures purely based on cell radio measurements.

Using UE location and satellite *ephemeris*, it is possible to estimate the remaining cell radio coverage time or the distance from UE location to a cell reference location, e.g. cell centre. It is possible to exploit satellite *ephemeris* because, even though LEO satellites mobility poses challenging conditions, they follow deterministic paths that can be known. The NW broadcasts the satellite *ephemeris* to UEs or it can use this information to anticipate which is the best candidate cell to handover to. Thus, new HO triggering conditions, which exploit location or time information, can be used in combination with measurement-specific conditions to enhance the mobility performance showed by measurement-based NR HO procedures.

As part of the findings in Part III, it was underlined that UEs feature a non-negligible measurement error. The low RSRP variation combined with the UE measurement error hampers the HO triggering and the HO decision. EMC-based 5G LEO satellite networks present characteristics that should be leveraged to enhance UE mobility performance. One of them is the full-correlation of large-scale radio propagation conditions between adjacent intra-satellite cells. Satellites provide NR access through multiple satellite beams that enable NR cells. This means that intra-satellite cells are radiated from the same point. Another important aspect is that the most relevant scenario for NTN is the rural environment, where likelihood of static LOS conditions are rather high. These factors enable a scenario where cell radio measurements can become dispensable. From the above, the hypothesis H4 is stated:

(**H4**) Intra-satellite mobility is characterized by fully-correlated radio propagation conditions - i.e. path loss, shadow fading and LOS - because cells are radiated from the same satellite. In such predictable scenario, a UE could handover across cells without requiring cell radio measurements.

Several 3GPP members have contributed with different proposals, e.g. [12] [13], however, no simulation results were provided to support them. This

part of the thesis covers this gap by: i) proposing two suitable HO solutions to enhance the UE mobility performance by exploiting the predictability of LEO satellites and ii) supporting the novel HO solutions with system-level results that validate the proposals.

Firstly, this part of the thesis proposes a location-based HO triggering event for validating the formulated hypothesis H3. The proposed solution exploits the distance between the UE location and the cells centre to enhance the NR A3 measurement event. Secondly, this thesis validates hypothesis H4 proposing a fully NW-controlled HO solution for intra-satellite mobility. The UE uses antenna gain predictions of the satellite beams to avoid cell radio measurements and thus the UE measurement error.

# 2 Objectives

The main goal of this part is to propose, simulate and analyze new HO solutions that enhance mobility performance, validating hypothesis H3 and H4. To this purpose, the following objectives were defined:

A. Propose concrete HO procedures to enhance UE mobility performance by exploiting the predictability of LEO satellites. The goal is to define HO solutions capable of: i) eliminating RLFs, ii) increasing DL SINR and iii) minimizing UHOs.

B. Investigate intra-satellite HO procedures that exploit the full-correlation of the path loss, the shadow fading and the LOS conditions between adjacent intra-satellite cells. The proposed algorithm shall not be impacted by the UE measurement error.

C. Evaluate through system-level simulations the mobility performance of the proposed HO solutions for UEs in rural and urban environments.

D. Identify the limitations of the proposed HO solutions and analyse their robustness against relevant sources of error.

# 3 Included Articles

**Paper E. Location-Based Handover Triggering for Low-Earth Orbit Satellite Networks**

This paper presents a new HO triggering event that uses UE location and satellite location information to enhance UE mobility performance with minimal impact on the 3GPP specifications. Based on 3GPP assumptions, UEs

have GNSS capabilities and satellites broadcast the cells centre ground location. Then, similarly to cell radio measurements, the UE periodically determines the distance changes between its own location and the cells centre location. This information is comprised in a location-based offset that is included as part of the NR A3 measurement event condition. The location-based offset includes several design parameters that can be set to *reward* appropriate target cells, *penalize* undesired target cells or both. Extensive system-level simulations are conducted to evaluate the mobility performance of the proposed location-based HO triggering event, which is used with the BHO and the CHO procedures.

**Paper F. Handover Solutions for 5G Low-Earth Orbit Satellite Networks**

This paper continues the work in Paper E with a twofold contribution. First, the paper presents a fully NW-controlled HO solution for intra-satellite mobility, which is based on geometric estimations that make radio measurements obsolete. Based on the full-correlated path loss and shadow fading between adjacent intra-satellite cells, the UE handovers across these cells using antenna gain predictions from serving and target cells. Second, extensive system-level simulations are conducted to analyse and compare the mobility performance of: i) the CHO procedure, ii) the CHO set with the location-based HO triggering event proposed in Paper E and iii) the HO solution presented in this paper. The system-level simulations are conducted for users in rural and urban environments. The channel model used can be found in Papers A and B. Furthermore, a sensitive study tests the robustness of the proposed HO enhancements against error sources not considered by the 3GPP which include: i) UE location error, pointing error of the satellite antenna and iii) radiation error of the satellite antenna.

# 4 Main Findings

**Eliminating RLFs and UHO events with minimal impact on the 3GPP specifications**

System-level simulation results in Paper E indicate that the use of the location-based HO triggering event enhances the mobility performance close to the DL SINR performance upper bound. In Paper D, it was shown that the measurement-based CHO procedure can eliminate RLFs at the expense of an increase of UHO events. The algorithm in Paper E allows the UE to capture the cells movement and use it to filter out undesired target cells and avoid UHOs. The CHO procedure configured with the location-based HO triggering event reaches the best achievable mobility performance by removing RLFs and UHOs. The elimination of UHOs maximizes the ToS in a cell,

which has a direct impact on the user experience because the UE spends less time exchanging HO control signalling. Furthermore, it is important to highlight that the HO algorithm is built on the 3GPP specifications for NTN (see 3GPP agreements in Section 1). The proposal requires minimum changes in the Release 17 specifications [14] [15]; the location-based offset limits which target cells are suitable candidates while cell radio measurements are still used to detect the appropriate instant to send the MR or access the target cells. The HO signalling remains as it is while the MR triggering and the CHO execution are optimized.

**Cell radio measurements can be neglected for intra-satellite mobility**

The usefulness of cell radio measurements depend on the UE accuracy to correctly measure the RSRP. The limited RSRP variation in NTN together with the UE measurement error present a non-negligible issue. In this thesis, system-level simulations have demonstrated that measurement-based HO procedures lead to sub-optimal mobility performance. Paper F presented a fully NW-controlled HO solution that exploits the full-correlated path loss and shadow fading among intra-satellite cells and uses satellite beam antenna gain predictions to handover. The provided system-level results validate the hypothesis H4 by showing that the proposed HO procedure eliminates RLFs and UHOs. This solution shows a mobility performance very similar to the location-based HO triggering event (Paper E), regardless of the UE environment. Note that the area of the UEs and the simulation time are configured to target only intra-satellite mobility events.

**The known movement of LEO satellites paves the way towards enhanced mobility performance**

The HO solutions presented in Papers E-F, have different flavours but both aim the same goal: enhance the mobility performance of current measurement-based HO procedures by exploiting the deterministic movement of LEO satellites. The system-level simulation results indicate that this area of research presents several benefits where by simple and small changes in the definition of the HO, the UE mobility performance is improved close to the upper bound performance to maximize the DL SINR.

**Adding error sources has no mobility performance impact on the proposed HO solutions**

Paper F also presents a sensitivity study that shows the robustness of the HO solutions proposed in this thesis. The study, conducted by system-level simulations, includes the radiation error of the satellite antenna, the pointing

error of the satellite antenna and the UE location error. All errors are time-invariant and normally distributed with standard deviation values selected from the available literature. The results indicate that none of these error sources have a relevant impact on the mobility performance.

**From rural to urban scenario without changes in the mobility performance**

In Paper F, the mobility performance of the BHO, the CHO, and the proposed HO procedures in this thesis were analysed for UEs in rural and urban environments. No major mobility performance differences were found among scenarios because of the characteristics of the reference scenario. A cell size of 50 km, satellite altitude of 600 km, 19 beams/cells per satellite and the use of EMC resulted in minor changes of the satellite elevation angle, i.e. from 79.4° to 100.6°. Since the satellite elevation angle remained high, most of the UEs stayed in LOS conditions with a low NLOS probability.

# References


[1] K.-I. Itoh, S. Watanabe, J.-S. Shih, and T. Sato, "Performance of Handoff Algorithm Based on Distance and RSSI Measurements," *IEEE Transactions on vehicular technology*, vol. 51, no. 6, pp. 1460–1468, 2002.

[2] H. Zhu and K.-s. Kwak, "Performance analysis of an adaptive handoff algorithm based on distance information," *Computer communications*, vol. 30, no. 6, pp. 1278–1288, 2007.

[3] S. Wang, M. Green, and M. Malkawi, "Adaptive handoff method using mobile location information," in *2001 IEEE Emerging Technologies Symposium on Broad-Band Communications for the Internet Era. Symposium Digest (Cat. No. 01EX508)*. IEEE, 2001, pp. 97–101.

[4] M.-m. Chen, Y. Yang, and Z.-d. Zhong, "Location-Based Handover Decision Algorithm in LTE Networks Under High-Speed Mobility Scenario," in *2014 IEEE 79th Vehicular Technology Conference (VTC Spring)*. IEEE, 2014, pp. 1–5.

[5] K. Kitagawa, T. Komine, T. Yamamoto, and S. Konishi, "A Handover Optimization Algorithm with Mobility Robustness for LTE Systems," in *2011 IEEE 22nd international symposium on personal, indoor and mobile radio communications*. IEEE, 2011, pp. 1647–1651.

[6] P. Muñoz, R. Barco, and I. de la Bandera, "On the Potential of Handover Parameter Optimization for Self-Organizing Networks," *IEEE Transactions on Vehicular Technology*, vol. 62, no. 5, pp. 1895–1905, 2013.

[7] I. Shayea, M. Ergen, M. H. Azmi, S. A. Çolak, R. Nordin, and Y. I. Daradkeh, "Key Challenges, Drivers and Solutions for Mobility Management in 5G Networks: A Survey," *IEEE Access*, vol. 8, pp. 172 534–172 552, 2020.

[8] H. Zhang and L. Dai, "Mobility Prediction: A Survey on State-of-the-Art Schemes and Future Applications," *IEEE Access*, vol. 7, pp. 802–822, 2018.

[9] "Solutions for NR to support Non-Terrestrial Networks (NTN) (Release 16)," 3GPP, TR 38.821 V1.0.0, 2019. [Online]. Available: https://www.3gpp.org/ftp/Specs/archive/38_series/38.821/

[10] "Report of 3GPP TSG RAN WG2 meeting #111-e Online," 3GPP, R2-2008701, 2020. [Online]. Available: https://www.3gpp.org/ftp/TSG_RAN/WG2_RL2/TSGR2_111-e/Docs/

[11] "Report of 3GPP TSG RAN WG2 meeting #112-e Online," 3GPP, R2-2100001, 2020. [Online]. Available: https://www.3gpp.org/ftp/TSG_RAN/WG2_RL2/TSGR2_112-e/Docs/

[12] "Further consideration on CHO in NTN," ZTE Corporation, Sanechips, 3GPP, R2-2108607, 2021. [Online]. Available: https://www.3gpp.org/ftp/tsg_ran/WG2_RL2/TSGR2_115-e/Docs

[13] "Remaining issues in NTN CHO," LG Electronics Inc., 3GPP, R2-2110229, 2021. [Online]. Available: https://www.3gpp.org/ftp/tsg_ran/wg2_rl2/TSGR2_116-e/Docs

[14] "NR; NR and NG-RAN Overall Description (Release 16)," 3GPP, TS 38.300 V16.6.0, 2021. [Online]. Available: https://www.3gpp.org/ftp/Specs/archive/38_series/38.300/

[15] "NR; Radio Resource Control (RRC) protocol specification (Release 16)," 3GPP, TS 38.331 V16.5.0, 2021. [Online]. Available: https://www.3gpp.org/ftp/Specs/archive/38_series/38.331/

# Paper E

## Location-Based Handover Triggering for Low-Earth Orbit Satellite Networks

Enric Juan, Mads Lauridsen, Jeroen Wigard, Preben Mogensen

The paper has been published in the
*IEEE 96th Vehicular Technology Conference (VTC2022-Spring), 2022.*

*The layout has been revised.*

# Abstract

*Broadband low Earth orbit (LEO) satellite constellations are a reality. The integration of satellite and terrestrial systems for mobile communications is taking-off with the development of non-terrestrial networks (NTN) and the ongoing deployment of private constellations. Due to the highly mobile nature of LEO satellites, one of the critical research areas is the design of the mobility mechanisms to ensure robust service continuity for the end-user. Recent studies in the domain of Earth-moving cells have shown that measurement-based handover (HO) triggering events cannot guarantee a low number of radio link failures without an increase in signalling and measurement reporting. In this work, we present a new HO triggering event that exploits the predictable movement of LEO satellites and uses the distance between the user's location and the centre of the moving cells on the ground. The performance of the proposed solution is evaluated with system-level simulations and compared against the measurement-based baseline HO and Rel-16 Conditional HO (CHO). It is found that the location-based HO triggering event completely eliminates the HO failures as well as unnecessary HOs and ping-pongs. As a result, the location-based HO triggering event extends the mean time-of-stay from values below 2 s to 4.8 s where the optimal mean time-of-stay is 4.9 s.*


# 1 Introduction

From the 2010s, LEO constellations have become a hot topic for industries and academics. While terrestrial systems can only cover about 6 % of the Earth's surface [1], satellite systems can provide broadband mobile communications anywhere at any time. In this quest for ubiquitous high-speed Internet, private companies are planning, manufacturing and deploying their LEO satellite constellations [2]. Examples of these systems are OneWeb, Starlink, Telesat, LeoSat and Kuiper. At the same time, 3GPP is working on a unified standard for terrestrial and satellite mobile communications. This concept, known as NTN, will be introduced for the first time in the upcoming Rel-17 of the 5G NR standard [3].

Among other scenarios, NTN targets LEO satellites at altitudes between 600 km and 1200 km, which move at approximately 7.5 km/s relative to the Earth. The vision is that these systems will provide 5G NR service on Earth through multiple satellite beams. This is a completely new scenario where the mobility management schemes require modifications, as captured in [4]. Especially for EMC, where the coverage area of each beam moves along with the satellite sweeping the Earth's surface, the satellite's mobility can lead to very frequent HO events. For example, for a satellite at an altitude of 600 km and a beam cell diameter of 50 km, a HO may occur approximately every 5 s. Frequent HO events increase the signalling overhead, which combined with

measurement inaccuracies and a low signal strength variation between cells in a region of overlap, can lead to a critical increase of the service failures and, therefore, long service interruptions.

In [5] we demonstrated that the UE-assisted network-controlled BHO fails to guarantee a robust service due to a late HO decision. Recently, the work in [6] showed that the Rel-16 CHO eliminates the RLFs and HOFs due to an earlier HO preparation but leads to a 60 % increase of the signalling overhead and measurement reporting as compared with the BHO. Both procedures are solely based on UE measurements, which have an impact on the HO triggering time and the HO decision. In terrestrial networks, standardized HO procedures are based on these measurements due to its simplicity and effectiveness. However, for NTN deployments, the 3GPP has suggested in [4] the use of additional triggering criteria since a purely measurement-based HO triggering (MHT) event may not be sufficient to reach optimal mobility performance.

LEO satellites follow deterministic trajectories. This implies that network and UE can estimate and track the movement of the cells to initiate the HO at the serving cell edge and towards the optimal target cell. In this paper, we propose a novel location-based HO triggering (LHT) event that exploits the distance between the UE's location and the location of the surrounding cells. Even though 3GPP has highlighted the importance of using alternative triggering criteria, neither specific solutions nor simulations results have been published. For this reason, we provide system-level simulations to show the strengths of our proposed solution. The performance of the LHT event is compared against the standardized BHO and CHO. The resulting evaluation shows that the LHT solution reduces the signalling overhead, removes the radio failures and maximises the time of stay in a cell.

The remaining of the paper is organized as follows. Section 2 reviews the main aspects of the conventional measurement-based HO triggering events and the related constraints when used in EMC. Section 3 describes the proposed location-based HO triggering solution. Section 4 introduces the scenario, UE's configuration and network parameters used for the system-level simulations. The KPIs used to evaluate the mobility performance and the system-level results are found in Section 5 and 6, respectively. Section 7 discusses the results and future research directions. Final conclusions are drawn in Section 8.

# 2 Limitations of the Measurement-based Handover Triggering in Earth-Moving Cells

One of the goals of mobility management is to ensure that connected UEs do not experience noticeable service interruption as they change connection from one cell to another. The HO is the connected-state mobility procedure that ensures this process. Typically, the HO relies on DL measurements performed by the UE to trigger the HO event. This means that a UE periodically measures the signal quality of its serving cell and neighbouring cells and once the configured HO event condition is fulfilled, the UE sends a MR to the network. Then, the network may command the UE to initiate the HO towards a certain target cell. This section focuses on the issues when the HO triggering condition of the HO event is purely based on radio measurements in EMC, which in this paper is referred to as MHT event.

In NTN, especially in EMC, the frequency of the HO events is mainly impacted by the movement of the satellites. As discussed in [5] and [6], the MHT events result in an increase of HOs towards the sub-optimal target cell. Fig. IV.1 intends to describe the limitations of using MHT events. It shows a simplified scenario consisting of a UE (red triangle) camping in serving *cell A* (light blue) and surrounded by three neighbouring cells (gray): *cell B*, *cell C* and *cell D*. Each satellite beam radiates a cell coverage area on the ground with a circular shape and radius $R_c$. As cells move from left to right, the UE experiences cell-edge conditions that might continuously trigger the measurement-based HO condition. This is due to UE's measurement inaccuracies and the cells' overlapping footprint. Besides, since the propagation distance is orders of magnitude greater than the cell size, there exist minor signal received power differences between cell centre and cell edge conditions, which also impacts the HO trigger.

Considering the scenario in Fig. IV.1, ideally the UE should remain connected to serving *cell A* until it is close enough to handover towards target *cell B*. In reality, the UE could attempt to connect to *cell C* and *cell D*, which may result in two cases. A first case where the UE connects to *cell D* and, due to cells movement, tries to handover back to *cell A*. Then, if *cell D* quickly moves away and disappears, the UE could not have enough time to communicate with *cell D* and initiate the HO again. This results in the UE declaring an RLF and going into idle state. In the second case, the UE might connect to *cell C* and immediately handover to *cell B*, unnecessarily staying for a very short time in *cell C*. Both cases are highly undesired since they increase the UE's power consumption, generate unnecessary signalling and lead to longer service interruptions which, ultimately, impacts the UE's service experience.

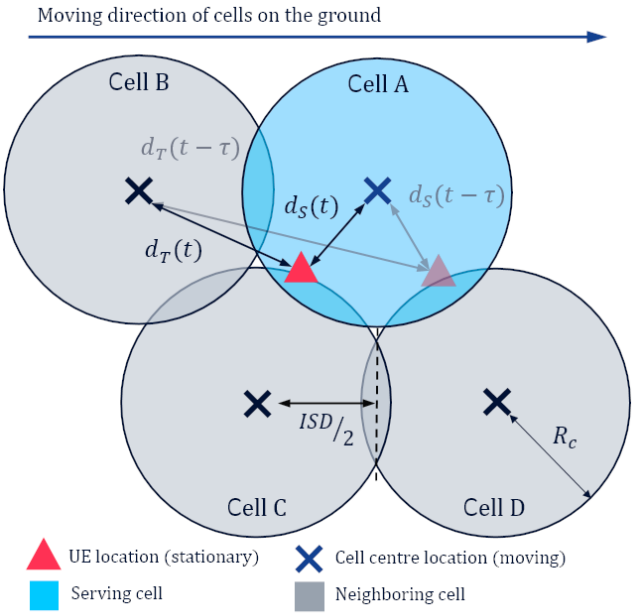


**Fig. IV.1:** Simplified scenario that depicts a UE being served by Earth-moving cells and exemplifies how the distances UE-cells centre change across time.

## 3 New Location-based Handover Triggering Event

The proposed LHT event exploits the UE's location and the location of the cells centre on the ground to determine the changes of the UE-cell centre distance. Such information, periodically collected by the UE, allows to capture the direction of the cells and can reduce the risk of a sub-optimal HO choice and minimize the impact of satellite's mobility. Such novel solution is based on: i) the UE has GNSS capabilities and ii) the network can broadcast location information of the cells. These assumptions are considered for Rel-17 by the 3GPP in [3].

The specification of the MHT event is modified to introduce an additional offset that comprises the location information. In this way, the impact on the 5G NR specifications is minimized because radio measurements remain a fundamental part of the HO triggering while cell movement is taken into account. We focus on the commonly used NR A3 event, even though the proposed solution can be applied with other relevant events in [7]. The NR A3 event relates to an intra-frequency HO initiated when the signal strength of target cell $T$ becomes stronger than serving cell $S$ by a certain HOM and for a certain TTT.

A simplified version of the A3 event containing the location-based offset $\Gamma_{S,T}$ can be seen below.

$$P_T(t) > P_S(t) + HOM + \Gamma_{S,T}(t\text{-}\tau, t) \quad \text{[dBm]} \quad \text{(E.1)}$$

where $P_S(t)$ and $P_T(t)$ are RSRP measurements (in dBm) from serving cell $S$ and target cell $T$, respectively, and $\Gamma_{S,T}(t\text{-}\tau, t)$ is the location offset (in dB) for the same cells pair $S$-$T$. A description of the calculation of $\Gamma_{S,T}$ is presented as follows.

As cells move, the UE samples the distances UE-cell centre $d$ at regular time intervals $\tau$, where $\tau$ follows the DL measurements sample rate. Fig. IV.1 shows a UE at two consecutive instances, $t$-$\tau$ and $t$. We denote the distance between the UE and its serving cell centre as $d_S$. Analogously, the distance between the UE and a candidate target cell is expressed as $d_T$. Given a serving and target cell pair $S$-$T$ and based on the estimated distances $d_S$ and $d_T$ at instants $t$-$\tau$ and $t$, the UE calculates the relative distance change for serving cell $\Delta d_S$ and target cell $\Delta d_T$ as below:

$$\begin{aligned} \Delta d_S(t\text{-}\tau, t) &= d_S(t) - d_S(t\text{-}\tau) \\ \Delta d_T(t\text{-}\tau, t) &= d_T(t) - d_T(t\text{-}\tau) \end{aligned} \quad \text{[m]} \quad \text{(E.2)}$$

The ratio $\xi_{S,T}$ is obtained by combining the expressions in (E.2) as:

$$\xi_{S,T}(t\text{-}\tau, t) = \frac{\Delta d_T(t\text{-}\tau, t)}{\Delta d_S(t\text{-}\tau, t)} \quad \text{[dB]} \quad \text{(E.3)}$$

$\xi_{S,T}$ could directly be used in (E.1) instead of $\Gamma_{S,T}$. Nonetheless, the location information can be further exploited to give the UE more control to filter out those undesired target cells and reach optimal performance. In (E.4), additional distance requirements are introduced. The sign of $\Delta d_S$ and distances $d_S$ and $d_T$ are considered. A positive value of $\Delta d_S$ indicates the serving cell centre is moving away from the UE, while a negative value reflects that the cell centre is approaching it. Distances $d_S$ and $d_T$ are used together with the cell radius $R_c$ to draw a *triggering area* near the geometric cell radius. We define the radius of an inner circle $R_c^- = R_c - \epsilon^-$ and the radius of an outer circle $R_c^+ = R_c + \epsilon^+$. Thus, the UE evaluates the HO triggering condition at the cell edge and towards those target cells immediately approaching as follows:

$$\Gamma_{S,T}(t\text{-}\tau, t) = \begin{cases} \xi_{S,T}(t\text{-}\tau, t) & \text{if } \Delta d_S > 0 \text{ and} \\ & \quad d_S > R_c^- \text{ and } d_T < R_c^+ \\ o_{penalty} & \text{otherwise} \end{cases} \quad \text{(E.4)}$$

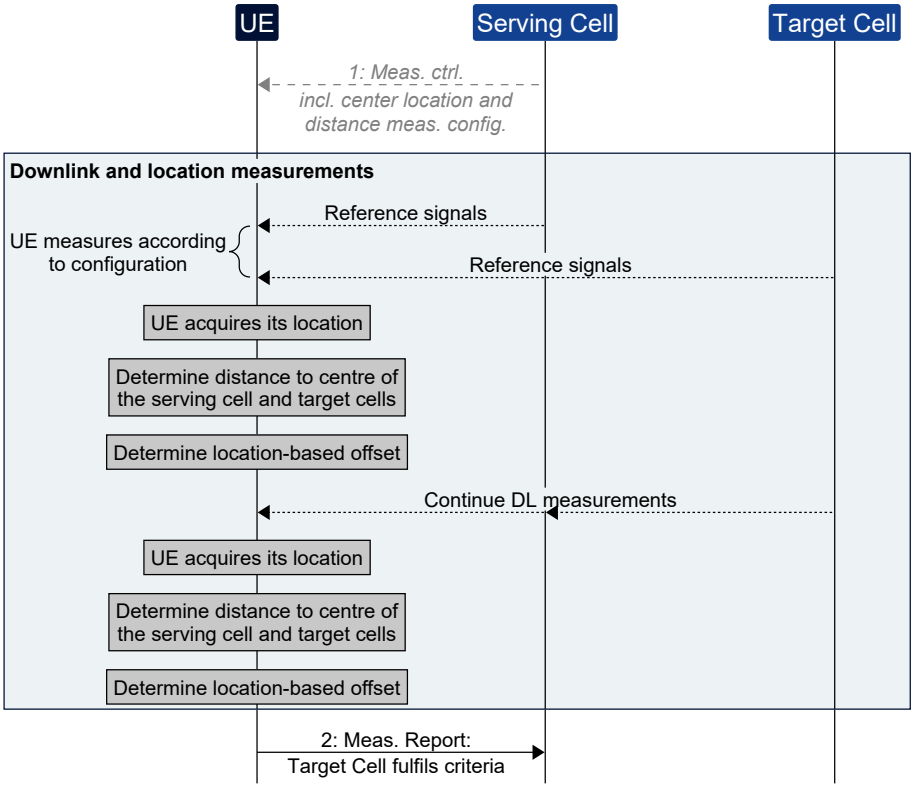


**Fig. IV.2:** Triggering of the measurement report based on downlink measurements and distance estimations.

The parameter $o_{penalty}$ is included to *penalize* those target cells that do not fulfill the distance constraints in (E.4). Further details are given later in Section 6.

Fig. IV.2 provides an illustration of the signalling between the UE and the network when the LHT event is used. Once the UE connects to the serving cell, the UE is configured with DL measurements and distance parameters. Similar to the BHO procedure, the UE periodically performs DL measurements but now also tracks distances $d_S$ and $d_T$. The UE periodically determines offset $\Gamma_{S,T}$ (see (E.4)) until the condition in (E.1) is fulfilled and the MR is sent to the serving cell. Since this solution only modifies the triggering of the MR, it is applicable to both standardized HO procedures: BHO and CHO.

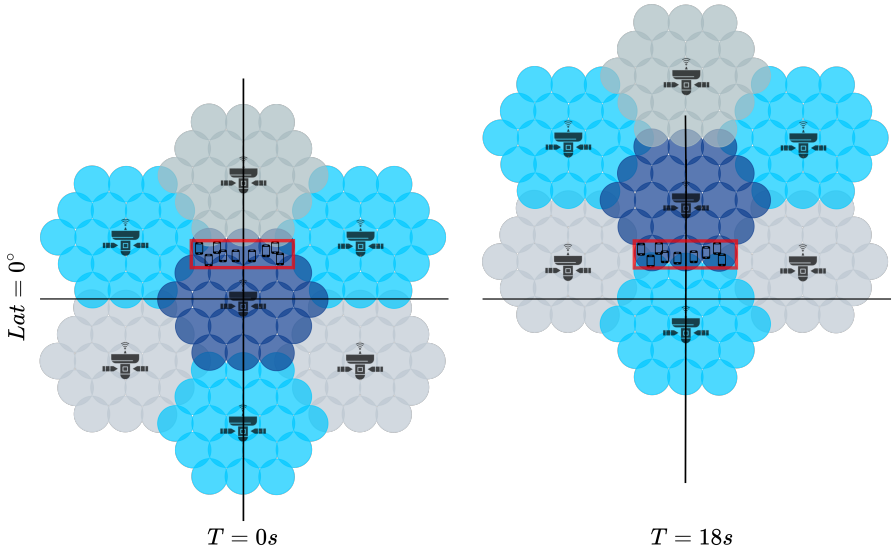


**Fig. IV.3:** Simulation scenario: 20 static UEs are served by 7 LEO satellites operating with Earth-moving cells. Beams with the same colour belong to the same satellite. Sizes of UEs, satellites and beams footprint are not to scale.

# 4 System Simulation Methodology

## 4.1 Simulation parameters

Fig. IV.3 depicts the simulated scenario: a constellation of 7 LEO satellites with gNB capabilities. The network implements EMC where each satellite beam corresponds to an NR cell. Following [4], we simulate satellites with 19 beams with a ground coverage diameter of 50 km, an inter-site distance (ISD) of 43.3 km and distributed in 3 concentric tiers. Besides, there is a cell overlapping of 50 % between cells in outer tiers of adjacent satellites.

A rural scenario is simulated where 20 static UEs are uniformly distributed along an area of 110 km $\times$ 35 km. The UE's measurement model includes a Gaussian error process. Such measurements are filtered at layer 1 and layer 3 following the specifications in [7]. The satellite payload characteristics are defined according to 3GPP technical report [4]. Uniform DL interference is generated by loading 25 % of the available PRBs per cell. Table IV.1 contains the main simulation parameters. Further details of the constellation, UE's configuration and network parameters are in [5].

System-level results are generated using a Nokia proprietary simulator that models NR PHY and MAC layers following 3GPP specifications. It operates at OFDM symbol resolution and offers a realistic analysis of mobility. It

has been used in 3GPP standardization and in scientific publications, e.g. [8] and [5]. Fifty simulations are combined varying the pseudo-random seed for each run to obtain statistically reliable results.

**Table IV.1:** System-level simulation assumptions.

| **Parameter** | **Values** |
|---|---|
| Satellite altitude | 600 km |
| Satellite antenna pattern | Section 6.4.1 in [9] |
| Satellite equivalent isotropic radiated power density | 34 dBW/MHz |
| 3 dB beamwidth | 4.4127° |
| Satellite Tx max Gain | 30 dBi |
| Satellite beam diameter | 50 km |
| UE Tx power | 23 dBm |
| Deployment scenario | Rural [10] |
| Shadow Fading ($\sigma$) | 0.3 to 7.4 dB [10] |
| Carrier frequency | 2 GHz (S-Band FDD) |
| Frequency reuse | FR1 |
| System Bandwidth | 10 MHz |
| Sub-carrier spacing | 15 kHz |
| Traffic model | Full Buffer |
| Background traffic load | 25 % PRBs |
| Radio Link Failure [7] | Qin/Qout threshold: $-6$ dB/$-8$ dB<br>T310 timer: 1000 ms<br>N310/N311: 1 |
| UE's measurement error ($\sigma$) | 1.72 dB |
| L3 filter coefficient K | 4 |
| Receiver type | LMMSE-IRC [4] |
| HO margin/Time-to-trigger | 0 dB/0 ms |
| Simulation time | 18 s (252 000 OFDM symbols) |

## 4.2 Radio Propagation Model

The work in [10] describes the adopted time-correlated radio propagation channel model. Large-scale variations of the LEO-to-Ground signal are realistically modelled considering the LOS transitions introduced by the satellite

movement as well as the changes in the propagation loss caused by buildings and objects near the UE. No fast fading is considered in this study.

### 4.3 Modelling of Conditional Handover

The HO modelling is modified to simulate the CHO procedure. It is assumed that the CHO preparation phase is executed free of failures since it takes place when the serving cell radio link is reliable and no outages are expected. A more exhaustive description of the modelling can be found in [6].

## 5 Key Performance Indicators

The following statistics were collected for this study:

### 5.1 Downlink Signal-to-interference-plus-noise Ratio

The DL SINR measures the quality of the received signal. It compares the strength of the signal from the serving cell against the level of undesired interference from the other cells and noise.

### 5.2 Radio Link Failures and Handover Failures

The RLF and HOF are relevant metrics to assess the robustness of the radio service. The RLF is declared when the signal quality drops below a threshold $Q_{out}$ during *T310* time length. In addition, the HOF is used to measure RLF and PDCCH failure during the HO procedure. Further details of the RLF and HOF declarations can be found in [8].

### 5.3 Time of Stay

The ToS is the time that a UE remains connected to the serving cell. It is an important KPI to assess the HO frequency and the signalling overhead due to PP and UHO. As reported in [8], the ToS in *cell A* is defined as the duration from when the UE sends a *HO complete* message to *cell A* to when the UE sends a *HO complete* message to another cell.

### 5.4 Unnecessary Handovers and Ping-pongs

As defined in [6], a UHO is declared when a UE handovers to a new cell and stays in that cell for less than 1 s. Similarly, a PP event is defined as a HO from *cell A* to *cell B* and handovers back to *cell A* within a certain ToS, e.g. 1 s.

# 6 Performance Results

This section presents the mobility performance of the BHO and the CHO procedures using the standardized MHT event and the proposed LHT event. HOM and TTT parameters of both triggering events are 0 dB and 0 ms based on [6]. The LHT event is configured with $R_c^- = 21$ km and $R_c^+ = 28$ km. These values are chosen considering that the $ISD/2$ is 21.65 km and the cell radius $R_c$ is 25 km. The LHT event is analysed for three schemes summarized in Table IV.2. These schemes depend on the value of $\xi_{S,T}$ and $o_{penalty}$ and aim to either only *reward* the relevant target cells, *penalize* undesired cell candidates or a combination of both. On top of the eight simulated cases - BHO and CHO procedures set with the MHT event and three schemes of the LHT event -, we include an optimal HO as a reference of upper bound performance. This case optimizes the DL SINR considering that the UE always receives the HO command and access the best cell at the right instant when target cell radio link becomes better than the serving cell radio link. The optimal HO does not include the impact of the UE's measurement error, signalling propagation delays or random access procedure.

**Table IV.2:** Configurations of the LHT event.

| **LHT schemes** | $\xi_{S,T}$ | $o_{penalty}$ |
|---|---|---|
| Reward (R) | $\Delta d_T / \Delta d_S$ | 0 |
| Penalty (P) | 0 | $10^6$ |
| Reward and Penalty (R,P) | $\Delta d_T / \Delta d_S$ | $10^6$ |

Fig. IV.4 shows the CDF of distance $d_S$ at HO completion time. Without loss of generality, only the BHO and the optimal HO are depicted. Using the MHT event, the HO takes place far within the cell and well beyond $R_c$, i.e. from 15 km to 29 km. This contrasts with the optimal HO performance which shows a range from 20.5 km to 24 km. This difference can be due to the combined impact of the UE's measurement error, the minor RSRP difference between cell centre and cell edge, i.e. 3 dB, and the signalling HO latency. Using the LHT event with a *penalty* approach, the HO occurs always after $R_c^-$. This means that $o_{penalty} = 10^6$ prevents the HO triggering until distance $d_S$ is greater than $R_c^-$. From there, $\Gamma_{S,T}$ takes $\xi_{S,T}$ value instead of $o_{penalty}$ and UEs start to initiate the HO procedure. How proactively the HO triggers depends on the *rewarding* value of $\xi_{S,T}$. Even though *reward* approaches anticipate the HO triggering as compared with the MHT event and involve more than 90 % of users completing the HO before $R_c$, when no *penalty* is used still 20 % of HO are completed before reaching a distance of 20.5 km. Due to radio impairments such as the UE's measurement inaccuracy, a performance

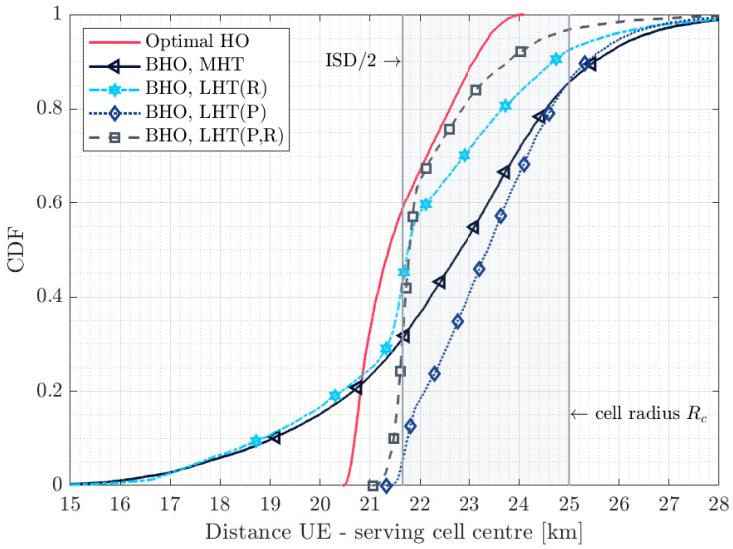


**Fig. IV.4:** Distribution of the distance UE-to-Serving Cell Centre at HO completion time for BHO procedure set with MHT and LHT events.

close to the optimal in terms of distance does not translate into accessing the right candidate cell. Thus, further analysis is needed to evaluate the overall mobility performance.

The DL SINR performance is presented in Fig. IV.5. Although the LHT event boosts the DL SINR, it does not show a relevant improvement as compared with the MHT event. This is because the CHO procedure, when only relies on DL measurements, already achieves a performance close to the optimal. The earlier HO preparation of the CHO enables a quicker reaction to the fast serving RSRP drop and, hence, reduces the number of failures. Such characteristic enhances the DL SINR performance but it leads to an increase of the UHO and PP rates, as explained in [6]. It is worth highlighting the improvement of the BHO procedure with the *reward* and *penalty* scheme. The *reward* anticipates the HO triggering, which addresses the core issue of the BHO procedure, while the *penalty* avoids UHO.

Fig. IV.6 depicts the HOF, UHO and PP rates. [6] showed that the CHO procedure removes the RLF and HOF at the cost of increasing the UHO and PP, i.e. signalling and measurement reporting. The *reward* scheme of the LHT event increases the UHO rate around 57 % and 91 % as compared with the BHO and CHO procedures with the MHT event. In contrast, the *penalty* scheme reduces the UHOs and PPs rates to 0, regardless of the HO procedure. The best performance in terms of RLF plus HOF, UHO and PP is achieved by the CHO procedure configured with a *penalty* scheme. The CHO procedure

eliminates the RLF and HOF with an earlier HO preparation and the *penalty* removes the UHO and PP by considering the distances to the cells centre.

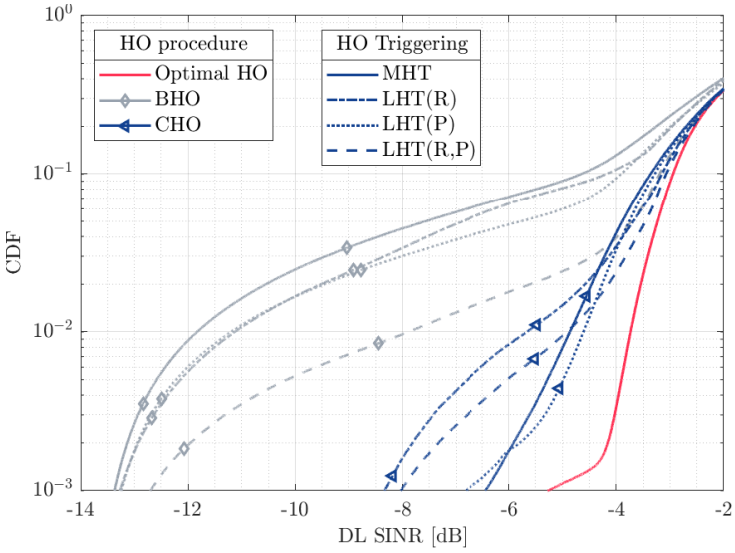


**Fig. IV.5:** Distribution of the DL SINR for BHO and CHO procedures configured with MHT and LHT events.

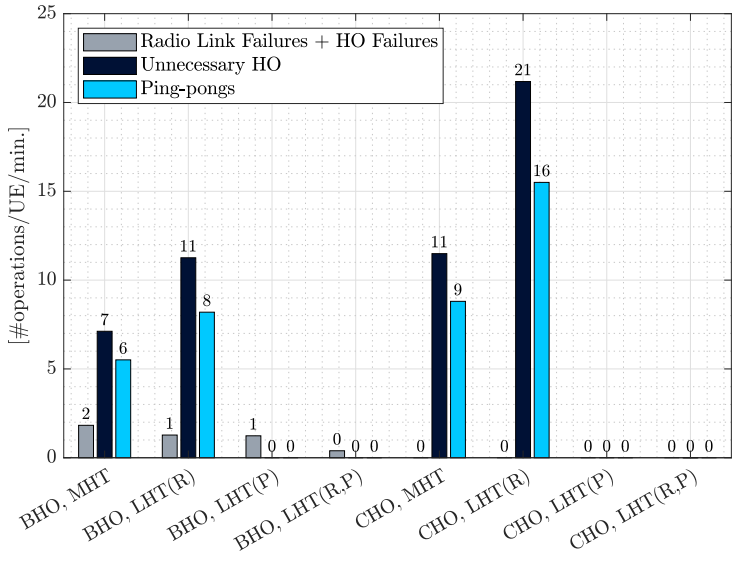


**Fig. IV.6:** HO failure, unnecessary HO and ping-pong rates for BHO and CHO procedures configured with MHT and LHT events.

In Fig. IV.7 the CDF of the ToS is presented. The MHT event shows mean ToS values below 2 s due to the high UHO rate seen in Fig. IV.6. The LHT event set with a *penalty* scheme extends the mean ToS to 4.8 s, independently of the HO procedure and presenting a close match with the optimal HO. As seen above, the *penalty* scheme removes UHO and PP, which translates into longer cell-stays at the serving cell. In addition, the CHO procedure configured with the LHT event and the *penalty* scheme presents a minimum ToS value of 2.5 s, the highest minimum value among all configurations.

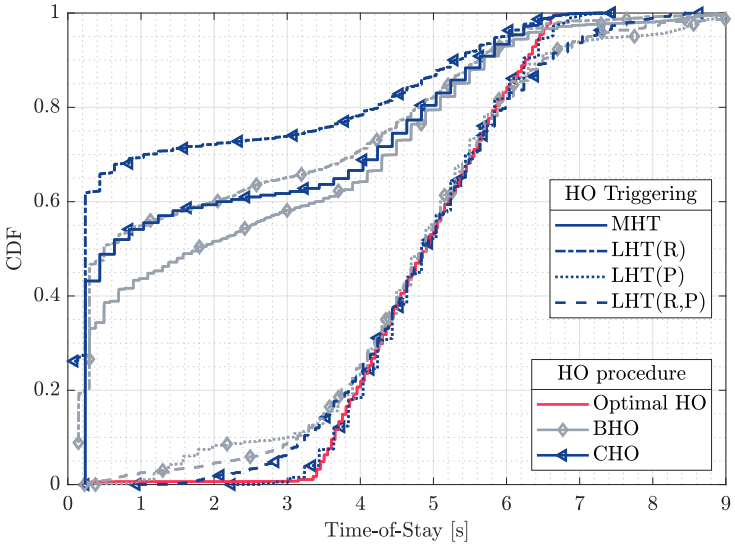


**Fig. IV.7:** Distribution of the time-of-stay in the serving cell for BHO and CHO procedures configured with MHT and LHT events.

# 7 Discussion and Future work

The research in [5] and [6] showed the limitations of measurement-based HO procedures in LEO-based NTN. The cost of improving the DL SINR is an increase of the UHO and the PP, which leads to sub-optimal mobility performance. Nonetheless, the predictable nature of satellite networks allows tapping the potential of additional information. This work explores the impact of including location information in the standardized HO triggering event. Through the parameters $\xi_{S,T}$ and $o_{penalty}$, the LHT event *rewards* and/or *penalizes* the candidate target cells. The system-level simulation results indicate that the LHT event, when *penalizes* the undesired target cells, enhances the 5G NR mobility performance and together with the CHO procedure achieves

the best performance. The BHO procedure can achieve similar mobility performance when combines the *reward* and *penalty* LHT schemes.

The proposed LHT successfully captures the cells' movement to filter the undesired target cells and drive the UE to the optimal target cells. Even though this may suggest mostly relying on location information, radio measurements are still relevant to detect the appropriate instant to handover as well as abrupt changes in the signal received power due to potential shadowing. It is worth highlighting that the location accuracy of the UE and cells centre is assumed ideal. Such assumption is not an issue considering the long communication distances (i.e. 600 km) and the cell diameter size (i.e. 50 km) over potential location inaccuracies of hundreds of meters.

In NTN, the HO events can be classified depending on whether the UE changes from one cell to another within the same satellite - i.e. intra-satellite HO - or the HO occurs among cells from different satellites - i.e. inter-satellite HO. The high degree of success of the LHT event can be explained by the fact that all the HO events in the simulations were intra-satellite HO. This case represents a particular arena where LOS conditions and shadow fading are fully correlated among cells since all satellite beams are radiated from the same transmission point. Together with the deterministic movement of the NTN cells, this fact results in a predictable scenario where the signal conditions become static between adjacent cells and hence the UE can rely on non-measurement information to reliably move among intra-satellite cells. Intra-satellite mobility enables a new space for simpler and more efficient HO solutions where a clever network should be able to dictate to the UE the best candidate cell without degrading the overall system performance.

# 8 Conclusions

We have proposed a new location-based handover triggering event and analysed its mobility performance in a low Earth orbit based non-terrestrial network implementing Earth-moving cells. The standardized measurement-based handover triggering event is modified to exploit the deterministic movement of the satellites and uses the location information of the users and the cell centres on the ground. In combination with radio measurements, the new handover event is triggered when the distance between the user's location and the cell centres on the ground meet the configured conditions. System-level simulations demonstrate that the novel location-based handover triggering event when used with the Rel-16 conditional handover is able to completely eliminate the handover failures, the unnecessary handovers and the ping-pongs. This reduces the signalling overhead and extends the time-of-stay in the serving cells from on average 1 s to 4.8 s.

# References

[1] S. Chen, Y.-C. Liang, S. Sun, S. Kang, W. Cheng, and M. Peng, "Vision, Requirements, and Technology Trend of 6G: How to Tackle the Challenges of System Coverage, Capacity, User Data-Rate and Movement Speed," *IEEE Wireless Communications*, 2020.

[2] O. B. Osoro and E. J. Oughton, "A Techno-Economic Framework for Satellite Networks Applied to Low Earth Orbit Constellations: Assessing Starlink, OneWeb and Kuiper," *IEEE Access*, 2021.

[3] 3GPP, "Solutions for NR to support Non-Terrestrial Networks (NTN) (Release 17)," RP-202908, 3GPP TSG RAN Meeting 90-e, Dec. 2020.

[4] ——, "Solutions for NR to support Non-Terrestrial Networks (NTN) (Release 16)," TR 38.821 V1.0.0, Dec. 2019.

[5] E. Juan, M. Lauridsen, J. Wigard, and P. E. Mogensen, "5G New Radio Mobility Performance in LEO-based Non-Terrestrial Networks," *IEEE GLOBECOM*, 2020.

[6] ——, "Performance Evaluation of the 5G NR Conditional Handover in LEO-based Non-Terrestrial Networks," *IEEE WCNC, 2022*.

[7] 3GPP, "TSG RAN, NR, RRC protocol specification (Release 16)," TS 38.331 V16.5.0, Jun. 2021.

[8] ——, "E-UTRA Mobility Enhancements in Heterogeneous Networks (Release 11)," TR 36.839 V0.7.1, Aug. 2012.

[9] ——, "Study on New Radio (NR) to support Non-Terrestrial Networks (Release 15)," TR 38.811 V15.2.0, Sept. 2019.

[10] E. Juan, M. Lauridsen, J. Wigard, and P. E. Mogensen, "Time-correlated Geometrical Radio Propagation Model for LEO-to-Ground Satellite Systems," *IEEE VTC-Fall*, 2021.

# Paper F

## Handover Solutions for 5G Low-Earth Orbit Satellite Networks

Enric Juan, Mads Lauridsen, Jeroen Wigard, Preben Mogensen

The paper has been published in the
*IEEE Access, 2022.*

*The layout has been revised.*

# Abstract

*Low-Earth orbit (LEO) satellite networks are meant to be fundamental to closing the digital divide, enabling new market opportunities and providing fifth-generation (5G) New Radio (NR) connectivity everywhere at any time. Despite the advantages of LEO deployments, these systems are characterized by a high mobility and a challenging propagation channel that compromise several procedures of the current 5G standards. One of the impacted areas is the radio mobility management, which is used to ensure continuous and satisfactory service while users handover among cells. Current research shows that the measurement-based 5G NR handover (HO) procedures, designed for terrestrial networks, fail to ensure optimal mobility performance. In this work, we provide a mobility performance analysis through extensive system-level simulations of state-of-the-art HO procedures for 5G NR over LEO satellite networks with Earth-moving cells. Furthermore, this article presents a novel antenna gain-based HO solution for intra-satellite mobility that exploits the predictability of the satellites movement and the antenna gain of the satellite beams, making UE's radio measurements obsolete. The system-level simulation results, which consider users in rural and urban scenarios, show that by exploiting the known satellite's trajectory, the UE eliminates service failures and undesired HO events, maximises the time-of-stay in a cell and experiences improved downlink signal-to-interference-plus-noise ratio. This article also includes a sensitivity study of the impact on the mobility performance of satellite-specific and UE-specific errors such as the UE's location error, the satellite beam's antenna radiation error and the satellite's pointing error. Finally, the impact of the UE's mobility is analyzed.*


# 1 Introduction

Internet has become something essential for society development and welfare, e.g. nowadays farmers need to be able to search for the best price to buy fertilizer and know when and where to sell their crops. Even though there has been an increase in Internet availability in recent years, a large percentage of the world's population remains unconnected; according to [1], less than 64 % of the population has Internet, which leaves 3 billion people offline. One of the main reasons for Internet access exclusion is the lack of available cellular infrastructure, especially in remote areas, where deploying fiber cable is not cost-effective.

Satellite technology aims to bridge the digital gap. By its nature, not being geographically constrained, it is ideal to deliver broadband connectivity to any location in the globe. Tens of thousands of satellites have been proposed to be deployed in LEO orbits - i.e., altitudes between 500 km and 1500 km. The Starlink constellation - backed by SpaceX - is currently authorized to deploy 4408 LEO satellites while the company has already launched more

than 2000 and envisions to have approximately 30 000 spacecrafts in orbit [2]. OneWeb's network, in the process of being completed in 2022, is planned to consist of 716 LEO satellites followed by a second phase with 6372 satellites [3]. Kuiper Systems, a subsidiary of Amazon, announced in 2019 a LEO deployment of 3236 satellites at altitudes between 590 km and 630 km [3]. Over the next decade, these three constellations alone envision to comprise more than 40 000 satellite systems into LEO, enabling a new time of space-based broadband services.

This new space race, driven by private companies, and the growth of demand for broadband services [1] have fueled the development of standards for NTN systems. Initially defined by the 3GPP in [4], NTN aims to complement TNs providing 5G and future sixth generation (6G) connectivity to unconnected areas through, among other systems, LEO satellites. Not limited only to provide connectivity in remote areas, NTN seeks to efficiently ensure 5G service availability anytime, anywhere, e.g. for critical communications in case of disaster and emergency, maritime communications and passengers on board of planes.

In contrast with GEO systems, LEO satellites feature high mobility but also reduced path loss, shorter transmission delays and lower production and launch costs. These systems operate in a revolving network at approximately 7.8 km/s relative to the Earth; at this speed a satellite circles the Earth in around 90 min. The movement of LEO satellites and thus signals from the RAN nodes leads to several issues. While in TN the RAN nodes are fixed, in LEO satellite networks, these nodes are constantly moving and triggering a high number of mobility events. Though the frequency of mobility events triggered by the satellite network will depend on the cell size - from 50 km to several hundreds of kilometers [5] -, the increment of these events might lead to an increase of the signalling overhead and potential service failures.

The target of connected-state mobility procedures is to ensure that the UE does not experience noticeable interruption or degradation of the service as it changes connection from one cell to the next one. The mobility procedure that must guarantee this is known as HO. Despite the advantages mentioned above, enabling 5G NR access over LEO satellite networks implies important challenges for the HO procedure. Some of those challenges include high HO frequency rate - which increases the control signalling between the UE and the NW -, long communication distances - which impact path loss, signal strength variation and propagation delays - and multiple high-gain beams radiated from the same satellite - which increases the DL interference experienced by the UE. A well-designed HO procedure is required to overcome these mobility challenges and to guarantee service continuity.

## 1.1 Related Work

There are research works in the literature addressing the topic of the HO over LEO satellite networks since the 1990s, which were motivated by the appearance of non-geostationary satellite projects such as Iridium and Globalstar constellations [6] [7]. These projects failed since they were not economically viable, launch costs were too high and hardware and software technologies were not mature enough.

In recent years, many companies have renewed the interest of providing ubiquitous Internet from space. A large body of investigations appeared after Starlink and OneWeb projects materialized and after the 3GPP reported in Release-15 the study to integrate satellite systems [4]. In [8], the authors proposed an inter-satellite HO strategy based on the *potential game* theory to reduce the average number of HO events and balance the constellation NW load. To reduce the HO delay and signalling cost, in [9], different HO procedures were proposed for a multi-layer network architecture which included GEO satellites, HAPS and terrestrial relay nodes. In [10], the authors focused on the inter-satellite HO for massive user terminals in mega-LEO constellations to maximize the quality of experience by establishing a HO model based on network-flows. A user-centric HO scheme for ultra-dense LEO satellite networks was proposed in [11]. The authors presented a solution to buffer user's downlink data in multiple satellites simultaneously to permit the terrestrial users to realize seamless HO and to address the frequent HO problem. In [12], the authors presented a reinforcement learning scheme where UEs make decisions autonomously to optimize the long-term throughput, meanwhile avoiding frequent HO events among non-terrestrial base stations. The above-mentioned proposals address approaches to optimize the HO over NTN, mainly focusing on the HO frequency problem. However, to the best of our knowledge, none of the works in the past literature considered 5G NR technology over NTN complying with the 3GPP specifications.

Based on the 3GPP technical reports [4] and [5] for Release-15 and Release-16, respectively, in [13] we demonstrated through system-level simulations that the conventional UE-assisted NW-controlled 5G NR HO - used in TNs and referred in this article as BHO - cannot ensure robust service continuity in 5G LEO satellite networks with EMC. Users experience frequent service outages due to a HO that is initiated too late when the serving cell radio link is already too weak to complete the HO process. Under the same scenario, we reported in [14] a mobility performance study of the Release-16 CHO which accomplishes to eliminate the service failures due to an earlier HO initiation. However, the analysis showed a 60 % increase of UHO events, as compared with the BHO procedure. Both mobility procedures, meant for TNs, strongly rely on UE's radio measurements. The 3GPP suggested in [5] considering

additional triggering criteria based on satellite's trajectory and UE's location to enhance mobility performance. In [15], we proposed the LHT event to exploit the distance information given by UE's location and knowledge of satellite's trajectory. Extensive system-level simulation results proved that the LHT event reduces the signalling overhead, eliminates the service failures and maximises the ToS in a cell. The best mobility performance was achieved by the CHO procedure configured to use the LHT event; here referred as location-based CHO (LCHO) procedure. Despite these works considered 5G NR over LEO satellite networks under 3GPP-compliant assumptions, these HO solutions were only analyzed with users in a rural environment, where radio propagation conditions are more favourable than in urban scenarios due to low and scattered buildings. Furthermore, these HO procedures are based on the reporting of the UE's radio measurements to the NW. Due to UE's radio measurement inaccuracy, this may lead to wrong HO decisions that increase the signalling overhead, which ultimately may compromise the UE's mobility performance.

## 1.2 Motivation and Contributions

The motivation behind this work stems from the lack of suitable HO solutions to support the development of 5G NR over LEO satellite networks and the need for system-level simulation results to support such solutions. Furthermore, the publicly available works in the literature that meet the latter only address users in rural scenarios. Overall, the novel contributions of this article cover several gaps of the literature and are summarized as follows:

- Discuss the state-of-the-art HO procedures to support 5G LEO satellite networks and the mobility challenges that these procedures shall overcome.
- Propose a novel fully NW-controlled antenna gain based HO (AGHO) solution for intra-satellite mobility that uses the UE's location, the antenna gain (AG) of the satellite beams and the known satellite's trajectory to avoid UE's radio measurements.
- Based on extensive system-level simulations, provide mobility performance analysis and comparison of the BHO, the CHO, the LCHO and the AGHO over 5G LEO satellite networks for users in rural and urban scenarios.
- Provide a sensitivity study that evaluates the mobility performance impact of UE-specific and satellite-specific errors on the LCHO and the AGHO solutions. The study considers the following sources of error: i) satellite beam antenna radiation, ii) satellite beam antenna steerability and iii) UE's location.

The rest of the paper is organized as follows. Section 2 describes the reference scenario and the main aspects impacting the HO procedure in LEO satellite networks. Furthermore, the section provides a comparison between terrestrial and LEO deployments, while it identifies the main limitations of measurement-based HO procedures. In Section 3, the HO enhancements analysed in this work are explained and compared. The simulation methodology and results from system-level simulation campaigns are then provided in Section 4 together with the definition of the KPIs used to evaluate the mobility performance of the different HO procedures. Finally, we draw the conclusions of this investigation and formulate recommendations for future research in Section 5.

# 2 Connected-mode Mobility in LEO satellite networks

This section first describes the reference scenario, then the main challenges and limitations of the HO procedure over LEO satellite networks are introduced. Finally, the section includes a discussion on the ongoing NTN standardization activities.

## 2.1 Reference scenario

Fig. IV.1 depicts the studied reference scenario where a LEO satellite network, at an altitude of 600 km, provides 5G NR coverage to a sparse number of users on the ground. Satellite systems operate as RAN nodes that through multiple satellite high-gain beams enable NR cells on the ground with a footprint diameter of 50 km. In NTN specifications, EFC and EMC are considered. The former entails that the satellite continuously adjusts the satellite beam pointing direction to fix the NR cell to a specific location on the Earth during a certain time period, while the latter option entails the satellite beam pointing direction is fixed and thus the beam footprint (i.e. NR cell) is moving on Earth. This study is carried out considering EMC, which entails highly mobile cells that will cause very frequent HO events. Fig. IV.1 aims to illustrate this phenomenon where stationary users continuously change serving cell due to cells movement, i.e. frequent HO events. These events can occur among cells from the same satellite, i.e. intra-satellite mobility, and among cells from different satellites, i.e. inter-satellite mobility.

As mentioned before, the connected-state mobility procedure that ensures users switching cells without noticeable service interruption is the HO procedure. The conventional HO procedure used in TNs (i.e. BHO) is based on specific reference radio signals measured by the UE, that are reported to the NW when a certain measurement-based condition is met. In this work,

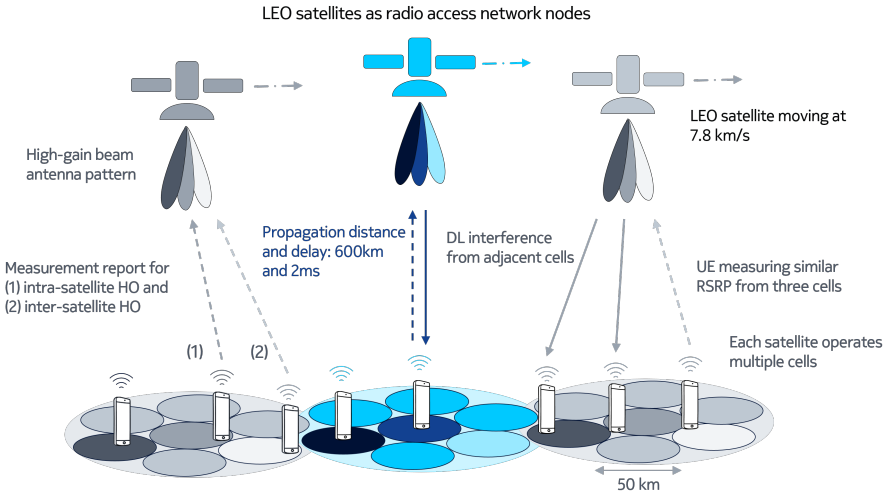


**Fig. IV.1:** LEO satellites as radio access network nodes providing 5G NR service to users on the ground.

the BHO procedure uses the common MHT event known as NR A3 event, which is triggered when the signal strength of target cell $T$ becomes HOM dB stronger than the signal strength of serving cell $S$ for a certain time called TTT. A simplified NR A3 event is given in (F.1), where $P_S(t)$ and $P_T(t)$ are the RSRP measurements (in dBm) from serving cell $S$ and target cell $T$, respectively. Further details of the NR measurement events can be found in [16].

$$P_T(t) > P_S(t) + \text{HOM} \qquad \text{[dBm]} \quad \text{(F.1)}$$

Once the above condition is met, the UE sends the MR to the NW via the serving cell. Based on the UE's radio measurements contained in the MR, the NW determines whether the target cell is appropriate to access and it commands the UE to initiate the HO towards that cell.

As mentioned above, the main goal of the HO procedure is to guarantee service continuity and, hence, ensure adequate user's experience. In LEO satellite networks, the UE's mobility performance is mainly challenged by satellites moving at high speed and altitude, which might lead to a malfunctioning of the measurement-based NR HO procedures. The following section explains the characteristics of the reference scenario and the mobility challenges to overcome in order to design new HO solutions.

**Table IV.1:** Main differences between the default values of the 3GPP-specific rural macro deployment in [17] and the reference LEO satellites network evaluated in this work.

| **Specific** | **Rural macro deployment** | **LEO satellites network** |
|---|---|---|
| Altitude RAN node | 35 m | 600 km |
| Maximum distance UE-RAN node | 10 km | 610 km (79.8° elevation angle) |
| Maximum propagation delay | 0.03 ms | 2 ms |
| Speed of RAN node (relative to Earth) | 0 km/h | 28 000 km/h |
| Cell radius | 10 km | 25 km |
| Cell visibility time (stationary UE) | ∞ | 3 to 7 s [15] |
| Cell RSRP variation in LOS (cell centre vs cell edge) | 50 dB | 3 dB |

## 2.2 Challenges and limitations

Below, the main physical differences between a typical terrestrial rural macro deployment and the reference scenario are described. Table IV.1 provides a summary of this comparison to support the explanation.

The NR HO procedures were designed to efficiently work in terrestrial deployments, where RAN nodes are fixed at altitudes of tens of meters, wireless communication distances are typically shorter than a few kilometers and mobility events are mainly triggered by the UE's mobility. The characteristics of LEO satellite networks are completely different. The reference scenario is characterized by LEO satellites constantly moving at an altitude of 600 km, where mobility events are mainly caused by the movement of satellites as they move much faster than UEs on the ground, approximately 7.8 km/s relative to the Earth (i.e. 28 000 km/h). While the 5G standard supports a maximum distance of 100 km, in LEO deployments the communication distances can escalate up to hundreds or thousands of kilometers. As Table IV.1 shows, in the reference scenario the maximum communication distance can be up to 610 km for a 79.8° elevation angle, as compared with the 10 km maximum distance of the rural macro deployment. Such increase in distance involves also an increase of the signal propagation delay; 0.03 s vs. 2 ms. Note that LEO satellite communications feature a propagation delay longer than a

transmission slot.

**Low RSRP variation and UE measurement error**

An important factor to consider is the RSRP variation in a cell. In TNs, there is a clear difference between the RSRP measured at cell centre and at cell edge. Considering the rural case in Table IV.1, the communication distance ranges from a few tens of meters (i.e. cell centre) up to 10 km (i.e. cell edge). Due to the logarithmic behaviour of radio signals attenuation, the maximum distance difference results in variations of some tens of dBs. This effect is not as pronounced in LEO satellite networks, where the distance between transmitter and receiver is orders of magnitude greater, regardless of the UE's location within the cell. The satellite-user distance can be more than 10 times longer than the cell size. In our reference scenario, the AG of the satellite beams is the main element that introduces changes in the RSRP. This is because the satellite-user distance changes from 600 km at cell centre to 600.5 km at cell edge (for a UE being served by the central satellite beam), which entails hardly any change in the free-space path loss, i.e. 154.03 dB vs. 154.04 dB.

Apart from the low RSRP variation, UEs have associated a certain measurement error. The 3GPP specifies in [18] a relative RSRP accuracy requirement of $\pm 2$ dB to be met at the input of the UE's L3 filter. The combination of these two aspects can challenge UEs to correctly distinguish the appropriate target cell to handover to. In Fig. IV.2, we depict the RSRP measured by a UE when using the BHO procedure. There is a maximum RSRP variation of 3 dB, where the RSRP ranges from $-108$ dBm at cell centre to $-111$ dBm at cell edge. It can be also observed that for some cells the RSRP range is even lower, i.e. approximately $-110$ to $-111$ dBm. The figure also shows the impact of the UE's measurement error. Especially in those instants when the UE is in between two cells, the UE cannot complete the HO at the optimal instant (e.g. $t = 19$ s and $t = 20$ s) or it handovers towards the wrong target cell (e.g. $t = 11$ s).

**High HO frequency and unnecessary HO events**

The high frequency of HO events caused by the movement of LEO satellites is more significant in EMC-based networks. For the scenario under study, the best achievable HO rate is an average of approximately 0.2 HO/UE/s. Ergo, the NW should handle per UE roughly a HO every 5 s. The low RSRP range combined with the UE measurement error may further increase the HO rate due to wrong HO decisions. If the number of UHO events significantly increases, the mobility performance and the user experience can be compromised.

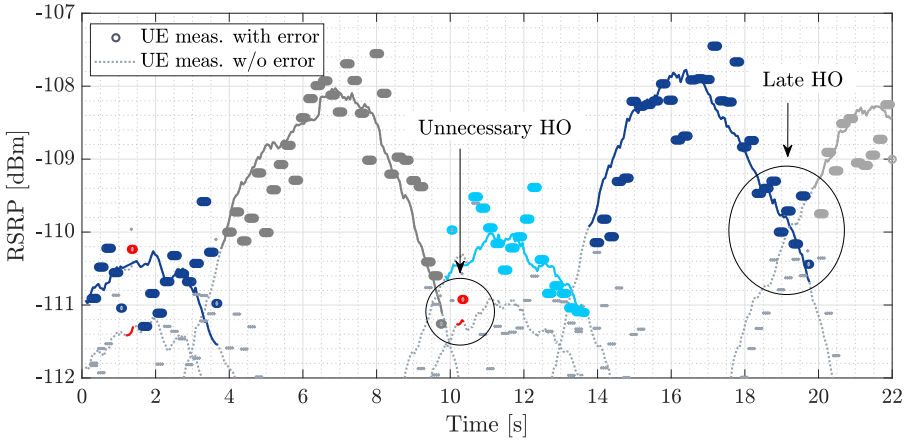


**Fig. IV.2:** Time trace of the RSRP measured by a UE when it is connected to a LEO satellite. There is limited RSRP variation experienced between cell centre and cell edge.

In [15], we discussed that HO procedures only based on UE's radio measurements may limit the mobility performance and increase the number of HO events towards sub-optimal target cells. Fig. IV.3 exemplifies some of the limitations of these procedures. The figure shows three snapshots of a scenario where a stationary UE (red triangle) is surrounded by three Earth-moving cells: *cell A*, *cell B* and *cell C*. The satellite beams radiate the cells on the ground with a circular shape. The radio coverage of the cells is depicted as an hexagon due to cells overlapping; this produces areas of a few kilometers where UEs detect similar RSRP from serving cell and neighbouring cells. The figure also includes time-traces of the RSRP variations with regards to the UE's location within the cell. In Fig. IV.3a, the UE is connected to *cell A* and located near the cell centre of *cell A*. As cells move from left to right due to satellite's movement, the radio coverage edge of *cell A* approaches the UE. Fig. IV.3b shows the UE in cell-edge conditions and located between the three cells. While the UE is in this area, it may continuously trigger measurement-based HO events due to the UE's measurement error and the low RSRP variation among cells. In order to minimize the HO rate and maximise the stay in each cell, it is optimal that the UE stays connected to *cell A* until it is close enough to handover towards *cell B*. However, the UE may connect to *cell C*, causing three undesired events:

- *Cell A*→*Cell C*→*Cell B*. Once the UE handovers from *cell A* to *cell C*, it may immediately handover to *cell B*. This results in an UHO event because it increases the signalling and makes a sub-optimal use of the available resources.
- *Cell A*→*Cell C*→*Cell A*. As in the previous case, the UE can handover

back to *cell A* to immediately handover towards *cell B*.

- *Cell A→Cell C→RLF*. After handovering from *cell A* to *cell C*, the UE may attempt to handover from *cell C* to *cell B* when is too late and then the UE declares a RLF and goes into idle-mode. If the UE does not execute the HO timely, the serving radio link becomes too weak because the cell moves away and the UE cannot communicate with the serving cell to initiate the HO (see Fig. IV.3c).

These cases are undesired and avoidable events since they increase the signalling overhead and the UE's energy consumption, lead to longer service interruptions and degrade the overall user experience.

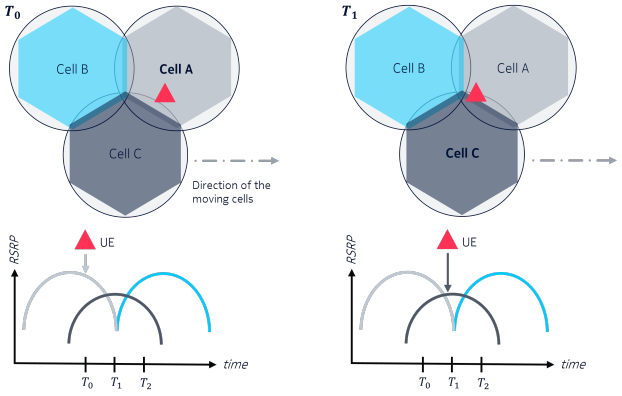


**(a)** UE at $T_0$: strong radio link with cell A

**(b)** UE at $T_1$: handover from cell A to cell C

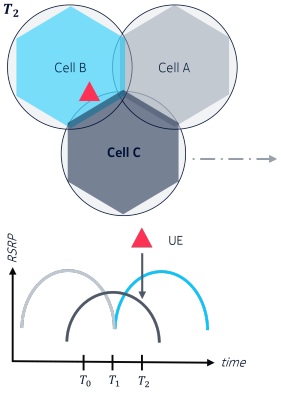


**(c)** UE at $T_2$: radio link with cell C fails

**Fig. IV.3:** Scenario that depicts the detected RSRP over time for a UE being covered by Earth-moving cells.

### Low DL SINR

Especially when cells are deployed with a FR1 scheme (i.e. all cells use the same frequency resources), UEs can experience poor DL SINR conditions when using the BHO procedure. Fig. IV.4 shows some of the issues of using this HO procedure to motivate the proposal of new HO solutions. The DL SINR traces correspond to a UE impacted by a high DL interference as a result of a single satellite radiating multiple NR cells on the ground. The UE, which is randomly selected, is configured with the BHO under three sets of HO control parameters, i.e. HOM and TTT. The *optimal HO* is also included as an upper-bound of the achievable DL SINR performance (Section 4.4 includes further details). None of the traces show values above 1 dB. The best DL SINR performance is achieved when the UE is configured with HOM = 0 dB and TTT = 0 s. However, this HO configuration increases the number of UHO events (e.g. $t = 12$ s). In [14] we discussed that measurement-based HO procedures are limited by such trade-off; improving the DL SINR entails an increase of UHO events. Note that the two other HO configurations present DL SINR values below −10 dB. These low values are a consequence of the inability of the BHO procedure to avoid RLFs, which strongly depend on the radio link quality experienced by the UE. Therefore, the BHO procedure is limited by a low DL SINR that increases RLFs, compromising the service continuity. Furthermore, the HO configuration that improves the DL SINR performance, increases the undesired HOs events.

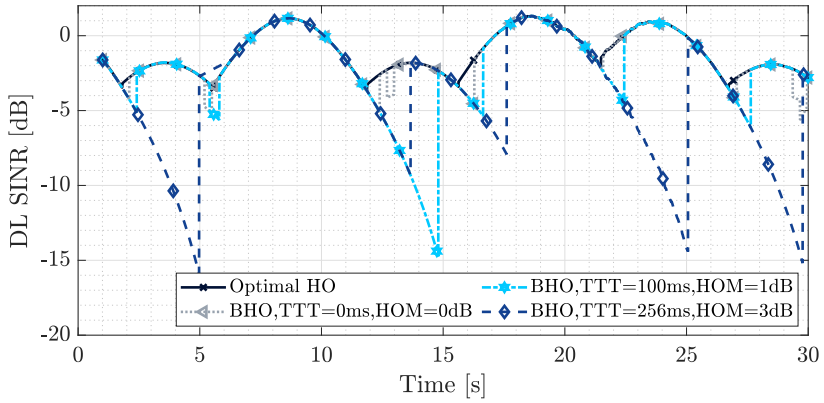


**Fig. IV.4:** Downlink signal-to-interference-plus-noise ratio (DL SINR) as a function of time, experienced by a UE connected through a LEO satellite network. The UE is configured with the BHO procedure under three HO configurations plus an optimized SINR-based HO procedure (upper-bound reference).

As discussed above, the BHO procedure was designed to function in terrestrial scenarios, the physical characteristics of which are quite different

from LEO deployments (see Table IV.1). These differences might cause a poor UE's mobility performance when using the BHO procedure. The key issues to address in order to design new HO solutions are summarized in the following points:

- *RSRP*. UEs detect RSRP from serving and neighbouring cells only within a 3 dB margin. If the HO procedure is purely based on UE's radio measurement, the low RSRP variation together with the UE's measurement error may cause to handover towards the wrong target cell.
- *HO frequency*. The movement of LEO satellites causes a high number of HO events. We aim to minimize the HO rate and maximize the time spent in each cell because an excess of signalling overhead and measurement reporting can compromise the mobility performance and the user experience.
- *DL SINR*. Serving radio link quality is limited by a strong DL interference from neighbouring cells. This not only impacts the throughput but also the mobility performance if DL SINR falls below a certain threshold, which might cause a RLF.

## 2.3 Related Standardization Activities

The 3GPP concluded a study item on NR NTN for Release-16. The outcome, including recommendations on future work, is provided in the technical report [5]. The target was to study the support of 5G NR to users on Earth through GEO, MEO and LEO satellites and HAPS. Each platform may implement multiple beams as NR cells. Among other architecture specifications, two types of payload were accounted: *transparent* and *regenerative*. The latter implies an NTN platform, e.g. LEO satellite, acting as a base station while the former entails a platform as a relay node for base stations on Earth.

In Release-17, the 3GPP introduced for the first time the satellite technology as part of the 5G specifications. The work item in [19] defined the required changes to enable basic operations of NR over NTN in FR1. The main challenges addressed are related to the mobility of the satellites since they introduce frequent changes of serving node and high time and frequency drifts. The work done by the 3GPP focused on GEO and LEO network scenarios with transparent payload, EFC and EMC configurations and UE with GNSS capabililities. Using its own position and the NTN *ephemeris*, a UE could pre-compensate the Doppler frequency shift, calculate the propagation delay variation between UE and satellite to estimate the full timing advance and benefit from location-based mobility procedures. The CHO procedure was agreed as a mobility procedure for NTN and could include new triggering criteria based on cells location and timing. Even though many companies

in the 3GPP proposed mobility enhancements for the CHO based on location and time conditions, there were no system-level simulation results on concrete enhancements to support the discussions.

At the time of writing, 3GPP is investigating enhancements to support NR operations over NTN in the context of Release-18. The new work item [20], started in May of 2022, will support new deployments in frequency bands above 10 GHz, enhance coverage for handset terminals with NW-verified UE location and address mobility and service continuity improvements for TN-NTN and NTN-NTN scenarios.

# 3 Analysed HO Enhancements

This section describes three HO enhancements compared to BHO procedure in Section 2.1: i) the CHO, ii) the LCHO and iii) the AGHO. Mobility performance evaluations of the CHO and the LCHO procedures are available in [14] and [15] but only for users in rural environments. This work includes a study of the novel AGHO procedure as a fully-network controlled HO strategy based on the estimated AG of the serving and target satellite beams.

## 3.1 Release-16 Conditional HO

In Release-16, the 3GPP specified the CHO procedure to improve the mobility robustness in terrestrial deployments. On this basis, our work in [14] demonstrated that the CHO enhances the UE's mobility performance in LEO-based NTN by reducing the risk of RLF at the expense of increasing UHO events.

The CHO ensures a robust mobility by preparing the HO in advance (with regard to the BHO). The principal difference is that the CHO decouples preparation and execution phases by configuring the UE with up to two triggering event conditions per candidate target cell. The first condition, also called preparation condition, is used by the UE to send the MR to the NW. This condition is triggered early enough to allow the network to reach the UE when the serving cell radio link is still under favourable conditions. The second condition, or execution condition, delays the HO execution and it is used by the UE to initiate the access towards the target cell when the target cell radio link becomes sufficiently good. These two conditions are based on UE's radio measurements. The specification permits to configure different measurements quantities for each of the conditions such as RSRP and RSRQ. Furthermore, the CHO may use different NR measurement events such as the NR A3 event, i.e. target cell becomes offset better than serving cell (see Section 2.1), and Event A5, i.e. serving cell becomes worse than threshold one and target cell becomes better than threshold two.

Fig. IV.5 illustrates the operational steps of the CHO procedure according to 3GPP specifications. In Step 1, once the first NR measurement event condition is fulfilled, the UE sends a MR to the serving cell with DL measurement details of the surrounding cells. The serving cell asks for HO preparation to the selected target cell(s) (Step 2-6). The specification allows the preparation of up to eight target cells. For the sake of simplicity, Fig. IV.5 shows only one target cell. The serving cell sends the CHO command comprising the radio resource control (RRC) reconfiguration information as well as the execution conditions for the prepared target cell(s) (Step 7). The execution conditions are set by the serving cell while the target cells provide the CHO command with the specific cell configuration. After reception of the CHO command, the UE does not immediately initiate the access to the target cell but evaluates the CHO execution condition (Step 8). Unlike BHO, the UE in Step 8 continues exchanging data with the serving cell until a target cell radio signal meets the CHO execution condition (Step 9). After Step 9, the UE executes the HO to access the target cell and the procedure follows as in the BHO. Fig. IV.5 shows a simplified signalling of the random access procedure and the HO completion since these are not part of the main focus of this paper. Further details about the CHO can be found in [21] and [16].

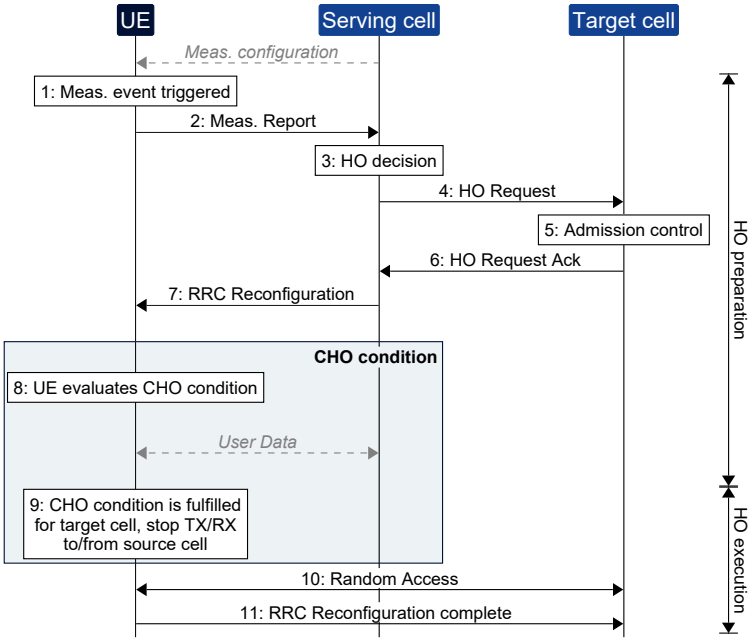


**Fig. IV.5:** Operational steps of the conditional HO (CHO) procedure, including the preparation and the execution conditions.

The main characteristics of the CHO procedure can be summarized as follows:

- *Decoupled HO preparation and HO execution phases*. This enables an earlier HO initiation when the serving cell radio link is in good conditions and delays the execution of the HO towards the target cell when the target cell radio link is strong enough.
- *Up to two HO triggering conditions purely based on UE's radio measurements*. CHO introduces preparation and execution event conditions. These events purely rely on radio measurements, which can limit the UE's mobility performance due to the reasons exposed in Section 2.2.
- *Reduced risk of service failure but increased signalling overhead and measurement reporting*. An earlier HO initiation means a more reactive HO procedure which reduces the probability of RLF declaration but it also increases the amount of UHO events if target cells are not carefully selected.

## 3.2 Location-based CHO

The BHO and the CHO procedures rely only on UE's radio measurements because of simplicity and effectiveness in TNs. However, in [14], we highlighted the existence of a trade-off between DL SINR and UHO events: DL SINR cannot be improved without increasing the signalling overhead and measurement reporting, which limits the stay in a cell and degrades the user experience.

LEO satellite systems follow orbits that are deterministic. The predictability of satellites movement implies that NW and/or UE may predict the cells radio coverage and exploit that information to optimize the HO procedure. Based on this principle and motivated by the discussions in [5], our work in [15] presented the LHT event, which is a novel HO triggering event that takes advantage of the cells location and UE's location.

The procedure starts with the NW broadcasting the centre locations of the moving cells. Note that in NTN, it is assumed that i) the NW has knowledge of the satellite *ephemeris* information (i.e. positions of the satellites and their orbits) and ii) the UE is aware of its own location. The UE periodically collects the satellite *ephemeris* broadcast by the NW and, together with its GNSS-based location, determines the changes of the UE-cell centre distances. This information is captured in a location-based offset, $\Phi_{S,T}(t)$, which is introduced in the NR measurement events to enhance the HO triggering process. In [15], it is proposed the following modification of the NR A3 event in (F.1):

$$P_T(t) > P_S(t) + \text{HOM} + \Phi_{S,T}(t) \qquad \text{[dBm]} \quad \text{(F.2)}$$

where $\Phi_{S,T}(t)$ is the location-based offset (in dB) for the cell-pair $S$-$T$.

$$\delta_S(t) = d_S(t) - d_S(t\text{-}\tau) \quad \text{[m]} \quad \text{(F.3)}$$

$$\delta_T(t) = d_T(t) - d_T(t\text{-}\tau) \quad \text{[m]} \quad \text{(F.4)}$$

$$\Psi_{S,T}(t) = \frac{\delta_T(t)}{\delta_S(t)} \quad \text{[dB]} \quad \text{(F.5)}$$

In a similar manner to DL measurements, the UE uses the location information provided by the NW to calculate distance UE-cell $S'$ centre ($d_S$) and distance UE-cell $T$'s centre ($d_T$) at periodic intervals $\tau$. In (F.3) and (F.4), the parameters $\delta_S$ and $\delta_T$ are calculated to capture the movement direction of cells $S$ and $T$. A positive value of $\delta_S$ denotes that cell $S$ is moving away from the UE, while a negative sign indicates that cell $S$ is approaching the UE. The cells movement information given by (F.3) and (F.4) is combined to obtain the cell-pair $S$-$T$ ratio $\Psi_{S,T}$, shown in (F.5).

$$\Phi_{S,T}(t) = \begin{cases} \Psi_{S,T}(t) & \text{if } \Delta_S > 0 \text{ and } d_S > \gamma_S \\ & \quad \text{and } d_T < \gamma_T \\ \Theta_P & \text{otherwise} \end{cases} \quad \text{[dB]} \quad \text{(F.6)}$$

The full definition of the location-based offset $\Phi_{S,T}$, given in (F.6), includes the parameters $\gamma_S$, $\gamma_T$ and $\Theta_P$. The purpose of $\Psi_{S,T}$ is to leverage cells movement and prompt the HO towards those cells approaching the UE. In [15], this aspect is referred to as a *reward* strategy and it takes effect when $\Delta_S$ is positive - i.e. serving cell $S$ is moving away - and the UE is at the geometrical edge of cell $S$. Distances $d_S$ and $d_T$ are evaluated against thresholds $\gamma_S$ and $\gamma_T$. The value of $\gamma_S$ is equal to half of the ISD and $\gamma_T$ is used to prevent UHO events to distant target cells, which can be triggered due to antenna side-lobes when only using UE's radio measurements.

Furthermore, (F.6) includes the constant $\Theta_P$ to *penalize* those candidate target cells that do not meet the conditions imposed by $\Delta_S$, $\gamma_S$ and $\gamma_T$.

According to [15], the LHT event successfully captures the movement of the cells to filter undesired target cells and direct the UE towards the optimal target cells. However, UE's radio measurements are still used to detect the appropriate time for the HO. In [15], BHO and CHO procedures are analysed under three schemes of the LHT event, which depend on the values of $\Phi_{S,T}$ and $\Theta_P$. These schemes aim to *reward*, *penalize* or both, *reward* and *penalize*, the candidate target cells. For this study we use the reported configuration achieving best mobility performance, which corresponds to the CHO procedure set with the *penalty* scheme. We refer to this configuration as the LCHO procedure.

Fig. IV.6 shows the operational steps to initiate the LCHO procedure. The UE not only measures reference radio signals but also periodically calculates

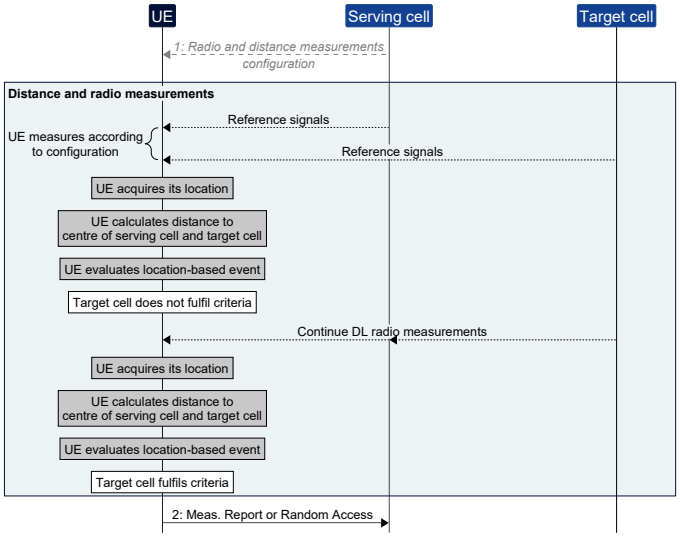


**Fig. IV.6:** Triggering of the measurement report or access to the target cell when using the location-based CHO (LCHO) procedure.

the distances UE-Cell centre using its location and the location of the cells. Once a target cell fulfils the criteria in (F.6), the UE sends the MR to the NW to initiate the HO preparation.

The most important features of the LCHO procedure, captured in [15], are listed below:

- *Enhances the mobility performance of the CHO procedure*. The LCHO accomplishes to eliminate service failures and UHO events and maximises the time in each cell. Thus, it overcomes the trade-off between DL SINR and signalling overhead shown by the CHO procedure.
- *Exploits the predictability of the satellites mobility*. NR measurement events are modified to exploit the deterministic movement of LEO satellites by using the distances between UE and ground centre of the cells.
- *UE's radio measurements are still relevant*. The procedure still relies on UE's radio measurements to detect the appropriate instant to handover towards the target cell. This may also account as a limitation due to UE's measurement error introduced in Section 2.2.
- *Additional control signalling*. This procedure relies on the location information reported by the NW. It also involves additional signalling between UE and NW to configure distance measurements in addition to configuration and reporting of UE's radio measurements.

### 3.3 Antenna Gain-based HO

As pointed above, specifications of the NR HO procedures can be enhanced by exploiting the predictability of the satellites movement. Initial steps were taken in [15], with a HO procedure that involves additional signalling between UE and NW to acquire cells centre and configure distance measurements. However, the procedure still relies on UE's radio measurements.

The usefulness of UE's radio measurements depends on UE's measurement accuracy. Section 2.2 highlights that the non-negligible measurement error, together with the low RSRP variation (see Table IV.1), can bring the UE to access the sub-optimal target cell. To overcome this issue, we present a novel fully NW-controlled HO solution that utilizes the AG of the satellite beams to bypass the UE's radio measurements and the effect of the measurement error. This approach is designed for intra-satellite mobility and aims to enhance the UE's mobility performance, while reducing the UE-NW signalling.

The motivation behind using the AGHO procedure stems from the fact that intra-satellite mobility represents a particular scenario where radio propagation conditions - i.e., line-of-sight, path loss and shadow fading - are assumed fully correlated between adjacent cells due to cells being radiated from the same satellite. This might result in a predictable scenario where signal conditions are static between satellite beams belonging to the same satellite. The full correlation of the radio propagation conditions together with the known movement of the cells enables a new space for novel HO solutions where the UE does not need to rely on radio measurements to reliably move among intra-satellite cells.

In the proposed approach, the NW is responsible for estimating the cells radio coverage based on the AG patterns of the satellite beams. Once an estimated target cell's AG becomes better than the serving cell's AG, the NW prepares that target cell and it sends a HO command to the UE. It is assumed that the NW knows the satellite *ephemeris* and the UE's location. In addition, the NW has knowledge of the antenna radiation pattern and the pointing vectors of the satellite beams. The AG of a satellite beam is calculated following the technical report [4], which defines the AG pattern of a typical reflector antenna with circular aperture.

The main elements of the AGHO procedure are described as follows, while Fig. IV.7 supports the explanation. We define $G(t)$ as the AG of a satellite beam, in dBi, at time $t$. The position vector of the satellite, relative to the Earth, is defined as $\vec{S}(t)$. The direction vector between satellite's location and UE's location is denoted as $\vec{SU}(t)$. The angle $\alpha$ refers to the angle measured from the bore-sight of a satellite beam's AG to the vector $\vec{SU}(t)$.

Given the serving satellite beam $S$ and the target satellite beam $T$, the NW estimates gains $G_S(t)$ and $G_T(t)$ at time $t$ based on the known AG patterns

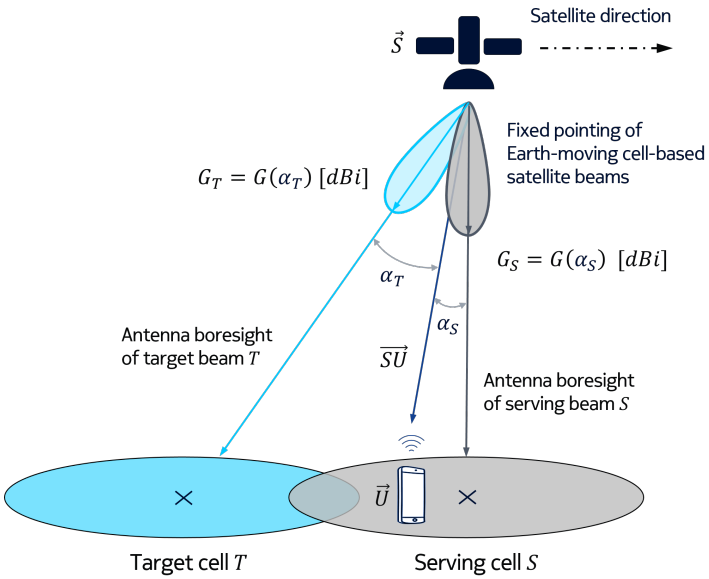


**Fig. IV.7:** Geometry of the antenna gain-based HO (AGHO) procedure.

and the angle $\alpha$ measured for satellite beams $S$ and $T$, i.e. $\alpha_S$ and $\alpha_T$, respectively. The proposed procedure operates estimating $G_S(t)$ and $G_T(t)$ at future instants $t_1, t_2$. These estimations require predicting future positions of the satellite along the orbit. Note that the estimations of $\vec{S}(t_1)$ and $\vec{S}(t_2)$ are conducted using linear regression from past instants, however, this could be done using orbit propagators or any other estimator.

As shown in Fig. IV.8, once $G_S(t)$ and $G_T(t)$ are estimated at instants $t_1, t_2$, the NW evaluates two conditions to carry out the HO decision. The first condition, in (F.7), is to detect when target cell's AG becomes better than serving cell's AG. The second condition (F.8) is introduced to avoid undesired handovers by predicting the target cell's AG at $t_2$, i.e. $G_T(t_2)$, and identify whether $G_T(t_2)$ increases or decreases. If both conditions are fulfilled, the NW, through serving cell $S$, sends the HO command to the UE with instructions to initiate the access towards target cell $T$.

$$G_S(t_1) < G_T(t_1) \qquad \text{[dBi]} \quad \text{(F.7)}$$

$$G_T(t_1) < G_T(t_2) \qquad \text{[dBi]} \quad \text{(F.8)}$$

The key points of the AGHO procedure are the following:

- *Intra-satellite mobility without UE's radio measurements.* The procedure bypasses the non-negligible UE's radio measurement error and captures

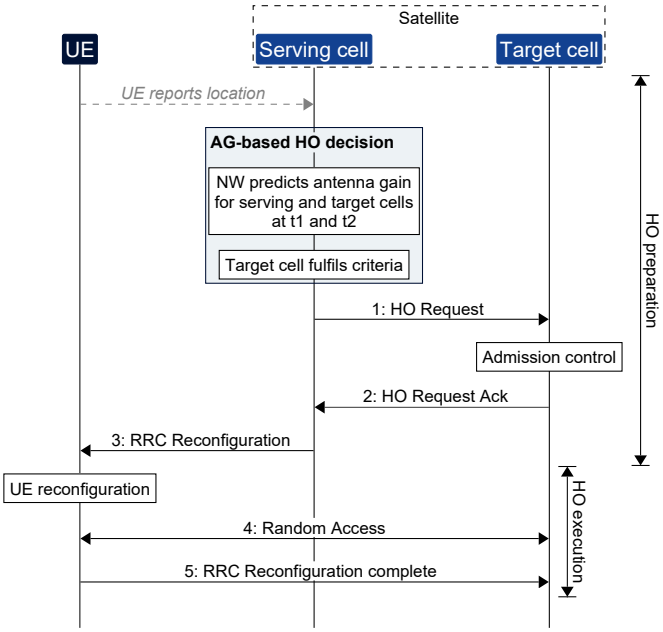


**Fig. IV.8:** Operational steps of the antenna gain-based HO (AGHO) procedure.

the crossover point among serving cell's AG and target cells' AG. Based on dual time domain, it avoids short stays in a cell and reduces UHOs events.

- *Reduced control signalling*. Reporting of UE's radio measurements can be reduced or avoided. This is important for satellites with a large number of cells; handling a heavy signalling load might require high-processing capabilities which added to a high HO frequency can compromise the UE's mobility performance.

- *Fully NW-controlled HO procedure*. Even though the NW still requires the reporting of the UE's location, the HO process is no longer assisted with UE's radio measurements. This might lead to a sub-optimal functioning in scenarios with abrupt changes of the radio propagation conditions.

- *Only for intra-satellite mobility*. The proposed solution is valid to handover among cells from the same satellite. However, it requires a different HO solution for inter-satellite mobility where radio propagation conditions are more likely to change from one cell to the next one.

## 3.4 Summary of the analysed HO procedures

This section has described state-of-the-art HO enhancements to improve the UE's mobility performance of the BHO procedure. Table IV.2 summarizes the key aspects of the studied HO procedures. The first HO enhancement - i.e. CHO - refers to a mobility procedure fully based on UE's radio measurements which decouples HO preparation and HO execution phases, enabling an earlier HO initiation. Furthermore, it is part of the 5G NR standard since Release-16. The LCHO solution, published in [15], is built on the basis of the NR HO procedures and it modifies the NR measurement events to include location information of the UE and the centres of the cells. It requires minimum changes in the 5G NR specifications and it can be considered a hybrid HO solution since it combines UE's radio measurements and location data. The UE needs GNSS capabilities and knowledge of the cells movement, requiring additional control signalling. Finally, the third HO enhancement - i.e. the AGHO - exploits the predictability of intra-satellite scenarios as well as avoids the non-negligible UE's radio measurement error. The HO is triggered based on geometrical estimations considering that UE's mobility is negligible with regard to the movement of the satellite and that the satellite's trajectory is known by the NW. In this way, the NW does not need the radio measurements reported by the UE to make the HO decision, which reduces the HO control signalling.

The NR HO procedures, that only use UE's radio measurements, might feature sub-optimal mobility performance. Such limitation can be addressed by exploiting the deterministic movement of LEO satellites either by combining radio measurements and location information or by enabling a clever NW, that detects the correct time to handover to the appropriate target cell.

**Table IV.2:** Summary of the HO procedures evaluated in this work.

| **HO procedure** | **Measurement quantity** | **Initiator** | **HO triggering condition** |
|---|---|---|---|
| BHO | Signal strength | UE | $P_T > P_S + HOM$ |
| CHO | Signal strength | UE | $P_T > P_S + HOM$ |
| LCHO | Signal strength and UE-cell distance | UE | $P_T > P_S + HOM + \Phi_{S,T}$ |
| AGHO | Satellite beam's antenna gain | NW | $G_S(t_1) < G_T(t_1)$, $G_T(t_1) < G_T(t_2)$ |

# 4 System-level performance evaluation

This section presents the mobility evaluation through system-level simulations of the HO enhancements detailed in Section 3. First, the system-level simulation methodology is explained including modelling assumptions, satellite details and 5G NR settings. Then, the definition of the KPIs and the mobility performance results are given. The section closes with a discussion of the main findings.

## 4.1 Simulation Methodology

Table IV.3 contains the main assumptions used to carry out the system-level simulations. Fig. IV.9 depicts the simulated EMC scenario: a constellation of 7 LEO satellites with on-board gNB capabilities enabling 5G NR access to 20 users on the ground. Every satellite enables 19 NR cells through 19 satellite beams, distributed on the ground in 3 concentric tiers. The antenna of a satellite beam provides a ground coverage diameter of 50 km. Cells on the ground show an approximately ISD of 43.3 km. Satellite radio specifics are set following the assumptions in [5]. The users are static and uniformly distributed within an area of 110 km $\times$ 35 km. Since the AGHO procedure is meant for intra-satellite mobility, the users area and the simulation time (i.e. 18 s) are specifically configured to target intra-satellite mobility events (see Fig. IV.9). The UE's measurement error follows a normal distribution. Radio measurements are filtered by the UE at layer 1 and layer 3 according to [16]. 25 % of the available PRBs per cell are artificially loaded to generate uniform DL interference. Further details of the simulation set-up can be found in [15].

Large-scale variations of the radio propagation conditions are modelled using the time-correlated radio propagation model reported in [22], which was designed considering the realistic changes of the propagation conditions in LEO-to-Ground links. Fast fading is not configured because it is assumed that the impact of fast fading is averaged out by UE's filtering.

The system-level simulation results are obtained with a Nokia proprietary simulation tool that models PHY and MAC layers according to NR specifications. The simulation tool offers realistic mobility analysis and it has been used in 3GPP standardization activities, e.g. [23], and research works, e.g. [24]. The simulation methodology follows a Monte Carlo approach [25]. The simulation procedure is repeated 1000 times using each time a different random seed and the simulation results are combined. The users distribution varies each simulation run with this methodology. Note that this is an important factor since the goal of this paper is to analyze UE's mobility performance and, therefore, a large number of mobility events is required.

**Table IV.3:** System-level simulation assumptions.

| **Parameters** | **Assumption** |
|---|---|
| Network deployment | LEO network with 7 satellites, 133 cells; 43.3 km of inter-site distance |
| UE deployment | 20 UEs uniformly distributed in rural or urban environments |
| Channel model | Mobility NTN channel model [22]; shadow fading ($\sigma$) 0.3 to 7.4 dB |
| Carrier configuration | 10 MHz bandwidth at 2 GHz (S-Band); FDD; FR1 |
| PHY numerology | 15 kHz sub-carrier spacing; 12 subcarriers per PRB |
| Satellite altitude | 600 km |
| Satellite transmit max gain | 30 dBi |
| Satellite beam antenna | Reflector with circular aperture (pattern in Section 6.4.1 in [4]); equivalent antenna aperture of 2 m; equivalent isotropic radiated power density of 34 dBW/MHz; 3 dB beamwidth of 4.4127° |
| Satellite beam diameter (on the ground) | 50 km |
| UE transmit power | 23 dBm |
| UE Tx/Rx antenna gain | 0 dBi per element |
| UE noise figure | 7 dB |
| DL/UL receiver type | LMMSE-IRC [5] |
| Traffic model | Full buffer |
| Background traffic load | 25 % PRBs |
| Radio Link Failure [16] | Qin: $-6$ dB, Qout: $-8$ dB; T310 timer: 1000 ms; N310/N311: 1 |
| UE's measurement error ($\sigma$) | 1.72 dB [18] |
| L3 filter coefficient K | 4 |
| Simulation time | 18 s (252 000 OFDM symbols) |

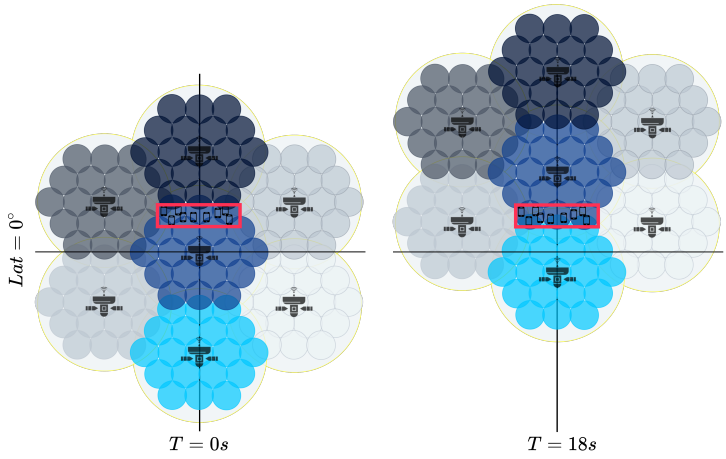


**Fig. IV.9:** Simulation scenario: 20 static UEs are served by 7 LEO satellites operating with Earth-moving cells. Beams with the same colour belong to the same satellite. Sizes of UEs, satellites and beams footprint are not to scale.

## 4.2 Configuration of the HO solutions

Each of the HO procedures is set with its optimal configuration. Table IV.4 contains the key HO parameters used to assess the HO solutions. The BHO and the CHO procedures are set with a HOM and a TTT equal to 0 dB and 0 ms, respectively. These values optimize the DL SINR, according to [14]. It is worth mentioning that the modelling of the CHO assumes that the CHO preparation phase is executed free of failures since it takes place when the serving cell radio link is reliable and no outages are expected. Furthermore, the system-level simulator considers any cell as a potential target cell, which means that CHO is executed without applying any filtering at NW side. More details are found in [14].

Regarding the LCHO procedure, the optimal configuration corresponds to the CHO set with the *penalty* scheme of the LHT event, i.e. $\Psi_{S,T} = 0$ dB and $\Theta_P = 10^6$ dB. The thresholds in (F.6) are set to $\gamma_S = 21$ km and $\gamma_T = 30$ km. The values were chosen considering that the $ISD/2$ is 21.65 km and the cell radius is approximately 25 km. The AGHO procedure is configured with $t_1 = 0.3$ s and $t_2 = 1.3$ s. At least 1 s of guard time is set between $t_1$ and $t_2$ to avoid UHO events and ensure that the target cell can provide sufficient time of coverage.

**Table IV.4:** Configured HO control parameters for the evaluated HO solutions in this work.

| HO procedure | Optimal HO parameters for the reference scenario |
|---|---|
| BHO | $HOM = 0\,\text{dB}$, $TTT = 0\,\text{ms}$ |
| CHO | $HOM = 0\,\text{dB}$, $TTT = 0\,\text{ms}$ ($2^{\text{nd}}$ condition) |
| LCHO | $HOM = 0\,\text{dB}$, $TTT = 0\,\text{ms}$,<br>$\Psi_{S,T} = 0\,\text{dB}$, $\Theta_P = 10^6\text{dB}$,<br>$\gamma_S = 21\,\text{km}$, $\gamma_T = 30\,\text{km}$ |
| AGHO | $t_1 = 0.3\,\text{s}$, $t_2 = 1.3\,\text{s}$ |

## 4.3 Key Performance Indicators

The following statistics were collected for this study:

- *Radio link failures* provide important information to evaluate the robustness and reliability of the radio link. A UE declares a RLF when the serving cell signal quality drops below a threshold $Q_{out}$ during *T310* time length. Further details of the RLF mechanism can be found in [23], [16] and [21].
- *Unnecessary Handovers and Ping-pongs*. An UHO event is declared when a user stays connected in a cell for less than a certain period, e.g. 1 s. As a subset of UHOs, PP events are declared when a user handovers from *cell A* to *cell B* and handovers back to *cell A* within a certain time, e.g. 1 s.
- *Geometric downlink signal-to-interference-plus-noise ratio*, in this article denoted as DL SINR, determines the quality of the received signal. This metric compares the signal strength that the user measures from the serving cell against the sum of interference power from the neighbouring cells and noise.
- *Time-of-stay* metric is defined as the time that a UE stays connected in a serving cell. It is relevant to assess the HO rate and the signalling overhead. The report [23] formally defines the ToS as the duration in *cell A* from when the UE sends a *HO complete* message to *cell A* to when the UE sends a *HO complete* message to another cell.

## 4.4 Mobility Performance Results

In this section we present the mobility performance of the BHO, the CHO, the LCHO and the AGHO solutions, which are tested for users in rural and urban scenarios. We also include the *optimal HO* as a reference of the best achievable performance. This *optimal HO* optimizes the DL SINR considering that the UE always receives the HO command and access the target cell with best DL SINR, at the optimal instant when target cell radio link quality becomes better than the serving cell radio link quality. There is no impact of the UE's measurement error on the *optimal HO*, control signalling propagation delays are correctly compensated and the random access procedure is executed without failures at the optimal time.

The results are organized as follows. First, the mobility performance is evaluated in terms of RLF rate. A high RLF rate indicates UEs experiencing long interruption periods and low DL SINR. Second, the UHO and PP rates provide a picture of the HO signalling overhead and the excess of measurement reporting. Some UEs could avoid RLFs but experience high rates of UHO/PP, which turns into an unnecessary use of resources and reduces the exchange of UE's data. Third, the DL SINR shows the result of the RLF performance. A consequence of reducing RLFs is the improvement of the radio link quality and, therefore, the DL SINR. Fourth, the ToS accounts for the time that a UE stays connected to the same cell. The goal is to minimize UHO and PP rates to maximise the ToS. Finally, we provide the UE-cell centre distance at HO completion time to show how close to the cell edge the UE completes the HO. Note that this metric does not distinguish among desired HO events and UHO events.

The RLF performance of users in rural and urban scenarios is depicted in Fig. IV.10. For the rural case, the three analysed HO enhancements are capable of eliminating the RLFs. For the urban case, the CHO is the only procedure able to keep the RLF rate close to zero. Nonetheless, the LCHO and the AGHO solutions present a rate of 0.1 operations/UE/min. The small difference is explained by the fact that CHO purely relies on UE's radio measurements and can react effectively to a channel state transition from LOS to NLOS. In contrast, LCHO and AGHO rely on geometric estimations that overlook the variations of the radio propagation conditions.

Fig. IV.11 provides the UHO rate and the PP rate. Similarly to the results in [14], the CHO procedure increases more than 70 % the UHO and PP rates, which results in a growth of the measurement reporting and the HO control signalling. The use of UE's location and satellite's pointing information prove to eliminate UHO events as observed for the LCHO and the AGHO cases. No relevant differences are observed for the different HO procedures under rural and urban conditions.

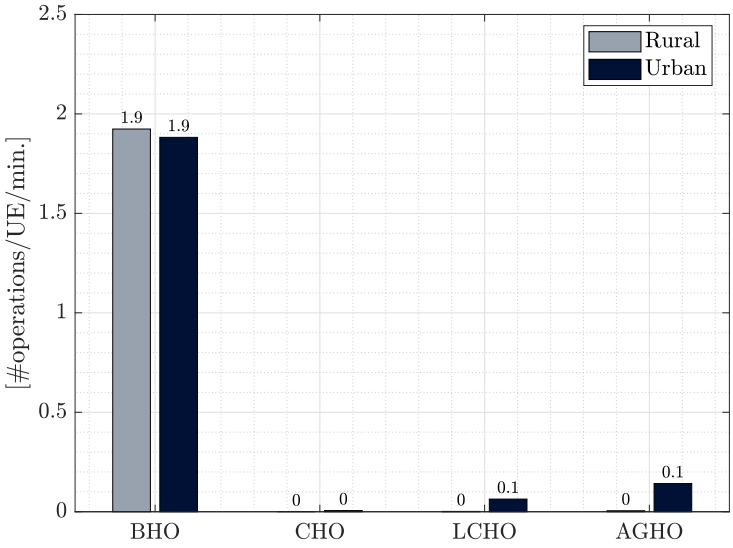


**Fig. IV.10:** Radio link failure (RLF) rates when using the baseline HO (BHO), the conditional HO (CHO), the location-based CHO (LCHO) and the antenna gain-based HO (AGHO) for users in rural and urban environments.

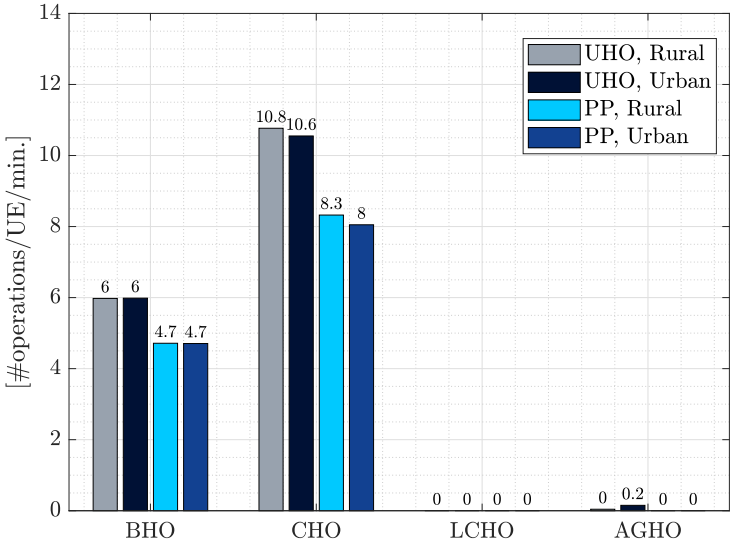


**Fig. IV.11:** Unnecessary HO (UHO) and ping-pong (PP) rates when using the baseline HO (BHO), the conditional HO (CHO), the location-based CHO (LCHO) and the antenna gain-based HO (AGHO) for users in rural and urban environments.

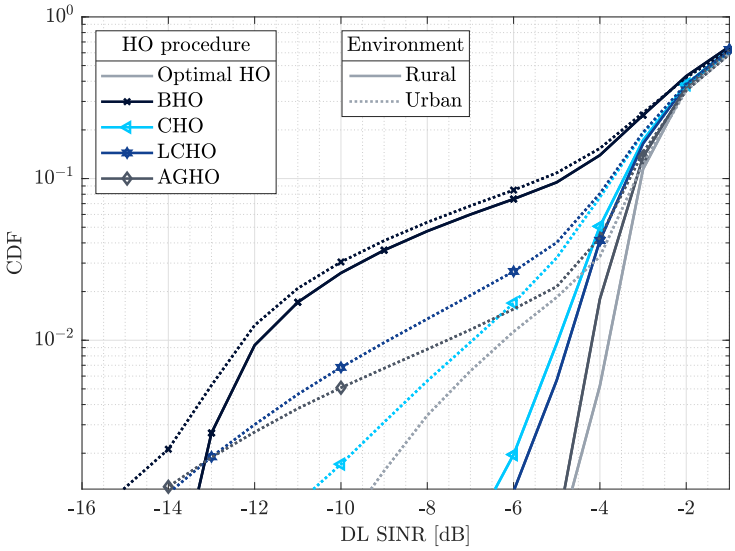


**Fig. IV.12:** CDF of the downlink signal-to-interference-plus-noise ratio (DL SINR) when the optimal HO, the baseline HO (BHO), the conditional HO (CHO), the location-based CHO (LCHO) and the antenna gain-based HO (AGHO) are used. Solid lines represent the performance for users in a rural environment and dotted lines refer to an urban environment.

Fig. IV.12 shows the CDF of the DL SINR corresponding to the analysed HO procedures in rural and urban scenarios. All the HO procedures present higher DL SINR values in rural conditions. As indicated in [26], in a rural scenario the likelihood of experiencing LOS conditions is higher as compared with an urban environment, where high-rise buildings might shadow users at higher elevation angles increasing the radio propagation losses. The *optimal HO* provides the upper-bound reference for both scenarios. For the rural case, where UEs are under almost-static LOS conditions, the AGHO shows the closest performance to the optimal, followed by the LCHO and the CHO procedures, respectively. This underlines the benefit of using alternative HO triggering criteria especially when radio conditions are fully-correlated among cells. Note that when urban conditions apply, in terms of DL SINR the CHO is the procedure showing a better robustness against varying LOS conditions.

Without loss of generality, the following performance results are shown only for the rural case. In Fig. IV.13, the CDF of the ToS is presented. LCHO and AGHO solutions achieve similar performance as compared with the *optimal HO*. As seen above, these two procedures are able to filter out UHO events, which maximises the ToS in the serving cell. Following this reasoning, when using the BHO and the CHO procedures, both with high UHO and PP rates, around 60 % of the stays in a cell are below 3 s. Note that the *optimal*

*HO* shows a ToS performance that falls within a range between 3 s and 7 s, approximately. This provides a magnitude of the HO frequency problem in the reference scenario; even using a flawless HO procedure, a UE executes a HO every 3-7 s.

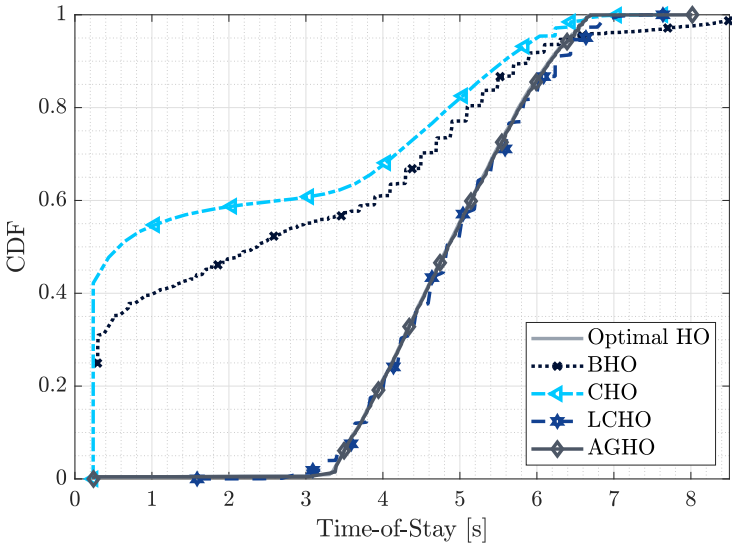


**Fig. IV.13:** CDF of the time-of-stay (ToS) when the optimal HO, the baseline HO (BHO), the conditional HO (CHO), the location-based CHO (LCHO) and the antenna gain-based HO (AGHO) are used in a rural environment.

Finally, Fig. IV.14 shows the CDF of the distance between the UE and the serving cell's centre at HO completion. The figure includes, in light grey, the overlapping area among cells that ranges from at least $ISD/2$ - i.e. 21.65 km - to the cell radius - i.e. 25 km. These results do not consider neither the impact of radio impairments such as the UE's measurement error nor the access to an undesired target cell. However, they provide a concise overview of where the HO takes place in the cell. The *optimal HO* shows that the benchmark distance ranges from 20.5 km to 24 km. The AGHO procedure follows a similar trend to the optimal but around 2 km before. Note that this can be explained since this procedure initiates the HO based on predictions at future times $t_1$ and $t_2$ (see Section 3.3). This suggests that the AGHO may be triggered shortly before the optimal time. For this evaluation, $t_1$ is equal to 0.3 s. Considering that the satellites moves at a speed of 7.8 km/s, this translates into a shift on the ground of 2.34 km, which fits with the observed in Fig. IV.14. It is also worth highlighting the difference among purely measurement-based procedures and geometry-based procedures, likely due to the combined impact of the UE's measurement error and the low RSRP difference between cell centre and cell edge (i.e. approximately 3 dB). The BHO and the CHO show 20 % of

the HO events occurring at distances between 15 km and 20.5 km, which can be linked to the high amount of UHO/PP events seen in Fig. IV.11.

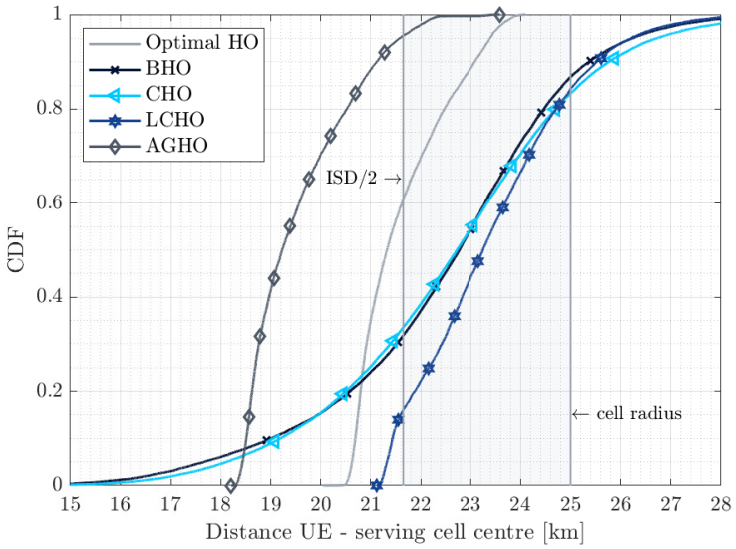


**Fig. IV.14:** CDF of the distance UE-serving cell centre at HO completion time when the optimal HO, the baseline HO (BHO), the conditional HO (CHO), the location-based CHO (LCHO) and the antenna gain-based HO (AGHO) are used in a rural environment.

## 4.5 Sensitivity analysis

Results shown above were obtained following the 3GPP specifications in [5], which contains realistic assumptions for system-level simulations with non-terrestrial systems. Despite the 3GPP reported the importance of using location-based HO triggering criteria, none of these assumptions considered inaccuracies in the location neither from the UEs nor the satellites. This section further analyses the robustness of those HO solutions that exploit location data. We investigate the impact of errors that could deteriorate the accuracy of the location data and degrade the UE's mobility performance.

Apart from UE's radio measurements, the LCHO procedure uses the UE's location, the satellite's position and the steering angles of the beams to estimate the centre of the cells. On the other hand, the AGHO solution also exploits UE's location and satellite's attitude besides the antenna radiation pattern of the satellite beams (see Section 3). Similarly as with radio measurements, these data sources could have associated a certain error that may alter the performance of the HO solutions.

To study the sensitivity of these error sources, a normally distributed error is introduced in the UE's location, the satellite's pointing accuracy and the

satellite beam's antenna radiation. These errors are time-invariant and differ among UEs, satellites and satellite beams, respectively. We conduct 1000 simulations varying the pseudo-random seed to ensure a sufficiently large number of samples. The outputs from all the realizations are later combined following a Monte Carlo approach to obtain statistically reliable results.

Five cases per HO procedure are considered to study the individual and the overall impact of these errors. The first case is the benchmark where no errors are considered. Second, we introduce a UE's location error with a $\sigma$ of 150 m. The 3GPP required in [27] a nominal positioning accuracy of 30 m in ideal conditions. The value for this study is set according to a worst case scenario where UEs do not feature GNSS coverage or the location is outdated due to, for example, UE's mobility. The third case covers a satellite's pointing inaccuracy of 0.35° ($\sigma$). This error translates into a shift of 3 km on the ground. The value is selected according to [28], which provides details of the Iridium's attitude, control and determination system. It is a low-accuracy case scenario since current attitude systems of LEO satellites feature more precise pointing control accuracy [2]. Fourth, an error in the antenna's radiation is introduced where the $\sigma$ is equal to 0.5 dB. We set a value higher than what can be found in the literature, e.g. [29]. Finally, the fifth case shows the impact of all the aforementioned errors combined.

Table IV.5 presents a summary of the main findings. There are minor differences in terms of DL SINR and HO distance but, overall, no relevant impact can be observed on the mobility performance, regardless of the HO procedure or the error. It is worth underlining that only the rural environment was taken into account for this part of the investigation.

**Table IV.5:** Summary of the impact of the satellite beam's antenna radiation error, the UE's location error and the satellite's control pointing error in a rural environment.

| Error source | Error [$\sigma$] | RLF [#op./UE/min] | UHO [#op./UE/min] | DL SINR $5^{th}$ percentile [dB] | Mean ToS [s] | Mean HO UE-cell distance [km] |
|---|---|---|---|---|---|---|
| | | | LCHO / AGHO | | | |
| None | - | 0.0 / 0.0 | 0.0 / 0.0 | -3.9 / -3.7 | 4.9 / 4.9 | 23.4 / 19.6 |
| Antenna gain | 0.5 dB | 0.0 / 0.0 | 0.0 / 0.1 | -3.9 / -3.9 | 4.9 / 4.9 | 23.4 / 19.6 |
| UE location | 150 m | 0.0 / 0.1 | 0.0 / 0.0 | -4.0 / -3.9 | 4.9 / 4.9 | 23.7 / 19.6 |
| Satellite pointing | 0.35° | 0.0 / 0.0 | 0.0 / 0.0 | -4.3 / -3.8 | 4.9 / 4.9 | 24.4 / 20.1 |
| Antenna gain, UE location, Satellite pointing | 0.5 dB, 150 m, 0.35° | 0.0 / 0.1 | 0.0 / 0.1 | -4.3 / -4.2 | 4.9 / 4.9 | 24.6 / 20.1 |

## 4.6 UE's mobility

Mobility performance has been typically impacted by UE's mobility in TNs [24]. Users have different speeds which can impact RSRP, communication latency and HO rate as they move. Despite the 5G specifications support UE speeds up to 500 km/h [30], in LEO satellite networks the mobility performance is dominated by satellites movement since they move much faster, i.e. 28 000 km/h.

We validate this assumption by analysing the mobility performance of users at 3, 30 and 500 km/h in a rural environment using the LCHO and the AGHO procedures. The RLF and the UHO rates, for the mentioned UE speeds and HO procedures, are provided in Table IV.6. The system-level simulation results confirm that UE's mobility has no relevant impact on the UE's mobility performance.

**Table IV.6:** Impact of the UE's mobility in terms of radio link failures (RLFs) and unnecessary HO (UHOs) when using the location-based CHO (LCHO) and the antenna gain-based HO (AGHO) procedures.

| HO Procedure | UE mobility [km/h] | RLF [#op./UE/min] | UHO [#op./UE/min] |
|---|---|---|---|
| LCHO | 3 | 0.0 | 0.0 |
| | 30 | 0.0 | 0.0 |
| | 500 | 0.0 | 0.0 |
| AGHO | 3 | 0.0 | 0.1 |
| | 30 | 0.0 | 0.0 |
| | 500 | 0.0 | 0.1 |

## 4.7 Summary of the results and discussion

Using extensive system-level simulations, this section has presented and analysed the UE's mobility performance of the BHO, the CHO, the LCHO and the novel AGHO solutions for EMC-based 5G LEO satellite networks. Furthermore, this paper contributes with a mobility analysis that considers UEs under rural and urban radio propagation conditions. The system-level simulation results support that measurement-based HO procedures require location information such as exploiting the known satellite trajectory and the UE's location.

Table IV.7 provides a summary of the main findings of this investigation. It is clear that LCHO and AGHO are the HO procedures achieving a mobility performance closer to the optimal. This underlines the relevance of using location data to select the appropriate target cell to handover to. Both solutions show similar performance in all the analysed KPIs. There are small differences in the distance UE-serving cell centre and the signalling load. The later intends to capture the measurement reporting and HO signalling load and is estimated considering the required signalling steps, the NR A3 event rate and the successful HO rate. Despite the AGHO shows the same signalling load as the optimal and a 25 % decrease as compared with the LCHO procedure, we consider the LCHO procedure a more suitable HO solution. This HO solution has a minimum impact on the 5G NR specifications, allows the UE to evaluate radio signal conditions and exploits the predictability of the satellites movement. Even though the AGHO has the advantage to avoid UE's radio measurements, the procedure is designed for intra-satellite mobility with continuous LOS conditions. The LCHO procedure can be used in intra-satellite and inter-satellite mobility and it is a more robust HO solution in scenarios characterized by abrupt RSRP changes, e.g. LOS to NLOS conditions.

As in TN, the environment surrounding the UE plays a part on the UE's mobility performance and the user experience. A UE in a rural environment with sparse and low clutter is likely to experience LOS conditions for longer periods since the probability of NLOS increases just for the lower elevation angles. On the other hand, urban scenarios are characterized by tall buildings, street canyons and, in essence, a shorter range of elevation angles with LOS conditions. Thus, it is important to evaluate the UE's mobility performance in rural and urban conditions to support the development of 5G LEO satellite networks. This article has contributed with novel system-level simulation results for users in rural and urban environments. With the simulation methodology used, there are no relevant differences in the results between both scenarios. This could be explained since the UE experiences a short range of elevation angles, i.e. from 79° to 101°. The used cell diameter, i.e. 50 km, combined with a low number of cells per satellite, i.e. 19, results in a satellite coverage with an approximate radius of 112 km. Considering that satellite altitude is 600 km, a UE at the edge of the satellite coverage will see a minimum elevation angle of 79.4°.

Despite the limited mobility performance differences comparing rural and urban environments, the magnitude of the mobility challenges is satellite deployment dependent. This means that the limitations of the HO procedures used in NTN will change based on cell size, constellation configuration or steerability of the satellite antennas. For instance, the scenario simulated in this paper consider a LEO satellite formation, distributed in 3 polar orbits, near the equator. As satellites move to larger latitudes, e.g. near polar re-

gions, LEO satellites will be closer to each other due to orbital propagation, which might result in more frequent HO events and higher inter-satellite interference. Thus, the UE's mobility performance can vary depending on the UE's location and the satellite formation, e.g. inclination of the satellite orbits.

# 5 Conclusion and future research

This article has provided a realistic system-level simulation analysis of the UE's mobility performance when using state-of-the-art handover solutions for 5G-based low-Earth orbit satellite networks. The study aims to support the development of non-terrestrial networks, thus, the simulation methodology follows 3GPP specifications and considers low-Earth orbit satellites with on-board gNB capabilities and Earth-moving cells. The baseline 5G NR handover, the 5G NR conditional handover, the location-based conditional handover and the novel antenna gain-based handover have been analyzed considering users in rural and urban environments. The antenna gain-based handover, which is a fully network-controlled handover procedure for intra-satellite mobility, exploits the known satellite's trajectory and the UE's location to avoid UE's radio measurements and, therefore, bypass the non-negligible impact of the UE's measurement error. The system-level simulation results indicated that the location-based conditional handover and the antenna gain-based handover achieved the best mobility performance, regardless of the user environment. Both procedures enhanced the handover triggering and the handover decision by eliminating radio link failures, unnecessary handovers, ping-pongs and, consequently, presented a downlink signal-to-interference-plus-noise ratio and a time-of-stay in a cell close to the optimal. Thus, the use of UE's location and satellite's movement information enhances the UE's mobility performance as compared with measurement-based handover procedures. Finally, we have presented a sensitivity analysis addressing UE-specific and satellite-specific errors that could impact the mobility performance. The system-level simulation results demonstrated that the location-based conditional handover and the antenna gain-based handover are robust against UE's location error, satellite's pointing error and satellite antenna's radiation error.

For future research directions in the field of handover procedures for low-Earth orbit satellite networks, it is worth investigating the performance of inter-satellite mobility procedures that, while exploiting the deterministic movement of these satellites, are also able to seamlessly react to abrupt changes of the received signal power due to variations of the line-of-sight conditions. Furthermore, future work should also involve the study of the proposed handover solutions under different satellite configurations such as Earth-fixed cells. The vision for future research in handover solutions should

focus on developing versatile procedures able to provide robust service continuity regardless of UE's radio capabilities, constellation deployment and satellite payload characteristics.

**Table IV.7:** Summary of the UE's mobility performance in rural and urban scenarios when using the baseline HO (BHO), the conditional HO (CHO), the location-based CHO (LCHO) and the antenna gain-based HO (AGHO) procedures. The optimal HO is included as the upper-bound performance.

| HO procedure | RLF [#op./UE/min] | UHO [#op./UE/min] | DL SINR $5^{th}$ percentile [dB] | Mean ToS [s] | HO signalling load [#op./UE/min] |
|---|---|---|---|---|---|
| | | | Rural / Urban | | |
| Optimal HO | 0.0 / 0.0 | 0.0 / 0.1 | -3.6 / -3.8 | 4.9 / 4.9 | 23.5 / 22.4 |
| BHO | 1.9 / 1.9 | 6.0 / 6.0 | -7.8 / -8.3 | 2.8 / 2.7 | 75.4 / 73.8 |
| CHO | 0.0 / 0.0 | 10.8 / 10.6 | -4.0 / -4.6 | 2.3 / 2.2 | 96.7 / 94.4 |
| LCHO | 0.0 / 0.1 | 0.0 / 0.0 | -3.9 / -4.8 | 4.9 / 4.9 | 49.0 / 46.8 |
| AGHO | 0.0 / 0.1 | 0.0 / 0.2 | -3.7 / -3.9 | 4.9 / 4.9 | 35.5 / 33.7 |

# References

[1] ITU, "2021 Measuring digital development: Facts and figures," ITU Publications, 2021. [Online]. Available: https://www.itu.int/en/ITU-D/Statistics/Pages/facts/default.aspx

[2] J. N. Pelton and S. Madry, *Handbook of Small Satellites: Technology, Design, Manufacture, Applications, Economics and Regulation*. Springer, 2020.

[3] N. Pachler, I. del Portillo, E. F. Crawley, and B. G. Cameron, "An Updated Comparison of Four Low Earth Orbit Satellite Constellation Systems to Provide Global Broadband," in *2021 IEEE International Conference on Communications Workshops (ICC Workshops)*, 2021, pp. 1–7.

[4] "Study on New Radio (NR) to support Non-Terrestrial Networks (Release 15)," 3GPP, TR 38.811 V15.2.0, 2019. [Online]. Available: https://www.3gpp.org/ftp/Specs/archive/38_series/38.811/

[5] "Solutions for NR to support Non-Terrestrial Networks (NTN) (Release 16)," 3GPP, TR 38.821 V1.0.0, 2019. [Online]. Available: https://www.3gpp.org/ftp/Specs/archive/38_series/38.821/

[6] E. Del Re, R. Fantacci, and G. Giambene, "Efficient Dynamic Channel Allocation Techniques with Handover Queuing for Mobile Satellite Networks," *IEEE Journal on Selected Areas in Communications*, vol. 13, no. 2, pp. 397–405, Feb 1995.

[7] G. Maral, J. Restrepo, E. del Re, R. Fantacci, and G. Giambene, "Performance Analysis for a Guaranteed Handover Service in an LEO Constellation with a Satellite-Fixed Cell System," *IEEE Transactions on Vehicular Technology*, vol. 47, no. 4, pp. 1200–1214, 1998.

[8] Y. Wu, G. Hu, F. Jin, and J. Zu, "A Satellite Handover Strategy based on the Potential Game in LEO Satellite Networks," *IEEE Access*, vol. 7, pp. 133 641–133 652, 2019.

[9] Y. Li, W. Zhou, and S. Zhou, "Forecast based Handover in an Extensible Multi-Layer LEO Mobile Satellite System," *IEEE Access*, vol. 8, pp. 42 768–42 783, 2020.

[10] S. Zhang, A. Liu, C. Han, X. Ding, and X. Liang, "A Network-Flows-Based Satellite Handover Strategy for LEO Satellite Networks," *IEEE Wireless Communications Letters*, vol. 10, no. 12, pp. 2669–2673, 2021.

[11] J. Li, K. Xue, J. Liu, and Y. Zhang, "A User-Centric Handover Scheme for Ultra-Dense LEO Satellite Networks," *IEEE Wireless Communications Letters*, vol. 9, no. 11, pp. 1904–1908, Nov 2020.

[12] Y. Cao, S.-Y. Lien, and Y.-C. Liang, "Deep Reinforcement Learning for Multi-User Access Control in Non-Terrestrial Networks," *IEEE Transactions on Communications*, vol. 69, no. 3, pp. 1605–1619, March 2021.

[13] E. Juan, M. Lauridsen, J. Wigard, and P. E. Mogensen, "5G New Radio Mobility Performance in LEO-based Non-Terrestrial Networks," in *2020 IEEE Globecom Workshops (GC Wkshps)*, Dec 2020, pp. 1–6.

[14] E. Juan, M. Lauridsen, J. Wigard, and P. Mogensen, "Performance Evaluation of the 5G NR Conditional Handover in LEO-based Non-Terrestrial Networks," in *2022 IEEE Wireless Communications and Networking Conference (WCNC)*, April 2022, pp. 2488–2493.

[15] E. Juan, M. Lauridsen, J. Wigard, and P. E. Mogensen, "Location-Based Handover Triggering for Low-Earth Orbit Satellite Networks," in *2022 IEEE 95th Vehicular Technology Conference (VTC2022-Spring)*, June 2022.

[16] "NR; Radio Resource Control (RRC) protocol specification (Release 16)," 3GPP, TS 38.331 V16.5.0, 2021. [Online]. Available: https://www.3gpp.org/ftp/Specs/archive/38_series/38.331/

[17] "Study on channel model for frequencies from 0.5 to 100 GHz (Release 17)," 3GPP, TR 38.901 V17.0.0, 2022. [Online]. Available: https://www.3gpp.org/ftp/Specs/archive/38_series/38.901/

[18] "NR; Requirements for support of radio resource management (Release 16)," 3GPP, TS 38.133 V16.5.0, 2020. [Online]. Available: https://www.3gpp.org/ftp/Specs/archive/38_series/38.133/

[19] "Solutions for NR to support Non-Terrestrial Networks (NTN) (Release 17)," 3GPP, RP-202908, TSG RAN Meeting 90-e, 2020. [Online]. Available: https://www.3gpp.org/ftp/tsg_ran/TSG_RAN/TSGR_90e/Docs

[20] "NR Non-Terrestrial Networks (NTN) enhancements (Release 18)," 3GPP, RP-213690, TSG RAN Meeting 94-e, 2021.

[21] "NR; NR and NG-RAN Overall Description (Release 16)," 3GPP, TS 38.300 V16.6.0, 2021. [Online]. Available: https://www.3gpp.org/ftp/Specs/archive/38_series/38.300/

[22] E. Juan, M. Lauridsen, J. Wigard, and P. E. Mogensen, "Time-correlated Geometrical Radio Propagation Model for LEO-to-Ground Satellite Systems," in *2021 IEEE 94th Vehicular Technology Conference (VTC2021-Fall)*, Sep. 2021, pp. 1–5.

[23] "E-UTRA Mobility Enhancements in Heterogeneous Networks (Release 11)," 3GPP, TR 36.839 V0.7.1, 2012. [Online]. Available: https://www.3gpp.org/ftp/Specs/archive/36_series/36.839/

[24] S. Barbera, P. H. Michaelsen, M. Säily, and K. Pedersen, "Mobility Performance of LTE Co-Channel Deployment of Macro and Pico Cells," in *2012 IEEE Wireless Communications and Networking Conference (WCNC)*, April 2012, pp. 2863–2868.

[25] R. Coates, G. Janacek, and K. Lever, "Monte Carlo Simulation and Random Number Generation," *IEEE Journal on Selected Areas in Communications*, vol. 6, no. 1, pp. 58–66, 1988.

[26] E. Juan, M. Lauridsen, J. Wigard, and P. E. Mogensen, "A Time-correlated Channel State Model for 5G New Radio Mobility Studies in LEO Satellite Networks," in *2021 IEEE 93rd Vehicular Technology Conference (VTC2021-Spring)*, April 2021, pp. 1–5.

[27] "Requirements for support of Assisted Global Navigation Satellite System (A-GNSS) (Release 17)," 3GPP, TR 38.171 V17.0.0, 2022. [Online]. Available: https://www.3gpp.org/ftp/Specs/archive/38_series/38.171/

[28] European Space Agency (ESA), "Iridium NEXT - Satellite Missions," accessed: 2022-05-09. [Online]. Available: https://earth.esa.int/web/eoportal/satellite-missions/i/iridium-next

[29] O. Breinbjerg, "High-Accuracy Spherical Near-Field Measurements for Satellite Antenna Testing," in *2017 11th European Conference on Antennas and Propagation (EUCAP)*, March 2017, pp. 2931–2934.

[30] I. Shayea, M. Ergen, M. H. Azmi, S. A. Çolak, R. Nordin, and Y. I. Daradkeh, "Key Challenges, Drivers and Solutions for Mobility Management in 5G Networks: A Survey," *IEEE Access*, vol. 8, pp. 172 534–172 552, 2020.

# Part V

# Conclusions

# Conclusions

The PhD dissertation proposes, simulates, and analyzes handover (HO) solutions to support the development of fifth generation (5G) New Radio (NR) over low-Earth orbit (LEO) satellite networks, specifically in Earth-moving cells (EMC) deployments. The focus is on 5G NR technology. First, the study analyzes the user equipment (UE) mobility performance of the conventional 5G NR HO procedure and the 5G NR conditional HO (CHO) procedure in 5G LEO satellite networks. The HO triggering and the HO decision, purely based on cell radio measurements, are identified as a constraint for the mobility performance due to the characteristics of LEO satellite networks. Therefore, enhancing the mobility performance of HO procedures in 5G LEO satellite networks is the main goal of the research. To that end, the deterministic movement of LEO satellites is acknowledged as the key element to exploit. Novel HO solutions, i.e. the location-based HO triggering event and the antenna gain based HO (AGHO) procedure, have been proposed, simulated and analyzed. Extensive system-level simulations demonstrate that the proposed HO solutions enhance the UE mobility performance as compared with the conventional 5G NR HO procedure and the 5G NR CHO procedure. The main contribution of the thesis is that UE location and satellite location can be used to substitute or complement cell radio measurements. The work motivates to exploit known satellite trajectory to achieve promising UE mobility performance in 5G LEO satellite networks.

## 1 Summary of the Main Findings

A summary of the research work together with the answers to the research questions is provided in the following.

*(Q1) For a given satellite elevation angle, what is the line-of-sight (LOS) probability for static users in rural and urban environments? What is the probability to transition from/to LOS/non line-of-sight (NLOS)? What is the variability of the shadow fading?*

To conduct realistic system-level simulations, the first part of this thesis has focused on the design of a radio propagation model suitable for mobility investigations with LEO satellites. The model accomplishes to capture the time-correlated variations of path loss, shadow fading, and visibility conditions, i.e. LOS and NLOS, caused by LEO satellites movement. The model parameters were fitted with data obtained through ray-tracing simulations. The proposed modelling follows a two-steps approach. First, a two-state Markov model predicts the LOS/NLOS states as a function of the satellite elevation angle observed by the UE. The LOS model analysis shows very close agreement as compared with ray-tracing simulation data. Second, the model predicts the path loss according to LOS/NLOS conditions by considering: i) free-space path loss, ii) clutter loss, and iii) shadow fading. The physically consistent approach includes ray contributions from a rooftop-to-street diffraction and a reflected ray. The ray-tracing data analysis showed that in NLOS conditions the latter is dominant for low elevation angles, whereas the former gains relevance as the satellite moves to higher elevation angles and the UE signal path becomes less obstructed. The model parameters are geometry-based to offer environment-specific properties. The proposed radio propagation model is founded on existing models from the international telecommunications union (ITU) and the 3rd generation partnership project (3GPP) and it can be used as a suitable extension of them. Finally, the model was implemented, tested and calibrated in the system-level simulator for the mobility investigations of this thesis.

By means of the proposed radio propagation model, we are able to answer the research questions in Q1. For instance, for a user in a rural environment with a satellite elevation angle of 80°, the LOS probability is 90 %, the probability to move from LOS to NLOS is 0.3 % and the shadow fading variability will depend on the elevation angle where visibility conditions change.

*(Q2) What is the reference signal received power (RSRP) variability experienced by UEs at cell centre and at cell edge? How the inter-cell interference from intra-satellite cells can impact the radio signal quality and the overall mobility performance? What is the optimal HO rate? What kind of enhancements can be done to improve the conventional HO procedure performance?*

The mobility performance of the conventional *break-before-make* UE-assisted network (NW)-controlled NR HO procedure, i.e. baseline HO (BHO), and the NR CHO procedure were analyzed to: i) gain insights on the characteristics of LEO satellite networks, ii) identify the limitations of these procedures, and iii) establish a baseline for later mobility studies.

The analysis of the BHO procedure indicated that this procedure cannot ensure service continuity. The study identified the following aspects impact-

ing the mobility performance:

i) There is a 3 dB RSRP variability from cell centre to cell edge.

ii) UEs feature a non-negligible measurement error. This measurement imperfection, which is modeled according to 3GPP requirements, impacts the HO triggering and the posterior HO decision.

iii) The serving cell radio link quality is limited by high inter-cell interference; more than 80 % of the simulated downlink signal-to-interference-plus-noise ratio (DL SINR) samples show values below 0 dB. This impacts the radio link failure (RLF) mechanism, the modulation and the coding schemes.

iv) EMC move on the ground at approximately 28 000 km/h due to satellite movement. The fast cell movement results in a fast degradation of the radio link quality, which increases RLFs and HO failure (HOF).

v) Despite a cell diameter of 50 km, the fast cells movement triggers a high number of HO events. The approximate lower bound of the HO rate is, on average, 0.2 HO/UE/s.

The study, which was conducted varying HO margin (HOM) and time-to-trigger (TTT) control parameters, revealed that the impact of these limitations results in a large number of RLFs, HOFs and ping-pong (PP) events. Further analysis found that the main issue of the BHO procedure was that a large part of the RLFs were caused by a too late HO, i.e. the HO is initiated when the UE is out of the serving cell radio coverage and the serving cell radio link is too weak to complete the HO procedure.

The mobility performance of the CHO procedure was also analyzed. The system-level simulation results showed that this procedure eliminates RLF and HOF due to an earlier HO triggering, at the expense of more than 60 % increase of unnecessary HO (UHO) events. The increase of UHO events increases the signalling overhead and the measurement reporting, which can compromise the mobility performance and the user experience. Thus, it was concluded that 5G NR HO procedures relying on NR measurement events, which are purely based on cell radio measurements, achieve sub-optimal mobility performance. Even when the UE avoids RLF and HOF, the combination of the low RSRP variability and the UE measurement error makes it difficult for the UE to correctly distinguish the appropriate target cell.

*(Q3) Can satellite ephemeris and UE location be used in the HO triggering criteria to initiate the HO at cell edge and towards the optimal target cell? Can location-based HO solutions maximize DL SINR, optimize the HO rate while reducing RLFs and UHO events?*

To mitigate the increase of signalling for enhancing the mobility performance, this thesis studied the benefits of exploiting the predictability of LEO satellites movement. Specifically, the location-based HO triggering (LHT) event was proposed, simulated and analyzed. This HO event modifies the NR measurement events to include a location-based offset that captures the distance changes between the UE location and the cells centre. The system-level simulation results indicate that RLF, HOF, UHO and PP events can be eliminated. Therefore, the use of the LHT event minimizes the HO rate and maximizes the time-of-stay (ToS) in a cell, which translates into UEs spending less time exchanging HO control signalling. The proposed event can be used with specified measurement-based NR HO procedures because it only modifies the triggering of HO events, i.e. the measurement report (MR) triggering and the CHO execution conditions.

*(Q4) Can the fact that there is a fully-correlated shadow fading be exploited? Can intra-satellite HO be triggered without using cell radio measurements bypassing the non-negligible UE measurement error?*

This thesis also investigated the possibility of using a HO procedure that does not require cell radio measurements. The goals were: i) to bypass the low RSRP variability and the UE measurement error, and ii) to achieve a mobility performance as close to the optimal as possible. To that end, the thesis has proposed a fully NW-controlled antenna gain-based intra-satellite HO procedure, that exploits the full-correlation of path loss, shadow fading and LOS conditions between adjacent intra-satellite cells. The proposed HO procedure uses antenna gain predictions of the satellite beams to indicate the UE the most appropriate target cell to handover to. The system-level simulation results demonstrated that this approach avoids RLF and UHO events.

Furthermore, the satellite beam antenna radiation error, the satellite beam antenna pointing error, the UE location error and the UE mobility were modelled and simulated to analyze their impact on the proposed HO solutions in terms of mobility performance. System-level simulation results showed that these error sources do not cause significant changes in the mobility performance.

# 2 Recommendations

The following recommendations are made from the presented conclusions:

1) Complement the 3GPP mobility studies to support NR over non-terrestrial network (NTN) with a radio propagation model that realistically cap-

tures the signal strength variations caused by satellite movement.

2) It is advised to exploit known satellite movement and complement cell radio measurements with UE location and cells centre location information. A sub-optimal mobility performance is expected for measurement-based 5G NR HO procedures in EMC-based 5G LEO satellite networks.

3) For intra-satellite mobility, the recommendation is to exploit known satellite movement together with the fully-correlated radio propagation conditions by means of satellite beam antenna gain predictions. Low RSRP variation and UE measurement error can degrade mobility performance.

# 3 Future Work

The work presented in this thesis is a first step towards the realization of mobility procedures for 5G-based LEO satellite networks.

The CHO procedure has been investigated considering that the preparation condition was faultlessly executed and the execution condition was evaluated for every potential target cell. It is recommended to study the use of a smarter NW that exploits the satellite movement and blocks the evaluation of undesired target cells.

The thesis presented two HO solutions that exploit the predictability of satellites movement. The analysis of these HO solutions was conducted for intra-satellite mobility in a EMC-specific deployment. The presented studies can be complemented by analyzing the mobility performance for inter-satellite mobility. Furthermore, it is recommended to study the performance of these solutions with satellites using Earth-fixed cells (EFC). Beyond these scenarios, it is advised to investigate HO solutions under different cell sizes, satellite payloads and constellation deployments.

The road towards a *network of networks* in sixth generation (6G) opens interesting research topics to explore such as the intra/inter-orbit satellite mobility, NTN-NTN mobility and TN-NTN mobility. Pedestrian UEs approaching urban areas, on board ships and in high-speed airplanes should be able to seamlessly connect to fixed terrestrial radio access networks (RANs), LEO satellite-based RANs and geosynchronous equatorial orbit (GEO) satellite-based RANs and handover among them without noticeable service interruption and without penalizing the user experience.

The use of a HO procedures without cell radio measurements has been investigated in this thesis. A possible research path is to investigate HO solutions that do not use cell radio measurements as the core part of the procedure but are still used to react to abrupt RSRP changes. Furthermore, the HO control signalling can be further explored to be reduced.

As a final research path, it is suggested that the proposed radio propagation model is complemented with real measurements campaign that provide realistic data to fit the model parameters.

# Part VI

# Appendix

# Paper G

## Are System-Level Simulation Results Sufficiently Reliable?

Enric Juan

# 1 Introduction

This appendix presents a study that evaluates the reliability of the system-level simulation results used in this PhD project. To that end, Section 2 studies the statistical *confidence* of these results based on the number of generated samples and simulation iterations. Additionally, the calibration process of the 3GPP channel model is described in Section 3. Details of the calibration and testing of the propagation model from Papers A-B are also included. Note than we refer to this model as *mobility model*. Section 4 explains the modelling of the UE measurement error. Further system-level simulation results showing the UE mobility performance as a function of the UE RSRP measurement accuracy are given to demonstrate UE sensitivity to the measurement error. Finally, the simulated LEO satellite deployment is compared against SpaceX Starlink, OneWeb and Amazon Kuipers deployments in Section 5 and the users density distribution is compared with population targets defined by the 3GPP in Section 6.

# 2 Confidence of the Simulation Results

This thesis has presented mobility performance results obtained by means of system-level Monte Carlo simulations [1]. The simulation tool is capable of reproducing the main processes of cellular networks, where mathematical underlying models mimic the stochastic nature of wireless links. It is designed to account for multi-cell and multi-user deployments, different channel propagation models and radio resource management algorithms. To realistically simulate these processes the simulator follows a Monte Carlo approach. This mathematical technique uses different random seeds to predict a set of outcomes leveraging a probability distribution for any uncertain variable. The simulation procedure is repeated many times, e.g. 1000 times, using each time a different random seed and the average of the results is calculated. Based on the law of large numbers theory, the idea is to produce a large enough number of outcomes to guarantee high statistical confidence of the results. The level of precision, or *confidence*, can be measured by means of confidence intervals (CIs); small intervals indicate more reliable results. These intervals depend on two parameters: the confidence level and the standard deviation from the mean of the samples distribution. A typical value of confidence level is 95 %. Thus, we are *confident* that 95 % of the generated samples fall between the lower and upper values of the interval.

This part of the thesis presents simple estimations of the CI based on a desired confidence level. Furthermore, it includes the estimation of the minimum required number of simulated samples to meet a certain confidence target. The latter is provided as a beneficial tool to know in advance the number

of required samples before running the simulations to make an efficient use of the available resources. The estimations are based on the simulated DL SINR samples collected for Paper F.

## 2.1 Estimation of the Confidence Intervals

The central limit theorem [2] states that taking sufficiently large random samples, the mean of a sample is normally distributed regardless of the distribution of the dataset from which the sample was taken. This is only possible if the dataset is larger than the number of samples.

Given a sequence of independent identically distributed random variables $x_1, x_2, ...x_N$ with mean $\mu$ and variance $\sigma^2$, the average $\bar{x}$ is defined as:

$$\bar{x} = \sum_{n=1}^{N} \frac{x_n}{N} \tag{G.1}$$

$$CI = \{\bar{x} - z \times \frac{\sigma}{\sqrt{N}}, \bar{x} + z \times \frac{\sigma}{\sqrt{N}}\} \tag{G.2}$$

The CI can be calculated using (G.2), where $\bar{x}$ is the sample mean, $z$ is the statistic associated with a certain CI, $\sigma$ is the sample standard deviation and $N$ is the sample size (i.e. number of simulated samples in our case). For a target of 95 % CI, the $z$-statistic is approximately 1.96[1].

In Paper F, $N = 35401445$ samples were generated to analyse the DL SINR. From that sample size, the distribution mean value is $\bar{x} = -2.22\,\text{dB}$ with standard deviation $\sigma = 2.52\,\text{dB}$. Given these parameters, the 95 % CI is given by:

$$\begin{aligned} CI &= \{-2.22 - 1.96\frac{2.52}{\sqrt{(35401445)}}, -2.22 + 1.96\frac{2.52}{\sqrt{(35401445)}}\} \\ &= \{-2.22 - 0.0008, -2.22 + 0.0008\} \\ &= \{-2.216, -2.214\} \end{aligned}$$

For the simulated number of samples $N$, the lower and upper bounds of the 95 % CI of the mean DL SINR are $\{-2.216, -2.214\}$dB, which indicates the high statistical confidence of the results in this thesis.

## 2.2 Minimum Number of Required Samples

Besides the DL SINR distribution, Paper C and F provided the $5^{th}$ percentile of the DL SINR. For the case of the CI for a proportion the proceeding is

[1]Statistically, 95 % of the area under a normal distribution curve is described as being $\pm 1.96$ standard deviations from the mean [3].

similar as the CI for means. In this case, the interval is estimated using the normal approximation of the Binomial proportion [4]. Given a certain percentile $\hat{p}$, the CI is estimated as follows:

$$CI = \hat{p} \pm z \times \sqrt{\frac{\hat{p}(1-\hat{p})}{N}} \tag{G.3}$$

The following justifies the minimum sample size required to guarantee statistical confidence given a certain interval. Following the procedure formulated in [5], for a 95 % confidence level, the estimate of $\hat{p}$ falling within a $\pm 5$ % interval is defined as:

$$\frac{1.96\sqrt{\hat{p}(1-\hat{p})/N}}{\hat{p}} < 0.05 \tag{G.4}$$

Given the above and for $\hat{p} = 0.05$, the number of required samples is given by:

$$N = \frac{(1.96)^2}{(0.05)^2}\frac{1-0.05}{0.05} = 29197 \tag{G.5}$$

This means that the number of uncorrelated DL SINR samples generated for Paper F is statistically sufficiently large given the minimum required limits.

## 2.3 Convergence of the Mean Value

Fig. VI.1 shows the mean value of the DL SINR distribution as a function of the Monte Carlo iterations (i.e. drops). The number of simulations ranges from 1 to 1000 drops. It can be observed a quick convergence after approximately 50 drops. In fact, after 7 drops the metric shows little variation with values between $-2.23$ dB and $-2.17$ dB. The corresponding 95 % CI, estimated at each step, is also included in the figure. In line with the calculations above, the CI present a small range even for the lower drops, i.e. 20-100 drops.

This section has provided a series of calculations and plots to evaluate the statistical confidence level of the system-level simulation results. The CI of the mean DL SINR presents a small range even for a reduced number of drops. Furthermore, it is demonstrated that the number of uncorrelated samples simulated for the $5^{th}$ percentile goes beyond the minimum required number of samples to ensure statistical confidence. Therefore, the outcome of these estimations indicate that the system-level simulation results in this thesis have high statistical reliability.

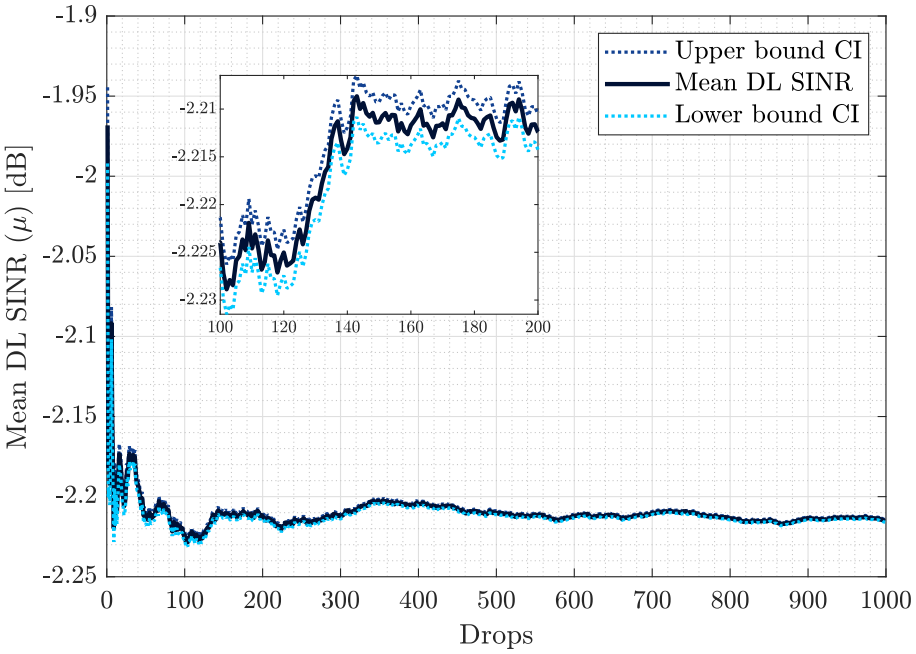


**Fig. VI.1:** Mean DL SINR as a function of the number of conducted Monte Carlo simulations.

# 3 Radio Propagation Models

Part I of this thesis discussed the relevance of correctly characterizing radio propagation conditions in order to investigate mobility solutions. The work in Paper C was conducted using the 3GPP model, while Papers D-F used the mobility model. The 3GPP model is defined in the technical report [6] for NTN channels, whereas the mobility model was designed for the purpose of carrying out mobility studies with LEO satellites (see Papers A-B for further details). Both models were implemented, tested and calibrated in the system-level simulator.

## 3.1 Calibration of the 3GPP Model

The 3GPP reported in [7] the process for calibration of the channel model in [6]. Based on the system-level assumptions in [7, Table 6.1.1.1-5], the members from the standardization body reported the simulated results of coupling loss (CL), geometry downlink signal-to-interference ratio (DL SIR) and geometry DL SINR. In [7, Table 6.1.1.2-1], it can be found the average performance for these metrics reported by the 3GPP members. The performance results for each company are available in the reports [8] [9].

In the early stages of this thesis, this model was implemented and calibrated in the simulator. Table VI.1 contains the main parameters used for the calibration according to 3GPP specifications. The system-level simulation results CL, DL SIR and DL SINR were extracted and compared against the results reported by the different 3GPP companies. Out of thirty calibration study cases in [7], the work in this project focused on the scenarios case-#9 and case-#10 which comprise:

i) Satellite orbit: LEO at an altitude of 600 km.

ii) Satellite parameter set #1.

iii) Central beam elevation: 90°.

iv) Terminal: Handheld.

v) Frequency band: S-band.

vi) frequency reuse (FR) schemes: FR1 (case-#9) and FR3 (case-#10).

Without loss of generality, Fig. VI.2 shows the geometric DL SINR cumulative distribution function (CDF). The results were generated for FR1 and FR3 and according to the parameters in Table VI.1. Furthermore, the figure includes the average DL SINR contributed by the other 3GPP members. The distribution shows an exact agreement between the simulated DL SINR and the reported values in [8] for both frequency reuse schemes. These results validated the implementation of the 3GPP model in the simulator and demonstrated that the outcome was reliable in terms of radio propagation.

## 3.2 Calibration of the Mobility Model

As explained at the beginning of this section, the mobility model from Papers A-B was also implemented, tested and calibrated in the system-level simulator. Fig. VI.3 compares the geometry DL SINR obtained with the 3GPP model and the mobility model. The results are obtained considering most of the assumptions in Table VI.1. For the mobility model, NLOS conditions are modelled. There is close agreement between both models, however, there are some differences at both ends of the distribution. For LOS conditions and at high elevation angles, the mobility model uses shadow fading values slightly smaller as compared with the 3GPP model, which may cause the differences at the high end of the CDF. At the lower end, the mobility model presents samples below $-6$ dB. This is probably due to UEs in NLOS conditions.

**Table VI.1:** Parameters for system-level simulator calibration.

| **Parameters** | **Assumption** |
|---|---|
| Satellite payload characteristics for DL | |
| Satellite altitude | 600 km |
| Satellite antenna pattern | Section 6.4.1 in [6]: Bessel function |
| Satellite equivalent isotropic radiated power density | 34 dBW/MHz |
| 3 dB beamwidth | 4.4127° |
| Satellite Tx max Gain | 30 dBi |
| Satellite beam ground diameter | 50 km |
| UE characteristics (handheld) | |
| UE transmit power | 23 dBm |
| Antenna type | (1,1,2) with omnidirectional antenna elements |
| UE antenna gain | 0 dBi per element |
| UE noise figure | 7 dB |
| Receiver type | LMMSE-IRC |
| Network and deployment parameters | |
| Carrier configuration | DL 30 MHz bandwidth at 2 GHz (S-Band); FDD; FR1 and FR3 |
| Deployment scenario [6] | NTN Rural |
| UE distribution | at least 10 UEs per beam with uniform distribution |
| Propagation conditions | line-of-sight (i.e. clear sky) |
| Shadow Fading ($\sigma$) [6] | 1.79 to 0.72 dB |
| Number of beams per satellite | 19-beams layout (i.e. 18 beams surrounding the central beam and allocated on 2 distinct tiers) considering wrap-around mechanism |
| Adjacent beam spacing | $\sqrt{3} \times \sin HPBW/2$ [rad] (based on 3 dB beam width of the satellite antenna pattern) |
| HO margin | 0 dB |
| UE attachment | RSRP |

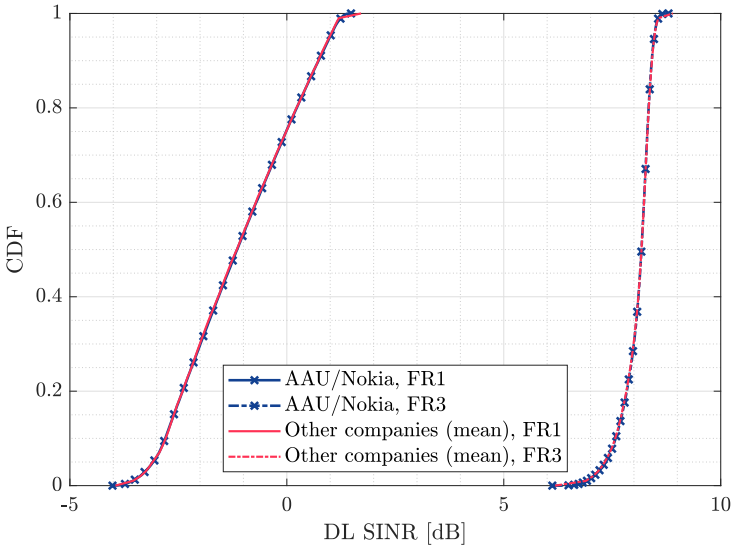


**Fig. VI.2:** Calibration of the 3GPP model: distribution of the geometric DL SINR for FR1 and FR3.

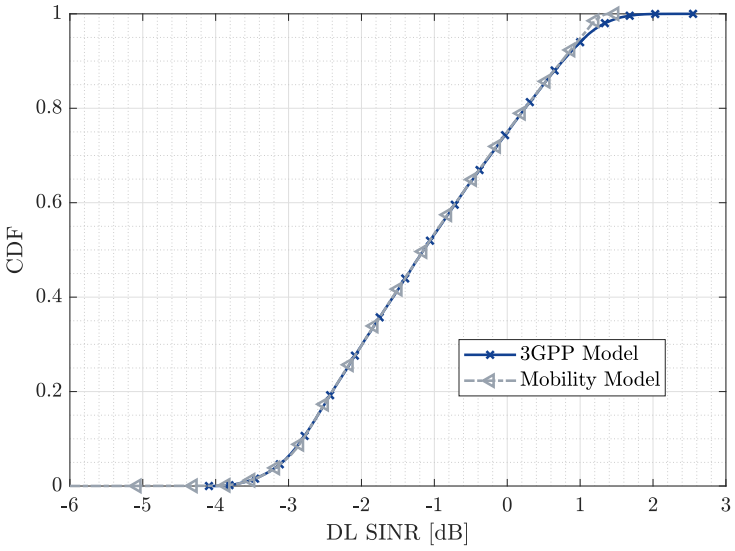


**Fig. VI.3:** Calibration of the mobility model: distribution of the geometric DL SINR for FR1.

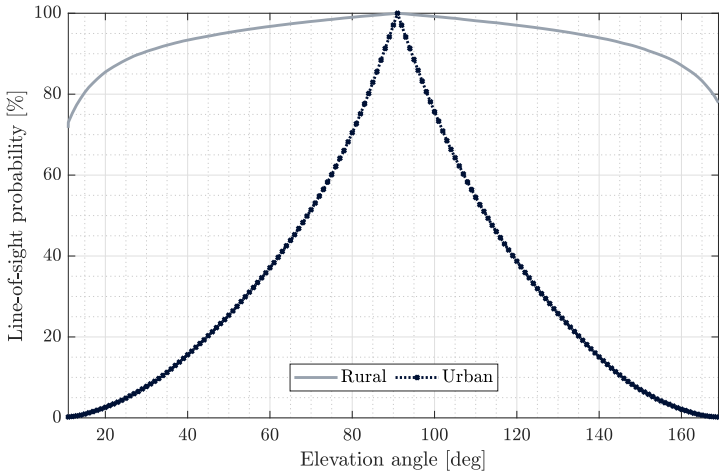


**Fig. VI.4:** Calibration of the mobility model: LOS probability for rural and urban environments.

Even though the mobility model enables realistic transitions between LOS and NLOS conditions, the studies of this thesis show a very low proportion of UEs in NLOS conditions. Paper F provides an explanation to this statement. This thesis has used a satellite deployment that leads UEs to a short range of elevation angles, i.e. from 79° to 101°. To support the justification, Fig. VI.4 presents the LOS probability for rural and urban environments simulated with the mobility model. Given the range 79°-101°, the rural case shows a LOS probability very close to 100 %. The urban case depicts LOS probabilities ranging from 70 % at 80° elevation angle to 100 % at 90° elevation angle.

# 4 Measurement Error Analysis

## 4.1 Modelling

This section describes the measurement error (ME) modelling present in the system-level simulator. As [10] specifies, the HO measurements are performed at layer-1 (L1), filtered and then forwarded to the layer-3 (L3) filter. Fig. VI.5 shows a simplified schematic of the measurement model found in chapter 9 of [10].

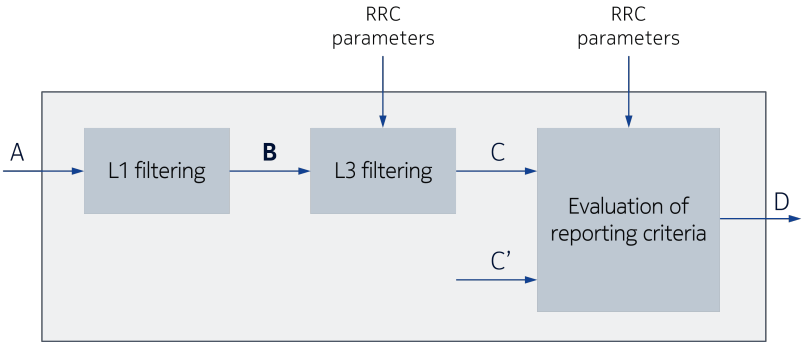


**Fig. VI.5:** Measurement model.

The measurement accuracy requirements in the specification TS38.133 [11] relate to point $B$ in Fig. VI.5. This means that the measurements after L1 filtering and before L3 filtering should fulfill the TS38.133 requirements. The simulation tool used for this thesis models the ME such that a normally-distributed error is separately added to each L1 measurement sample. Then, the ME at point $B$ depends on the error distribution for each individual measurement and the L1 sliding window length. The following details the procedure to correctly model the normally-distributed ME at point $B$ considering that these are combined after L1 filter and the requirements in [11].

In Long-Term Evolution (LTE) and NR, the RSRP accuracy requirements are specified so that the ME is within the bounds with 90 % probability. For example, a measurement accuracy of $\pm 2$ dB means that the ME is within $\pm 2$ dB with 90 % probability. We make use of the formulation in [12] to derive the standard deviation given a certain probability.

Let $X$ be a random variable normally-distributed, independent with mean $\mu = 0$ and variance $\sigma^2$. The probability that $X$ lies in the range $\{-\delta, +\delta\}$ is given by the following expression:

$$P(-\delta \leq X \leq \delta) = \text{erf}\left(\frac{\delta}{\sigma\sqrt{2}}\right) \tag{G.6}$$

Let ME samples at point $A$, $X_1, X_2, ..., X_n$, be random variables normally-distributed and independent. Assuming that these samples are distributed with mean $\mu = 0$ and variance $\sigma_a^2$, the probability that a sample lies in the range $\{-\delta, +\delta\}$ is:

$$P(-\delta \leq X \leq \delta) = \text{erf}\left(\frac{\delta}{\sigma_a\sqrt{2}}\right) \tag{G.7}$$

By extension, the standard deviation $\sigma_a$ of the ME at point $A$, such that the probability of the ME lying in the interval $\{-\delta, +\delta\}$ is 0.9, is:

$$\sigma_a = \frac{\delta}{\sqrt{2}\,\mathrm{erfinv}(0.9)} \tag{G.8}$$

As explained above, the measurement samples at point $B$ are combined by the L1 filter. This means that that the variance of the ME after L1 filtering (i.e. point $B$) results from linearly combining individual variances. Considering $L$ as the L1 filter length, the variance $\sigma_b^2$ of the combined distributions is given by:

$$\sigma_b^2 = \mathrm{Var}\left(\frac{1}{L}\sum_{i=1}^{L} X_i\right) = \frac{1}{L^2}\sum_{i=1}^{L}\mathrm{Var}\left(\bar{X}_i\right) = \frac{\sigma_a^2}{L} \tag{G.9}$$

Thus, the standard deviation $\sigma_b$ after L1 filtering, assuming that the error lies within the bounds $\{-\delta, +\delta\}$ with 90 % probability is set as:

$$\sigma_b = \frac{\delta\sqrt{L}}{\sqrt{2}\,\mathrm{erfinv}(0.9)} \tag{G.10}$$

Up to this point, the modelling of the ME from one cell has been described. However, measurement events compare measurements from two different cells. This means that two filtered RSRP measurements are compared against each other, which results in a combination of two already-combined errors. The following is assumed for the calculation of the error standard deviation $\sigma_{b'}$ when comparing two RSRP measurements:

i) All RSRP measurements are taken using the same L1 filtering length $L$.

ii) ME is normally distributed with zero mean.

iii) All RSRP ME samples are independent and identically distributed.

Since two RSRP samples are compared, the combined difference of these two measurements is also normally distributed. Hence, the variance $\sigma_{b'}^2$ is defined as:

$$\sigma_{b'}^2 = \sigma_b^2 + \sigma_b^2 = 2\,\sigma_b^2 = 2\frac{\sigma_a^2}{L} \tag{G.11}$$

Considering the expressions (G.6) and (G.11), the required error standard deviation $\sigma_{b'}$ for relative RSRP measurements with 90 % error bound is given by the general form:

$$\sigma_{b'} = \frac{\delta\sqrt{L}}{\sqrt{4}\,\mathrm{erfinv}(0.9)} \tag{G.12}$$

The simulator is configured to use an L1 filtering sliding window of 4 samples (i.e. $L = 4$) and the 3GPP requires a relative measurement accuracy of $\delta = \pm 2\,\text{dB}$. Therefore, the ME standard deviation used in the simulator is:

$$\sigma_{b'} = \frac{2\,\text{dB}}{\text{erfinv}(0.9)} = 1.7196\,\text{dB} \tag{G.13}$$

## 4.2 Impact on the UE Mobility Performance

The ME impact in terms of RLFs, UHOs and HO attempts on the BHO procedure is depicted in Fig. VI.6. The figure shows the increase of these key performance indicators (KPIs) as a function of the accuracy range $\delta$. The $\delta$ reference is $\pm 2\,\text{dB}$, which is the range found in [11] for relative RSRP accuracy in normal conditions. Tighter accuracy requirements lead to a better HO performance because the UE detects more precisely the appropriate target cell.

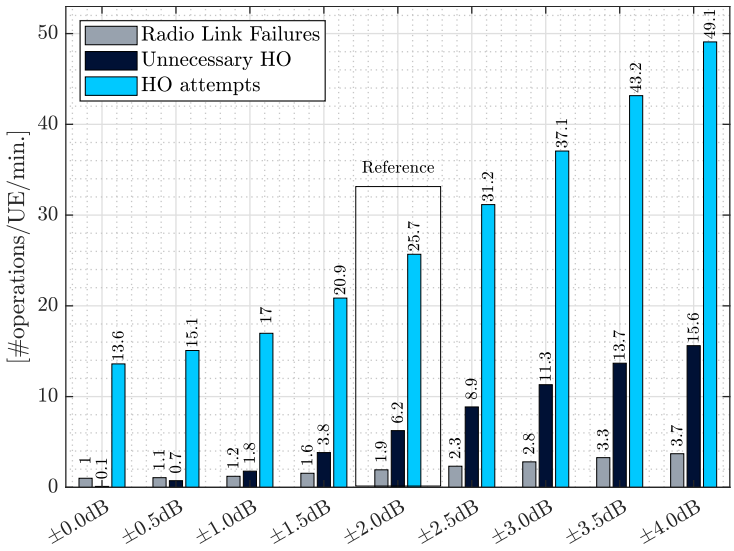


**Fig. VI.6:** Impact of the ME on the UE mobility performance in terms of RLFs, UHOs and HO attempts when using different measurement accuracy requirements.

# 5 LEO Satellite Constellations

The simulation work in this thesis has followed the 3GPP specifications for NTN. In [7], the 3GPP reported system-level simulation assumptions including satellite altitude, beam size and beam layout distribution, among other

parameters. This sections aims to compare the simulated satellite beam deployment against the three front-runner broadband constellation projects carried out by the private companies SpaceX, OneWeb and Amazon.

In Fig. VI.7, we demonstrate the number of required satellites to provide global coverage depending on the satellite beam footprint size. To that end, we consider the 3GPP configuration of 19 beams per LEO satellite, satellite altitude of 600 km and estimate the number of satellites varying the beam size. These estimations considered a beam footprint with a circular shape. The figure also includes the number of satellites of SpaceX Starlink [13], OneWeb [14] and Amazon Kuiper [15]. For the OneWeb case, the beam radius is estimated based on the beam coverage area because the beam footprint is highly elliptical.

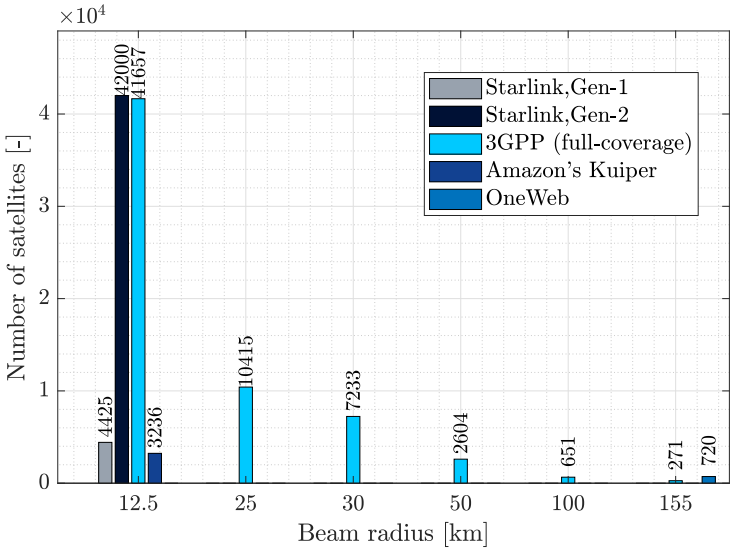


**Fig. VI.7:** Comparison of 3GPP, SpaceX's Starlink, OneWeb and Amazon's Kuiper deployments in terms of number of satellites as a function of the satellite beam size.

The system-level simulations of this thesis assumed 19 beams with a footprint diameter of 50 km. Considering such configuration as the reference, to provide ubiquitous coverage the constellation would need approximately 10 415 satellites (i.e. 197 885 satellite beams). Assuming circular beams, Starlink and Kuiper constellations aim for beams with a radius of approximately 12.5 km. SpaceX has plans to deploy approximately 42 000 LEO satellites in different orbits, while Amazon aims for 3236 LEO satellites. Assuming 19 satellite beams per satellite and a satellite beam size of 25 km (diameter), the required number of LEO satellites to provide global coverage is roughly 41 657 satellites. Despite the number of beams per satellite for Starlink and

Kuiper are not publicly available, we can assume that Starlink satellites implement a low number of beams per satellite, while Kuiper satellites will feature higher complexity antenna systems with larger number of satellite beams.

# 6 UE Distribution

The main goal to enable satellite-based NR access is to bring connectivity to rural and remote areas, thus, the UE density must be set accordingly. This section discusses the UE distribution used in the system-level simulator.

The simulation methodology considers UEs randomly dropped following an uniform distribution over a sphere with radius $R_E = 6371\,\text{km}$. Furthermore, we consider a full-buffer traffic model, therefore, UEs are always active exchanging data with the NW. For Papers C-D, 20 UEs where randomly located within an area of $55\,\text{km} \times 55\,\text{km}$ (i.e. $3718\,\text{km}^2$), whereas for Papers E-F, the area of the UEs was changed to $111\,\text{km} \times 33\,\text{km}$ (i.e. $3025\,\text{km}^2$). The purpose of this modification was to ensure that UEs only triggered intra-satellite mobility events. These cases present a UE density of $0.005\,\text{UEs}/\text{km}^2$ and $0.007\,\text{UEs}/\text{km}^2$, respectively.

The report [7] contains performance targets for simulation analysis, despite it states that the values should not be considered as strict requirements. The pedestrian usage scenario for rural coverage considers an overall UE density of $100\,\text{UEs}/\text{km}^2$ for UEs with an activity factor[2] of 1.5 %. Then, considering only simultaneously active UEs, the UE density is equal to $1.5\,\text{UEs}/\text{km}^2$.

Even though the 3GPP targets are meant for throughput performance to ensure a certain downlink (DL) and uplink (UL) experienced data rate, they provide a reference in terms of UE density. The simulation work in this thesis shows a UE density lower than the 3GPP targets. However, this thesis has focused on UE mobility performance where the key factor is to simulate enough mobility events covering all the possible UE locations within the deployed cells. To that purpose, as mentioned above, we follow a Monte Carlo approach where the simulation procedure is repeated a large number of times, e.g. 1000 iterations, to obtain reliable statistics. Considering Paper F where 1000 iterations were simulated, the combined simulation results consider mobility events from $20 \times 1000$ UE locations (i.e. $7\,\text{UEs}/\text{km}^2$).

[2]The activity factor is defined in [16] as the percentage value of the amount of simultaneous active UEs to the total number of UEs.

# References

[1] R. Coates, G. Janacek, and K. Lever, "Monte Carlo Simulation and Random Number Generation," *IEEE Journal on Selected Areas in Communications*, vol. 6, no. 1, pp. 58–66, 1988.

[2] S. G. Kwak and J. H. Kim, "Central Limit Theorem: the Cornerstone of Modern Statistics," *Korean journal of anesthesiology*, vol. 70, no. 2, pp. 144–156, 2017.

[3] M. Liu, "Optimal Number of Trials for Monte Carlo Simulation," *VRC–Valuation Research Report*, 2017.

[4] L. D. Brown, T. T. Cai, and A. DasGupta, "Confidence Intervals for a Binomial Proportion and Asymptotic Expansions," *The Annals of Statistics*, vol. 30, no. 1, pp. 160–201, 2002.

[5] G. Pocovi, B. Soret, M. Lauridsen, K. I. Pedersen, and P. Mogensen, "Signal Quality Outage Analysis for Ultra-Reliable Communications in Cellular Networks," in *2015 IEEE Globecom Workshops (GC Wkshps)*. IEEE, 2015, pp. 1–6.

[6] "Study on New Radio (NR) to support Non-Terrestrial Networks (Release 15)," 3GPP, TR 38.811 V15.2.0, 2019. [Online]. Available: https://www.3gpp.org/ftp/Specs/archive/38_series/38.811/

[7] "Solutions for NR to support Non-Terrestrial Networks (NTN) (Release 16)," 3GPP, TR 38.821 V1.0.0, 2019. [Online]. Available: https://www.3gpp.org/ftp/Specs/archive/38_series/38.821/

[8] Thales, "System Level Calibration Results for NTN on DL transmissions," 3GPP, R1-1913404, 3GPP TSG-RAN1 Meeting #99. [Online]. Available: https://www.3gpp.org/ftp/Meetings_3GPP_SYNC/RAN1/

[9] ——, "System Level Calibration Results for NTN on UL transmissions," 3GPP, R1-1913405, 3GPP TSG-RAN1 Meeting #99. [Online]. Available: https://www.3gpp.org/ftp/Meetings_3GPP_SYNC/RAN1/

[10] "NR; NR and NG-RAN Overall Description (Release 16)," 3GPP, TS 38.300 V16.6.0, 2021. [Online]. Available: https://www.3gpp.org/ftp/Specs/archive/38_series/38.300/

[11] "NR; Requirements for support of radio resource management (Release 16)," 3GPP, TS 38.133 V16.5.0, 2020. [Online]. Available: https://www.3gpp.org/ftp/Specs/archive/38_series/38.133/

[12] N. Lebedev, "Special functions and their applications."

[13] "The bandwidth of the Starlink constellation and the assessment of its potential subscriber base in the USA," SatMagazine. [Online]. Available: http://www.satmagazine.com/story.php?number=1026762698#:~:text=The%20diameter%20of%20the%20cell,area%20of%20379%20square%20kilometers.

[14] I. Del Portillo, B. G. Cameron, and E. F. Crawley, "A Technical Comparison of Three Low Earth Orbit Satellite Constellation Systems to Provide Global Broadband," *Acta astronautica*, vol. 159, pp. 123–135, 2019.

[15] J. Hindin, "TECHNICAL APPENDIX: Application of Kuiper Systems LLC for Authority to Launch and Operate a Non-Geostationary Satellite Orbit System in Ka-band Frequencies," Washington DC: Federal Communications Commission, 2019. [Online]. Available: https://www.fcc.gov/

[16] "SA; Service Requirements for the 5G System (Release 18)," 3GPP, TS 22.261 V18.6.0, 2022. [Online]. Available: https://www.3gpp.org/ftp/Specs/archive/22_series/22.261/

ISSN (online): 2446-1628
ISBN (online): 978-87-7573-834-2

AALBORG UNIVERSITY PRESS